

SAN FRANCISCO-
OAKLAND BAY BRIDGE
SELF-ANCHORED SUSPENSION BRIDGE
EVALUATION OF THE ASTM A354 GRADE BD RODS

SAN FRANCISCO- OAKLAND BAY BRIDGE SELF-ANCHORED SUSPENSION BRIDGE EVALUATION OF THE ASTM A354 GRADE BD RODS

CONTRIBUTORS:

California Department of Transportation

Brian Maroney
Ade Akinsanya
Bob Brignano
Tony Anziano
Ken Terpstra
William Casey

Bolt Consultants

Alan Pense
Herbert Townsend
Louis Raymond
Karl Frank
Sheldon Dean
Thomas Langill
Robert Heidersbach
Douglas Williams

Design Joint Venture T.Y. Lin International/ Moffatt & Nichol

Marwan Nader
Hayat Tazir
Carol Choi

California Department of Transportation Materials Engineering and Testing Services

Keith Hoffman
Gary Thomas
Mazen Wahbeh
Rami Boundouki

Bay Area Management Consultants

Ted Hall
Steve Matty
Jeffrey Gorman
Stephen Christoffersen
Alan Cavendish-Tribe

California Transportation Commission

Stephen Maller
Dina Noel

SAN FRANCISCO-
OAKLAND BAY BRIDGE
SELF-ANCHORED SUSPENSION BRIDGE

EVALUATION OF THE ASTM A354 GRADE BD RODS

SEPTEMBER 30, 2014

TABLE OF CONTENTS

EXECUTIVE SUMMARY	ES-1
<hr/>	
1. INTRODUCTION AND BACKGROUND	1-1
<hr/>	
1.1 San Francisco–Oakland Bay Bridge	1-1
1.2 High-Strength, Large-Diameter Rods (A354BD) in the SAS	1-5
1.3 Failure of Pier E2 Embedded Rods at Shear Keys S1 and S2 (2008)	1-9
1.4 Other A354BD Rods on the SAS	1-14
1.5 Testing Program	1-15
Test I	1-18
Test II	1-20
Test III	1-22
Test IV	1-24
Test V	1-26
Test VI	1-28
<hr/>	
2. MECHANICAL TESTING AND BORESCOPE EXAMINATION	2-1
<hr/>	
2.1 Borescope Investigations	2-1
2011 Borescope Investigation of E2 Shear Key Rod Holes	2-3
2013 Borescope Investigation of E2 Shear Key Rod Holes	2-4
2.2 Tests I, II, and III	2-7
2.2.1 Test I: Field Hardness Test	2-8
2.2.2 Test II: Laboratory Tests	2-10
2.2.3 Test II: Modified (II-M)	2-18
2.2.4 M-Shapes	2-25
2.2.5 Test III: Full-Diameter Tension Test	2-26
2.2.6 Test III Modified (III-M)	2-36
2.2.7 Summary	2-41
<hr/>	
3. STRESS CORROSION TESTING	3-1
<hr/>	
3.1 Test IV – Stress Corrosion Testing: “Townsend Test”	3-1
3.1.1 Test Rig Design	3-1
3.1.2 Test Protocol	3-5
3.1.3 Test Results at Job Site (Phase 1, 2, 3, 4, and 5)	3-7

3.1.4 Post-Fracture Analysis at Lab (Phases 1, 2, 3, 4, and 5).....	3-11
3.1.5 Summary of Results	3-14
3.2 Test V — Incremental Step Load Testing: “Raymond Test”	3-15
3.2.1 Test Protocol and Test Rigs	3-15
3.2.2 FEM Validation	3-21
3.2.3 Summary of Results	3-24
3.2.4 Conclusions.....	3-29
3.3 Test VI — Additional Verification Testing: “Gorman Test”	3-29
3.3.1 Part 1: Extended RSL Testing.....	3-30
3.3.2 Part 2: Sustained Load Testing.....	3-31
3.3.3 Summary of Results and Conclusions, Test VI.....	3-33
4. TESTING PROGRAM SUMMARY AND RECOMMENDATIONS	4-1
4.1 Background and Objectives	4-1
4.2 Summary of Results of Tests I, II, and III	4-2
4.3 Summary of Results of Test IV	4-3
4.4 Summary of Results of Test V	4-6
4.5 Summary of Results of Test VI	4-7
Part 1	4-7
Part 2	4-7
4.6 Summary and Recommendations	4-8
4.6.1 Summary	4-8
4.6.2 Conclusions and Recommendations	4-8
5. GLOSSARY, ABBREVIATIONS, AND ACRONYMS	5-1
6. REFERENCES	6-1
7. APPENDICES	7-1
A. Presentations to TBPOC	
B. E2 Shear Keys S1/S2 Design Alternatives	
C. S1/S2 Alternative Load Path (Shimming) Report	
D. A354BD Rods Project Specifications	
E. Hood Canal Floating Bridge Report (3/20/2014 Revision)	
F. Borescope Investigation of Pier E2 Rods Holes, SMR Reports (2011 and 2013)	
G. BAMC’s Borescope Report (04/17/2014 Revision 3)	
H. E2 Shear Key Rod Failure Fracture Analysis Report	
I. Theory of Hydrogen Embrittlement and Stress Corrosion Cracking	
J. Test I, II, III, M-Shape, II-M, III-M Reports	
K. Test IV Plans and Field Reports	
L. Test IV Post-Fracture Analysis Reports	
M. Test V Details and Data Report	

N. Test VI Details and Data Report

O. Field Inspection Report on the Tower Anchorage Anchor Rods

LIST OF FIGURES

Figure 1.1-1: <i>Plan and Elevation of San Francisco–Oakland Bay Bridge New East Span</i>	1-2
Figure 1.1-2: <i>Self-Anchored Suspension Bridge</i>	1-4
Figure 1.1-3: <i>Pier E2 Details</i>	1-4
Figure 1.2-1: <i>A354BD Rods Across SFOBB-SAS</i>	1-6
Figure 1.2-2: <i>A354BD Rods on the SAS</i>	1-8
Figure 1.3-1: <i>E2 Cap Beam During Construction (Photo taken 10/19/2009)</i>	1-10
Figure 1.3-2: <i>Top of Pier E2 Cap Beam at S1/S2 during Construction (Photo taken 1/12/2011)</i>	1-11
Figure 1.3-3: <i>Shear Keys S1/S2, Rods, Pipe Sleeves, and Top Hat Details</i>	1-11
Figure 1.3-4: <i>First Indication of Rod Failure</i>	1-12
Figure 1.3-5: <i>Rod Failure Timeline</i>	1-12
Figure 1.3-6: <i>A354BD Rods at Pier E2 — Break Locations</i>	1-13
Figure 1.3-7: <i>Pier E2 Shear Key S1/S2 Fractured Rod</i>	1-13
Figure 1.3-8: <i>Conditions for Hydrogen Embrittlement Cracking</i>	1-14
Figure 1.5-1: <i>Test I — Field Hardness Test</i>	1-19
Figure 1.5-2: <i>Test II — Laboratory Tests</i>	1-21
Figure 1.5-3: <i>Test III — Full Diameter Tension Test</i>	1-23
Figure 1.5-4: <i>Test IV — Stress Corrosion (Townsend) Test</i>	1-25
Figure 1.5-5: <i>Test V — Raymond Test</i>	1-27
Figure 2.1-1: <i>Location of Shear Keys S1 (Left) and S2 (Right) on Pier E2</i>	2-1
Figure 2.1-2: <i>Cross-Sectional View of Shear Key and Shear Key Anchor Rods Setup</i>	2-2

Figure 2.1-3: *Anchor Rod Setup*..... 2-2

Figure 2.1-4: *Top Hat Detail* 2-2

Figure 2.1-5: *Borescope* 2-3

Figure 2.1-6: *Exposed Rod at Pier E2* 2-3

Figure 2.1-7: *Standing Water in the Rod Hole* 2-4

Figure 2.1-8: *Debris on the Bearing Plate* 2-4

Figure 2.1-9: *Various Debris on the Bearing Plate (1)* 2-4

Figure 2.1-10: *Various Debris on the Bearing Plate (2)* 2-4

Figure 2.1-11: *Location of Fractured Rods on Shear Keys S1 (Left) and S2 (Right), including the Five Extracted Rods at the Time of the Borescope Inspection — Four More Rods Were Extracted Later*..... 2-5

Figure 2.1-12: *S2-H6 Borescope Snapshot* 2-6

Figure 2.1-13: *S2-A6 Borescope Snapshot*..... 2-6

Figure 2.1-14: *S2-H6 Borescope Snapshot* 2-6

Figure 2.1-15: *S2-H6 Borescope Snapshot* 2-6

Figure 2.1-16: *S2-A8 Borescope Snapshot*..... 2-6

Figure 2.1-17: *S2-A8 Borescope Snapshot*..... 2-6

Figure 2.2-1: *In-Situ Hardness Testing*..... 2-9

Figure 2.2-2: *Hardness Reading Layout on Various Diameters of Rods* 2-9

Figure 2.2-3: *Average Hardness for 2" Rods (Left) and 3" Rods (Right)* 2-10

Figure 2.2-4: *Average Hardness for 3.5" Rods (Left) and 4" Rods (Right)* 2-10

Figure 2.2-5: *HRC Tester*..... 2-11

Figure 2.2-6: *Hardness, Chemistry and CVN Coupon Extraction Layout* 2-12

Figure 2.2-7: *Hardness Test Measurement Layout* 2-12

Figure 2.2-8: *Chemical Testing Analysis Layout*..... 2-13

Figure 2.2-9: *Chemical Testing Analysis Layout*..... 2-13

Figure 2.2-10: *Charpy Testing Machine*..... 2-14

Figure 2.2-11: *Test I and II Average Hardness Values for Group 3 (Left) and Group 4 (Right)*..... 2-15

Figure 2.2-12: *Test I and II Average Hardness Values for Group 7 (Left) and Group 8 (Right)*..... 2-15

Figure 2.2-13: *Test I and II Average Hardness Values for Group 9 (Left) and Group 12 (Right)*..... 2-16

Figure 2.2-14: *Test I and II Average Hardness Values for Group 13 (Left) and Group 14 (Right)*..... 2-16

Figure 2.2-15: *Test I and II Average Hardness Values for Group 15* 2-16

Figure 2.2-16: *Average CVN Values, Test II and Circumferential Values of 2008 Rods from Test II-M*..... 2-17

Figure 2.2-17: *Test Coupon Locations on Rod Pieces* 2-19

Figure 2.2-18: *Hardness Measurements*..... 2-19

Figure 2.2-19: *Chemistry Sample*..... 2-20

Figure 2.2-20: *Tensile Coupon and CVN Sets*..... 2-20

Figure 2.2-21: *Test II-M Traverse Readings (1)*..... 2-21

Figure 2.2-22: *Test II-M Traverse Readings (2)*..... 2-21

Figure 2.2-23: *Test II-M Traverse Readings (3)*..... 2-21

Figure 2.2-24: *HRC Readings at 90° Angle (1)*..... 2-22

Figure 2.2-25: *HRC Readings at 90° Angle (2)*..... 2-22

Figure 2.2-26: *HRC Readings at 90° Angle (3)*..... 2-22

Figure 2.2-27: *Circumference CVN*..... 2-23

Figure 2.2-28: *Centerline CVN* 2-24

Figure 2.2-29: *Specimens Layout, per Test Procedures*..... 2-25

Figure 2.2-30: *Sample Coupon* 2-25

Figure 2.2-31: *Group 7 Sample with Cut Samples*..... 2-26

Figure 2.2-32: *Group 7 Coupon* 2-26

Figure 2.2-33: *Group 7 HRC Readings on Surfaces A and B*..... 2-26

Figure 2.2-34: *Layout of Samples Extracted for Test III*..... 2-27

Figure 2.2-35: *Full-Size Tensile Testing at Laboratory* 2-28

Figure 2.2-36: *Schematic of Coupon (Left), and Actual Test III Coupon (Right)*..... 2-28

Figure 2.2-37: *Tensile and Charpy Sample Layout*..... 2-29

Figure 2.2-38: *Rockwell C hardness Testing Layout*..... 2-29

Figure 2.2-39: *Knoop Hardness Coupon* 2-30

Figure 2.2-40: *Knoop Hardness Testing* 2-30

Figure 2.2-41: *Scanning Electron Microscope*..... 2-31

Figure 2.2-42: *Average CVN Values, Test III and Circumferential Values of 2008 Rods from Test II-M*..... 2-33

Figure 2.2-43: <i>HRC Readings, Test III</i>	2-34
Figure 2.2-44: <i>Fracture Surface Zones</i>	2-34
Figure 2.2-45: <i>Fracture Initiation Zone (30 μm)</i>	2-35
Figure 2.2-46: <i>Fracture Propagation Zone (30 μm)</i>	2-35
Figure 2.2-47: <i>Final Fracture Zone (30 μm)</i>	2-35
Figure 2.2-48: <i>Banded Features (50,000 μm)</i>	2-36
Figure 2.2-49: <i>Thread Root Examination (500,000 μm)</i>	2-36
Figure 2.2-50: <i>Test Coupon Locations on Rods</i>	2-37
Figure 2.2-51: <i>Hardness Measurements</i>	2-37
Figure 2.2-52: <i>Chemistry Sample</i>	2-38
Figure 2.2-53: <i>Tensile Coupon and CVN Sets</i>	2-38
Figure 2.2-54: <i>Full-Diameter Tensile Test</i>	2-39
Figure 2.2-55: <i>Test III-M Traverse HRC Measurements</i>	2-39
Figure 2.2-56: <i>Circumference CVN</i>	2-40
Figure 2.2-57: <i>Centerline CVN</i>	2-40
Figure 3.1-1: <i>Test Rig for Full-Length Rods</i>	3-3
Figure 3.1-2: <i>Test Rig for Full-Length Rods during Setup</i>	3-3
Figure 3.1-3: <i>Test IV in Progress under Protective Tent</i>	3-4
Figure 3.1-4: <i>Test Rig after Rod Failure Showing the Effects of the Energy Released when Fracture Occurs</i>	3-4
Figure 3.1-5: <i>Venting of Test Solution</i>	3-6
Figure 3.1-6: <i>Fracture Preservation Operation</i>	3-7
Figure 3.1-7: <i>Typical Plot of Load vs. Test Time, Showing Step Increases in Load Until Failure at 0.85 Fu (Rod 1)</i>	3-8
Figure 3.1-8: <i>Plot of Electrode Potential and pH vs. Test Time (Rod 11)</i>	3-9
Figure 3.1-9: <i>Test IV — Townsend Test Results Comparison</i>	3-12
Figure 3.1-10: <i>Test IV Failure Loads for A354BD Rods</i>	3-13
Figure 3.1-11: <i>Load Displacement Graphs for Rods 14–17</i>	3-14
Figure 3.2-1: <i>Bend Test Machine for Incremental Step Loading, Manufactured by FDI</i>	3-16
Figure 3.2-2: <i>A Charpy-sized, Single Edge Notched Bend, ASTM E1290 SEN(B), Specimen</i>	3-17

Figure 3.2-3: A Charpy-sized, Threaded Specimen for Determining $K_{I\phi}$ 3-17

Figure 3.2-4: Machining Plan for a 3-inch Diameter Rod..... 3-18

Figure 3.2-5: Rod Sample with Specimens Removed..... 3-18

Figure 3.2-6: Schematic of a (10/5/2,4) Step Loading Profile to Determine Threshold for the Hardness of Steel ≥ 33 HRC to 45 HRC 3-20

Figure 3.2-7: Definition of Crack Initiation Load, P_i Load and Threshold Load, P_{th} 3-20

Figure 3.2-8: Test IV Model Mesh 3-22

Figure 3.2-9: Test V Model Mesh 3-22

Figure 3.2-10: Estimated Rod F_u vs. Specimen Threshold Load..... 3-23

Figure 3.2-11: EHE Threshold Force Ultimate and Stress Intensity..... 3-24

Figure 3.2-12: Effect of Applied Polarization Potential on the Measured K_{Isc} and $K_{I\phi}$ -EHE 3-26

Figure 3.2-13: Test V 2008 SCC Specimen Fracture Load in Salt Water Adjusted to Test IV Hardness of 37 HRC and Rod Potential (F_u -SCC) 3-27

Figure 3.2-14: Test V 2010 and 2006 EHE Specimen Fracture Load in 3.5% Salt Water Adjusted to Test IV Rod Potential (F_u EHE) and Hardness (HRC)..... 3-28

Figure 3.3-1: Test V, 4-hr and Test VI, 8-hr, 16-hr Threaded EHE-RSL for Shear Key (Top)..... 3-30

Figure 3.3-2: Threaded Test V and VI: F_u -EHE vs Loading Rate at $-1.06V_{sce}$ 3-31

Figure 3.3-3: Components of the Sustained Load Test Rigs 3-32

Figure 3.3-4: Three Sustained Load Test Rigs Undergoing Final Check-out Prior to Calibration 3-32

Figure 4.3-1: Test IV Failure Loads for A354BD Rods 4-4

Figure 4.3-2: Test IV EHE Threshold and Applied Load Summary..... 4-4

Figure 4.3-3: Load Displacement Graphs for Rods 14 -17 (2013 Galvanized and Ungalvanized) 4-5

Figure 4.4-1: Test V Specimen SCC Failure Load in Salt Water at Rods Potential (F_u)..... 4-6

Figure 4.5-1: Test V and Test VI Load Rating 4-7

LIST OF TABLES

Table 1.2-1: <i>List of A354BD Components on the SAS</i>	1-7
Table 1.2-2: <i>Supplemental Protection Barrier</i>	1-9
Table 1.4-1: <i>Pier E2 2008 vs. 2010 Rod Comparison Summary</i>	1-15
Table 1.5-1: <i>List of Tests</i>	1-16
Table 1.5-2: <i>SAS A354BD Rod and Bolt Data and Testing Program Summary</i>	1-17
Table 2.1-1: <i>Summary of Borescope Investigations</i>	2-5
Table 2.1-2: <i>Summary of Water Sample Testing at WJE</i>	2-7
Table 2.2-1: <i>A354BD Hardness Requirements</i>	2-8
Table 2.2-2: <i>ASTM A354 Chemical Requirements</i>	2-14
Table 2.2-3: <i>Chemical Analysis Results, Test II</i>	2-17
Table 2.2-4: <i>Chemical Analysis Results, Test II-M</i>	2-23
Table 2.2-5: <i>Coupon Tensile Testing Results, Test II-M</i>	2-24
Table 2.2-6: <i>ASTM A354 Mechanical Requirements</i>	2-29
Table 2.2-7: <i>Full-Diameter Tensile Strength Results, Test III</i>	2-32
Table 2.2-8: <i>Coupon Tensile Strength Results, Test III</i>	2-32
Table 2.2-9: <i>Test III-M Chemical Analysis</i>	2-40
Table 2.2-10: <i>Coupon Tensile Testing Results, Test III-M</i>	2-41
Table 2.2-11: <i>Full Size Tensile Testing Results, Test III-M</i>	2-41
Table 2.2-12: <i>Test I, II, III, and III-M Results Summary</i>	2-41
Table 3.1-1: <i>Test IV Rods</i>	3-5

Table 3.1-2: *Test IV Loading Schedule for Under and Over 2 ½" Diameter*..... 3-6

Table 3.1-3: *Test IV Results* 3-10

Table 4.1-1: *Comparison of 2006, 2008, 2010, and 2013 Rods*..... 4-2

Table 4.2-1: *Test I, II, III, and III-M Results Summary* 4-3

EXECUTIVE SUMMARY

Shear Key S1 and Shear Key S2 of the Self-Anchored Suspension (SAS) Bridge superstructure of the east span of the San Francisco-Oakland Bay Bridge (SFOBB) were connected to Pier E2 at the east side by means of 96, 3-inch diameter, galvanized ASTM A354 Grade BD (A354BD) anchor rods fabricated and installed inside the Pier E2 concrete bent cap in 2008 (2008 Rods). In early March 2013, after erection of the superstructure and load transfer was completed, the rods were pre-tensioned to 70% of their minimum specified ultimate tensile strength (F_u). A few days after tensioning was completed, during the first two weeks of March 2013, 32 of the 96 anchor rods fractured. All 32 fractures occurred at or near the threaded engagements at the bottom ends of the rods. Failure of the rods ceased after the pre-tension level in the remaining rods was reduced to 0.40 F_u in mid-March. All of these 96 rods at Shear Key S1 and Shear Key S2 were abandoned and an alternative anchoring system was successfully designed and installed.

Although the 2008 rods are no longer in service, their failure raised concerns about the long-term performance of the remaining A354BD rods on the SAS. An initial metallurgical investigation concluded that the 2008 rods failed as a result of hydrogen embrittlement. The California Department of Transportation undertook a testing program of unprecedented scale to further examine the cause of failure, and to evaluate the suitability of all other A354BD rods on the SAS Bridge¹. This testing program was designed with the guidance of a team of preeminent experts in the fields of fasteners, metallurgy and materials science, chemical engineering, fracture mechanics, and hydrogen embrittlement. This team is principally responsible for the contents of this Executive Summary. As summarized below, this program encompassed the following main components.

1 — REVIEW OF EVENTS LEADING TO BREAKAGE OF RODS AND REVIEW OF CONSTRUCTION AND FABRICATION DOCUMENTS

The 3-inch diameter 2008 rods were installed into 7-inch diameter pipe sleeve assemblies that include an 8-inch diameter chamber at the bottom (top-hat), to allow for tensioning and grouting. These assemblies were installed inside the Pier E2 concrete cap beam prior to placement of concrete. A review of construction documents revealed that rods were exposed to water that had entered the pipe sleeve assemblies enclosing the rods prior to grouting and tensioning. Also, water was found in the rod cavities during the in-situ boroscope examinations that followed the removal of a few fractured rods. Accordingly, there is no doubt that the rods were exposed to water at the time of tensioning. This is significant because water is a source of hydrogen that could cause embrittlement when a rod is tensioned above its critical threshold load.

¹The A354BD rods have been discussed in several meetings with the Toll Bridge Program Oversight Committee. Appendix A provides material presented on 7/24/2014 and 8/28/2014.

2 — FIELD HARDNESS MEASUREMENTS

Because previous studies have shown that susceptibility to hydrogen embrittlement increases with increasing hardness, in-situ measurements were made on virtually all accessible rods (1210 of 2306) on the SAS. The results showed that rod hardness was generally uniform and within the ASTM A354 specification. This finding is significant because it makes it unlikely that there are rods with hardness higher than allowed in the ASTM specifications, and as such, with unusually high susceptibility to hydrogen embrittlement.

3 — LABORATORY DETERMINATION OF CHEMICAL COMPOSITION AND MECHANICAL PROPERTIES

Groups of rods representing the various sizes, tension levels, and locations on the SAS were selected for detailed laboratory testing to determine chemical composition and hardness. These results showed that the material properties were generally uniform and within specifications. Although not required by specification, Charpy impact toughness tests were also conducted. These tests showed that the toughness of the majority of the remaining rods is within normal ranges for this material. Charpy tests performed on samples of the 2008 rods, however, showed significantly lower toughness values.

4 — TENSION TESTS OF FULL-DIAMETER RODS

As a further step in investigating the properties of the remaining rods, tensile tests were conducted to measure actual breaking strengths of full-diameter rods from the selected groups. Along with the full-diameter tensile tests, hardness profiles, chemical composition, Charpy impact tests, and reduced-section tensile specimens were tested. Again, these tests generally indicated that the properties of the remaining rods are within specified ranges.

5 — TOWNSEND TEST FOR SUSCEPTIBILITY TO HYDROGEN EMBRITTLEMENT OF FULL-DIAMETER RODS

The Townsend Test for Stress Corrosion Cracking (SCC) or hydrogen embrittlement susceptibility was performed on full-diameter rods selected from the various groups of SAS rods. This test is named after and was designed, together with the assistance of other team members, by Dr. Herbert Townsend, who conducted a small scale version of this test in 1972. The 1975 paper by Dr. Townsend summarizing his work of 1972 is fundamental to the field of hydrogen embrittlement. The selected rods were representative of the population of rods on the SAS in terms of hardness range, diameter, and thread forming. In this test, the tensile load is increased very slowly (in steps) until a threshold load level is established for the onset of cracking due to hydrogen embrittlement. The slow rate of loading is essential to detect the effects of hydrogen that requires time for diffusion. With applied loads up to 1.86 million pounds, the scale of this test is unprecedented for hydrogen embrittlement testing.

To determine the threshold load for hydrogen entering the steel from the environment due to corrosion (environmental hydrogen), the rods were loaded while immersed in salt water containing 3.5% sodium chloride. The main results of these tests are:

- The 2008 rods failed by hydrogen embrittlement at the same load (0.70 F_u) that resulted in failure on the SAS, and with similar fracture characteristics. This result provides confirmation that the Townsend Test duplicates the actual performance of these rods.
- All other groups of rods exhibited threshold loads greater than their design loads, indicating that the remaining rods are not susceptible to failure by hydrogen embrittlement at the design loads, even under the worst-case scenario of exposure to salt water as long as the galvanized coating remains intact.

- A comprehensive study of the mechanical and chemical properties of the rods conducted after the Townsend Test indicates that the greater susceptibility to hydrogen embrittlement of the 2008 rods is correlated with lower toughness.

To explore the possibility that hydrogen already present in the steel (internal hydrogen) could have contributed to the low threshold of the 2008 rods, the Townsend Test was repeated in air, without exposure to salt water. These tests showed a complete absence of hydrogen embrittlement. This result clearly demonstrates the following:

- Failures of the 2008 rods in the wet Townsend Tests occurred as a result of environmentally induced hydrogen embrittlement.
- The 2008 rods would not have failed if they were protected from water.

6 — RAYMOND TEST FOR SUSCEPTIBILITY TO HYDROGEN EMBRITTLEMENT WITH SMALL SAMPLES CUT FROM FULL-DIAMETER RODS

The Raymond Test is a slow, rising step-load laboratory bend test for susceptibility to hydrogen embrittlement. This test is named after and was conducted, with input from other team members, by Dr. Louis Raymond, who developed a national standard test for establishing hydrogen embrittlement thresholds (ASTM F1624). It was conducted with two types of small specimens cut from full-size rods. In one type, a pre-crack was introduced into rectangular bars to establish material susceptibility according to fracture mechanics procedures. These results were consistent with previously published tests of pre-cracked specimens of this material. A second type of specimen included the threaded portion of the as-built rod without a pre-crack. Testing these specimens gave results that were consistent with the results of the Townsend Test, thus providing independent confirmation of the results obtained with full-diameter rods.

7 — GORMAN TEST TO VALIDATE THE RESULTS OF THE RAYMOND TEST AT LONGER TIMES

The Gorman Test was intended to further verify that the hydrogen embrittlement thresholds determined in the accelerated 80-hour Raymond Test are valid at longer test times. The concept for this test was developed by Dr. Jeffrey Gorman, who specializes in materials. This was approached in two phases. In phase one, hold times for the rising step-load tests of pre-cracked specimens were increased by up to four times without any change in results, thus validating the thresholds obtained in the initial Raymond Test. In phase two, threaded specimens are being subjected to static loads for up to 5000 hours to further validate the Raymond thresholds. Phase one is complete and phase two is still in progress and is scheduled to be completed in March 2015.

CONCLUSIONS

All results of this study indicate that the 2008 rods on E2 failed by environmentally induced hydrogen embrittlement because they were tensioned above their hydrogen embrittlement threshold while simultaneously immersed in water, which served as the source of hydrogen. The low hydrogen embrittlement threshold of the 2008 rods is likely due to rod fabrication methods.

There is no evidence that hydrogen present in the steel prior to installation or tensioning contributed to the 2008 rod failures. On the contrary, the Townsend Test performed on the 2008 rods in salt solution and in the dry confirmed that without the presence of water, these rods would not have failed.

All remaining A354BD rods on the SAS exhibit hydrogen embrittlement thresholds that are higher than their pre-tension stress levels and are safe. All A354BD rods on the SAS were designed to have both primary corrosion protection (galvanization) and supplemental corrosion-protection measures, such as dehumidification, paint sys-

tem, or grout, which would prevent corrosion and further rule out any future possibility of hydrogen embrittlement. Such measures already have been implemented except for painting the Pier E2 top housing shear key and bearing rods.

RECOMMENDATIONS

The testing program results show that the A354BD rods on the SAS exhibit hydrogen embrittlement thresholds that are higher than their pre-tension stress levels and therefore are safe against environmentally induced hydrogen embrittlement as long as the galvanized coating remains intact.

Based on the findings of this investigation, nothing further is needed to ensure the integrity of the SAS A354BD rods, other than providing a supplementary barrier to the Pier E2 top housing shear key and bearing rods, and application of customary maintenance procedures, and shall be specified in the SAS Maintenance Manual.

Caltrans Construction field personnel recently observed the presence of water at the bottom of the tower, near a number of A354BD anchor rods. The source of this water shall be fully investigated and addressed. It is noted that this is not a stress corrosion cracking issue, as the rods are pre-tensioned to levels that are lower than their hydrogen embrittlement threshold. However, this may lead to long-term corrosion and needs to be addressed.

Bolt Consultants

Alan Pense, Ph.D., NAE

Herbert E. Townsend, Ph.D., P.E.

Louis Raymond, Ph.D., P.E.

Douglas E. Williams, P.E.

Karl H. Frank, Ph.D., P.E.

Jeffrey Gorman, Ph.D., P.E.

Sheldon W. Dean Jr., Sc.D., P.E.

Robert Heidersbach, Ph.D., P.E.

Thomas Langill, Ph.D.

1. INTRODUCTION AND BACKGROUND

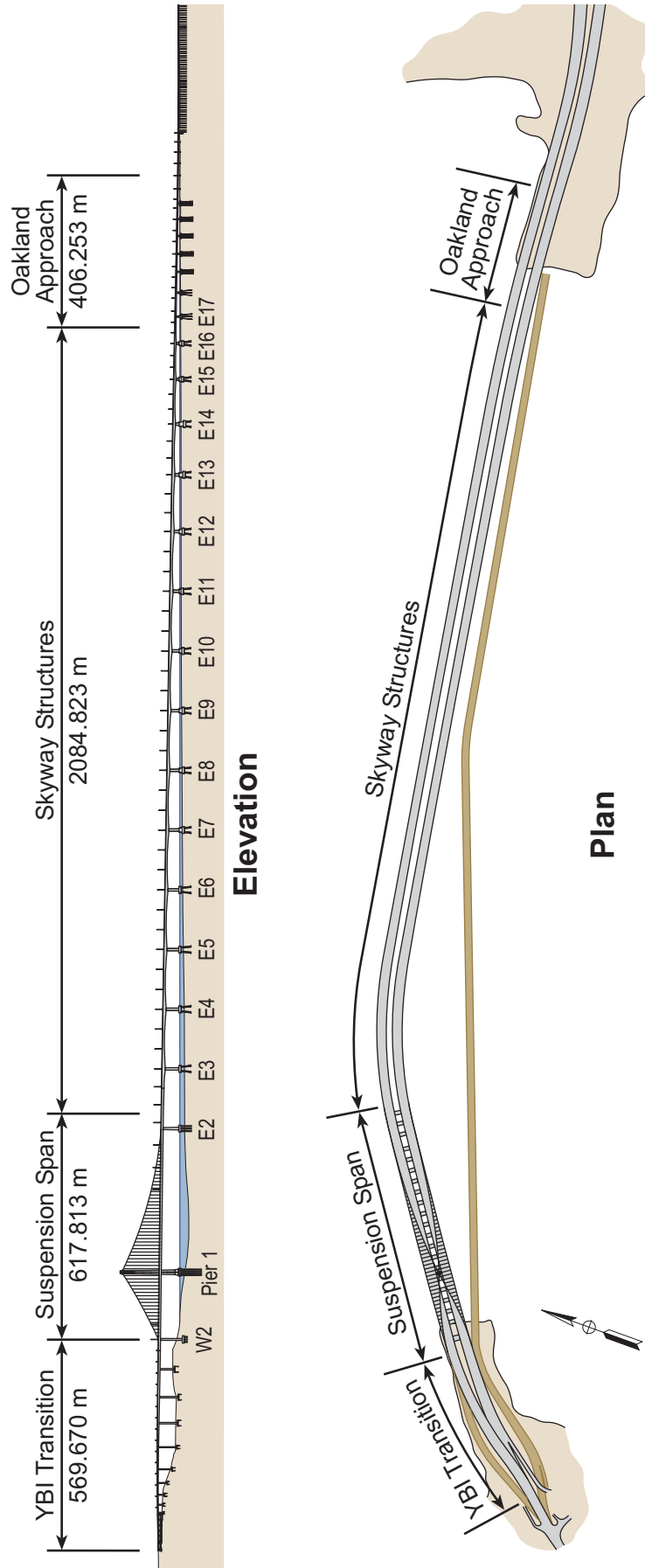
During the first two weeks of March 2013, 32 of the 96 three-inch-diameter, ASTM A354 Grade BD (A354BD) high-strength rods at Pier E2 fractured at their lower ends. These rods were used to tie-down the S1 and S2 shear keys of the Self-Anchored Suspension (SAS) bridge superstructure to the east pier. The fractures occurred a few days after the rod tensioning, and a few months before the scheduled opening of the New East Span of the San Francisco–Oakland Bay Bridge (SFOBB). With a 30% failure rate, it was decided that all of these 96 rods at Shear Keys S1 and S2 would be abandoned and an alternative anchoring system would be designed and constructed. In addition, the California Department of Transportation undertook a testing program of unprecedented breadth and depth to ascertain the cause of the rod failures and to evaluate the suitability of all other A354BD rods on the bridge. The remainder of this chapter provides general background on the bridge, details on the rod failures, and an introduction to the testing program. Details on the steps that were taken to ensure the safety of the bridge and achieve the seismic safety opening of the eastern spans on schedule are provided in Appendices B and C.

1.1 SAN FRANCISCO–OAKLAND BAY BRIDGE

The new East Span of the San Francisco–Oakland Bay Bridge (SFOBB) consists of four (4) main components (see Figure 1.1-1):

- The Oakland Touchdown structure (OTD), a low-rise, post-tensioned concrete box girder reaching the Oakland shore
- The Skyway, a segmental concrete box girder
- The Self-Anchored Suspension Span (SAS), an asymmetric, single tower, single cable, dual orthotropic box girders, self-anchored suspension bridge (see Figure 1.1-2).
- The Yerba Buena Island Transition Structures (YBITS), a post-tensioned concrete box girder that connects the SAS to the east portal of the Yerba Buena Island Tunnel

Figure 1.1-1: Plan and Elevation of San Francisco–Oakland Bay Bridge New East Span



The Self-Anchored Suspension (SAS) Bridge consists of dual orthotropic box girders suspended from a cable that is supported on the 160 m tower located off of the eastern shore of the Yerba Buena Island. The SAS spans 565 m between the east pier (E2) and the west pier (W2). The bridge is asymmetric with a 385 m main span of over the navigational channel, and a 180 m back span to the west of the tower. The main cable is anchored at the east end of the main span and loops around the west bent through deviation saddles. The suspenders are splayed to the exterior sides of the box girders and are spaced at 10 m. The bridge carries a pedestrian path on the south side of the eastbound deck.

The tower is composed of four shafts interconnected with shear links along its height; each shaft is a stiffened pentagonal steel box section that tapers along the height. The tower is fixed to a 6.5 m deep pile cap with anchor rods and dowels. The pile cap consists of a steel moment resisting frame encased with concrete and is supported on 13, 60-m long, 2.5-m diameter cast-in-drilled-hole (CIDH) concrete piles.

While the tower carries most of the bridge dead load, it is not the primary element that carries the bridge seismic loads. Piers E2 and W2 are designed to provide the main lateral seismic support of the bridge. The west piers are reinforced concrete columns that are monolithically connected to the prestressed cap beam forming the west bent. The west bent is supported on gravity footings cast into Yerba Buena Island (YBI) rock.

The east pier (Pier E2) is composed of two reinforced concrete piers and a prestressed concrete cap beam (see Figure 1.1-3). The prestressed cap beam supports the superstructure on four bearings and four shear keys. The bearings are primarily designed to carry the vertical loads (with the capacity to carry the lateral loads) while the shear keys are designed to carry all the lateral loads. The bearings have spherical bushing assemblies capable of large rotations about the transverse axis of the bridge, thus providing an almost true pin connection. Sixteen 2.5 m diameter cast-in-steel shell (CISS) concrete piles support the east bent. These vertical piles are about 100 m long and are founded on firm soil layer below the Young Bay Mud.

Figure 1.1-2: Self-Anchored Suspension Bridge

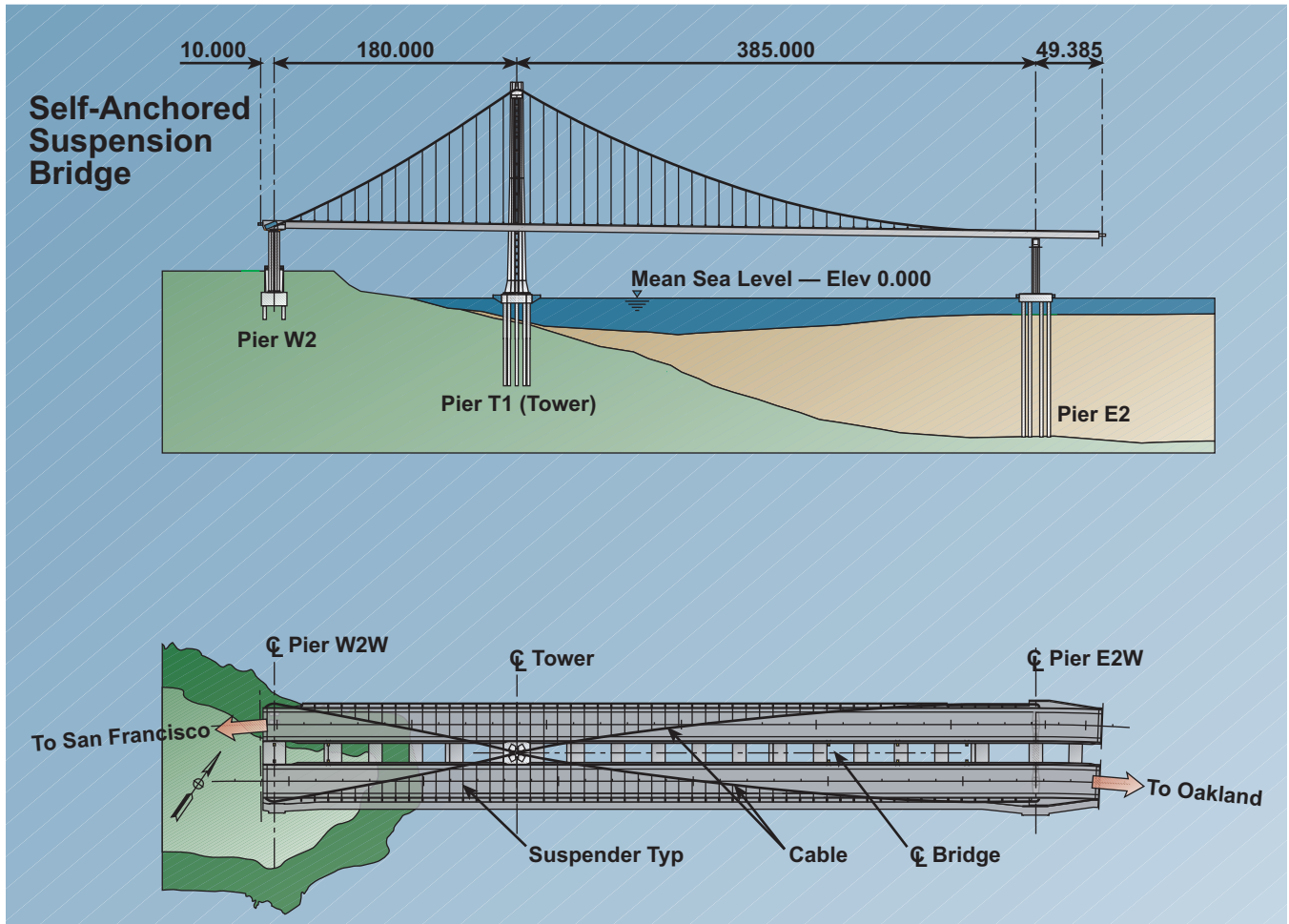
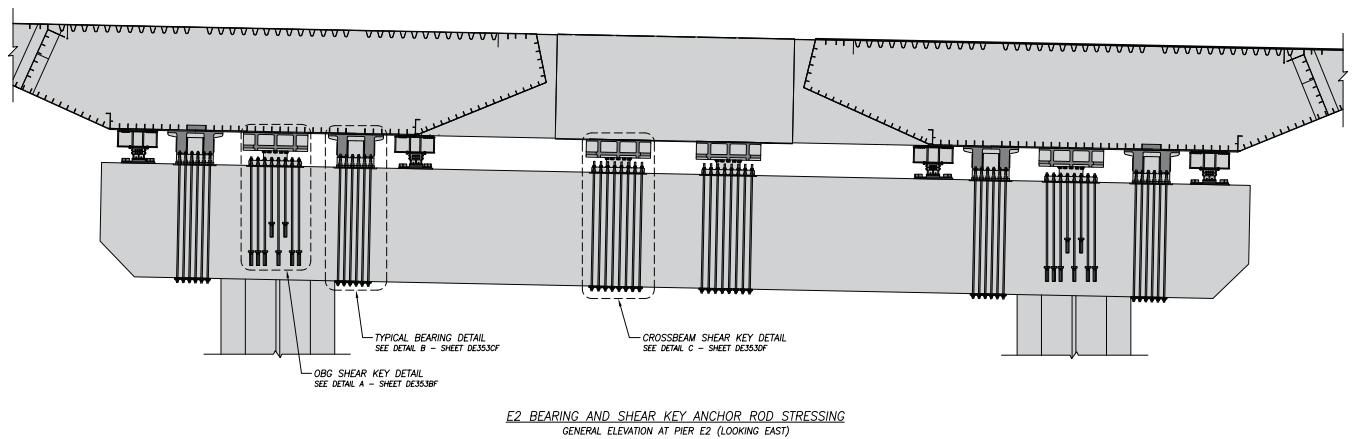


Figure 1.1-3: Pier E2 Details



For the majority of the structural elements and their connections, the demands from the Safety Evaluation Earthquake (SEE) controlled the design. In addition, critical elements are capacity protected. In the case of the shear keys and bearings at Pier E2, a safety load factor of 1.4 was applied to the SEE demands to provide a more robust design based on input from the Seismic Safety Peer Review Panel (SSPRP).

1.2 HIGH-STRENGTH, LARGE-DIAMETER RODS (A354BD) IN THE SAS

The majority of large-diameter high strength rods on the SAS were specified to conform to A354BD. The project Special Provisions included additional requirements for A354BD bolts and rods, such as conformance to the provisions of ASTM A143 and using dry blast cleaning in lieu of acid pickling prior to galvanizing. In addition, Magnetic Particle Testing (MT) was included by change order for A354BD rods and bolts that were to be tensioned in excess of 0.50 Fu. Additionally, some A354BD rods and bolts at lower tension levels also had MT included, such as PWS Anchor Rods (Main Cable). Appendix D includes the above referenced specifications and requirements.

The A354BD rods on the SAS are classified in 17 groups; an additional group is added to represent the 2013 Pier E2 replacement rods. The groups account for the locations of A354BD rods on the SAS, and other characteristics that differentiate the rods. The locations of the various components are identified in plan and elevation views of the SAS on Figure 1.2-1. The list of rod groups including rod diameter and pre-tension levels is presented on Table 1.2-1. Photographs of all the rods as installed in the structural component are shown in Figure 1.2-2.

Figure 1.2-1: A354BD Rods Across SF0BB-SAS

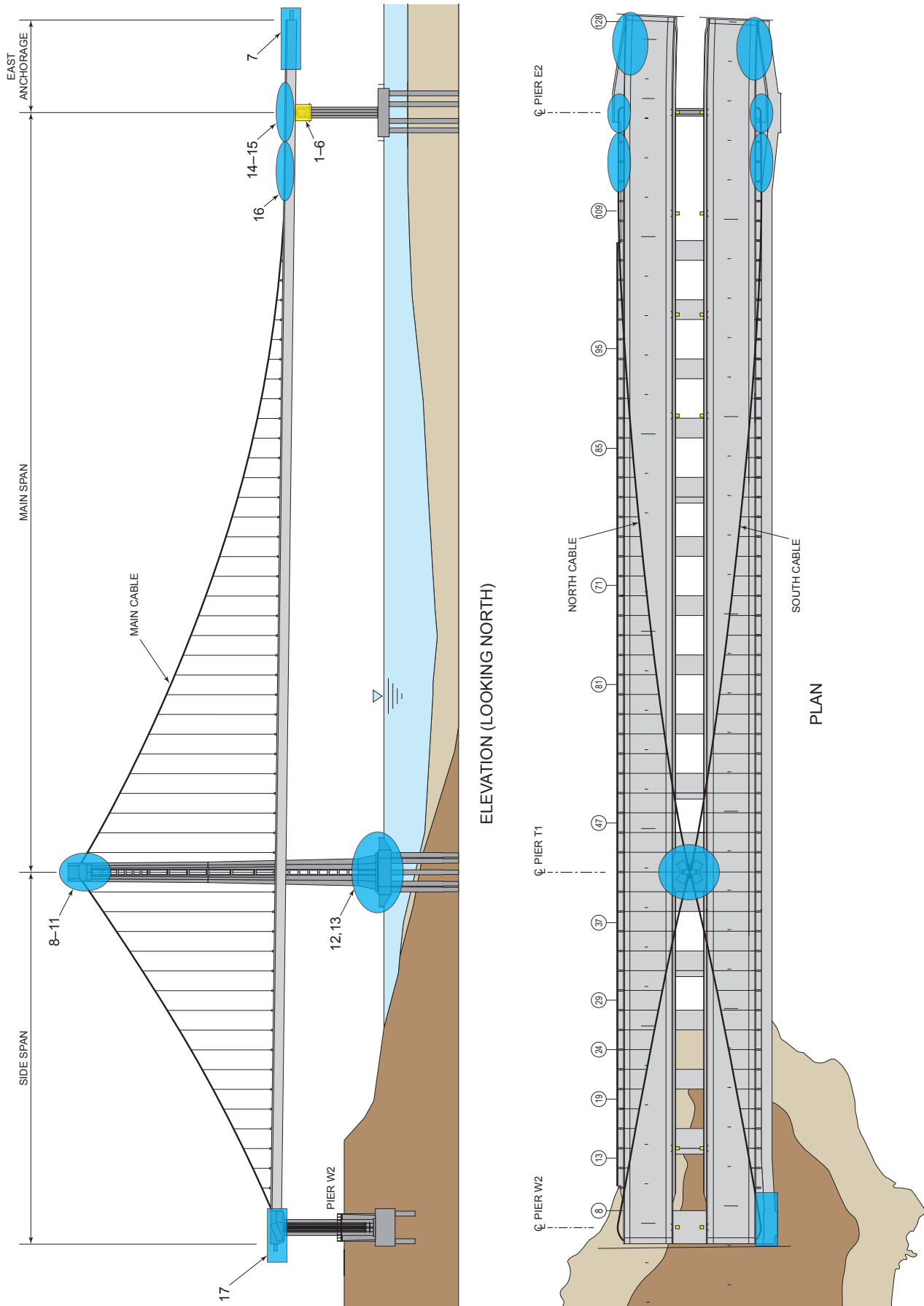


Table 1.2-1: List of A354BD Components on the SAS

Location	Group No.	Description	Quantity Installed	Diameter mm (in)	Sustained Tension (Fraction of Fu)	Average Hardness ⁽¹⁾
Pier E2	1	Shear Key (S1/S2) Anchor Rods (2008) — Bottom	96 ⁽²⁾	76 (3)	0.70	37
	2	Shear Key and Bearing Anchor Rods (2010) — Bottom	192 ⁽³⁾	76 (3)	0.70	34
	3	Shear Key Rods — Top Housing	320	76 (3)	0.70	35
	4	Bearing Rods — Top Housing	224	51 (2)	0.70	35
	5	Spherical Bushing Assembly Rods	96	25 (1)	0.61	36
	6	Bearing Retainer Ring Plate Assembly Bolts	336	25 (1)	0.40	35
Cable Anchorage	7	PWS Anchor Rods (Main Cable)	274	89 (3 1/2)	0.32	35
Top of Tower	8	Tower Saddle Tie Rods	25	102 (4)	0.68	35
	9	Tower Saddle Turned Rods (@ Splices)	108	76 (3)	0.45	37
	10	Tower Saddle Grillage Anchor Bolts	90	76 (3)	0.10	34
	11	Tower Outrigger Boom Bolts	4	76 (3)	0.10	39
Bottom of Tower	12	Tower Anchorage Anchor Rods (76 mm (3-inch) Dia.)	388	76 (3)	0.48	34
	13	Tower Anchorage Anchor Rods (102 mm (4-inch) Dia.)	36	102 (4)	0.37	33
East Saddles	14	East Saddle Anchor Rods	32	51 (2)	0.10	37
	15	East Saddle Tie Rods	18	76 (3)	0.20	33
East Cable	16	Cable Bracket Anchor Rods	24	76 (3)	0.16	36
Pier W2	17	Bikepath Anchor Bolts	43 ⁽⁴⁾	30 (1 1/4)	N/A	36
Pier E2 (New)	18	2013 Replacement Anchor Rods (CCO 312)	8	76 (3)	0.70	35

Notes:

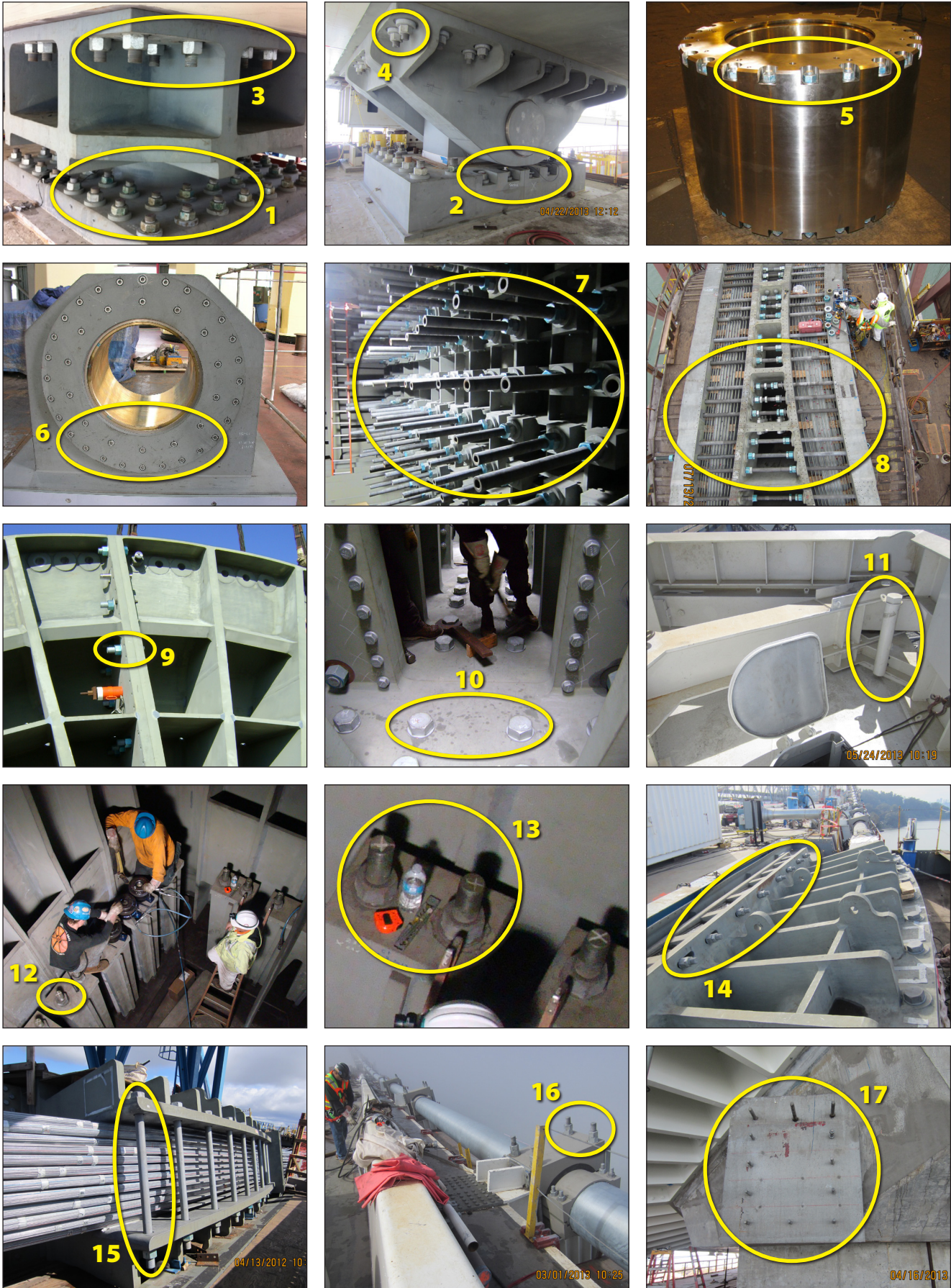
(1) Based on Mill Test Reports

(2) Rods no-longer in use; detensioned and replaced with Saddle Design Alternative

(3) Eight rods in Group 2 were removed for testing and replaced with Group 18 rods.

(4) Rods no longer in use due to alternative architectural design.

Figure 1.2-2: A354BD Rods on the SAS



All the A354BD rods on the SAS were galvanized for corrosion protection. In addition to galvanization, a second corrosion-protection system was specified using at least one of the following: dehumidified environment, grout sleeves or paint system. See Table 1.2 - 2. Supplemental corrosion barriers have been successfully used on other bridges (see Appendix E).

Table 1.2-2: Supplemental Protection Barrier

Rod Data			Supplemental Protection Barrier Per Design*		
Group ID	A354BD Rod Location	Sustained Tension (%Fu)	Dehumidified	Primer	Grout
1	Pier E2 Shear Key (S1/S2) Anchor Rods (2008) — Bottom	70		●	●
2	Pier E2 Shear Key and Bearing Anchor Rods (2010) — Bottom	70		●	●
3	Pier E2 Shear Key Rods — Top Housing	70		●	
4	Pier E2 Bearing Rods — Top Housing	70		●	
5	Pier E2 Spherical Bushing Assembly Rods	61		●	
6	Pier E2 Bearing Retainer Ring Plate Assembly Bolts	40		●	
7	PWS Anchor Rods (Main Cable)	32	●		
8	Tower Saddle Tie Rods	68	●		
9	Tower Saddle Turned Rods (@ Splices)	45	●		
10	Tower Saddle Grillage Anchor Bolts	10	●		
11	Tower Outrigger Boom Bolts	10		●	
12	Tower Anchorage Anchor Rods (76 mm (3-inch) Dia.)	Tower	48	●	
		Pile Cap	48		●
13	Tower Anchorage Anchor Rods (102 mm (4-inch) Dia.)	Tower	37	●	
		Pile Cap	37		●
14	East Saddle Anchor Rods	10	●		
15	East Saddle Tie Rods	20	●		
16	Cable Bracket Anchor Rods	16		●	
17	W2 Bikepath Anchor Bolts	N/A		●	

* Primary protection is provided by galvanization. Supplemental protection is also specified on all rods as noted in this table.

1.3 FAILURE OF PIER E2 EMBEDDED RODS AT SHEAR KEYS S1 AND S2 (2008)

The 3-inch diameter A354BD rods that anchor the bottom parts of shear keys S1 and S2 to the Pier E2 bent cap were fabricated and installed in 2008. These rods were pre-assembled into pipe sleeve assemblies that included a chamber at the bottom (top-hat). The entire system was placed into the capbeam prior to the concrete pour in December 2008. The length of these rods varies between 9-ft and 17-ft long. To allow for the movement of the shear keys during load transfer, the anchor rods were recessed into 8-inch diameter top hat chambers during construction (from 2008 to 2013). Figure 1.3-1 show Pier E2 after the cap beam was completed, and Figure 1.3-2 shows the top of the rod pipe sleeves. It is noted that the rods were exposed to water during construction (refer to Appendices F and G).

Figure 1.3-3 schematically illustrates the rod pipe sleeves, top hat details, and grout tubes. Construction documents indicate that the grout tubes were rerouted upwards into a U-shape, so that the inlet ends of the tubes exit from the top of the E2 concrete cap beam. After load transfer of the SAS was completed and Shear Key S1 and Shear Key

S2 were in their final positions, the anchor rods were lifted to connect to the shear keys. Construction documents indicate that grout was placed between January 22 and January 24, 2013 and was allowed to cure for 28 days before the rods were tensioned. The anchor rods at Shear Key S2 were tensioned first on March 1, 2013; the anchor rods at Shear Key S1 were tensioned on March 2, and March 5, 2013. The rods were tensioned using hydraulic jacks to a pressure equivalent to a maximum of 0.75 of the minimum specified ultimate tensile strength (F_u) in the rods to achieve a final sustained tension of 0.70 F_u ($F_u = 140$ ksi) after seating of the nuts and washers.

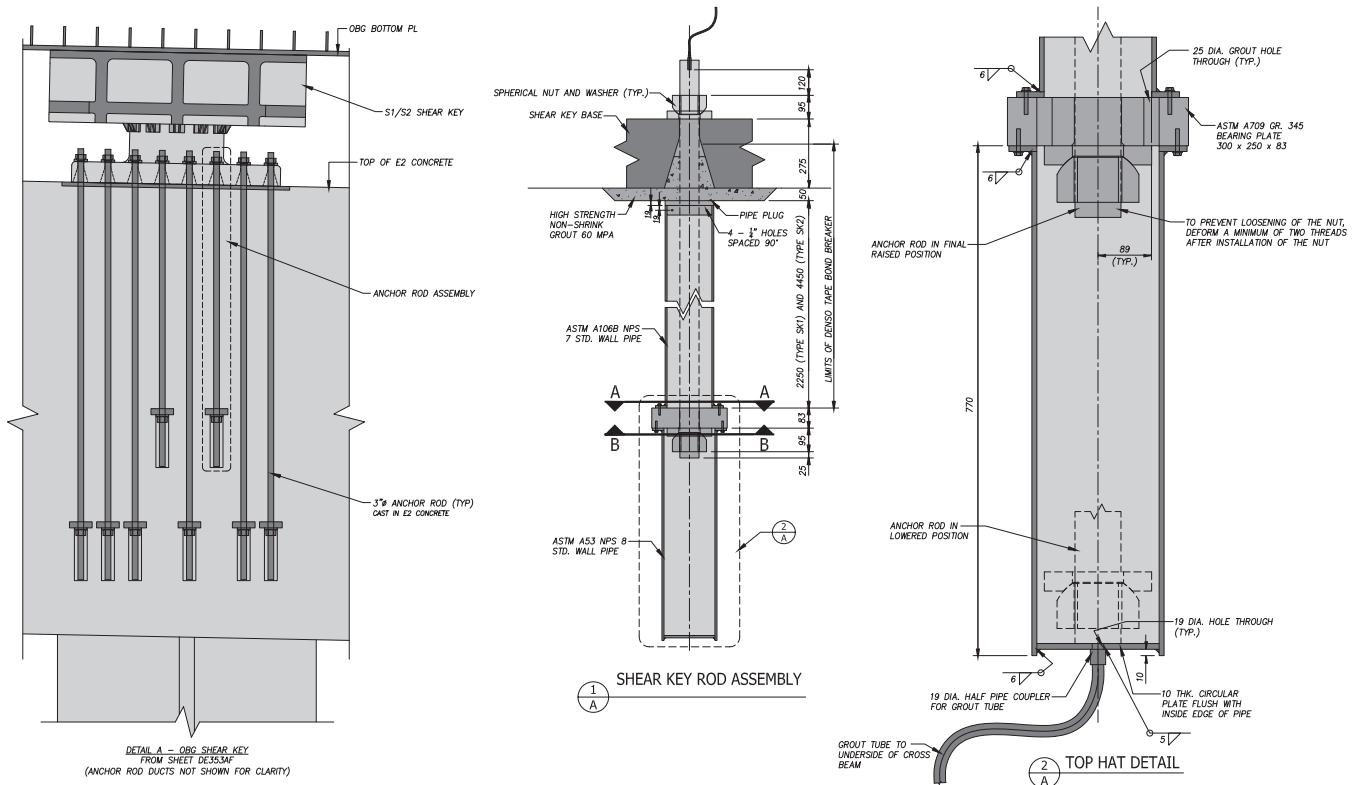
Figure 1.3-1: E2 Cap Beam During Construction (Photo taken 10/19/2009)



Figure 1.3-2: Top of Pier E2 Cap Beam at S1/S2 during Construction (Photo taken 1/12/2011)



Figure 1.3-3: Shear Keys S1/S2, Rods, Pipe Sleeves, and Top Hat Details



On March 8, 2013, a few days after the anchor rods were tensioned, Caltrans Construction personnel observed that the nuts on nine shear key rods had lifted about 2 inches above the washers, indicative of rod failure (see Figure 1.3-4). Within the next four days, another 20 nuts were found to be in a similar condition. It was then decided to reduce the tension on the remaining rods to 0.40 Fu to avoid further failures while the situation was being evaluated. During that process, three more rods failed, bringing the total number of failed rods to 32 in 14 days. Figure 1.3-5 provides a histogram of the rod failure timeline.

Figure 1.3-4: First Indication of Rod Failure



Figure 1.3-5: Rod Failure Timeline

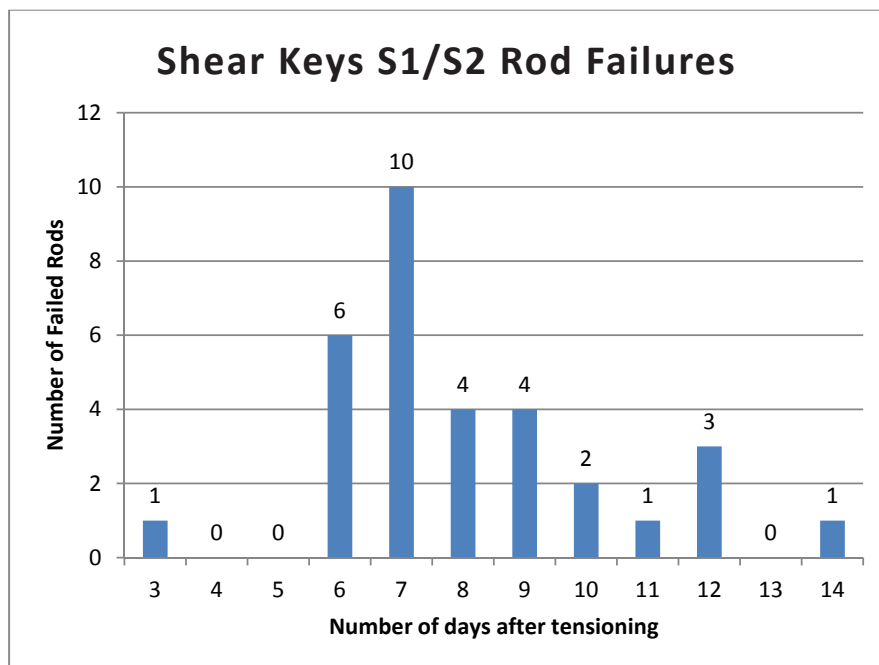


Figure 1.3-6: A354BD Rods at Pier E2 — Break Locations

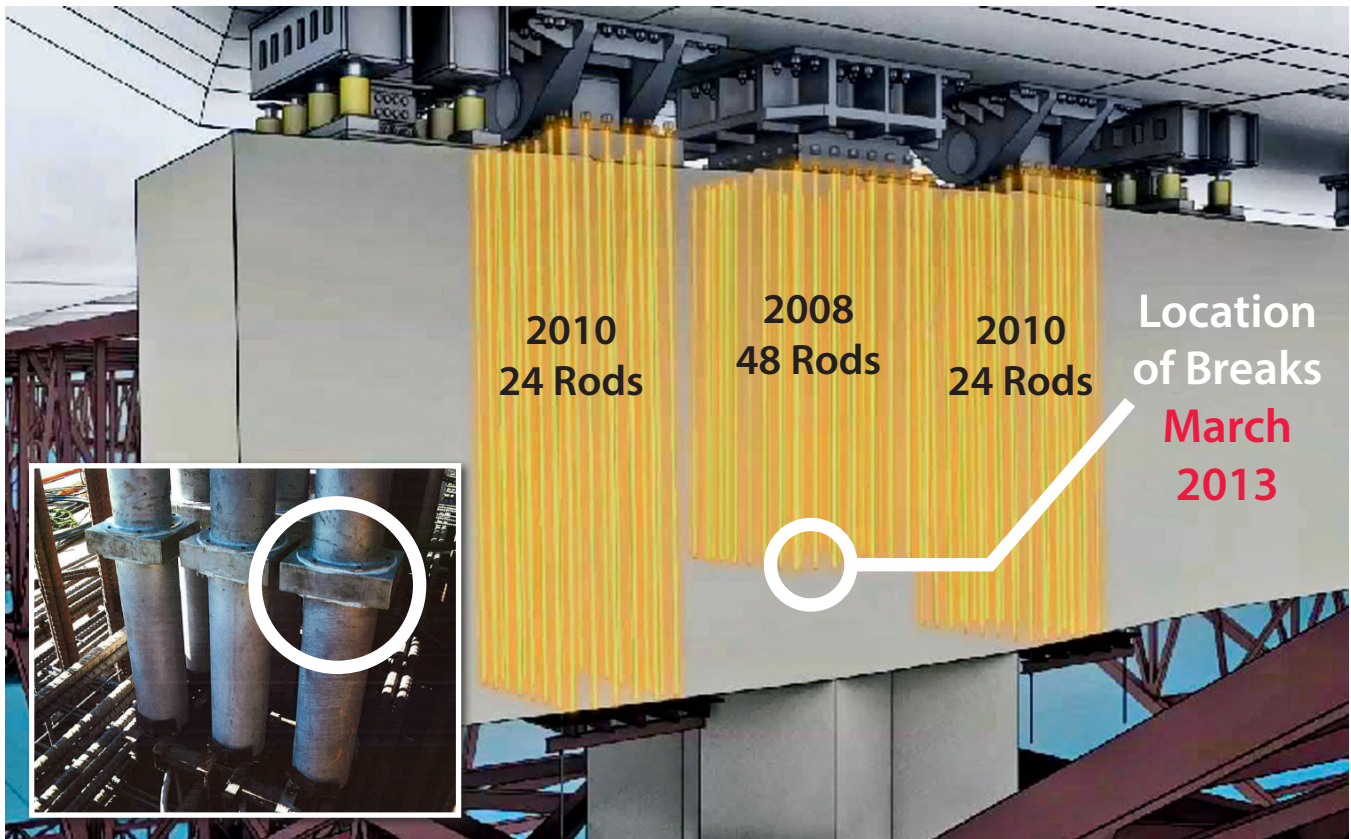
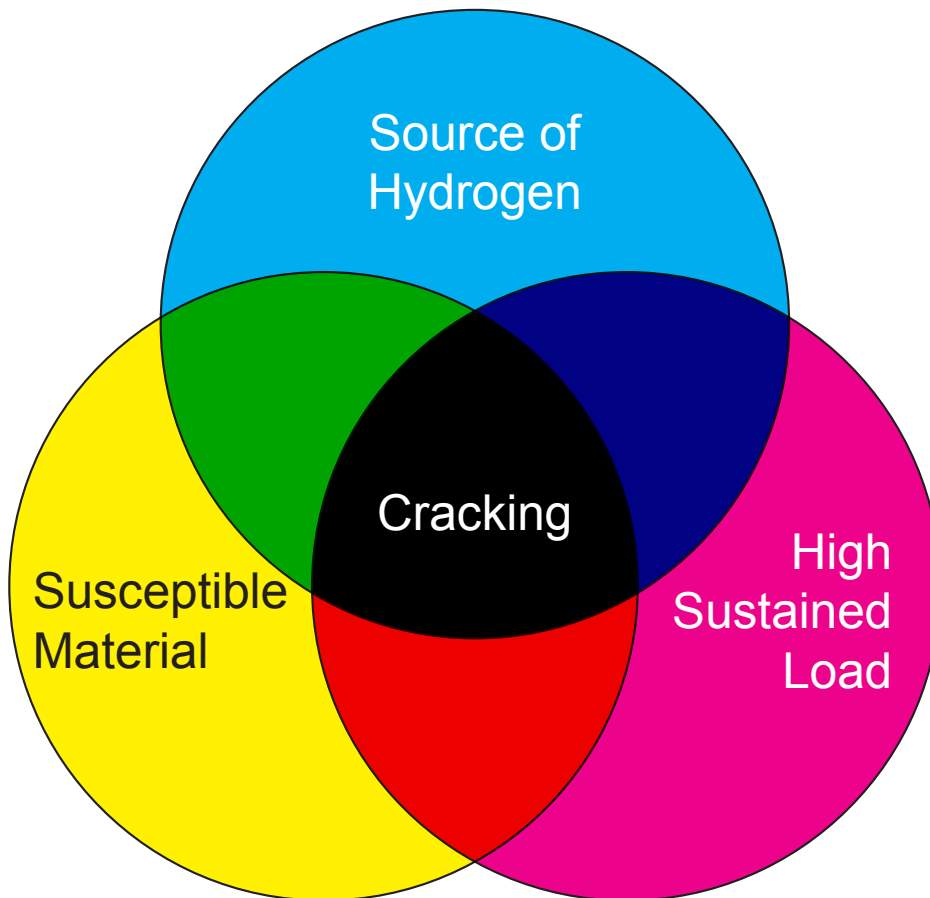


Figure 1.3-7: Pier E2 Shear Key S1/S2 Fractured Rod



All of the failed rods fractured at or near the bottom nut connection (See Figure 1.3-6). To investigate what had happened and determine the cause of the failures, it was decided to extract a sample population of the failed rods for testing and analysis. Due to the limited overhead clearance, removing the rods required raising each rod by increments and cutting it into lengths of one to two feet. Figure 1.3-7 shows two such pieces of rods with the fractured sections. The initial failure analysis report identified hydrogen embrittlement as the failure mechanism of the S1 and S2 shear key anchor rods. The report with the findings is provided in Appendix H.

Appendix I provides a summary on the theory of hydrogen embrittlement (HE), which requires three essential factors to be simultaneously present as shown in Figure 1.3-8.

Figure 1.3-8: Conditions for Hydrogen Embrittlement Cracking

A borescope was used to perform an in-situ examination of the un-retrievable pieces of the broken rods on March 13 and 14, 2013 by METS personnel. This examination successfully photographed the lower fracture surface and unexpectedly revealed the presence of water and evidence of voids in the grout in the top hat in four out of five locations. The results of the borescope examination and chemical analysis of the water extracted from on pipe sleeve are provided in Section 2.1.

Before the preliminary failure analysis was completed, the Design Team decided not to rely on any of the remaining 2008 rods in the S1 and S2 shear keys and proceeded to develop a new design to clamp the shear keys to the substructure. The new design at E2 is provided in Appendix B. When the schedule showed that the construction of the new design would not be completed until December 2013, the Design Team proposed using the lateral load capacity of the bearings (through the installation of shims) to allow for the opening of the new east span of the SFOBB on schedule in September 2013 (refer to Appendix C for details).

1.4 OTHER A354BD RODS ON THE SAS

All other A354BD rods on the SAS were identified, inventoried, and re-inspected (visually). A thorough review of fabrication and construction records was performed to compare fabrication processes, material test results, and construction procedures for the 2008 failed rods. It was noted that except for the tower foundation anchor rod, all A354BD rods were supplied by the same fabricator. Table 1.4-1 provides a comparison between the 2008 rods and 2010 rods at Pier E2 based on the review of the records. Some of the key differences between the failed 2008 rods and the other rods on the bridge are that the MT of the threads was not performed on the 2008 rods, and that the 2008 rods were fabricated using a different process. Another significant difference between the two groups of rods

is exposure to water. As seen in the construction photos and from the borescope investigation, the bottoms of the 2008 anchor rods (where failure occurred) were exposed to standing water.

Table 1.4-1: Pier E2 2008 vs. 2010 Rod Comparison Summary

2008 (32 Failed Rods)	2010 (Rods in Service)
• No Vacuum Degassing	• Vacuum Degassing
• Double Heat Treatment	• Single Heat Treatment
• No Magnetic Particle Testing (MT)	• MT of threads
• Water removed from base of Rod several times during construction	• Through Bolts • No standing water issue
• Fabricated and Installed in 2008 • Tensioned in March 2013	• Installed and Tensioned in April 2013 +/-
• After rod failure, pockets of water/air discovered in grouted Top Hat	• Through Bolts • No indications of grouting issues
• Electrochemical potential ~ -1.01 Vsce	• Electrochemical potential ~ -0.92 Vsce
• Thread deformation to prevent nut loosening	• No thread deformation

1.5 TESTING PROGRAM

A testing program was developed to evaluate the suitability of the various types of A354BD rods used in the SAS to perform their function during their design life of 150 years. The A354BD rods must perform at their permanent tension levels, with essentially no risk of failure, whether due to mechanical overload or time-dependent mechanisms. The testing was designed to:

- Verify that the mechanical properties and chemical composition of all types of A354BD rods used on the bridge were as specified, and to evaluate the uniformity of these properties across the various lots.
- Determine the resistance to Hydrogen Embrittlement (HE) / Stress Corrosion Cracking (SCC) of the rods in use on the bridge.
- Test the failed rods manufactured in 2008 using the same testing protocols that were used for the other rods in use on the bridge to ascertain the similarities and differences between the failed rods and other groups of rods.
- Evaluate the potential for other failures.

To address the above objectives, the testing program is composed of six parts: Test I, Test II, and Test III for the conventional mechanical properties and chemistry testing, and Test IV, Test V, and Test VI for the time-dependent SCC testing. A summary of the Testing Program is provided in Table 1.5-1, Table 1.5-2, and Figure 1.5-1 through Figure 1.5-5. Prior to these tests, in-situ borescope examination was performed, as well as a review of fabrication and construction records. A brief description of Tests I through VI is provided in this section.

Test details and results are provided in Section 2 for the mechanical and chemical testing and in Section 3 for all the time-dependent stress corrosion testing.

Table 1.5-1: List of Tests

Test I	Test II	Test III	Test IV	Test V	Test VI
Field Test (in-situ)	Laboratory Test on Stick-Out or Spares	Full-Diameter Test on Removed Rods or Spares	Stress Corrosion Test (Townsend) on Removed Rods or Spares	Incremental Step Loading Technique (Raymond Test)	Additional Verification (Gorman Test)
<ul style="list-style-type: none"> • Hardness 	<ul style="list-style-type: none"> • Rockwell C Hardness • Chemistry • Charpy V-Notch (when available) 	<ul style="list-style-type: none"> • Full-Diameter Tension Test • Coupon Tension Test • Rockwell C Hardness • Knoop Micro-Hardness • Metallurgical Analysis • Fracture Analysis • Galvanization Chemistry 	<ul style="list-style-type: none"> • Time-Dependent Stress Corrosion Test • Rockwell C Hardness • Knoop Micro-Hardness • Charpy V-Notch • Chemistry • Metallurgical Analysis • Fracture Analysis • Galvanization Chemistry • Electrode Potential 	<ul style="list-style-type: none"> • Reduced Sample Size Test • SCC/HE Threshold 	<ul style="list-style-type: none"> • Reduced Load Rates • Part 1: Extended Step Load Test • Part 2: Sustained Load Test (SLT)

Table 1.5-2: SAS A354BD Rod and Bolt Data and Testing Program Summary

Group #	Location	Rod/Bolt Data					Tests							
		Structural Component	Quantity Installed	Nominal Diameter [in]	Length (ft)	Sustained Tension in Service % Fu (UTS)	I in-situ hardness (# of specimens)	II Laboratory test (# of specimens)	III Full Diameter Tension + Lab (# of specimens)	IV Full Diameter Stress Corrosion test		V Incremental Step Loading (ISL) Technique (# of specimens)	VI (Additional Verification) (# of specimens)	
										Test Rig ID (& Rod #)	Phase No.			
1		Shear Key (S1/S2) Anchor Rods (2008) — Bottom	96 ⁽¹⁾	3	10–17	0.70	87	14	2	12 & 13 18 & 19	3 & 5	4	2	-
2		Shear Key and Bearing Anchor Rods (2010) — Bottom ⁽³⁾	192 ⁽²⁾	3	22–23	0.70	138	-	4	1, 2, 3 & 4	1	4	-	-
3	Pier E2	Shear Key Rods — Top Housing ⁽³⁾	320	3	2–4.5	0.70	287	12 (spares)	4 (spares)	-	-	-	4 (spares)	6 to 15
4		Bearing Rods — Top Housing	224	2	4	0.70	224	7 (spares)	2 (spares)	5	2	1 (spare)	2 (spares)	-
5		Spherical Bushing Assembly Rods	96	1	2.5	0.61	-	-	-	-	-	-	-	-
6		Bearing Retainer Ring Plate Assembly Bolts	336	1	0.2	0.40	-	-	-	-	-	-	-	-
7	Cable Anchorage	PWS Anchor Rods (Main Cable)	274	3 1/2	28–32	0.32	266	43	1 (spare)	8 & 9: Rolled Threads 10 & 11: Cut Threads	2	2 with Rolled Threads 2 with Cut Threads	2 with Rolled Threads 2 with Cut Threads	-
8		Tower Saddle Tie Rods	25	4	6–18	0.68	19	2 (spares)	1 (spare)	7	2	1 (spare)	1 (spare)	-
9	Top of Tower	Tower Saddle Turned Rods (@ Splines)	108	3	2	0.45	20	2	-	-	-	-	-	-
10		Tower Saddle Grillage Anchor Bolts	90	3	1	0.10	-	-	-	-	-	-	-	-
11		Tower Outrigger Boom Bolts	4	3	2	0.10	-	-	1 (spare)	-	-	-	-	-
12	Bottom of Tower	Tower Anchorage Anchor Rods (76 mm (3-inch) Dia.)	388	3	26	0.48	226	6	1	6	2	1	2	-
13		Tower Anchorage Anchor Rods (102 mm (4-inch) Dia.)	36	4	26	0.37	36	3	-	-	-	-	1	-
14	East Saddles	East Saddle Anchor Rods	32	2	3	0.10	16	2	1 (spare)	-	-	-	-	-
15		East Saddle Tie Rods	18	3	5	0.20	8	1	-	-	-	-	-	-
16	East Cable	Cable Bracket Anchor Rods	24	3	10–11	0.16	12	-	-	-	-	-	-	-
17	Pier W2	Bikepath Anchor Bolts	43 ⁽⁴⁾	1 1/4	1.5	NA	-	-	-	-	-	-	-	-
18	Pier E2 (New)	2013 Replacement Anchor Rods (CCO 312)	8	3	22–23	0.70	-	-	-	14 & 15: Galvanized 16 & 17: Ungalvanized	4	2 Galvanized 2 Ungalvanized	2	-

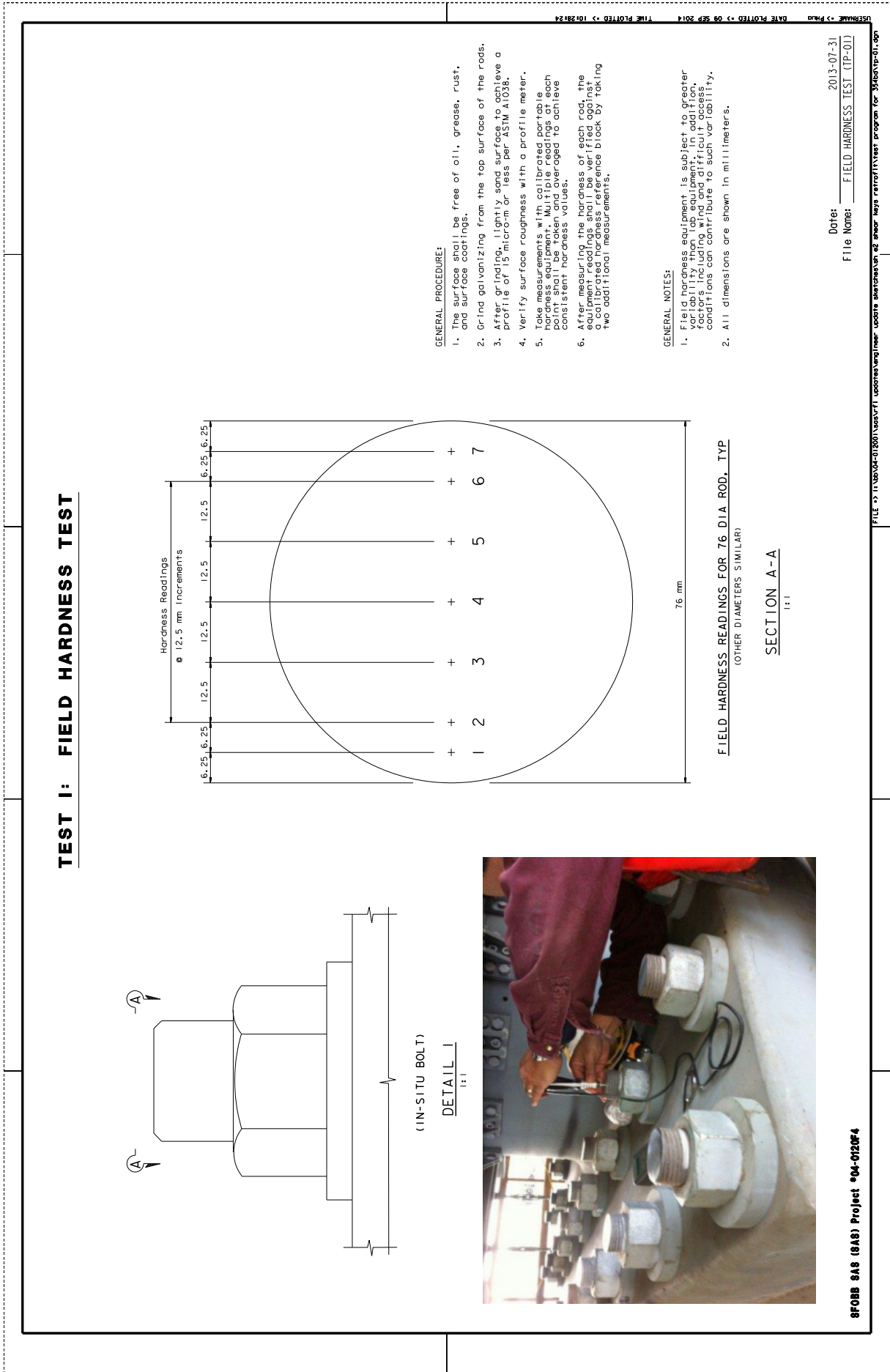
Notes:

- (1) Rods no longer in use; detensioned and replaced with Saddle Design Alternative
- (2) Eight rods in Group 2 were removed for testing and replaced with Group 18 rods
- (3) Group 2 and Group 3 rods are from the same heat
- (4) Rods no longer in use due to alternative architectural design
- (5) Several tests are performed for each specimen in this table

Test I

Test I consists of field hardness testing to characterize the various lots of rods and determine their hardness across the rod cross section, considering that high-hardness (or high-strength), low-alloy steels are generally more susceptible to stress corrosion cracking than lower-strength steels. Consequently, the initial work undertaken was to survey the rods in the structure and to determine their hardness. The hardness of the 2008 rods, which fractured in service, was measured as part of this effort to provide a basis for comparison with the other rods. The other rods came from two manufacturers and several heat treatment batches. To ensure the rods were reasonably uniform and properly manufactured, field hardness testing of 1,252 rods was performed. Approximately 45,000 field hardness measurements were taken in Test I. These data provided a means to evaluate the variability or uniformity of the rod hardness. See Figure 1.5-1 for details.

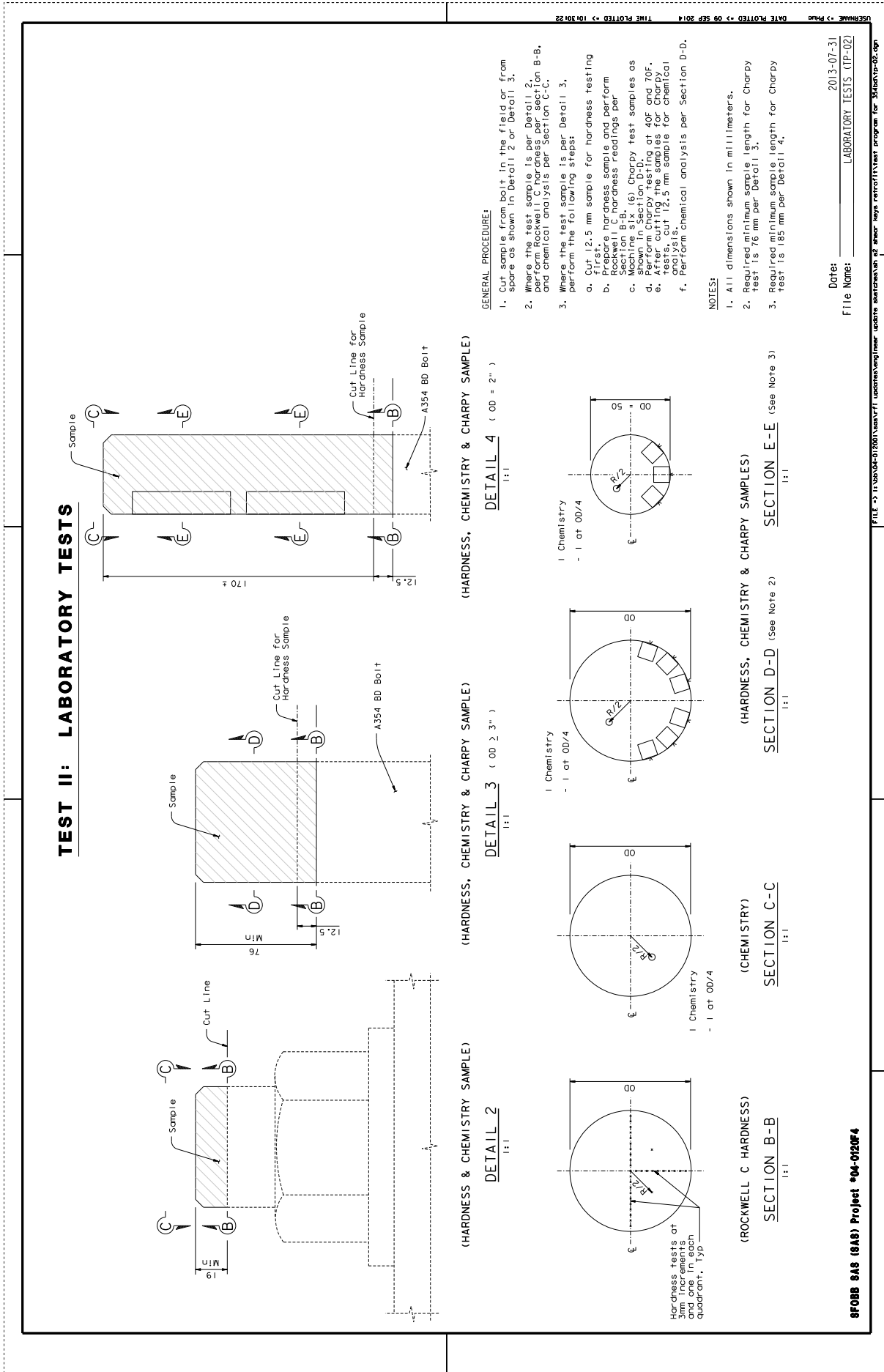
Figure 1.5-1: Test I — Field Hardness Test



Test II

Test II consists of laboratory testing for hardness, impact toughness, and chemical composition. This is to determine basic mechanical properties (hardness and toughness) and to characterize the chemical composition of the rods. This test was performed on small specimens cut from spare rods or in-service rods that were accessible and had enough length in the stick-out beyond the nut. The hardness measurement portion of Test II was for comparison with Test I, to correlate field hardness methods with lab hardness methods. See Figure 1.5-2 for details.

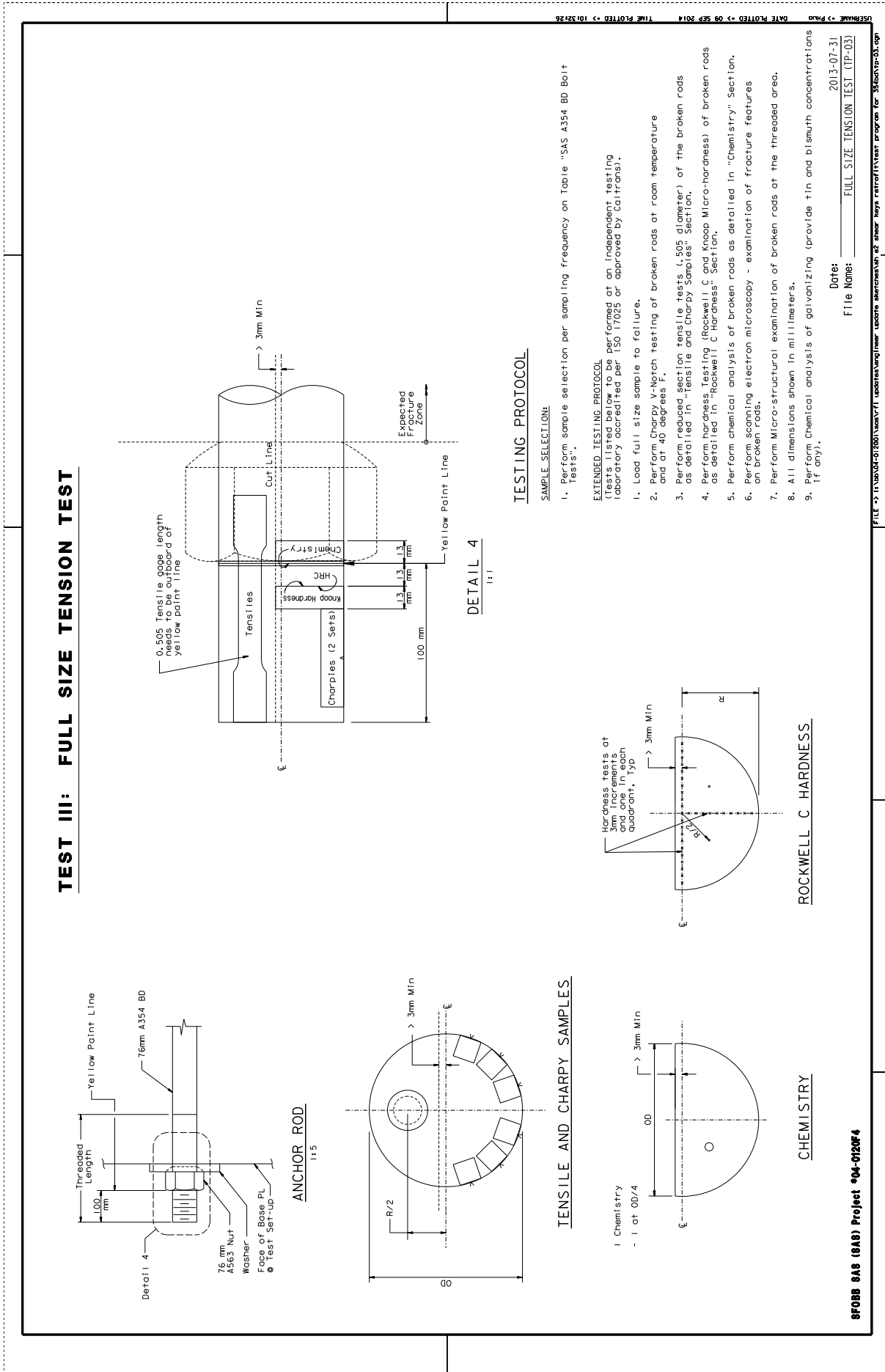
Figure 1.5-2: Test II — Laboratory Tests



Test III

Test III was included in the testing plan to verify that the full-diameter rod tensile strength matches the tensile strength determined in typical material quality control tests such as those performed using reduced-size specimens during rod manufacturing. See Figure 1.5-3 for details.

Figure 1.5-3: Test III — Full Diameter Tension Test



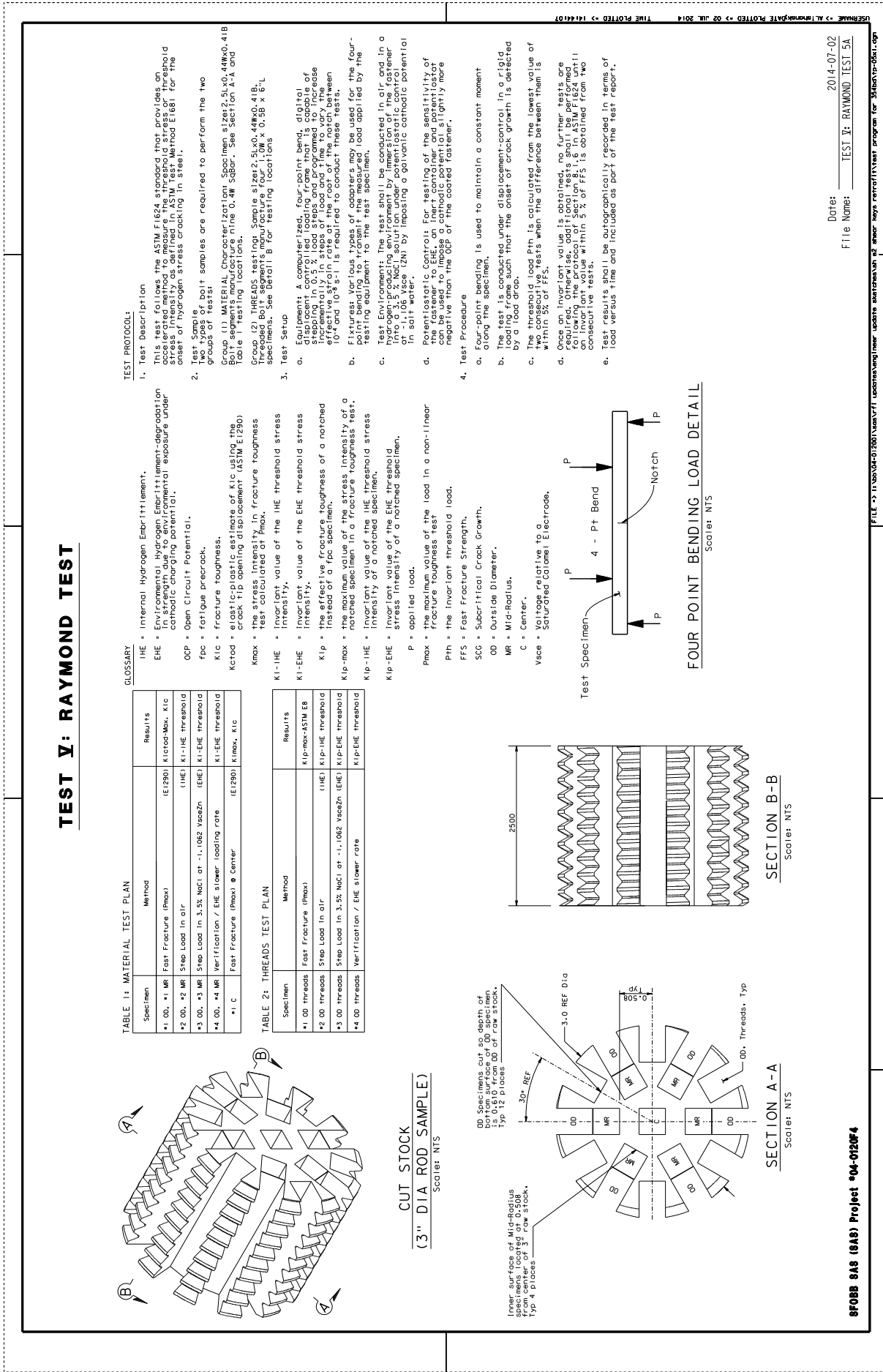
Test IV

Test IV is the full-diameter Stress Corrosion Cracking (SCC) test, also referred to as the “Townsend Test”. This test was developed to directly address the failure of the 2008 rods and to compare the resistance of other rods on the bridge to SCC. The Townsend Test is an accelerated stress corrosion cracking test that was modeled after Dr. Townsend’s 1975 work [3] to confirm Boyd and Hyler’s earlier study of high-strength bolts [2]. The objective of Test IV is to determine the susceptibility threshold load (% Fu) of the Self-Anchored Suspension Span rods to stress corrosion cracking in their threaded and galvanized condition (without introducing a pre-crack). Full-diameter rods are installed in specially designed and fabricated test rigs that include environmental chambers containing salt water (3.5% NaCl solution) to submerge threaded parts of the rod. The applied load is increased incrementally by means of hydraulic jacks and held at each step for 48 hours up to a maximum load of 0.85 Fu. This is sufficiently above the highest sustained load of 0.70 Fu for the A354BD rods in the structure. Furthermore, step loads beyond 0.85 Fu were not performed for safety reasons. In the event the rod does not fail at the maximum applied load (0.85 Fu) after being held for 140 hours, the rod is then pulled to failure. Seventeen rods were tested for SCC and an additional two for IHE in these rigs for a total of 19 rods. Following the failure of the rods, a post-fracture evaluation was performed to ascertain the cause of failure by examining the fracture surface under a scanning electron microscope, and to further characterize the microstructure of the alloy and provide other pertinent characteristics. See Figure 1.5-4 for details.

Test V

Test V, also referred to as the “Raymond Test” is based on ASTM F1624/F2660 protocol that establishes a procedure to determine the susceptibility of steel to hydrogen-induced failures. It does so by determining the threshold load for the onset of subcritical crack growth using standard fracture mechanics analysis on irregular-shaped specimens such as notched bars and actual threaded rod specimens. The testing also used a 3.5% NaCl solution environmental chamber. Test V was included in the testing program to corroborate the thresholds obtained in Test IV by using a different testing method and benefit from increased sample quantities by using multiple small test specimens for each rod group. Test V was employed as a well tested and often used method as a check for Test IV and later used to expand the program and test other variables. In addition, small specimens were available for Test V when samples of sufficient length were not available for Test IV. Test V also included tests of specimens with fatigue pre-cracks to determine the critical stress intensity factor for growth of SCC cracks, KISCC. Measurement of KISCC was of interest since it is an indication of the steel’s resistance to SCC. Furthermore, step loads beyond $0.85 F_u$ can be performed without safety concerns associated with the full-size testing in Test IV. See Figure 1.5-5 for details.

Figure 1.5-5: Test V — Raymond Test



Test VI

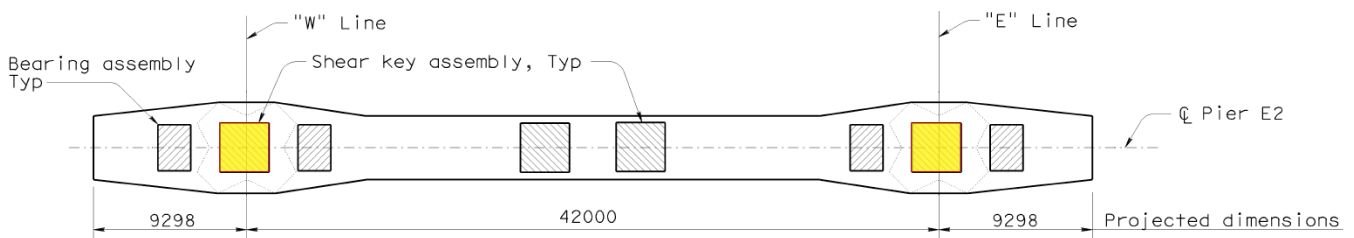
Test VI, also called the “Gorman Test,” is an additional validation of the SCC thresholds obtained in Test V. This test is performed in two parts. The first is essentially Test V with an extended time step, to further verify that longer hold times do not lower the threshold. The second part follows a sustained load protocol. It consists of loading small-size samples submerged in a 3.5% NaCl environmental chamber to loads near the threshold level and sustaining the load for an extended time, orders of magnitude longer than used in Test IV and Test V. This test is generally consistent with ASTM E1681.

2. MECHANICAL TESTING AND BORESCOPE EXAMINATION

2.1 BORESCOPE INVESTIGATIONS

A total of 288 A354BD bearing and shear key anchor rods have been installed in the Pier E2 cap beam, per the contract requirements; 96 of these 3-inch hot-dip galvanized rods are shear key anchor rods that were embedded in concrete at the Pier E2 cap beam. The shear key anchor rods were fabricated in 2008 and assembled inside pipe sleeves in Shear Keys S1 and S2 after release to the jobsite. The locations of the shear keys (S1 and S2) are highlighted in Figure 2.1-1. The area around the pipe sleeves was grouted five years later, in 2013.

Figure 2.1-1: Location of Shear Keys S1 (Left) and S2 (Right) on Pier E2



As shown in Figure 2.1-2, Figure 2.1-3, and Figure 2.1-4, the details of the rods in S1 and S2 are different from the details for the bearing anchor rods. The embedment of the shear key E2 rods in concrete prevents access from below. Prior to installation of the shear keys, the rods had to be flush with the pier E2 top surface; therefore, pipe sleeves were installed below the bearing plate to allow for the rods to be temporarily lowered. The area inside the temporary pipe sleeve was to be grouted after each rod was raised to its final position during installation of the shear key.

Figure 2.1-2: Cross-Sectional View of Shear Key and Shear Key Anchor Rods Setup

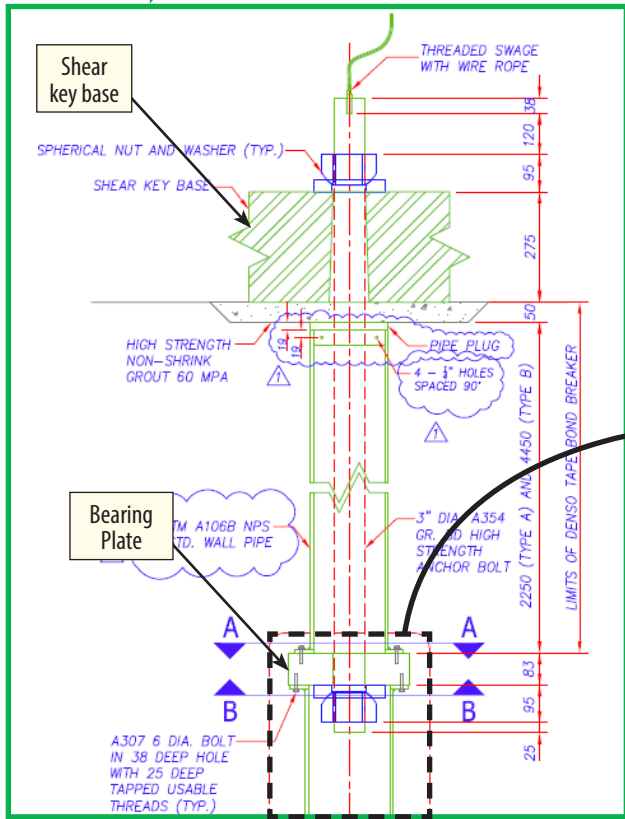
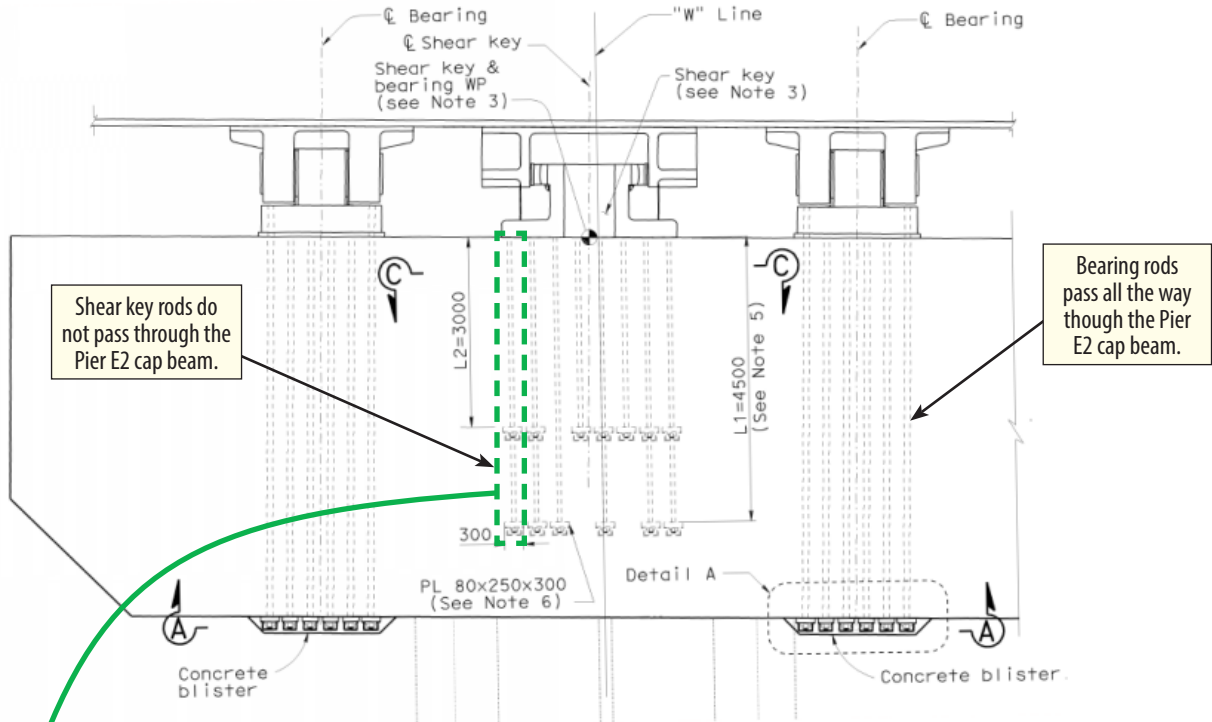


Figure 2.1-3: Anchor Rod Setup

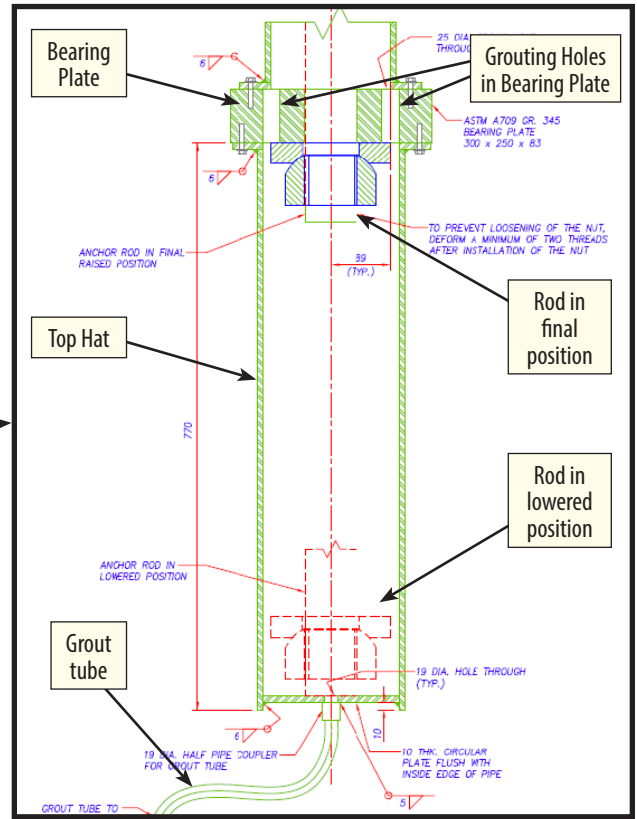


Figure 2.1-4: Top Hat Detail

2011 Borescope Investigation of E2 Shear Key Rod Holes

After the Pier E2 concrete pour, the rod holes were left open, exposing them to atmospheric conditions and accumulation of debris. The Contractor periodically extracted the water and used compressed air to remove debris. In order to prevent future water and debris intrusion, the Contractor covered the holes with plywood.

Construction requested METS to later inspect the interior of the rod holes to assess the condition of the rods. The borescope inspection of various rods was performed at Shear Keys S1 and S2 on Aug. 8, 2011, with a GE XL Go Videoprobe Borescope (Figure 2.1-5). Prior to the borescope inspection of the anchor rod sleeve, an initial visual inspection of the accessible area was conducted.

Figure 2.1-5: Borescope



The visible portion of the rods exhibited rust stains on the threaded portion of the rod. No physical damage to the threads was documented (see Figure 2.1-6).

Figure 2.1-6: Exposed Rod at Pier E2



SUMMARY OF OBSERVATIONS:

See Figure 2.1-7 through Figure 2.1-10 for borescope images. For the full report of the borescope inspections, please refer to Appendix F.

During the random investigation, the rods exhibited zinc corrosion products. Various types of debris were discovered in the holes throughout the investigation. Standing water was observed in some locations.

Figure 2.1-7: Standing Water in the Rod Hole



Figure 2.1-8: Debris on the Bearing Plate



Figure 2.1-9: Various Debris on the Bearing Plate (1)



Figure 2.1-10: Various Debris on the Bearing Plate (2)

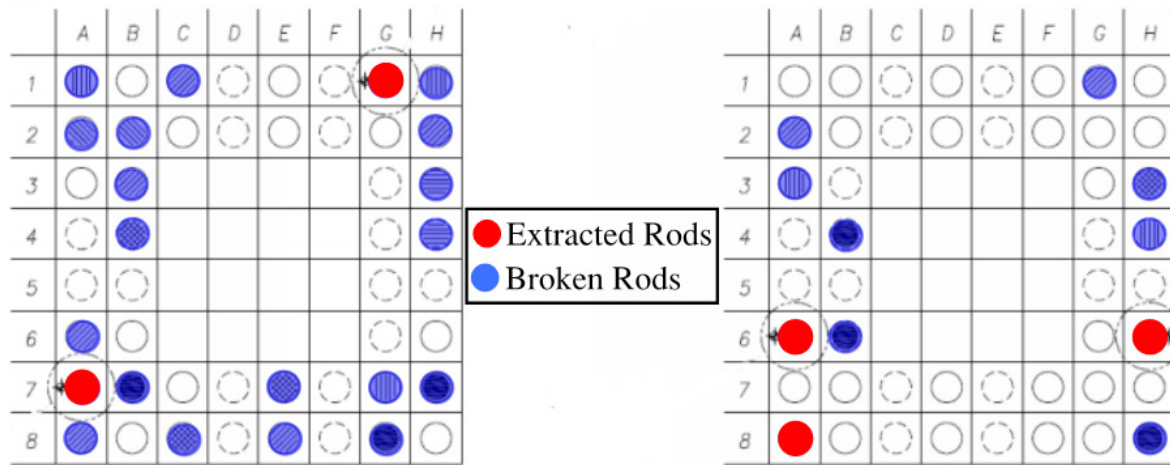


2013 Borescope Investigation of E2 Shear Key Rod Holes

Once the grouting was complete, in March 2013, thirty-two (32) of the shear key anchor rods fractured shortly after tensioning. The top portions of nine of the rods were extracted in segments for fracture analysis, but it was not possible to retrieve the bottom fracture surfaces. The Department requested that METS investigate the interior of the rod holes with a borescope to evaluate the in-situ conditions and provide images of the fracture region.

Out of the 32 fractured rods, five locations, as highlighted in Figure 2.1-11, were accessible for borescope inspection after removal of the following rods: S2-H6, S2-A6, S1A7, S1-G1 and S2-A8. Four more rods were extracted later.

Figure 2.1-11: Location of Fractured Rods on Shear Keys S1 (Left) and S2 (Right), including the Five Extracted Rods at the Time of the Borescope Inspection — Four More Rods Were Extracted Later



SUMMARY OF OBSERVATIONS:

For the full report of the borescope inspections, please refer to Appendix F. For additional information, see Appendix G.

In four out of five inspected locations, standing water was observed in the bottom of the anchor rod holes as shown in Figure 2.1-12 and Figure 2.1-14 through Figure 2.1-17. In rod hole S2-A6, where water was not visible (Figure 2.1-13), corrosion was evident. In three of five locations, gaps were discovered between the washer and the spherical nut suggesting the nut had dropped and rotated. The flat surfaces of the spherical nut and a small portion of the fracture are shown in Figure 2.1-14. The close up of Figure 2.1-14 is shown in Figure 2.1-15 where the fracture surface is almost flush with the spherical nut face. Signs of corrosion were evident on the spherical nut face as shown on Figure 2.1-15. A summary of findings are compiled in Table 2.1-1.

Table 2.1-1: Summary of Borescope Investigations

Date	Rod ID	Borescope Examination		
		Water in pipe sleeve	Movement of the rod assembly inside the top-hat	Corrosion products
4/17/13	S1-G1	Yes	Yes	Yes
3/14/13	S1-A7	Yes	Yes	
3/12/13	S2-H6	Yes	Yes	
3/13/13	S2-A6	No	No	Yes
3/13/13	S2-A8	Yes	Yes	

Figure 2.1-12: S2-H6 Borescope Snapshot

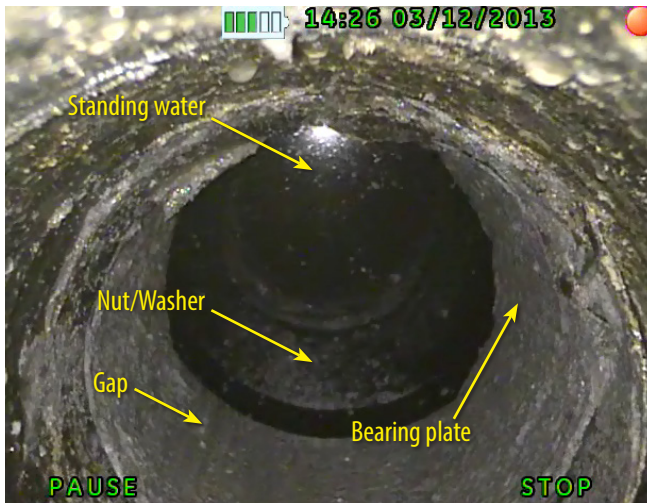


Figure 2.1-13: S2-A6 Borescope Snapshot



Figure 2.1-14: S2-H6 Borescope Snapshot

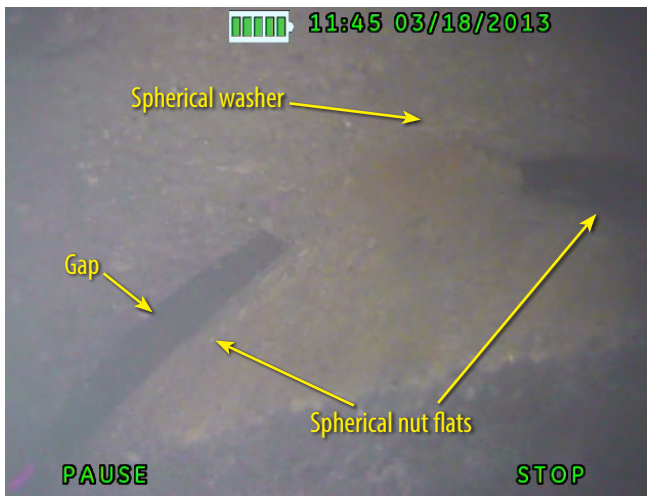


Figure 2.1-15: S2-H6 Borescope Snapshot

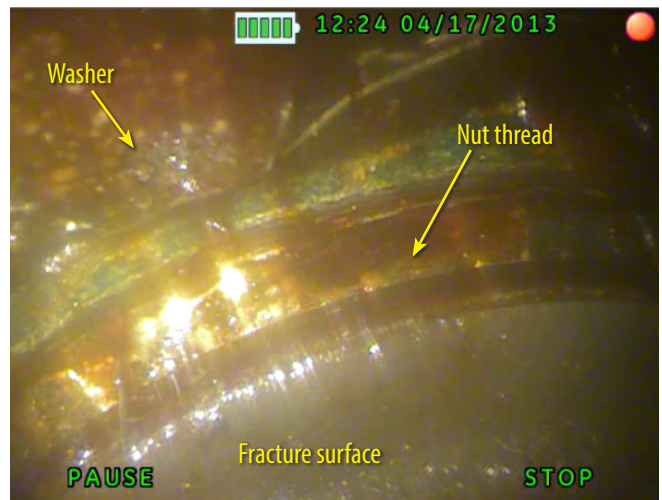


Figure 2.1-16: S2-A8 Borescope Snapshot

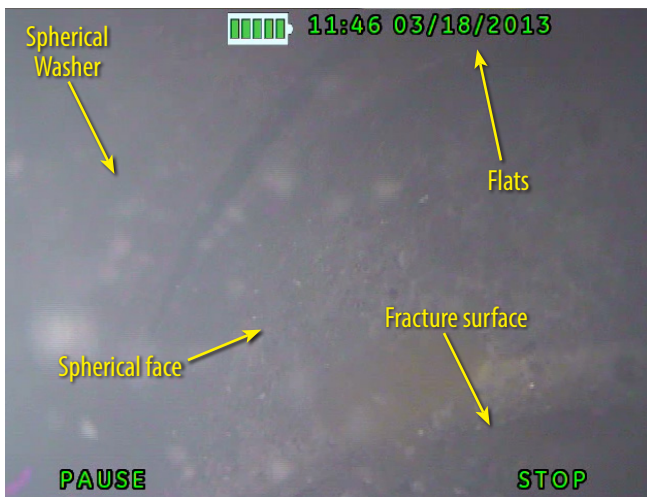


Figure 2.1-17: S2-A8 Borescope Snapshot



A water sample was taken for testing from the S2-A8 sleeve in Pier E2. The water sample was taken after the rod failed and was extracted. The sample was tested for pH and conductivity, as well as levels of chloride, sodium,

calcium, sulfate, nitrate, potassium, magnesium, nitrite, carbonate, bicarbonate, chromium, iron, zinc, aluminum, total dissolved solids, and organic compounds. The results are summarized in Table 2.1-2. For further details of the tests performed, refer to Appendix F.

Table 2.1-2: Summary of Water Sample Testing at WJE

Parameter	Result
pH	13.04
Conductivity	31 mS
Chloride	44 mg Cl ⁻ /L
Sulfate	128 mg SO ₄ ²⁻ /L
Nitrate	1.5 mg NO ₃ ²⁻ /L
Nitrite	293 mg NO ₂ ⁻ /L
Sodium	3940 mg Na ⁺ /L
Potassium	990 mg K ⁺ /L
Magnesium	ND
Calcium	96 mg Ca ²⁺ /L
Carbonate*	2,040 mg/L as CaCO ₃
Bicarbonate	ND
Organic Compounds	ND
Chromium	<1 mg Cr/L
Iron	ND
Aluminum	29.2 mg Al/L
Zinc	32.8 mg Zn/L
Total Dissolved Solids	11,200 mg/L

ND = Not Detected

* Value is for anions similar in acid strength to carbonate and reported as carbonate

2.2 TESTS I, II, AND III

Initial testing of the fractured A354BD anchor rods suggested hydrogen embrittlement as the mechanism for failure. Following the failure of the 32 rods manufactured in 2008, determining the susceptibility and mechanical properties of the remaining rods was necessary. Accordingly, Caltrans developed a testing program to determine the condition of these intact anchor rods. The locations of the A354BD rods on the bridge were categorized into 17 groups, as follows:

- Group 1 Pier E2 Shear Key (S1/S2) Anchor Rods (2008) — Bottom
- Group 2 Pier E2 Shear Key and Bearing Anchor Rods (2010) — Bottom
- Group 3 Pier E2 Shear Key Rods — Top Housing
- Group 4 Pier E2 Bearing Rods — Top Housing
- Group 5 Pier E2 Spherical Bushing Assembly Rods
- Group 6 Pier E2 Bearing Retainer Ring Plate Assembly Bolts
- Group 7 PWS Anchor Rods (Main Cable)

- Group 8 Tower Saddle Tie Rods
- Group 9 Tower Saddle Turned Rods (@ Splices)
- Group 10 Tower Saddle Grillage Anchor Bolts
- Group 11 Tower Outrigger Boom Bolts
- Group 12 Tower Anchorage Anchor Rods (3-Inch Diameter)
- Group 13 Tower Anchorage Anchor Rods (4-Inch Diameter)
- Group 14 East Saddle Anchor Rods
- Group 15 East Saddle Tie Rods
- Group 16 Cable Bracket Anchor Rods
- Group 17 W2 Bikepath Anchor Bolts

2.2.1 Test I: Field Hardness Test

The first test (Test I) determined the hardness values, which correlate to tensile strength, of the rods already installed in the field. Steel with high tensile strength, and high hardness, is generally more susceptible to hydrogen embrittlement. The Test I data provided the Department with a basic understanding of the potential susceptibility and variability of the mechanical properties of the installed rods.

ASTM A354 specifications require the hardness values of the rods to conform to specified ranges, as shown in Table 2.2-1. ASTM F606 specification requires the HRC values to be met at mid-radius locations.

Table 2.2-1: A354BD Hardness Requirements

Size, in.	Grade	Hardness Rockwell C (HRC)	
		Minimum	Maximum
¼ to 2½	BD	33	39
Over 2½	BD	31	39

Rod Selection

Of the 2,306 rods in the 17 groups, 1,210 rods were tested in the field. The remaining rods were not accessible to the inspection team to perform in-situ testing. The rods that were not accessible were in Group 5 (E2 Bearing Assembly Spherical Bushing Rods), Group 6 (E2 Bearing Retainer Ring Assembly Bolts), Group 10 (Grillage Bolts), Group 11 (Tower Outrigger Bottom Bolts), and Group 17 (W2 Bike Path Anchor Rods).

Test Method

Field hardness testing was performed using the Ultrasonic Contact Impedance (UCI) hardness testing method (Figure 2.2-1). The test utilizes a portable machine, the GE Kautkramer MIC 10, which applies a 10-kg load. A calibration block was utilized to ensure accuracy of the portable tester in accordance with the manufacturer’s recommendations. The test has a ±2 HRC margin of error in the results.

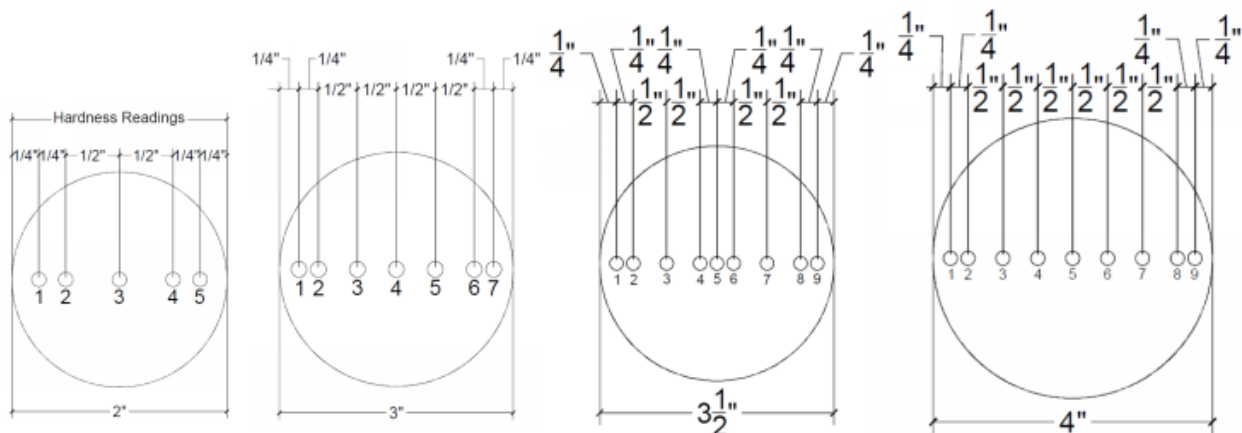
Figure 2.2-1: In-Situ Hardness Testing



The following is the test procedure for the in-situ hardness testing:

1. Galvanizing was ground off the top surface of the rods using a grinder.
2. Suitable sand paper was lightly applied after grinding to achieve a surface profile of 15 μm or less, per ASTM A1038.
3. A profile meter was used to ensure surface roughness met the requirements of ASTM A1038.
4. The surface was cleaned to remove any oil, grease, dust, rust, and surface coatings.
5. Measurements were taken across the diameter of the rod at five locations on the 2-inch rods, seven locations on the 3-inch rods, and nine locations on the 4-inch rods, as shown in Figure 2.2-2. Five readings were taken at each location; the highest and lowest values were discarded and the remaining values were averaged. The first and last locations across the diameter were ¼ inch from the edges of the rods for all diameters.
6. Two readings were made on a calibration block after each bolt was tested to verify the calibration of the equipment to within ±2 HRC.

Figure 2.2-2: Hardness Reading Layout on Various Diameters of Rods



Summary of Results

For the full report of the testing results, please refer to Appendix J.

The Test I (Field Hardness Test) results are summarized in Figure 2.2-3 and Figure 2.2-4. The crosses indicate the maximum and minimum limits of HRC measurement at mid-radius per ASTM A354 and ASTM F606. The bars represent the range of data acquired in the field hardness testing.

Test I results were found to be as expected for quenched and tempered material, with lower hardness values at the core due to slower cooling rates and higher hardness values near the edges because of more rapid cooling rates. No significant outliers suggesting major manufacturing deficiencies were detected.

Figure 2.2-3: Average Hardness for 2" Rods (Left) and 3" Rods (Right)

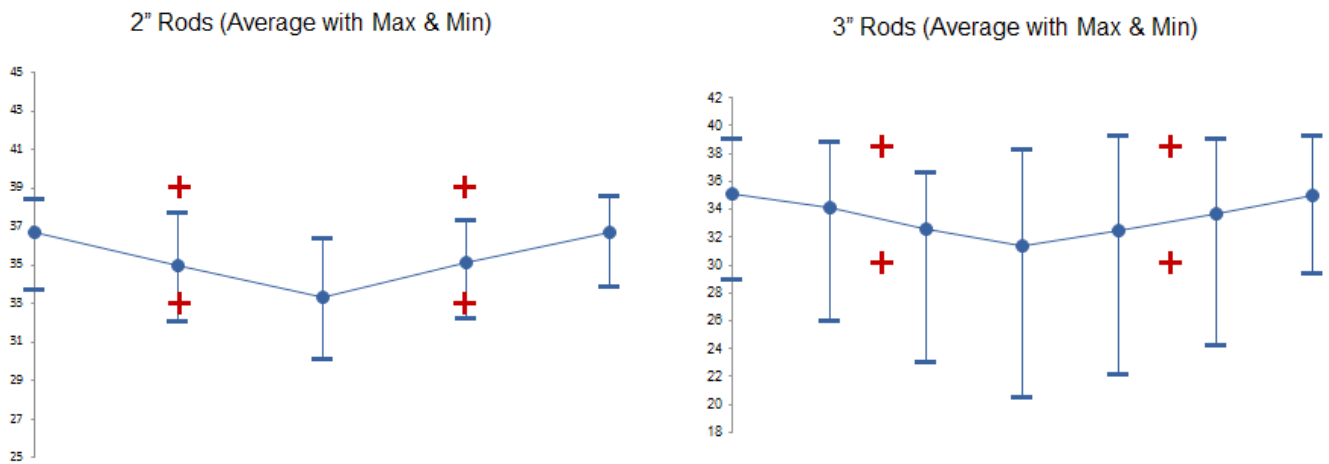
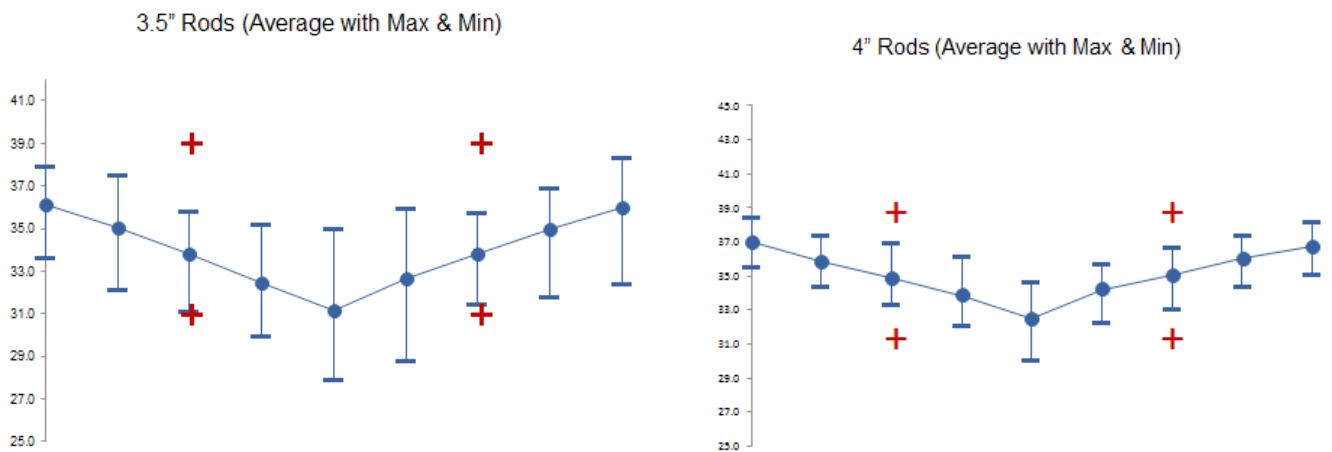


Figure 2.2-4: Average Hardness for 3.5" Rods (Left) and 4" Rods (Right)



2.2.2 Test II: Laboratory Tests

Laboratory testing (Test II) consisted of hardness testing, spectrochemical analysis, and Charpy impact testing (where enough material was available). The testing was performed on small samples removed from the unstressed ends of rods in the field or from spare rods. This testing was performed to determine the basic mechanical properties (hardness and toughness) and characterize the chemical composition of the rods. The mechanical properties of the steel provide the basic information necessary to assess the susceptibility of the rods to hydrogen embrittlement.

Hardness testing was performed with calibrated Rockwell C hardness testing equipment, allowing for the UCI testing in Test I to be verified. These tests also characterize the variability of the material.

Rod Selection

The samples were removed from the groups of rods where material was available and accessible. Samples from Group 3 (Pier E2 Shear Key Rods – Upper), Group 4 (Pier E2 Bearing Rods – Upper), and Group 8 (Tower Saddle Tie Rods) were from spare rods of the same material heat as the rods in the field. Samples were taken from the field for Groups 7, 9, 12, 13, 14, and 15.

Testing coupons were extracted from the rod specimens in the locations shown in Figure 2.2-6. Where sufficient material was available, Charpy coupons were extracted for testing as well.

Test Methods

Laboratory Rockwell C Hardness (HRC)

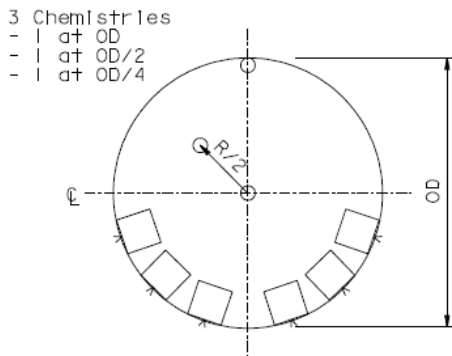
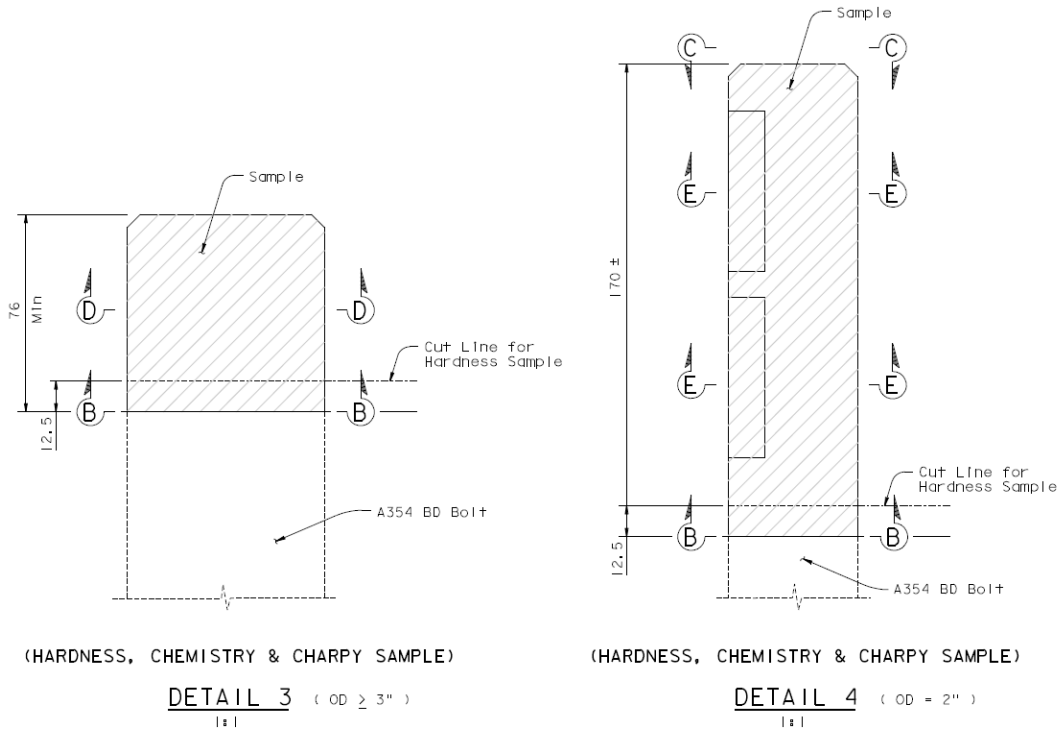
Each test coupon is cut with a saw using a cutting fluid that reduces heat input. Since surface preparation is crucial for the hardness testing, the surfaces are then polished to a dull shine to achieve the required surface profile. This surface profile provides a clean testing surface and ensures accurate and reproducible results. The test is typically performed with a Rockwell Hardness Tester as shown in Figure 2.2-5.

Figure 2.2-5: HRC Tester



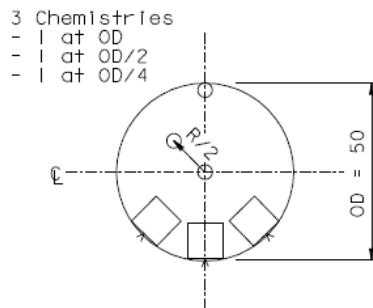
Hardness testing was performed at locations across the diameter and radius at 3-mm increments, in accordance with ASTM E18 requirements. As noted in Figure 2.2-7, an additional measurement was taken at mid-radius in each quadrant.

Figure 2.2-6: Hardness, Chemistry and CVN Coupon Extraction Layout



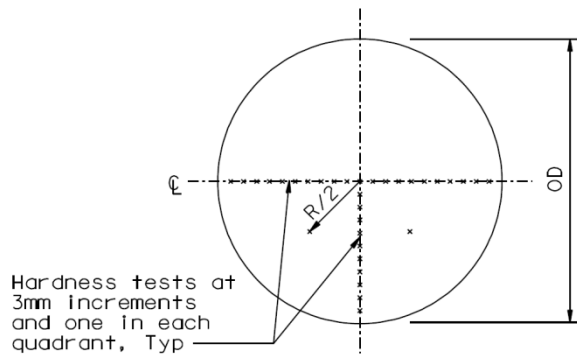
(HARDNESS, CHEMISTRY & CHARPY SAMPLES)

SECTION D-D
1:1



SECTION E-E
1:1

Figure 2.2-7: Hardness Test Measurement Layout



Chemistry (Lab)

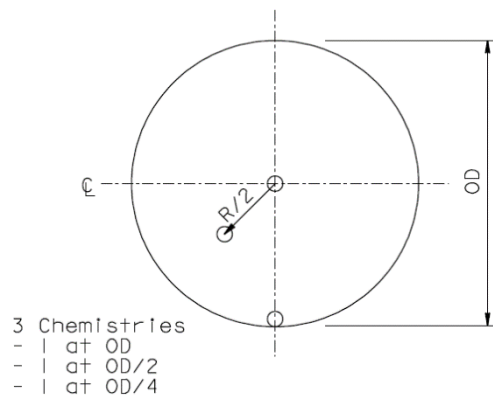
The chemical test measures the chemical composition of steel substrate utilizing Optical Emission Spectroscopy (OES). During this test, chemistry test specimens are extracted from the test rods using an abrasive saw with cooling liquid. To ensure the specimens are homogeneous and free from pits or voids, the surface is ground with an abrasive belt or disk. Upon extraction of the specimen, it is placed on a calibrated OES machine (see Figure 2.2-8) and a spark is applied to the test coupon. The energy of the spark causes the electrons in the sample to emit light that is converted into a spectral pattern. The intensities of the peaks are measured and qualitative and quantitative analyses of the material composition are performed with the OES analyzers.

Figure 2.2-8: Chemical Testing Analysis Layout



Three chemistry samples were analyzed from each rod using the OES method: close to the edge of the rod, at the center, and at mid-radius. These locations are shown in Figure 2.2-9.

Figure 2.2-9: Chemical Testing Analysis Layout



In accordance with ASTM A354 specifications, the material was tested for carbon (C), manganese (Mn), phosphorus (P), and sulfur (S). The ASTM requirements for these elements are shown in Table 2.2-2. Although not required by ASTM, the rods were also tested for aluminum (Al), chromium (Cr), cobalt (Co), columbium (Nb), copper (Cu), molybdenum (Mo), nickel (Ni), silicon (Si), titanium (Ti), and vanadium (V).

Table 2.2-2: ASTM A354 Chemical Requirements

Element	Alloy Steel	
	Heat Analysis, %	Product Analysis, %
Carbon for sizes through 1-1/2 in	0.30 to 0.53	0.28 to 0.55
Carbon for sizes larger than 1-1/2 in	0.35 to 0.53	0.33 to 0.55
Manganese, min	0.60	0.57
Phosphorus, max	0.035	0.040
Sulfur, max	0.040	0.045
Alloying Elements	A	A

^A Steel, as defined by the American Iron and Steel Institute, shall be considered to be alloy when the maximum of the range given for the content of alloying elements exceeds one or more of the following limits: manganese, 1.65%; silicon, 0.60%; copper, 0.60% or in which a definite range or a definite minimum quantity of any of the following elements is specified or required within the limits of the recognized field of constructional alloy steels; aluminum, chromium up to 3.99%, cobalt, columbium, molybdenum, nickel, titanium, tungsten, vanadium, zirconium, or any other alloying elements added to obtain a desired alloying effect.

Charpy V Notch (Lab)

The ASTM A354 specifications do not require Charpy V-Notch (CVN) testing, so there are no defined acceptance criteria.

Nevertheless, the Charpy test, which measures the toughness of the material, is of interest since toughness is a measurement of a material’s ability to resist fracture. Steels are generally tougher at higher temperatures and more brittle at lower temperatures. Due to limited availability of test samples, most samples were tested at 40°F and 70°F.

The standard Charpy specimens were extracted using wire Electrical Discharge Machining (EDM) closest to the surface of the rod. Once specimens were extracted, they were machined to the standard size (10 mm × 10 mm × 55 mm). A V-notch was then made at the center of each specimen. The notch had edges that were at 45° from the centerline in both directions and was 2 mm deep with a 0.25-mm radius at the tip. The notches were oriented for the fracture travel from the outside of the rod towards the interior of the rod, similar to the crack propagation direction for a full-size rod. See Figure 2.2-10 for a Charpy testing machine.

Figure 2.2-10: Charpy Testing Machine



Samples were removed from the stick-out end of the rod as shown in Figure 2.2-6. CVN testing was performed in accordance with ASTM E-23. The rods in Group 14 (East Saddle Anchor Rods) did not have enough material to extract samples for this test.

Summary of Results

For the full report of the testing results, please refer to Appendix J.

Rockwell C Hardness

The HRC lab values were found to be similar to the in-situ testing results. The results from field testing (Test I) have an accuracy within ± 2 HRC. Per ASTM E18, the Test II values have a maximum error of ± 1 HRC. The results of the laboratory testing (Test II) were mostly within 3 HRC of the field testing value. Average results are shown in Figure 2.2-11 through Figure 2.2-15; the Test I results are averages of hundreds of measurements, whereas Test II results are averages of fewer than 10 measurements.

In general, the core of the rod had lower hardness values than the edge of the material. This is indicative of slower cooling rates at the core during the heat treatment process, which is expected because these rods were all quenched and tempered and is not an indication of problems. Additionally, during laboratory testing, it was observed that several of these samples had lower hardness values closer to the edge, creating an “M-Shape” appearance. This also appears in Test I results but not in the average of the test values. See Section 2.2.4 for additional testing related to the "M-Shape" hardness profile.

Figure 2.2-11: Test I and II Average Hardness Values for Group 3 (Left) and Group 4 (Right)

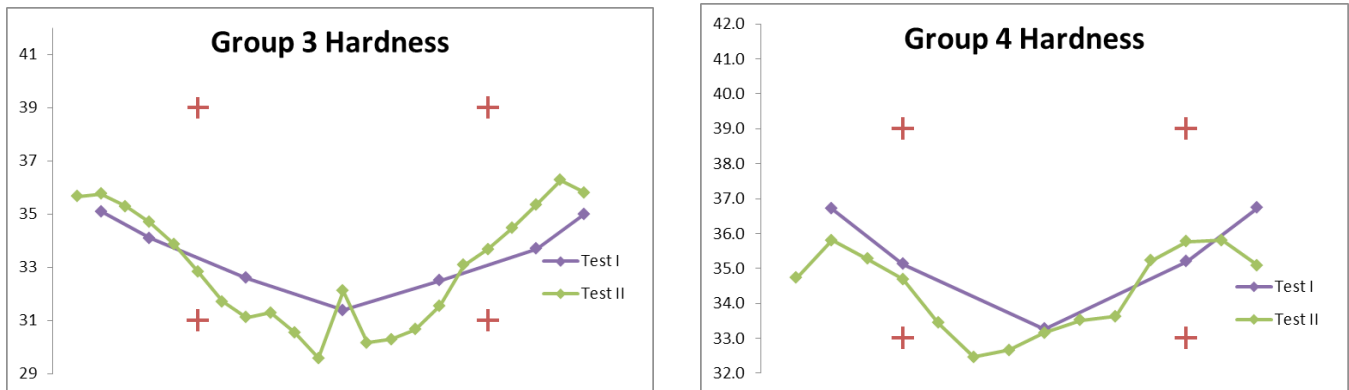


Figure 2.2-12: Test I and II Average Hardness Values for Group 7 (Left) and Group 8 (Right)

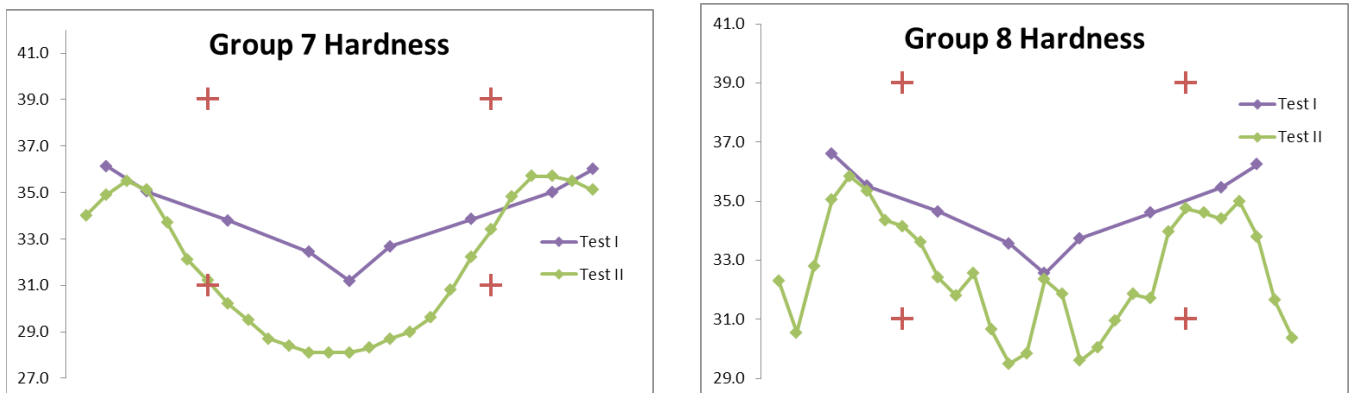


Figure 2.2-13: Test I and II Average Hardness Values for Group 9 (Left) and Group 12 (Right)

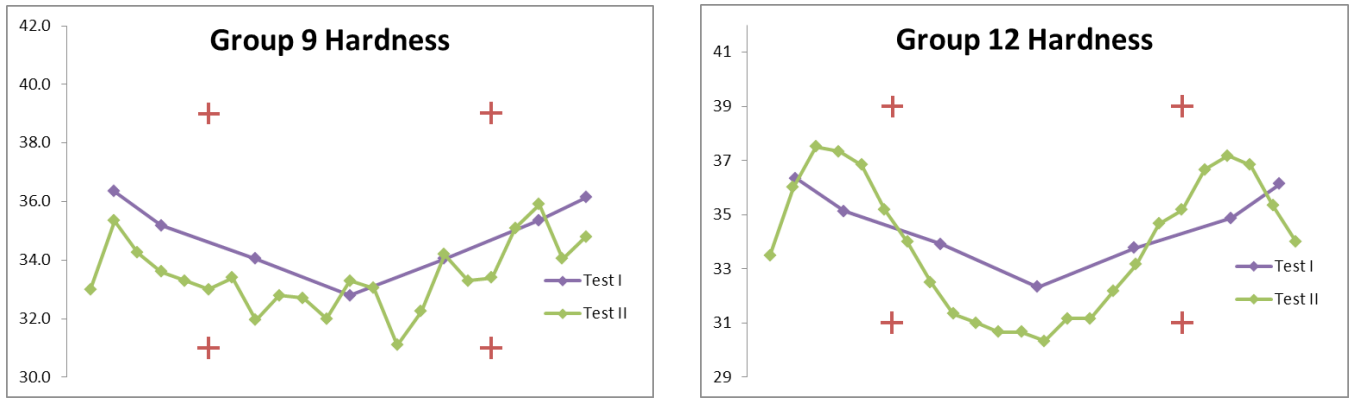


Figure 2.2-14: Test I and II Average Hardness Values for Group 13 (Left) and Group 14 (Right)

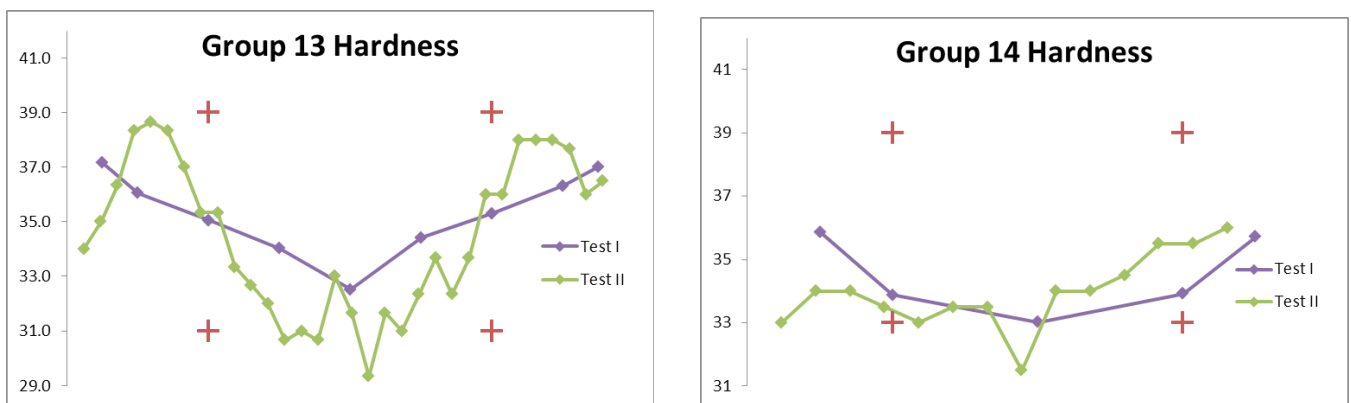
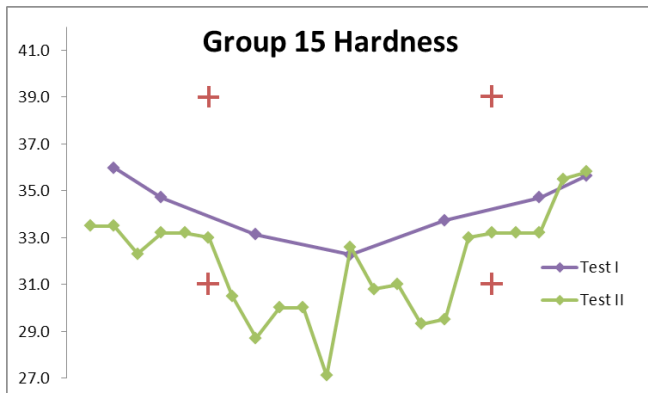


Figure 2.2-15: Test I and II Average Hardness Values for Group 15



Chemical Testing

All spectrochemical analyses of the steel were found to be in conformance with A354BD chemical requirements. Averages are shown in Table 2.2-3.

Table 2.2-3: Chemical Analysis Results, Test II

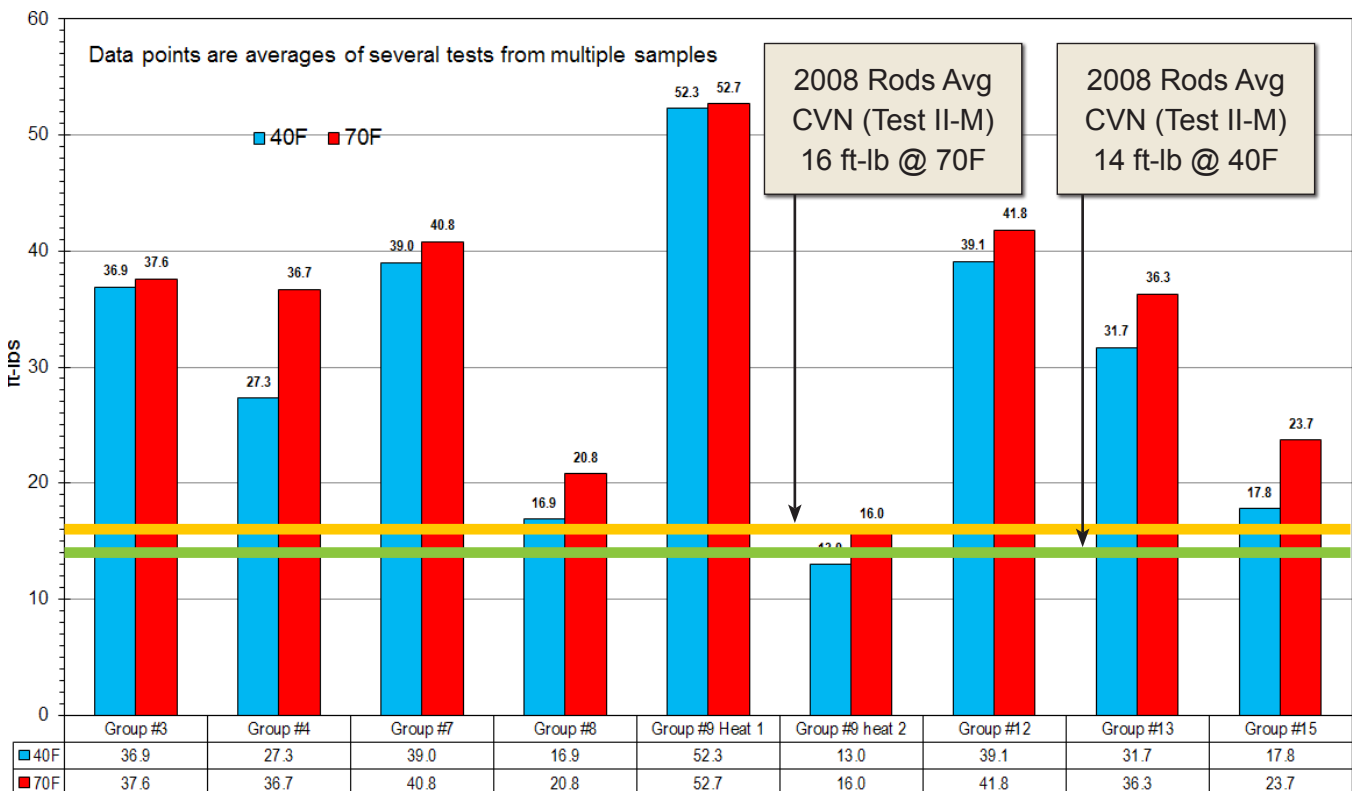
	C	Cr	Cu	Mn	Mo	Ni	P	Si	S
ASTM 354BD Requirements	0.33 to 0.55	-	-	0.57 min	-	-	0.040 max	-	0.045 max
Group 3	0.43	0.94	0.22	0.86	0.16	0.14	0.02	0.28	0.04
Group 4	0.42	0.94	0.21	0.87	0.19	0.09	0.02	0.26	0.03
Group 7	0.42	1.05	0.17	0.97	0.19	0.1	0.01	0.21	0.02
Group 8	0.43	1.08	0.18	0.99	0.16	0.14	0.01	0.35	0.02
Group 9	0.43	1.08	0.11	0.97	0.2	0.1	0.01	0.35	0.02
Group 12	0.38	1.03	0.31	0.93	0.16	0.11	0.01	0.27	0.02
Group 13	0.4	0.97	0.26	0.94	0.16	0.12	0.01	0.24	0.02
Group 14	0.4	0.97	0.19	0.89	0.16	0.11	0.01	0.27	0.02
Group 15	0.42	0.96	0.2	0.84	0.17	0.14	0.01	0.28	0.03

Additionally, the galvanized coatings of the samples were checked for tin and bismuth. The maximum tin content was found to be 0.007 and the maximum bismuth content was 0.014; these amounts are not considered to be significant or harmful to the material.

Charpy V Notch Testing

As shown in Figure 2.2-16, the Charpy values vary depending on rod group and heat batch. The lowest observed values were found in Groups 8 and 9, Heat #2, which were from the same fabrication batch. Note that ASTM A354 specifications do not require CVN testing, so there are no defined acceptance criteria.

Figure 2.2-16: Average CVN Values, Test II and Circumferential Values of 2008 Rods from Test II-M



2.2.3 Test II: Modified (II-M)

Purpose

Test II-M was performed to determine basic mechanical properties (hardness and toughness) and characterize the chemical composition of the rods that had already failed in service. The testing was similar to Test II but performed on pieces of rods extracted from Pier E2 shear key anchor rods. The intent of this testing was to contribute to the analysis of the root cause of failure and for comparison with other A354BD rods. Test II-M consisted of Rockwell C Hardness testing, chemical analysis, Charpy impact testing, and coupon tensile testing.

Rod Selection

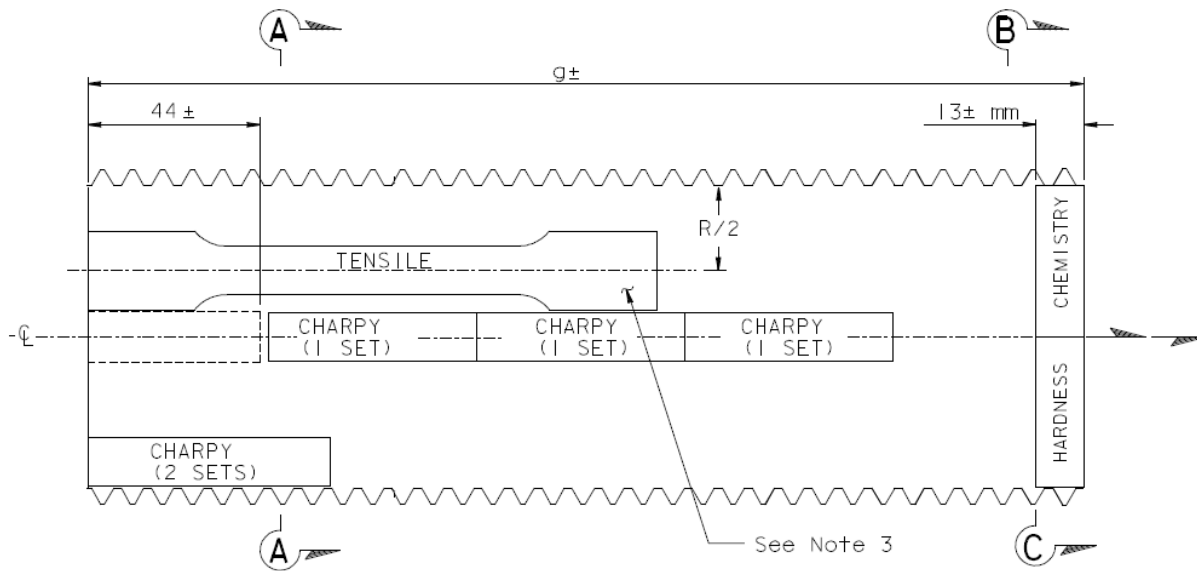
The rods from Group 1 (Pier E2 Shear Key (S1/S2) Anchor Rods(2008) – Bottom) were extracted after fracture and the pieces were sequentially numbered. Group 1 rods were not tested previously in Test I through Test III; Test II Modified and Test III Modified were designed to address these specific rods. Fourteen rod pieces were selected for testing:

- Rod ID S1-G6 — Item 08-08 — Heat MIS-26
- Rod ID S2-H5 — Item 08-09 — Heat MIS-26
- Rod ID S2-B4 — Item 08-10 — Heat MIS-27
- Rod ID S2-H4 — Item 08-11 — Heat MIS-27
- Rod ID S1-A2 — Item 08-12 — Heat MJF-28
- Rod ID S1-B3 — Item 08-13 — Heat MJF-28
- Rod ID S1-H2 — Item 08-14 — Heat MJF-29
- Rod ID S1-A1 — Item 08-15 — Heat MJF-29
- Rod ID S2-G8 — Item 08-16 — Heat MJF-30
- Rod ID S2-H3 — Item 08-17 — Heat MJF-30
- Rod ID S1-H1 — Item 08-18 — Heat MJF-31
- Rod ID S2-B2 — Item 08-19 — Heat MJF-31
- Rod ID S1-G7 — Item 08-20 — Heat MJF-32
- Rod ID S1-H7 — Item 08-21 — Heat MJF-32

Test Methods

The coupons were extracted per Figure 2.2-17 for each test: one tensile coupon, four sets of Charpy specimens, a minimum of one chemical sample and hardness readings across the diameter.

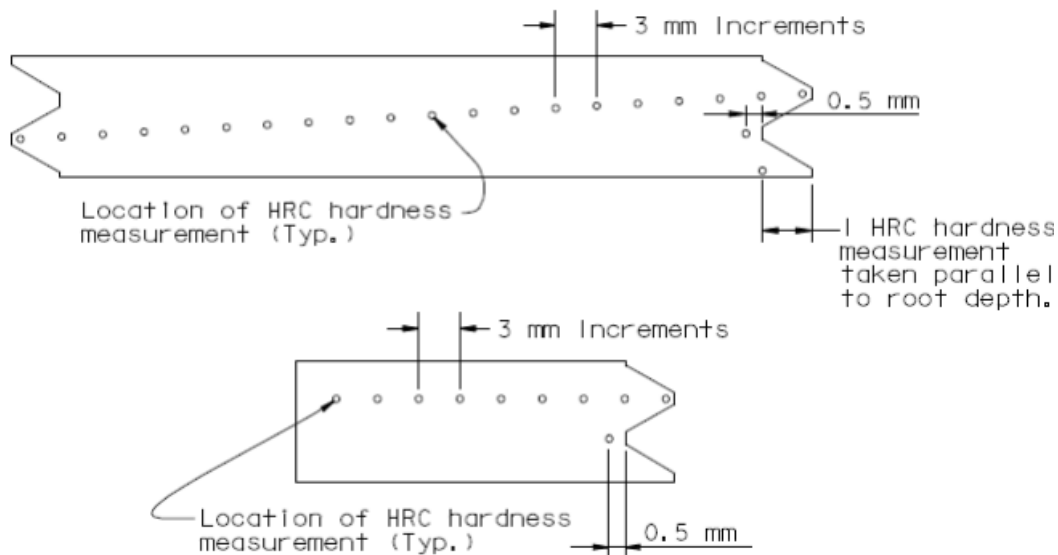
Figure 2.2-17: Test Coupon Locations on Rod Pieces



HRC Hardness

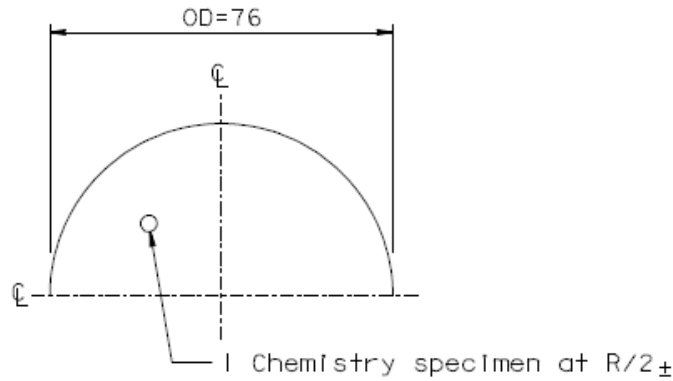
The hardness readings were performed along two perpendicular traverses. The readings for the HRC measurements were separated by 3 mm throughout the cross-section; see Figure 2.2-18.

Figure 2.2-18: Hardness Measurements



Chemical Test

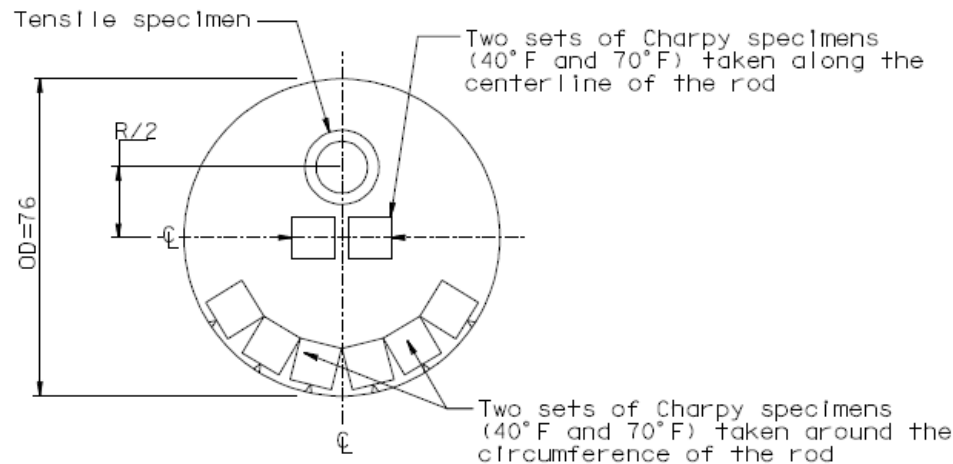
Chemistry sample were removed at mid-radius (see Figure 2.2-19). The laboratory used a minimum of three samples to ensure the accuracy of the results.

Figure 2.2-19: Chemistry Sample**Charpy V Notch Impact Test**

Four sets of Charpy specimens were removed from the rod – two sets were from the centerline longitudinal to the rod axis and two sets were from around the circumference of the rod; see Figure 2.2-20. The tests were performed at 40°F and 70°F. Refer to Section 2.2.2 for sample extraction and testing procedure details.

Tensile Test

The tensile specimen is extracted at mid-radius; see Figure 2.2-20. All samples were cut by EDM and then machined down.

Figure 2.2-20: Tensile Coupon and CVN Sets*Summary of Results*

For the full report of the testing results, please refer to Appendix J.

Rockwell C Hardness Testing

The HRC acceptance criteria for A354BD rods are at mid-radius. The results at mid-radius are in conformance, although they are at the higher end of the range. See Figure 2.2-21 through Figure 2.2-23 for reference on the traverse results; the rods are split into groups of four or five rods per graph for clarity.

Figure 2.2-21: Test II-M Traverse Readings (1)

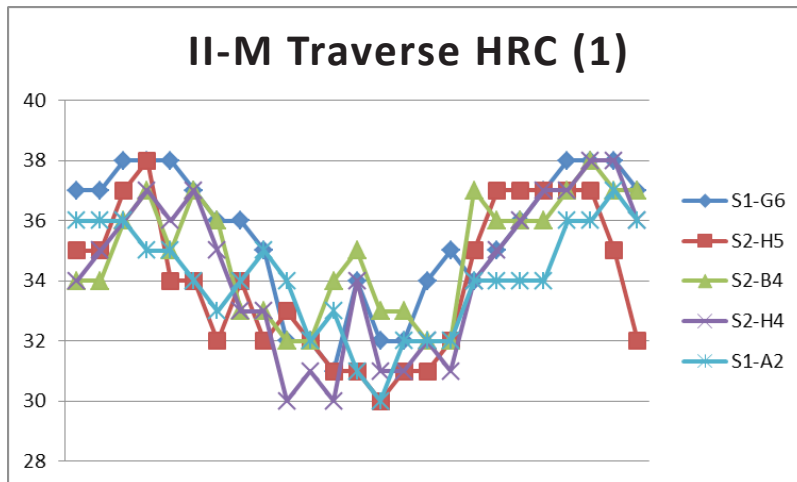


Figure 2.2-22: Test II-M Traverse Readings (2)

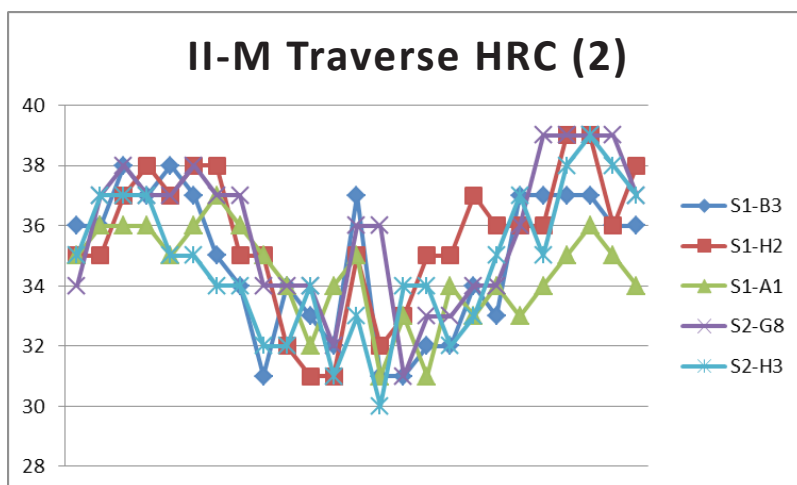
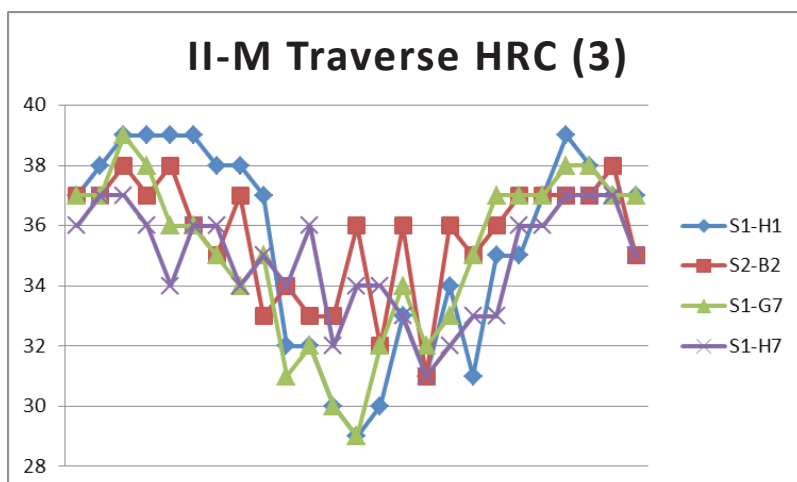


Figure 2.2-23: Test II-M Traverse Readings (3)



Additionally, the rods were tested at the 90° traverse and the results were found to be consistent. The hardness values of the rod from center to edge are represented in each graph from left to right; see Figure 2.2-24 through Figure 2.2-26 for reference.

Figure 2.2-24: HRC Readings at 90° Angle (1)

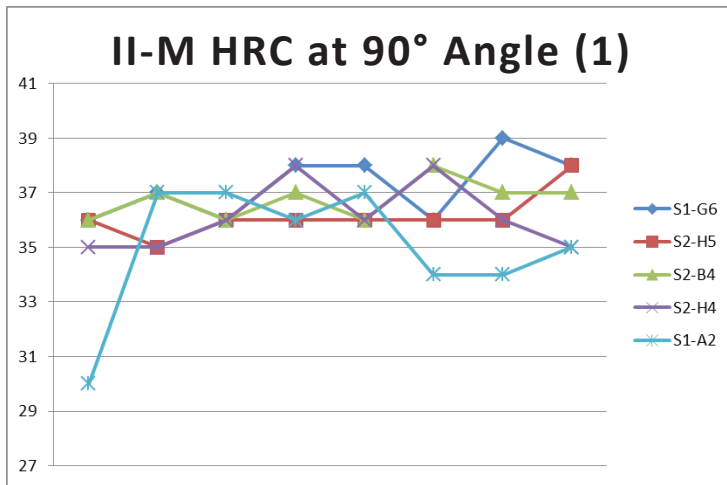


Figure 2.2-25: HRC Readings at 90° Angle (2)

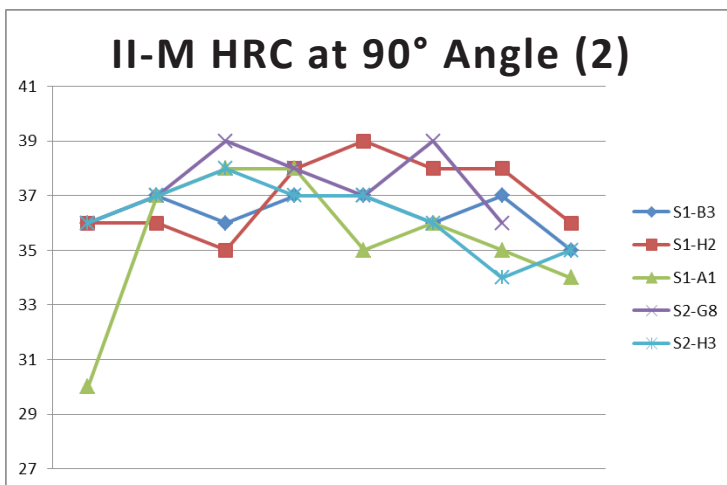
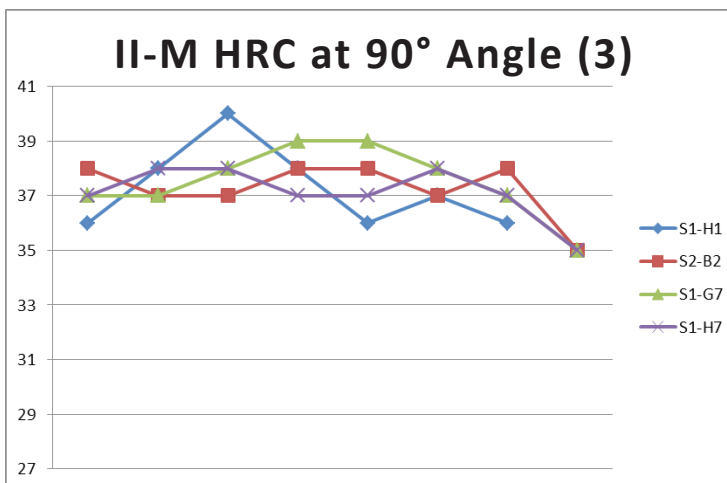


Figure 2.2-26: HRC Readings at 90° Angle (3)



Chemical Analysis

The results of the chemical analysis were found to be in conformance with the A354BD requirements; see Table 2.2-4 for reference.

Table 2.2-4: Chemical Analysis Results, Test II-M

	Al	C	Cr	Co	Cb	Cu	Mn	Mo	Ni	P	Si	Si	Ti	V
ASTM	-	0.33–0.55	-	-	-	-	Min 0.57	-	-	Max 0.040	-	Max 0.045	-	-
S1-G1	<0.005	0.42	0.99	0.01	<0.005	0.21	0.96	0.16	0.1	0.012	0.24	0.039	<0.005	0.03
S2-H5	<0.005	0.45	1	0.01	<0.005	0.21	0.97	0.16	0.1	0.012	0.24	0.038	<0.005	0.03
S2-B4	<0.005	0.45	1.01	0.01	<0.005	0.22	0.98	0.16	0.1	0.013	0.24	0.04	<0.005	0.03
S2-H4	<0.005	0.42	1	0.01	<0.005	0.21	0.96	0.16	0.1	0.012	0.24	0.042	<0.005	0.03
S1-A2	<0.005	0.43	0.99	0.01	<0.005	0.21	0.96	0.16	0.1	0.011	0.24	0.038	<0.005	0.03
S1-B3	<0.005	0.42	0.99	0.01	<0.005	0.21	0.95	0.16	0.1	0.011	0.24	0.036	<0.005	0.03
S1-H2	<0.005	0.44	0.99	0.01	<0.005	0.21	0.95	0.16	0.1	0.011	0.25	0.04	<0.005	0.03
S1-A1	<0.005	0.44	1.01	0.01	<0.005	0.21	0.97	0.16	0.1	0.012	0.24	0.043	<0.005	0.03
S2-G8	<0.005	0.44	1	0.01	<0.005	0.21	0.95	0.16	0.1	0.011	0.24	0.039	<0.005	0.03
S2-H3	<0.005	0.42	1	0.01	<0.005	0.21	0.95	0.16	0.1	0.011	0.24	0.042	<0.005	0.03
S1-H1	<0.005	0.44	1	0.01	<0.005	0.21	0.97	0.16	0.1	0.012	0.24	0.042	<0.005	0.03
S2-B2	<0.005	0.42	0.99	0.01	<0.005	0.21	0.95	0.16	0.1	0.011	0.24	0.038	<0.005	0.03
S1-G7	<0.005	0.41	0.99	0.01	<0.005	0.21	0.97	0.16	0.1	0.012	0.24	0.039	<0.005	0.03
S1-H7	<0.005	0.43	0.99	0.01	<0.005	0.21	0.96	0.16	0.1	0.012	0.24	0.038	<0.005	0.03

Charpy V Notch Test

See Figure 2.2-27 and Figure 2.2-28 for a summary of the results. See Figure 2.2-16, which summarizes the CVN results from Test II and Test II-M. The ASTM A354 specifications do not require CVN testing, so there are no defined acceptance criteria.

Figure 2.2-27: Circumference CVN

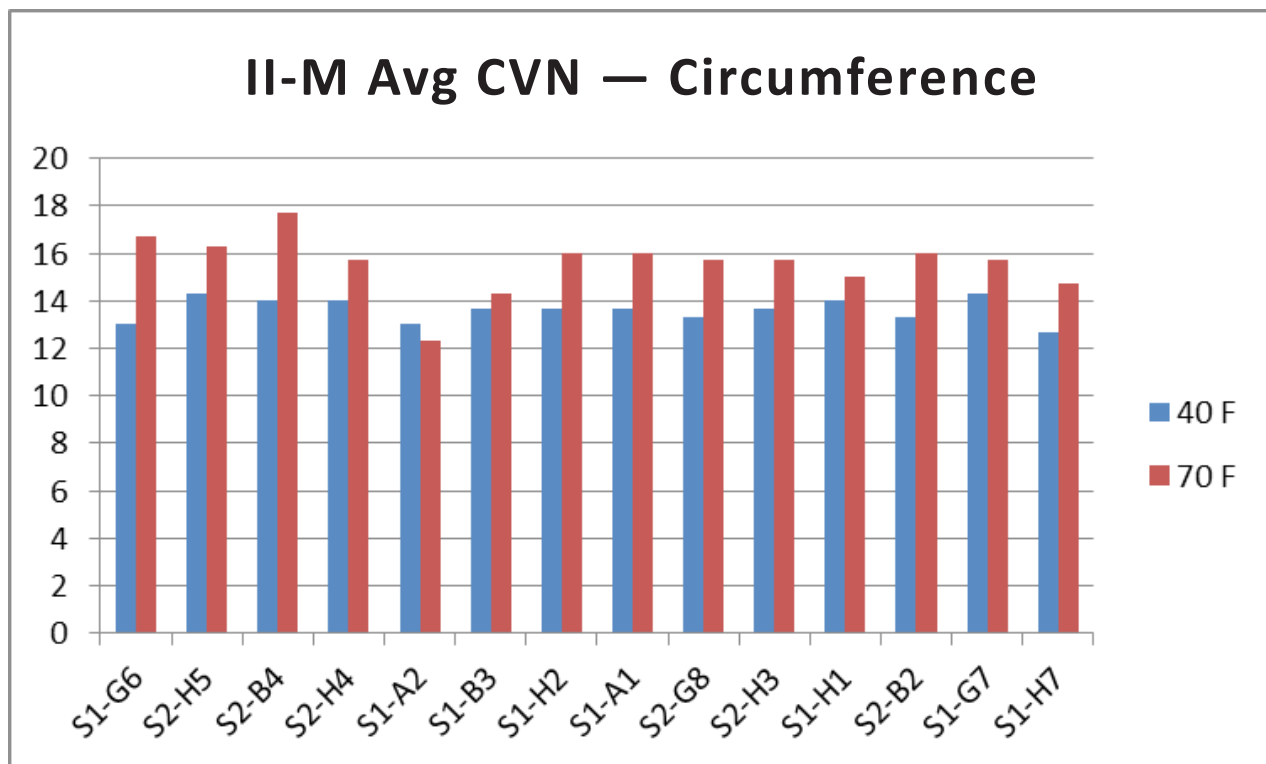
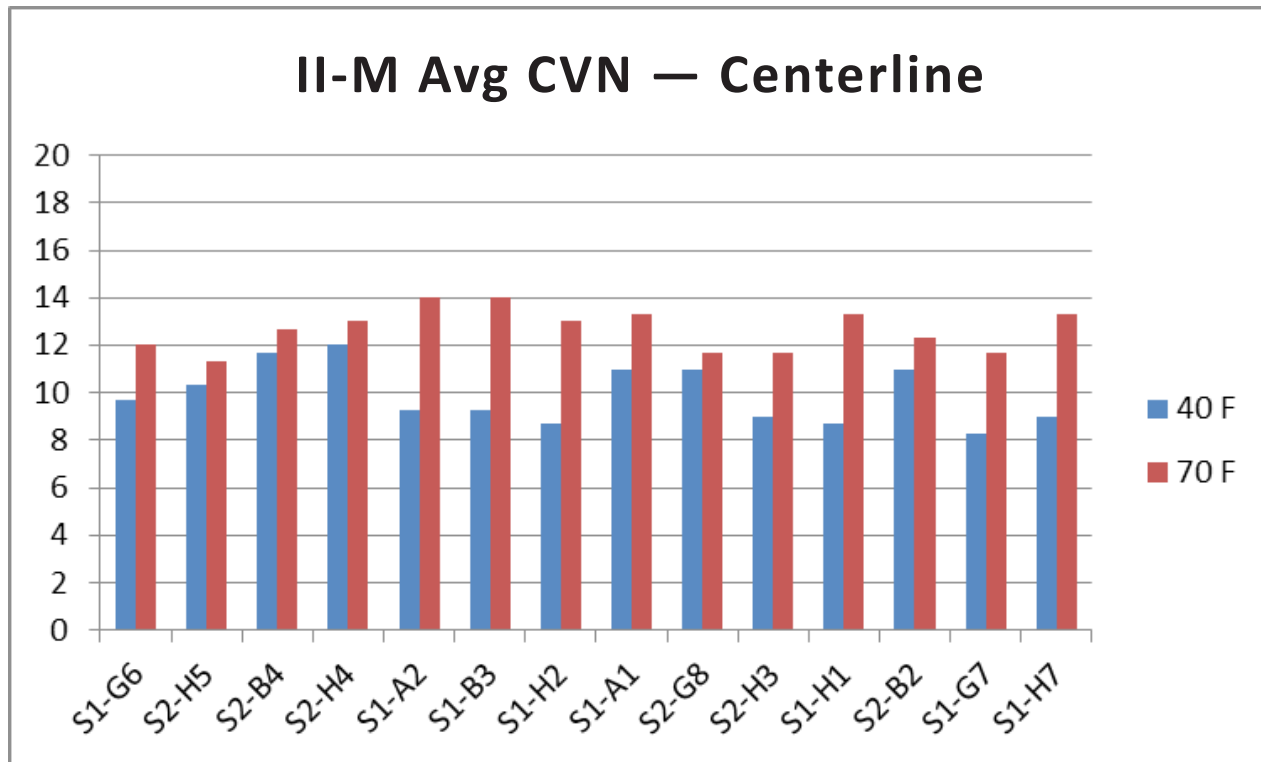


Figure 2.2-28: Centerline CVN



Coupon Tensile Testing

The tensile and yield strength values were found to be in conformance with the minimum values required by the ASTM requirements; however, the sample from rod S1-H1 failed with 13% elongation while the rest were close to the minimum elongation requirements. It is noted that Rod S2-B2 is from the same material heat (MJF-31) as Rod S1-H1, and the sample from Rod S2-B2 had 16.5% elongation. The maximum elongation for samples from all rods was found to be 16.5%. See Table 2.2-5.

Table 2.2-5: Coupon Tensile Testing Results, Test II-M

ASTM Req.	Tensile Strength (psi)	Yield Strength (psi)	Elongation (%)	Reduction of Area (%)
	Min. 140000	Min. 115000	Min. 14%	Min. 40%
S1-G6	159000	134000	15%	47.8%
S2-H5	162000	139000	15%	44.5%
S2-B4	167000	145000	14%	45.0%
S2-H4	163000	140000	15%	46.2%
S1-A2	156000	131000	16.5%	46.8%
S1-B3	161000	137000	15%	46.5%
S1-H2	163000	142000	15.5%	47.4%
S1-A1	159000	133000	15%	44.8%
S2-G8	162000	140000	14.5%	46.8%
S2-H3	165000	142000	15%	46.2%
S1-H1	170000	149000	13%	42.1%
S2-B2	160000	137000	16.5%	47.4%
S1-G7	160000	138000	14%	44.1%
S1-H7	160000	135000	15%	46.6%

2.2.4 M-Shapes

During hardness testing of the rods, the general shape of the hardness readings indicated a softer core and increasingly harder material toward the edges. Some rods appeared to have lower hardness values immediately adjacent to the edges of the rod; together, the values formed what is referred to as “M-Shape” hardness profile across the diameter of the rod. M-Shape hardness profile testing was performed to determine whether the observed hardness profiles near the edge of the A354BD rods on the SAS Bridge are accurate or a result of testing procedure.

Testing Procedure

For this purpose, two rods that represented extreme examples of M-Shaped hardness profiles, as determined by previous HRC measurements on cross-sections, were selected by the Augmented Design Team:

- Rod ID 7-II-E-028 (PWS Anchor Rods, Rolled Threads, 3.5” diameter)
- Rod ID 13-II-cE-9 (Tower Anchor Bolt, Cut Threads, 4” diameter)

The Rockwell C Hardness method is based on the penetration of a conical diamond indenter into the surface of a specimen under fixed load. As a result, any motion of the surface might produce invalid results. In cases of threaded rods, some of these edges have insufficient support, which may cause rocking or flexing of the specimen; this will add to the travel distance of the indenter, thereby producing a lower hardness value. A procedure was established to evaluate the rod without being concerned about the rocking effect.

Using water jet methods, one rectangular solid specimen was cut from each of the cross sections previously used to determine Test II hardness profiles. These specimens were cut to be 0.4 in. × 0.4 in. × T (thickness of disc); see Figure 2.2-29 and Figure 2.2-30. These specimens were cut so that one surface (Surface A in Figure 2.2-29) was parallel to the outer edge of the original cross-section at a depth of 0.1 in. ± 0.05 in. and the opposite surface (Surface B) was at a depth of 0.5 in. ± 0.05 in. The cut made by the water jet method was measured to be about 0.01 inches in width.

Figure 2.2-29: Specimens Layout, per Test Procedures

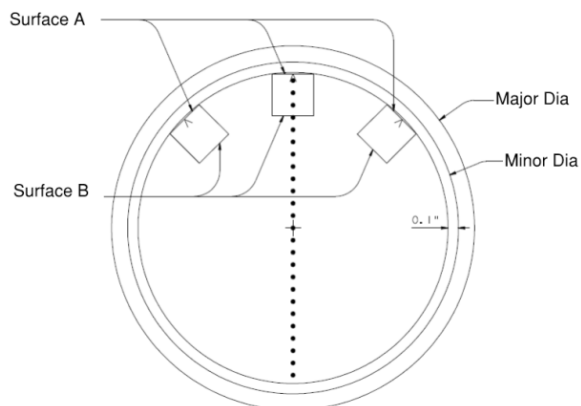
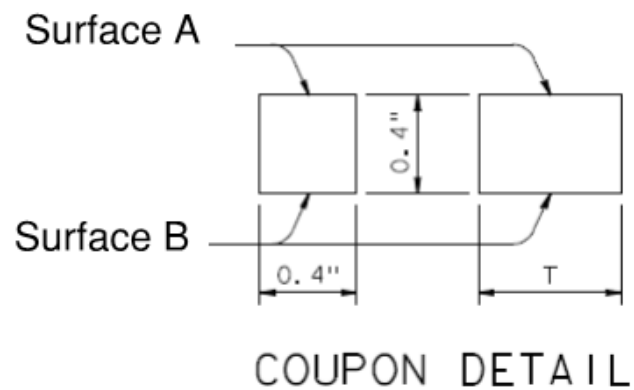


Figure 2.2-30: Sample Coupon

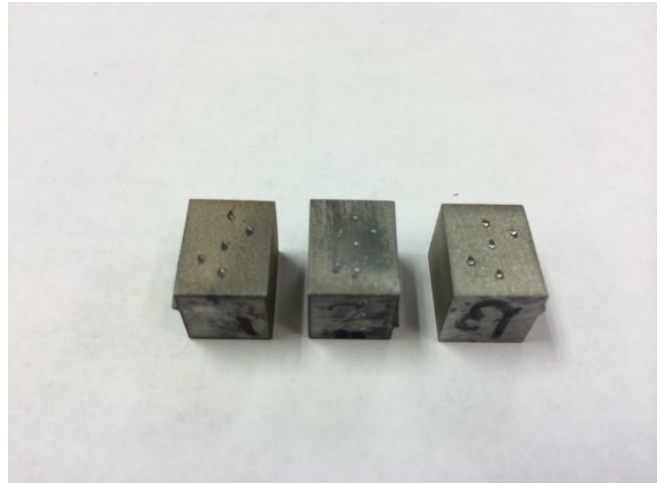


Five HRC measurements were taken on Surface A, per ASTM E18. Surface A was then sanded to achieve a smooth surface without any HRC impressions. Five additional HRC measurements were taken on Surface B, per ASTM E18. See Figure 2.2-31 and Figure 2.2-32 for laboratory specimens extracted. Surfaces A and B were then compared to the hardness values previously measured on cross-sections at 0.1 in. and 0.5 in. during Test II.

Figure 2.2-31: Group 7 Sample with Cut Samples



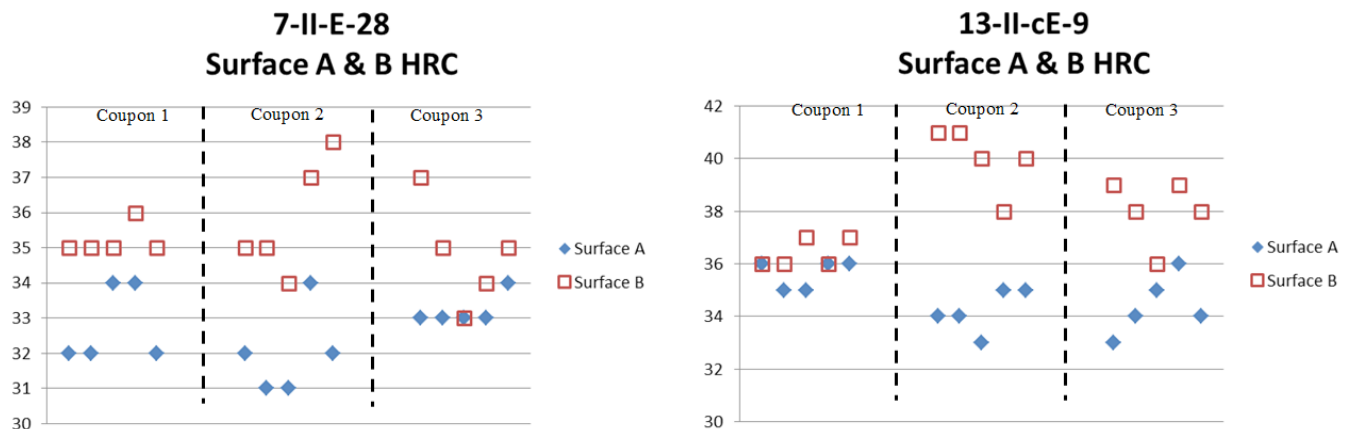
Figure 2.2-32: Group 7 Coupon



Test Results Summary

The hardness values of Surface A and Surface B are shown in Figure 2.2-33 for both rods. In both cases, Surface B indicated higher hardness values than Surface A.

Figure 2.2-33: Group 7 HRC Readings on Surfaces A and B



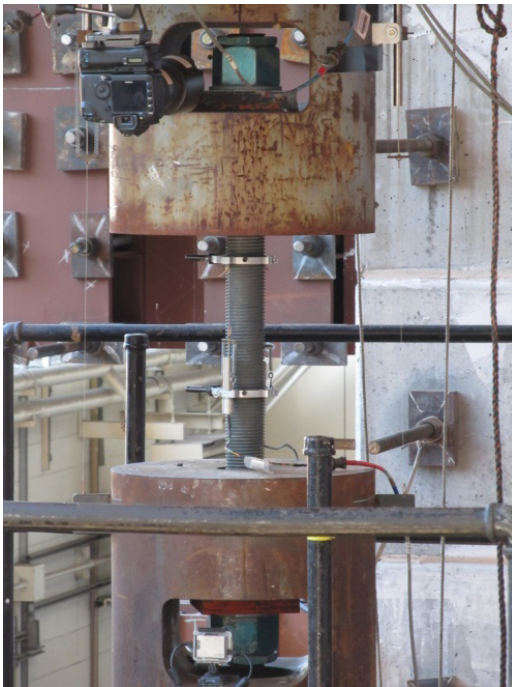
The hardness measurements at 0.1 inches and 0.5 inches below the thread root confirmed those determined by the “M-Shape” profile in cross-section since Surface B showed a higher average value than Surface A and the results were not an artifact or error in the hardness profiles of these two specimens.

For the full report of the testing results, please refer to Appendix J.

2.2.5 Test III: Full-Diameter Tension Test

The full-diameter tension test (Test III) was initiated to further analyze the A354BD rods and to correlate the mechanical properties to tensile strengths. The fractured specimens were also used to perform in-depth fracture analysis to better understand the fracture mechanisms. It was expected that the full-diameter testing would provide a better baseline for comparing the failed 2008 rods to the other rods.

Figure 2.2-35: Full-Size Tensile Testing at Laboratory

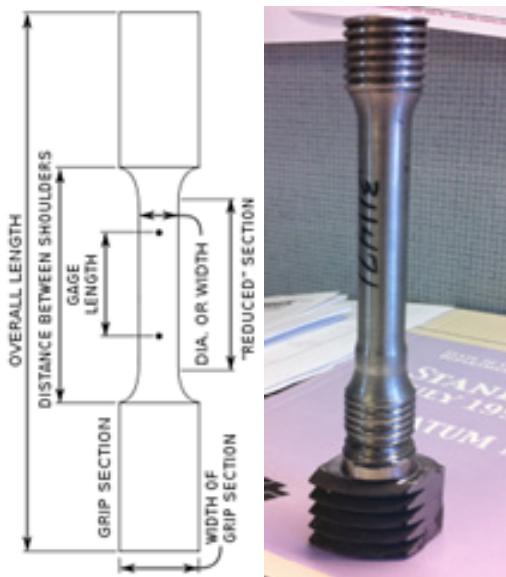


For samples that were being tested full-diameter, the load was applied axially through sufficient thread engagement to develop full strength of the product until failure. The acceptance criteria for full-diameter testing is specified by ASTM A354, Table 3, where the yield and tensile strength are the only measurements evaluated.

Coupon Tensile Test

Coupon tensile testing is a reduced-size tensile test, per ASTM F606, using specimens with diameters of 0.5 in. and gage lengths of 2 in. (as shown in Figure 2.2-36). The load is applied axially until failure. After failure, the two pieces are fitted closely together and the overall length measured for elongation. The diameter is measured at the point of failure to determine the reduction of area.

Figure 2.2-36: Schematic of Coupon (Left), and Actual Test III Coupon (Right)



The acceptance criteria for coupon tension testing are specified by ASTM A354, as shown in Table 2.2-6.

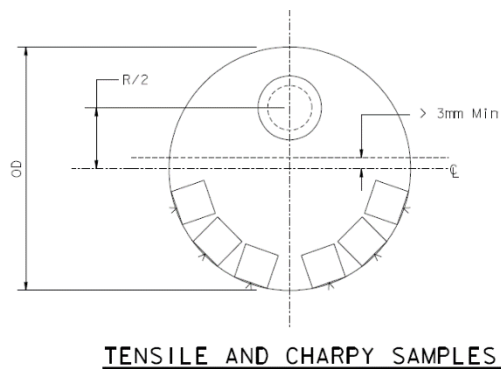
Table 2.2-6: ASTM A354 Mechanical Requirements

Grade	Size, In.	Tensile Strength, min, psi	Yield Strength (0.2% offset), min, psi	Elongation in 2 in. min, %	Reduction of Area, min, %
BC	1/4 to 2-1/2, incl	125 000	109 000	16	50
BC	Over 2-1/2	115 000	99 000	16	45
BD	1/4 to 2-1/2, incl	150 000	130 000	14	40
BD	Over 2-1/2	140 000	115 000	14	40

Charpy V Notch Test

Similar to Test II, the test was performed at 40°F and 70°F on samples removed from the closest region to the surface of the rod, as seen in Figure 2.2 - 37. Refer to Section 2.2.2 for sample extraction and testing procedure details. The rod in Group 14 did not have enough material to extract samples for this test.

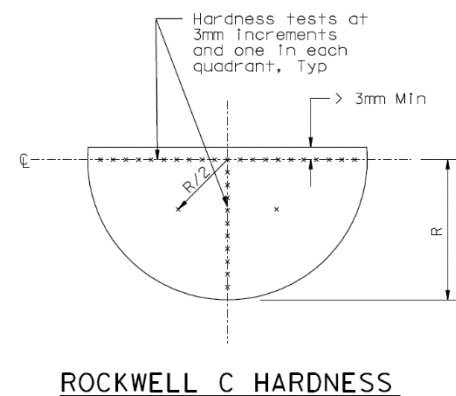
Figure 2.2-37: Tensile and Charpy Sample Layout



Rockwell C Hardness

Similar to Test II, the readings were performed in 3-mm increments across the diameter, beginning 3 mm from the circumference of the rod, and along a radial traverse perpendicular to the full-diameter measurements as shown in Figure 2.2-38. Refer to Section 2.2.2 for testing procedure details.

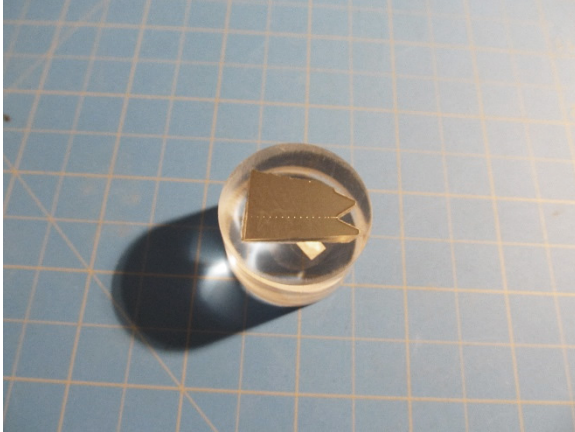
Figure 2.2-38: Rockwell C hardness Testing Layout



Knoop Micro-Hardness

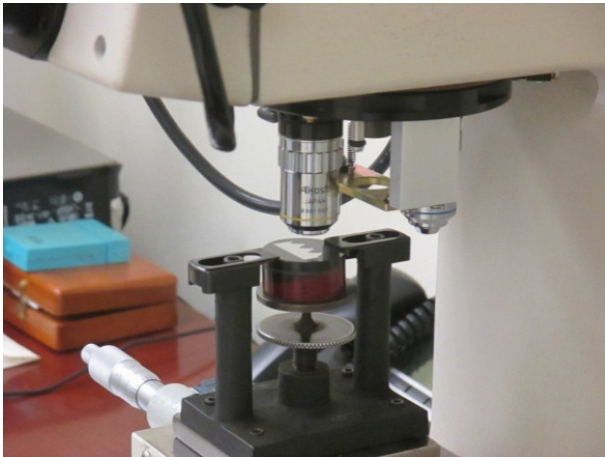
Knoop micro-hardness testing was performed per ASTM E384 specifications. Readings were taken along the same line as the HRC readings, evaluating the microhardness of material by applying a 500-gram load into the material and creating a small diamond indentation. The indenter tip is an extended pyramid diamond. The diagonal length of these indentations is measured. The indentations are shown in Figure 2.2-39.

Figure 2.2-39: Knoop Hardness Coupon



To perform this test, the surface profile was prepared per ASTM E3. Knoop Hardness samples require a mirror finish attained by following the recommended practice for preparing cross sections of metal for microscopic examination. See Figure 2.2-40.

Figure 2.2-40: Knoop Hardness Testing



Metallurgical and Fracture Analysis

After full-size testing of the rods, the fracture surface was visually assessed to detect the various zones of fracture: fracture initiation, fracture propagation, and the final fracture.

The types of failure observed on the rod fracture surfaces were evaluated using Scanning Electron Microscopy (SEM), which generates images based on the interaction of the electrons with the material. Images of the fracture surface were analyzed for fracture type as a result of tensile overload, which was represented by dimples and cleavage morphology. Additionally, the homogeneity of the material was analyzed by looking for banded features or inclusions. See Figure 2.2-41 for a typical microscope used for metallurgical analysis.

Figure 2.2-41: Scanning Electron Microscope

Chemical Analysis

Chemical analysis was performed using the Optical Emissions Spectroscopy (OES) and Inductively Coupled Plasma Mass Spectroscopy (ICP) methods. In accordance with A354BD standards, the material was tested for carbon, manganese, phosphorus, and sulfur. In addition to the ASTM requirements, the rods were tested for aluminum, chromium, cobalt, niobium, copper, molybdenum, nickel, silicon, sulfur, titanium, and vanadium.

Zinc Coating Analysis

The galvanized layer of the rods was also tested using the ICP method in order to check for chemical composition of the material.

Summary of Results

For the full report of the testing results, please refer to Appendix J.

Full-Diameter Tensile Test

All full-diameter tests were in conformance with A354BD requirements for tensile strength. See summary of tensile strength results in Table 2.2-7. The full-diameter tensile strengths correlate with the reduced-size tensile strengths.

Table 2.2-7: Full-Diameter Tensile Strength Results, Test III

		Test III Tensile Strength (psi)	ASTM Min. Req. (psi)
Group 2	Sample 1	158300	140000
	Sample 2	158300	140000
	Sample 3	157900	140000
	Sample 4	158400	140000
Group 3	Sample 1	156300	140000
	Sample 2	153900	140000
	Sample 3	156500	140000
	Sample 4	157800	140000
Group 4	Sample 1	158400	150000
	Sample 2	157200	150000
Group 7	Sample 1	158600	140000
Group 8	Sample 1	151300	140000
Group 11	Sample 1	167000	140000
Group 12	Sample 1	158850	140000
Group 14	Sample 1	150400	140000

Coupon Tensile Test

All coupon tensile tests were in conformance with A354BD requirements for tensile strength, yield strength, elongation, and reduction of area. See summary of results in Table 2.2-8.

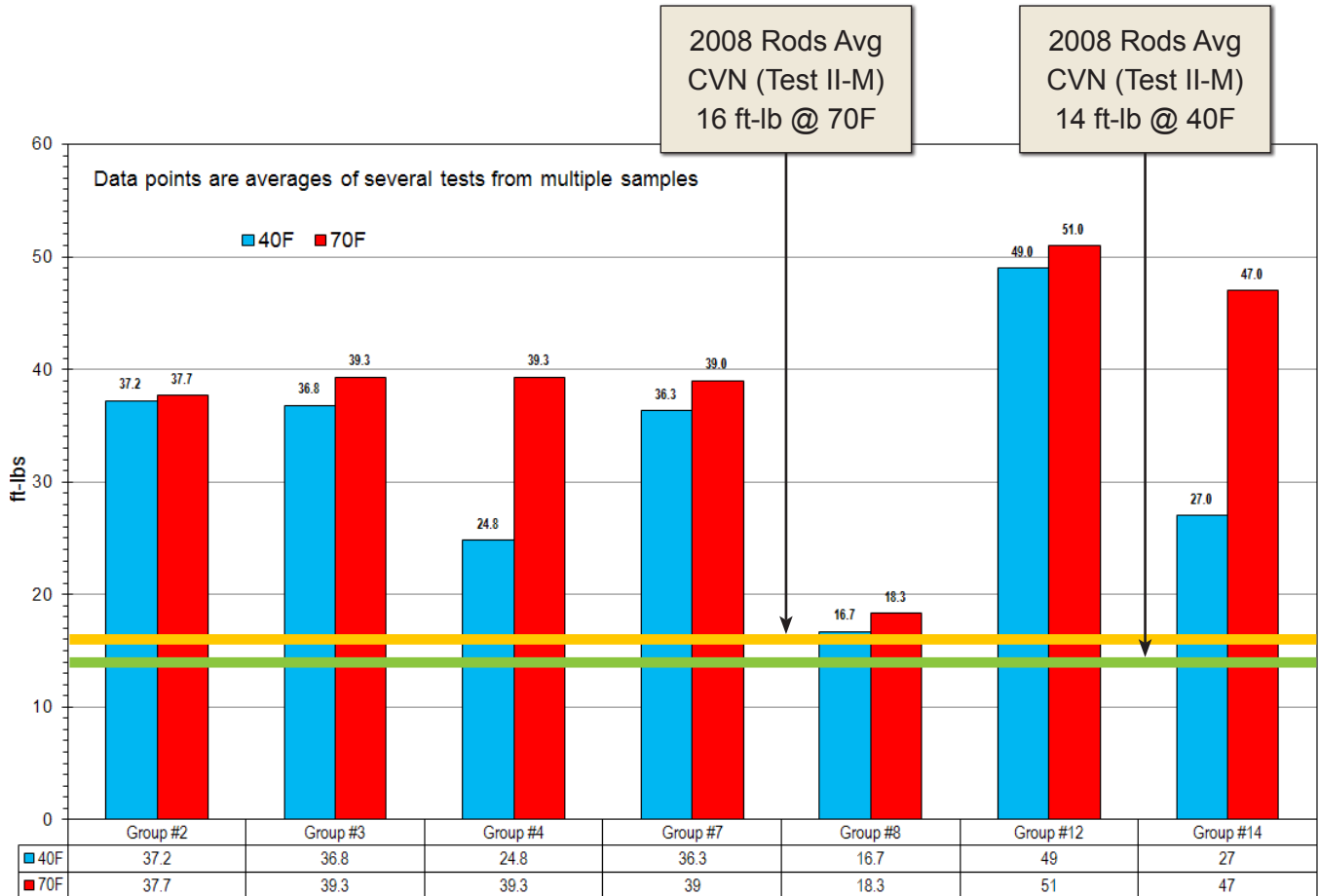
Table 2.2-8: Coupon Tensile Strength Results, Test III

	ASTM Req.	Tensile Strength (psi)	Yield Strength (psi)	Elongation (%)	Reduction of Area (%)
		Min. 140000 (except Group 4 Min 150000)	Min. 115000	Min. 14%	Min. 40%
Group 2	Sample 1	160000	140000	17.0%	53.5%
	Sample 2	157000	138000	19.0%	53.4%
	Sample 3	157000	139000	17.5%	54.0%
	Sample 4	160200	143100	16.8%	52.3%
Group 3	Sample 1	156300	140900	18.5%	54.3%
	Sample 2	157600	138900	19.0%	54.6%
	Sample 3	156400	137800	17.5%	53.9%
	Sample 4	159100	141200	18.0%	53.0%
Group 4	Sample 1	159900	146700	17.0%	50.4%
	Sample 2	156600	144400	15.0%	46.6%
Group 7	Sample 1	158300	138800	17.0%	53.1%
Group 8	Sample 1	161500	136400	17.0%	49.3%
Group 12	Sample 1	163300	147600	17.0%	54.8%

Charpy V Notch Test

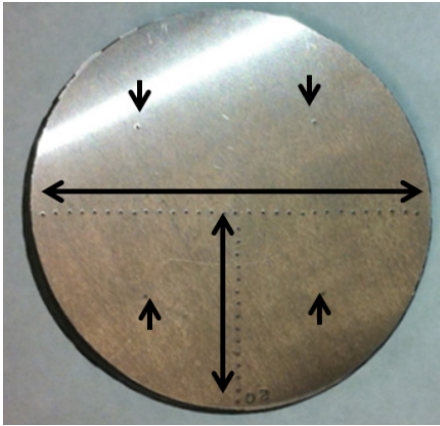
The lowest observed values were found in Group 8. See Figure 2.2-42 for a summary of the results. For a comparison, see Figure 2.2-16, which summarizes the CVN results from Test II and Test II-M. The ASTM A354 specifications do not require CVN testing, so there are no defined acceptance criteria.

Figure 2.2-42: Average CVN Values, Test III and Circumferential Values of 2008 Rods from Test II-M



Rockwell C Hardness

All samples were tested for HRC and the results are shown in Appendix A. The hardness values were typically lower at the cores of the rods than close to the edges. All average hardness values of the rods met the ASTM A354 requirement at mid-radius. The locations tested are shown in Figure 2.2-43.

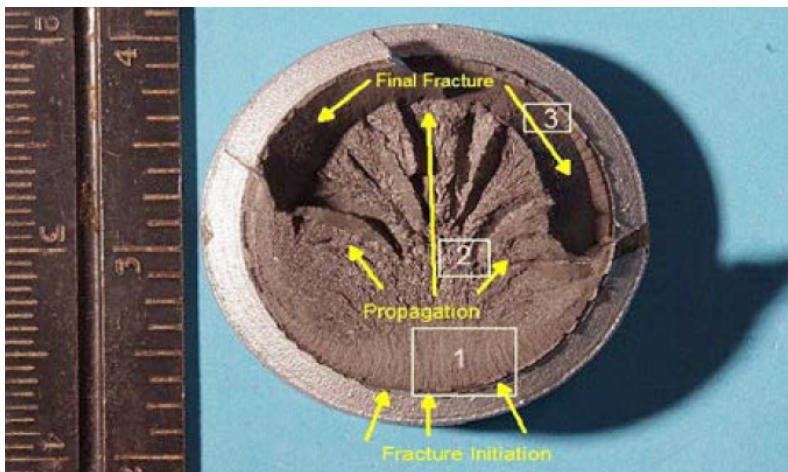
Figure 2.2-43: HRC Readings, Test III

Knoop Micro-Hardness

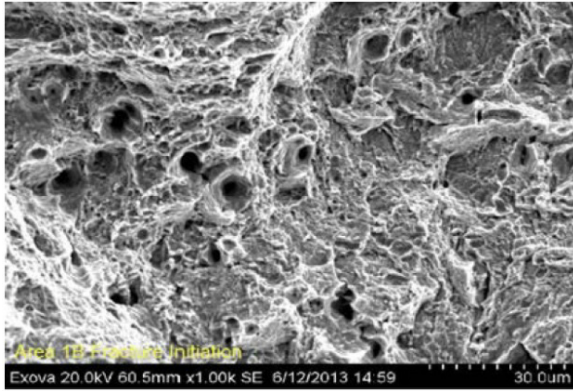
Since Knoop micro-hardness comes from a small indentation, it is more sensitive to surface and microstructural features. This provides a larger range of readings, so the Knoop micro-hardness results are not as uniform as the HRC readings. Additionally, there are no ASTM acceptance criteria requirements for Knoop micro-hardness in A354BD specifications. The test was performed for comparison purposes with the HRC measurements through conversion and they were found to be in correlation with the HRC values.

Metallurgical and Fracture Analysis

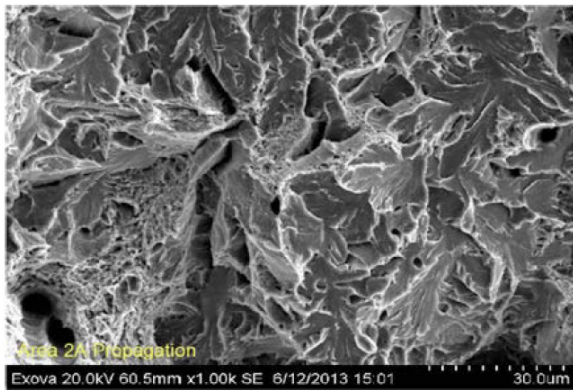
SEM analysis was performed on all of the fractured surfaces after full-diameter tension testing. The zones of fracture were identified and divided between fracture initiation, propagation, and final fracture, as shown in Figure 2.2-44. All rods tested were found to have similar features.

Figure 2.2-44: Fracture Surface Zones

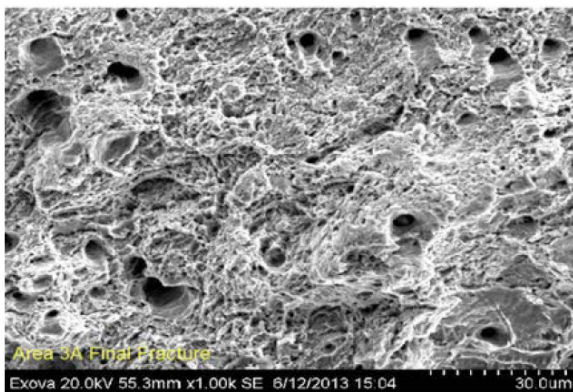
Based on the morphology of the fracture surfaces, initiation of the failures of all of the rods was due to ductile tearing, although later stages of the fracture involved some cleavage. As shown in Figure 2.2-45, the fracture initiation zone shows dimples or “cup and cone” features typical of ductile fracture; in this area, these features indicate that failure was caused by tensile overload.

Figure 2.2-45: Fracture Initiation Zone (30 μm)

As the crack propagates, the propagation area shows fracture features of both cleavage and ductility (see Figure 2.2-46).

Figure 2.2-46: Fracture Propagation Zone (30 μm)

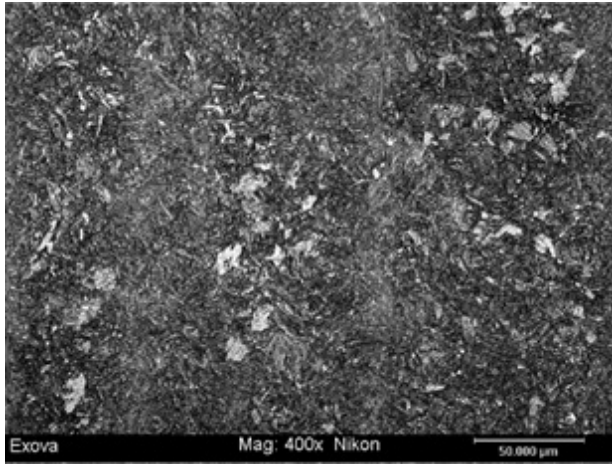
The final fracture zone shows dimpled ductile tearing (as shown in Figure 2.2-47). Final fracture occurs when the remaining material is insufficient to sustain the applied load.

Figure 2.2-47: Final Fracture Zone (30 μm)

The micro-images of the material indicated an essentially tempered martensitic structure across the diameter. However, there were some vertical banded features present that indicated a nonhomogeneous material. These features are identified by the alternating dark and light color sequence, as shown in Figure 2.2-48. Evaluation of micrographs from Test III, and from the post-fracture analysis phase of Test IV, indicates that the banding is common

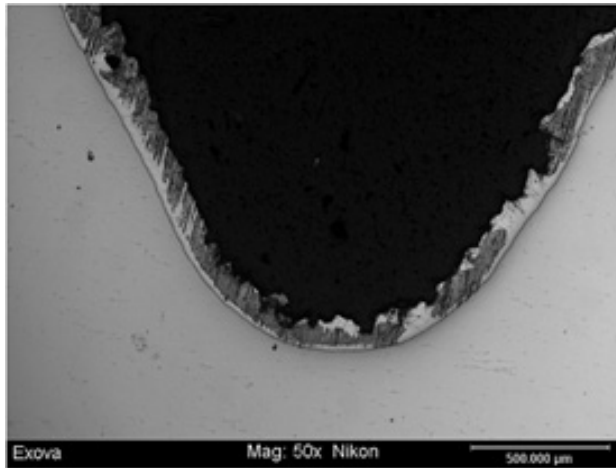
in 3-inch diameter A354 BD rods made of SAE 4140 steel. The non-homogeneity of the material, which causes the banding, is a probable result of minor variations in the chemical composition of the steel coupled with variations of temperature across the diameter during various heat treatment steps.

Figure 2.2-48: Banded Features (50,000 μm)



An examination was performed on selected thread roots adjacent to the fracture surface, such as is shown in Figure 2.2-49.

Figure 2.2-49: Thread Root Examination (500,000 μm)



Chemical Analysis

In accordance with ASTM A354, the material is to be tested for carbon, manganese, phosphorus, and sulfur. In addition to the ASTM requirements, the rods were tested for aluminum, chromium, cobalt, niobium, copper, molybdenum, nickel, silicon, sulfur, titanium and vanadium. All spectrochemical testing of the steel substrate was found to be in conformance with the A354BD chemical requirements.

2.2.6 Test III Modified (III-M)

The testing was similar to Test III but performed on pieces extracted from Pier E2 shear key anchor rods. Test III-M was performed in order to determine basic mechanical properties (hardness and toughness) and characterize the chemical composition of the rods that had already failed in service. The intent of this testing was to contribute to the analysis of the root cause of failure and for comparison with the other A354BD rods. Test III-M

consisted of Rockwell C Hardness testing, chemical analysis, CVN testing, coupon tensile testing, and full-diameter tensile testing.

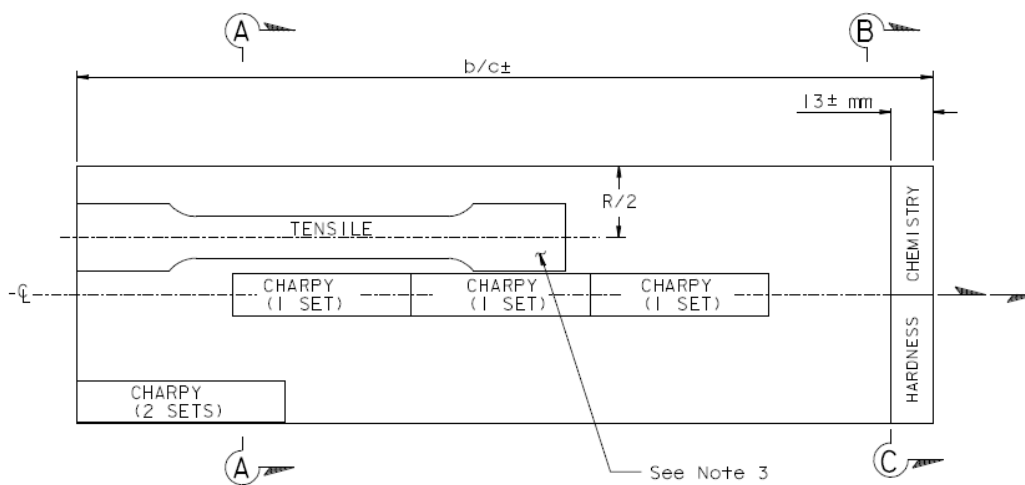
Rod Selection

The rods from Group 1 (Pier E2 Shear Key (S1/S2) Anchor Rods (2008) – Bottom) were extracted after fracture and the pieces were sequentially numbered. The threaded Pieces A and D of Rod S1-H3, Item 08-01, were tension tested (full-diameter) and the shank Pieces C and D from the same rod were used to obtain samples for the other tests. Pieces A and B were from the top of the rod, and Pieces C and D were from the bottom of the rod. Group 1 rods had not been tested previously in Test I through III; Test II Modified and III Modified were designed to address these specific rods.

Test Methods

The coupons were extracted per Figure 2.2-50 for each test: one tensile coupon, four sets of Charpy specimens, minimum of one chemical sample, and hardness readings across the diameter.

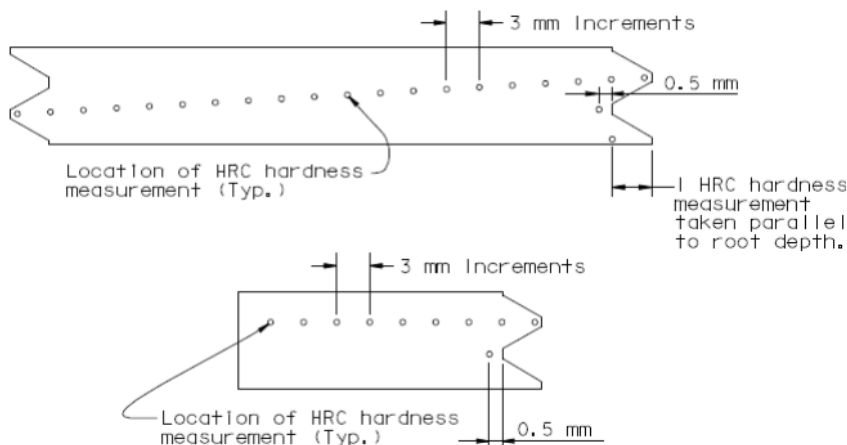
Figure 2.2-50: Test Coupon Locations on Rods



HRC Hardness

The hardness readings were performed along two perpendicular traverses. The readings for the HRC measurements were separated by 3 mm throughout the entire cross-section; see Figure 2.2-51.

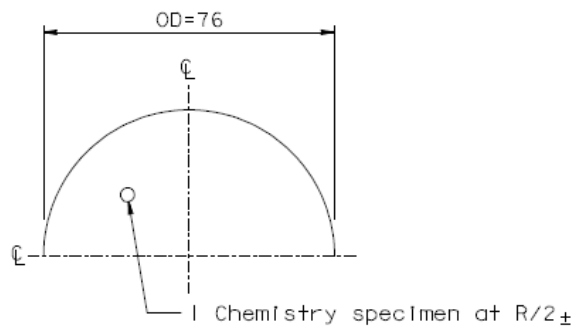
Figure 2.2-51: Hardness Measurements



Chemical Test

Chemistry samples were removed at mid-radius (see Figure 2.2-52). The laboratory used a minimum of three samples to ensure the accuracy of the results.

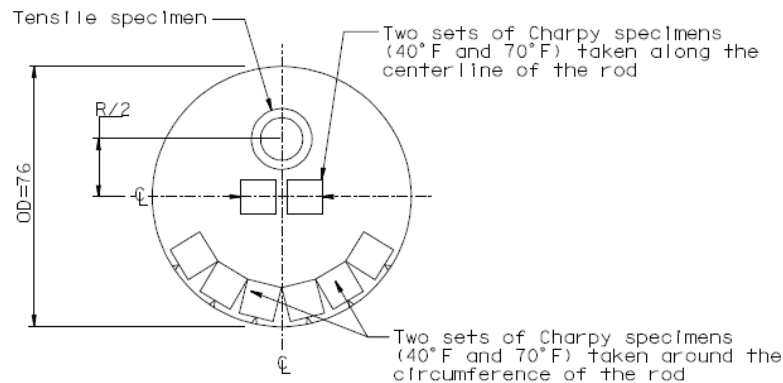
Figure 2.2-52: Chemistry Sample



Charpy V Notch Test

Four sets of Charpy specimens were removed from the rod — two sets were from the centerline longitudinal to the rod axis and two sets were from around the circumference of the rod; see Figure 2.2-53. The tests were performed at 40°F and 70°F. Refer to Section 2.2.2 for sample extraction and testing procedure details.

Figure 2.2-53: Tensile Coupon and CVN Sets



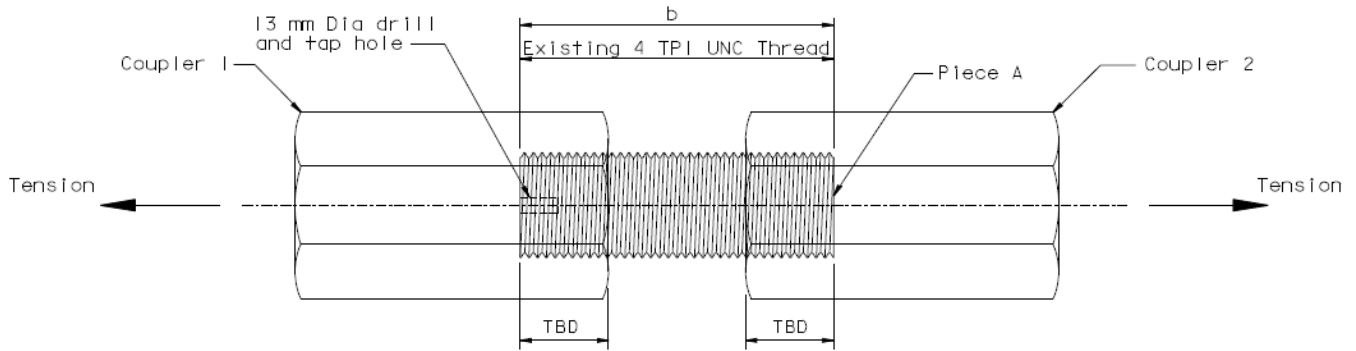
Coupon Tensile Test

Tensile specimens were extracted at mid-radius. See Figure 2.2-53. All samples were cut by EDM and then machined down.

Full-Diameter Tensile Test

The shanks were threaded to engage into the couplers used in testing set-up (see Figure 2.2-54) in preparation for full-diameter testing. The samples were instrumented to provide load-displacement curves and record the load and displacement at failure. The samples were then loaded to failure.

Figure 2.2-54: Full-Diameter Tensile Test



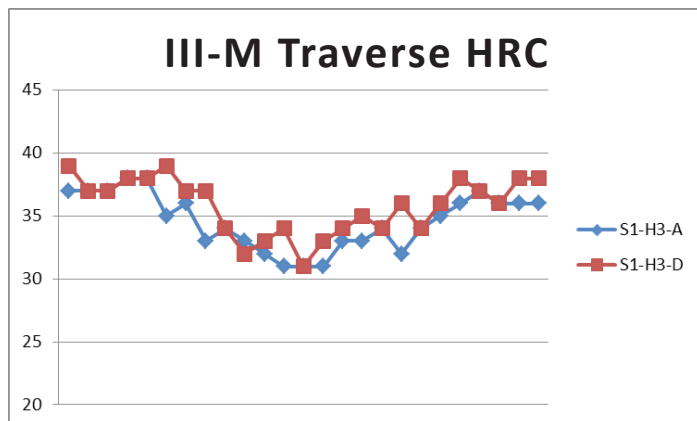
Summary of Results

For the full report of the testing results, please refer to Appendix J.

Rockwell C Hardness Testing

The HRC acceptance criteria for A354BD are at mid-radius. Although the results are at the higher end of the range of conformance, the results at mid-radius are in conformance. See Figure 2.2-55 for reference.

Figure 2.2-55: Test III-M Traverse HRC Measurements



Chemical Analysis

The results of the chemical analysis were in conformance with the A354BD requirements. See Table 2.2-9 for reference.

Table 2.2-9: Test III-M Chemical Analysis

	ASTM Req	S1-H3-A	S1-H3-D
Al	-	<0.005	<0.005
C	0.33–0.55	0.43	0.42
Cr	-	1	1.01
Co	-	0.01	0.01
Cb	-	<0.005	<0.005
Cu	-	0.21	0.21
Mn	Min 0.57	0.96	0.96
Mo	-	0.16	0.16
Ni	-	0.1	0.1
P	Max 0.040	0.012	0.012
Si	-	0.23	0.23
Si	Max 0.045	0.039	0.042
Ti	-	<0.005	<0.005
V	-	0.03	0.03

Charpy V Notch Test

See Figure 2.2-56 and Figure 2.2-57 for a summary of the results. For a comparison, see Figure 2.2-16, which summarizes the CVN results from Test II and Test II-M. The ASTM A354 specifications do not require CVN testing, so there are no defined acceptance criteria.

Figure 2.2-56: Circumference CVN

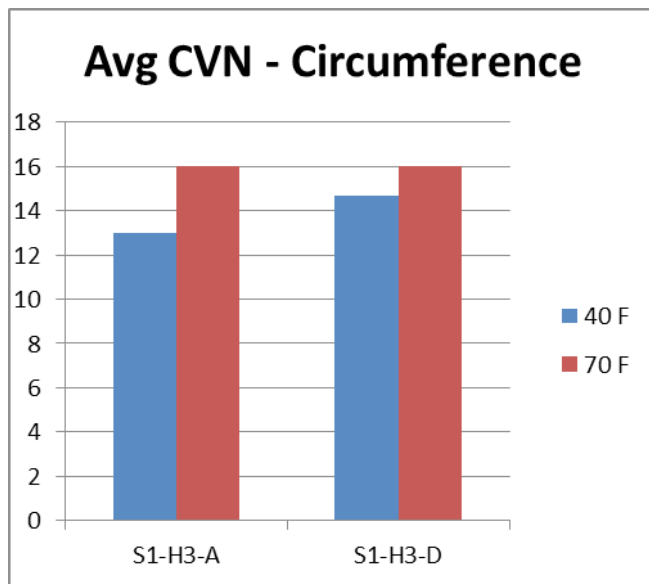
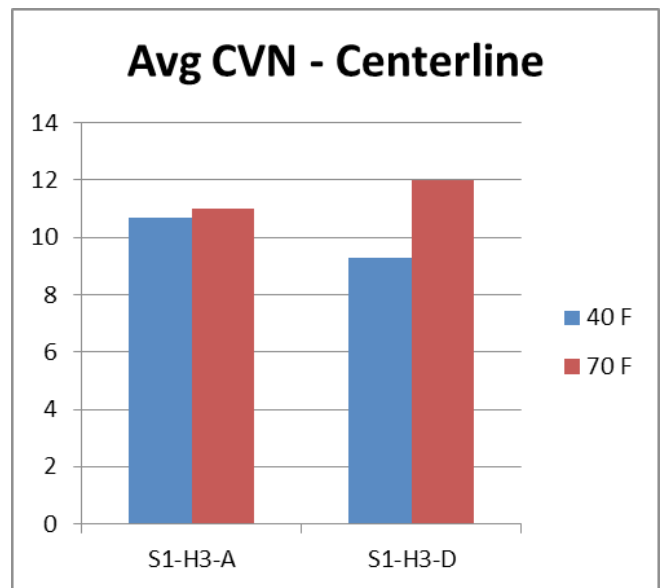


Figure 2.2-57: Centerline CVN



Coupon Tensile Testing

The mechanical testing performed on the rods was found to be in conformance with ASTM requirements. The elongation and reduction of area were closer to the limit, which may indicate brittle characteristics. See Table 2.2-10 for a summary of results.

Table 2.2-10: Coupon Tensile Testing Results, Test III-M

ASTM Req.	Tensile Strength (psi)	Yield Strength (psi)	Elongation (%)	Reduction of Area (%)
	Min. 140,000	Min. 115,000	Min. 14%	Min. 40%
S1-H3-A	159,000	133,000	14.5%	46.0%
S1-H3-D	160,000	135,000	15%	48.2%

Full-Diameter Tensile Testing

For the full-diameter tensile tests, full-diameter samples were pulled to failure. The tension test is performed similar to Test III by placing the samples in controlled tension until failure, in accordance with ASTM F606. Both rods met the minimum requirement for A354BD. See Table 2.2-11.

Table 2.2-11: Full Size Tensile Testing Results, Test III-M

ASTM Req.	Tensile Strength (psi)
	Min. 140,000
S1-H3-A	159,631
S1-H3-D	162,981

2.2.7 Summary

Table 2.2-12 provides a summary of the mechanical properties based on Tests I, II, III, and III-M.

Table 2.2-12: Test I, II, III, and III-M Results Summary

		Summary of Tests I, II, III, and III-M (all rods)			
		2006 Rods	2008 Rods	2010 Rods	2013 Rods
Mechanical Testing	Hardness — Lab (R/2) (HRC)	35	36	34	35
	Hardness — Lab (Edge) (HRC)	34	38	35	36
	Toughness — CVN (ft-lb)	35	14	37	48
	Full Size Tensile (ksi)	159	161	153	162

3. STRESS CORROSION TESTING

3.1 TEST IV — STRESS CORROSION TESTING: “TOWNSEND TEST”

The objective of Test IV is to determine the threshold load levels for hydrogen embrittlement of full-diameter galvanized A354BD rods in the SAS. It is intended that the results will serve as a guide to identifying safe load levels and, if necessary, suggest remedial action for galvanized fasteners exposed to a marine environment on the SAS.

To achieve this goal, full-diameter A354BD rods representing a variety of sizes, compositions, and manufacturing-process variables were exposed to salt water while simultaneously and slowly applying an increasing tensile load until failure. This testing concept is based on 1975 research by Townsend [3] successfully used to determine the effects of galvanized coatings on the thresholds for both internal hydrogen embrittlement (IHE) and environmental hydrogen embrittlement (EHE) of pre-cracked, quenched-and-tempered SAE 4140 steel bars. A main difference is that the 1972 tests used specimens with fatigue pre-cracks, while the Test IV protocol used as-built threaded full diameter rods without introducing intentional pre-cracks.

3.1.1 Test Rig Design

A typical test rig is shown in Figure 3.1-1. The rig shown is intended for testing full-length rods and it includes chambers containing 3.5% sodium chloride (salt) solution surrounding the threaded regions at both ends. This solution is widely used throughout industry for EHE testing of high-strength steels. In addition, a 3.5% sodium chloride solution is considered to be a reasonable simulant of environments that could develop in threaded areas of anchor rods exposed to marine environments if corrosion protective measure were not applied.

In cases where full-length rods were not available for testing, a smaller, threaded-end segment of the rod was tested in a single wet chamber located at the dead end of the rig at the left in Figure 3.1-1, with the load applied to a coupled jacking rod at the stressing end of a shorter test rig. Detailed drawings of all test rigs are included in Appendix K.

Tensioning of the rods is similar to the method used to load rods on the SAS. Hydraulic jacks, shown at the stressing end to the right in Figure 3.1-1, were used to apply a tensile load above the target level. The nut is then snug-tightened and the hydraulic pressure is released to allow the rod to seat itself within a tolerance of -0/+10 kips of the target load. Strain gauges are used to monitor the load on the rods during the load application and throughout the entire duration of Test IV.

During all tests except the last two tests without wet chambers, electrode potential with respect to a reference electrode and the pH of the test solution were monitored. For Rods 1 to 4 only, electrode potentials were continuously measured against a hot dip galvanized A325 bolt, and these potential measures were verified in the laboratory in the ensuing post-fracture analysis against a saturated calomel electrode (SCE). For Rods 1 to 4 only, pH values were continuously measured by a pH probe, but the measurement bulb on the pH probes accumulated a deposit from the test solution and did not match measurements with pH paper. For the remaining tests, pH and potential were measured manually by use of pH paper and SCE at each load step.

Deliberate coating defects, also referred to as intentional holidays, were placed in the thread roots of three consecutive threads at the region of the initial engagement with the nut by use of a diamond impregnated wire. The intentional holidays were intended to locally remove the galvanized coating and to promote the galvanic deposition of hydrogen on the steel surfaces at the roots of threads.

In the case of full-length rods with wet chambers at both ends, the defects were introduced around the full circumference of the first three engaged threads at the dead end only. For the shorter rods with wet chambers only at the dead end, the defects were introduced only to the top third of the circumference of the first three engaged threads.

Other features of Test IV include:

- Two sets of four strain gauges were mounted at 90-degree intervals around the rod circumference to detect axial and bending stresses.
- Elongation and rotation during jacking were measured by use of displacement transducers at the stressing end.
- Temperatures of the rods, the test solution, and the ambient air were continuously monitored by use of thermocouples.
- Acoustic emission (AE) sensors were placed to provide warnings when final fracture was about to occur, thus providing safety to test personnel as a primary objective. A secondary objective was to assess if AE can detect the onset of cracking.
- The test rigs were surrounded with sand bags, steel plates, and k-rail for safety purposes.
- The test rigs were sheltered from rain and direct sunlight by use of tents.

See Figure 3.1-2 and Figure 3.1-3 for an overall view of the test rigs. Figure 3.1-3 shows tanks of NaCl solution, a siphon system to replenish solution continuously, and access on the stressing end to tighten the nut. Figure 3.1-4 shows the test rig and the rod at the end of the test, after fracture.

Figure 3.1-1: Test Rig for Full-Length Rods

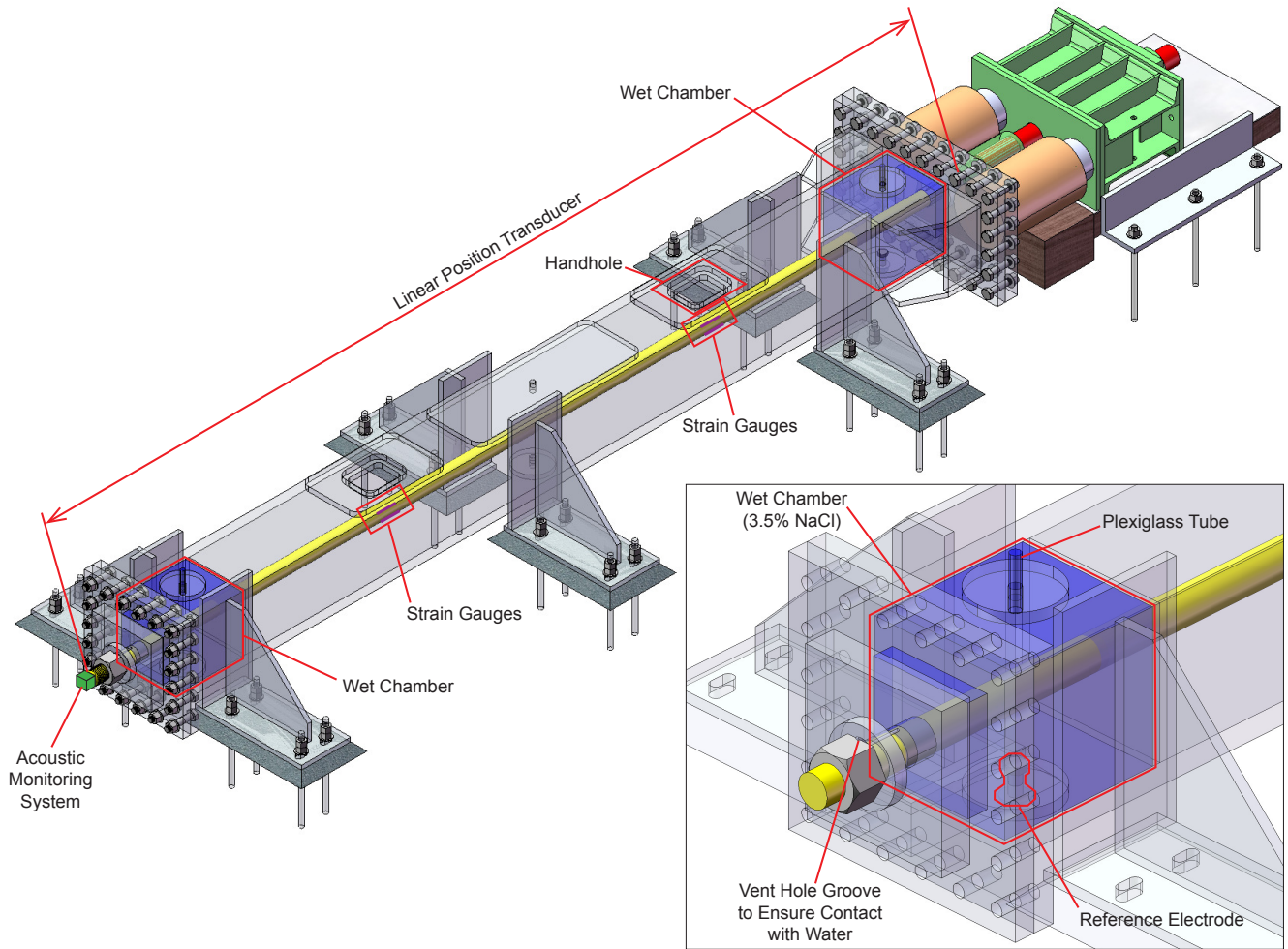


Figure 3.1-2: Test Rig for Full-Length Rods during Setup



Figure 3.1-3: Test IV in Progress under Protective Tent



Figure 3.1-4: Test Rig after Rod Failure Showing the Effects of the Energy Released when Fracture Occurs



3.1.2 Test Protocol

The test protocol was designed based on the work described in the 1975 Townsend publication [3]. Details of the test protocol are included in Appendix K, and the highlights are summarized below.

Table 3.1-1 lists rods selected for Test IV. These included full-length rods when available. The rods ranged in diameter from 2 to 4 inches, with both cut and rolled threads, and both galvanized and ungalvanized. These rods represent a range of steel compositions, steelmaking practices, and fracture toughness.

Prior to testing, all rods were checked for cracks by use of magnetic particle inspection, and cleaned.

Table 3.1-1: Test IV Rods

Group No.	Rod	Identification	Thread Type	Dia. (in)
2	1	Pier E2 Bearing Anchor Rods (2010) — Bottom Rod ID B1-F4	Cut	3
	2	Pier E2 Bearing Anchor Rods (2010) — Bottom Rod ID B2-F5	Cut	3
	3	Pier E2 Shear Key Anchor Rods (2010) — Bottom Rod ID S3-D2	Cut	3
	4	Pier E2 Shear Key Anchor Rods (2010) — Bottom Rod ID S4-E2	Cut	3
4	5	Pier E2 Bearing Rods — Top Housing Spare Rod	Rolled	2
12	6	Tower Anchorage Anchor Rods Vulcan, Rod ID b2W-6	Cut	3
8	7	Tower Saddle Tie Rods Rod ID 5	Rolled	4
7	8	PWS Anchor Rods (Main Cable) Rolled Threads, Rod ID E-118, Heat OYI	Rolled	3.5
	9	PWS Anchor Rods (Main Cable) Rolled Threads, Rod ID W-074, Heat OTD	Rolled	3.5
	10	PWS Anchor Rods (Main Cable) Cut Threads, Rod ID E-036, Heat OTD	Cut	3.5
	11	PWS Anchor Rods (Main Cable) Cut Threads, Rod ID E-110, Heat OOF	Cut	3.5
1	12	Pier E2 Shear Key (S1/S2) Anchor Rods (2008) — Bottom Rod ID S2-A8, Heat MJF-32, Top Threads	Cut	3
	13	Pier E2 Shear Key (S1/S2) Anchor Rods (2008) — Bottom Rod ID S2-A8, Heat MJF-32, Bottom Threads	Cut	3
18	14	Pier E2 2013 Replacement Anchor Rods (CCO 312) Rod ID EB-2-03, Galvanized	Cut	3
	15	Pier E2 2013 Replacement Anchor Rods (CCO 312) Rod ID EB-2-08, Galvanized	Cut	3
	16	Pier E2 2013 Replacement Anchor Rods (CCO 312) Rod ID SK-3-06, Ungalvanized	Cut	3
	17	Pier E2 2013 Replacement Anchor Rods (CCO 312) Rod ID SK-3-13, Ungalvanized	Cut	3
1	18	Pier E2 Shear Key (S1/S2) Anchor Rods (2008) — Bottom Rod ID S1-A7, Bottom Threads, Dry Test	Cut	3
	19	Pier E2 Shear Key (S1/S2) Anchor Rods (2008) — Bottom Rod ID S2-H6, Bottom Threads, Dry Test	Cut	3

The loading schedule for Test IV is shown in Table 3.1-2. The rate of loading is intended to be sufficiently slow to permit diffusion of hydrogen and slow crack growth, yet fast enough to allow testing to be completed within 24 days. The average rate of load increase shown in Table 3.1-2, up to 0.85 Fu, is approximately one-half that used to establish thresholds of one-inch square bars in the 1975 research by Townsend [3]. In those cases, where the load reached 0.85 Fu, or when the onset of crack growth was suspected, the rods were held for six days. After the six-day hold without evidence of cracking, the rods were pulled to failure, which generally occurred above 1.0 Fu.

For all the wet chambers in the test rigs, the spherical washer has a groove to permit venting of the NaCl solution (See Figure 3.1-5). This is to ensure flow of the NaCl solution to the first thread of the nut and remove any trapped air. After verifying the flow of the NaCl solution, the groove is sealed with a piece of closed cell backer rod, which is held in place with plumber’s putty. Because this operation happens with the rod under load, the acoustic emissions (AE) are continuously monitored for safety during this operation.

Figure 3.1-5: Venting of Test Solution



Table 3.1-2: Test IV Loading Schedule for Under and Over 2 1/2" Diameter

Rods with Diameter 2 1/2" and under		
Load %Fu	Stress, ksi	Days
30	45	2
40	60	2
50	75	2
55	83	2
60	90	2
65	98	2
70	105	2
75	113	2
80	120	2
85	128	6

Rods with Diameter over 2 1/2"		
Load %Fu	Stress, ksi	Days
30	42	2
40	56	2
50	70	2
55	77	2
60	84	2
65	91	2
70	98	2
75	105	2
80	112	2
85	119	6

Following the fracture of a rod in a test setup, the fracture surfaces are preserved with the following steps:

1. The fracture surface and adjacent threads are cleaned with water to remove NaCl from the wet chamber solution and sand from the protective sandbags placed behind the rod.
2. The cleaned areas are dried with compressed air, a heat gun, or a blow drier.
3. The dried areas are sprayed with denatured alcohol to capture any residual water.
4. The areas are dried again with compressed air, a heat gun, or a blow drier.
5. The cleaned and dried fracture surfaces are preserved with WD-40 (See Figure 3.1-6).
6. The pieces of the rods with fracture surfaces are stored in an air-conditioned office with additional WD-40 periodically applied until they are sent to a lab for the post-fracture analysis.

Figure 3.1-6: Fracture Preservation Operation



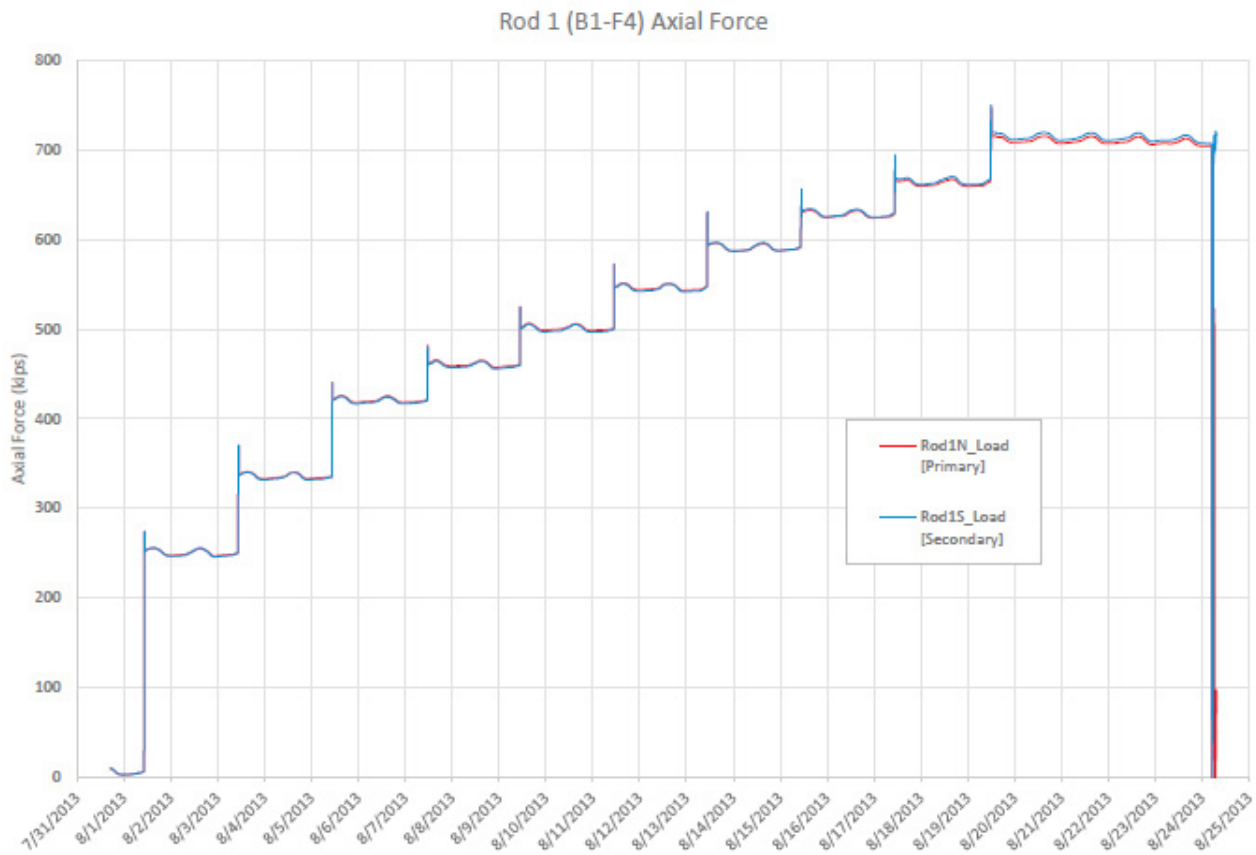
3.1.3 Test Results at Job Site (Phase 1, 2, 3, 4, and 5)

See Appendix K for test data.

A typical loading sequence is shown in Figure 3.1-7. In this case, the load was increased stepwise to 0.85 F_u , where it was held until it fractured after 113 hours.

Figure 3.1-7: Typical Plot of Load vs. Test Time, Showing Step Increases in Load Until Failure at 0.85 Fu (Rod 1)

1330 SE 6th Ave.
Portland, Oregon 97214
Ph (503) 239-6000
Fax (503) 239-6100
www.vgoinc.com



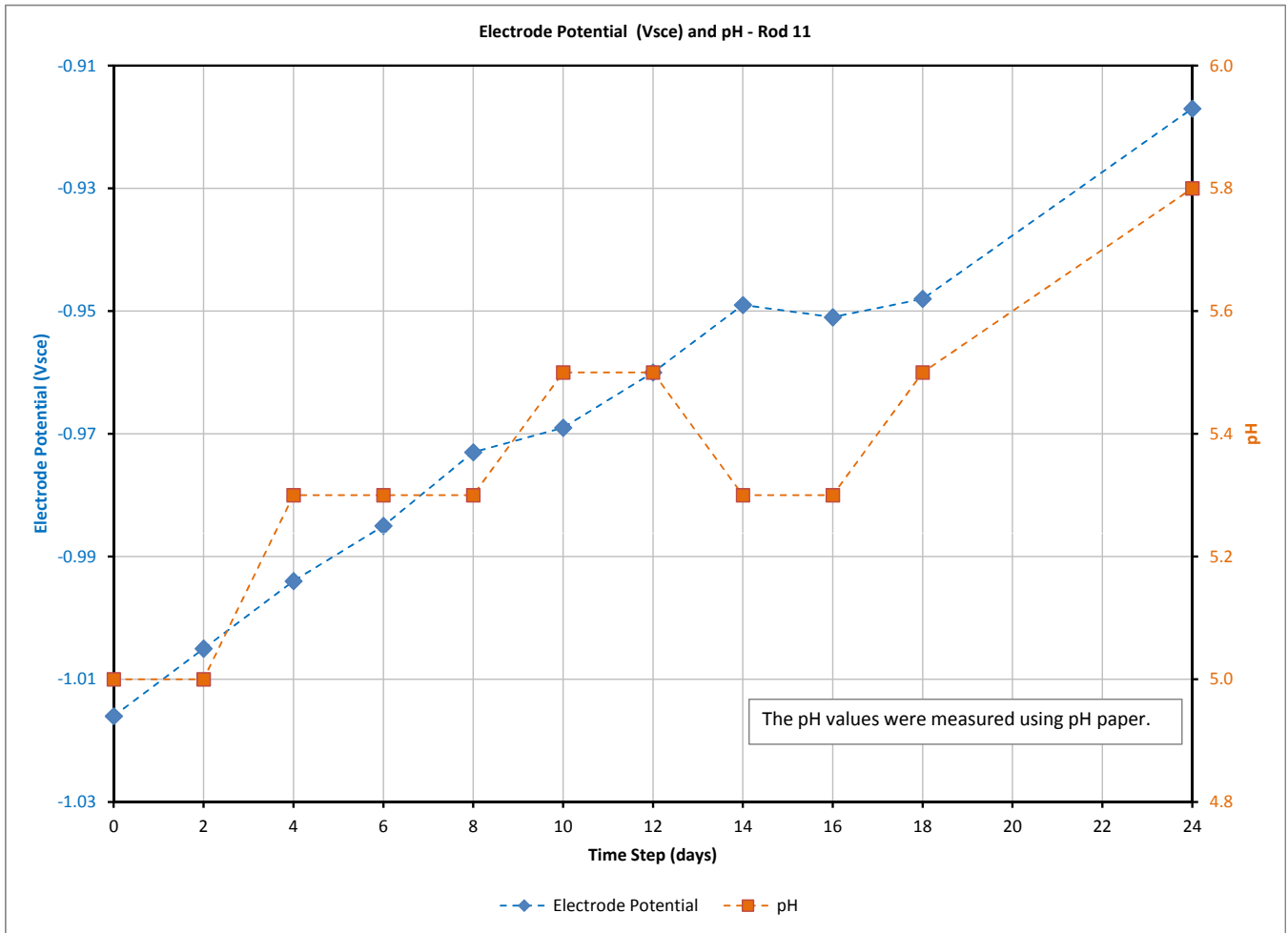
Electrode potentials of the rods and pH of the test solution typically varied during the course of the test as typified by Figure 3.1-8. Increasing pH with time is attributable to the buildup of zinc ions in solution resulting from corrosion of the galvanized rod.

Electrode potentials measured during testing of the rods generally started at a level that is significantly less negative than the potential of $-1.06 \text{ V}_{\text{SCE}}$ normally exhibited by pure zinc and ordinary galvanized coatings. This result can be attributed to the composition and structure of the galvanized rod coatings, which were found to consist mainly of iron-zinc intermetallic compounds. The fact that the potentials of the iron-zinc intermetallic compounds are less negative than pure zinc means that galvanic activity and driving force for hydrogen evolution are also reduced. These results are significant because EHE thresholds for high-strength steels are known to increase as the electrode potential rises to less negative levels [3, 4].

Figure 3.1-8 also shows that the electrode potential becomes less negative with time during the test. This rise is consistent with the selective dissolution of zinc from the coating, leaving behind a coating increasingly rich in iron, and less galvanic.

Subsequent to the tests of Rods 1 to 4, potentials were measured directly against a SCE at each load step.

Figure 3.1-8: Plot of Electrode Potential and pH vs. Test Time (Rod 11)



The results of Test IV are summarized in Table 3.1-3.

Table 3.1-3: Test IV Results

Phase No.	Group ID	Rod No.	Max Load %Fu	Field Max Hardness HRC @ 1/4" from O.D. ⁽¹⁾	Lab Average Hardness HRC at Root ⁽²⁾⁽³⁾	Impact Toughness CVN ft-lbs @ 40F	Potential at FiN/Al Load Volts vs Saturated Calomel Electrode ⁽⁴⁾⁽⁵⁾	Intergranular Cracking Detected in SEM?	EHE Threshold %Fu ⁽⁶⁾
1	2	1	85	37	37	37	-0.92	Yes	80
	2	2	80	36	37	37	-0.92	Yes	75
	2	3	111	36	39	37	-0.90	No	85
	2	4	85	35	36	38	-0.93	Yes	80
2	4	5	101	34	40	29	-0.88	No	85
	12	6	117	35	38	39	-0.87	No	85
	8	7	111	34	36	20	-0.96	No	85
	7	8	110	32	35	50	-0.91	No	85
	7	9	118	36	39	36	-1.01	No	85
	7	10	110	33	38	39	-0.99	Yes	80
	7	11	120	37	41	34	-0.92	Yes	80
3	1	12	70	37	36	14	-1.01	Yes	65
	1	13	70	34	35	15	-1.01	Yes	65
4	18	14	109	35	N/A	48	-0.96	No	85
	18	15	110	36	N/A	48	-0.94	No	85
	18	16	113	37	N/A	47	-0.70	No	85
	18	17	115	36	N/A	47	-0.70	No	85
5	1	18	115	36.5	N/A	N/A	Dry Test	No	85
	1	19	115	35.5	N/A	N/A	Dry Test	No	85

Notes

1. OD = Rod Outside Diameter
2. At ~2 mm from root for HRC
3. Hardness for Rods 1-4 is 5-11 are HRC hardness taken at 0.12 mm or 0.4 mm from the thread root as reported by PFAs 1 through 3.
4. Potentials for Rods 1-4 are the average of potentials measured at the lab on parts of the rod that were wet during the test.
5. Potentials for all others were measured in-situ at end of test and reported by VGO.
6. In accordance with normal practice (e.g., ASTM E1681), the threshold values given in Table 3.1-3 represent the last load step at which cracking was not detected.
7. N/A indicates data not yet available to date.

In 1975, KIScc thresholds for precracked, galvanized 4140 bars with a hardness of HRC 37 was found to be 30 KSI-in^{1/2} [3]. However, application of fracture mechanics equations fails to predict the observed EHE thresholds in terms of the fractional Fu observed for threaded rods. For example, the Bueckner equation for 3-inch-diameter rods with an EHE threshold of 0.75 Fu gives a value of 60 KSI-in^{1/2}, double that of precracked bars. This demonstrates that the fracture mechanics solutions are not sufficient to predict EHE thresholds for threaded rods that do not have pre-cracks, as suggested by the work of Olsen [5].

3.1.4 Post-Fracture Analysis at Lab (Phases 1, 2, 3, 4, and 5)

See Appendix L for Post Fracture Analysis (PFA) Reports.

Phase 1 – 2010 Pier E2 – Rods 1–4

Of the 2010 previously exposed rods (Nos. 1 to 4), three failed at loads of 0.85, 0.80, and 0.85 Fu. The remaining rod (No. 3) did not fracture until pulled to failure at the end of the test. By convention, EHE thresholds are defined as the last load sustained without evidence of crack initiation. This leads to the threshold values of 0.80, 0.75, 0.85, and 0.80 Fu, for Rods 1-4, respectively, as shown in Table 3.1-3. Assuming that these rods are representative of an identical group, the threshold can be taken conservatively as 0.75 Fu.

Fracture surfaces of the 2010 rods exhibited varying degrees of brittle failure originating at the initial engaged threads. Rod 3, which did not break during the step-load test and had to be pulled to failure, had the fewest intergranular features. Given the characteristics of the fracture surfaces, and the fact that tests were conducted in salt water, it is reasonable to conclude that Rods 1, 2, and 4 fractured as a result of EHE. A 'holiday' intentionally created in the galvanizing by rubbing a 0.012-inch-diameter diamond wire in the root of the three threads centered on the location of the first engaged thread of the nut. For Rods 1-4, the holiday was created on the dead end, while the jacking end was left as-is. Rod 1 and Rod 2 broke at the jacking end without any artificial holiday, while Rod 3 and Rod 4 broke at the dead end at the holiday. This indicates that initial coating defects are not required for the occurrence of EHE.

Each fracture surface was carefully examined for any evidence of crack arrest. A crack arrest would suggest that the fracture duration spanned a load step and so would be important in evaluating the results of the Townsend Test. No crack arrest was found on any of the fracture faces examined. Rod 2 had a ridge feature that initially appeared to be a crack arrest during visual examination, but detailed examination of this feature on both fracture surfaces and from both sides of the longitudinal specimens revealed that the ridge feature was an anomaly that is probably related to the high inclusion count of that rod. It is concluded that a true threshold was achieved with Test IV.

Phase 2 – Other Rods (with Cut or Rolled Threads) – Rods 5–11

None of the rods in this group failed until being pulled to failure at the end of the test. With the exception of Rods 6, 10, and 11, which were the only rods in Phase 2 with cut threads, all broke at locations away from the thread engagement with the nut and showed no evidence of intergranular cracking in the SEM examination. This indicates that rolled threads have a significant beneficial effect, even in the case of Rod 7 (Group 8) with low toughness.

Rod 6, with cut threads, did not break but rather had stripped threads during the pull to failure final step after reaching 0.85Fu. No Wet MT found an indication in the rod at the first thread engagement with the nut. The rod was bent to get a fracture surface at the first thread engagement with the nut. No Intergranular cracking was observed during the SEM examination, indicating an EHE threshold of 0.85 Fu.

Rods 8 through 11 are all 3.5-inch diameter PWS anchor rods. Rod 8 and Rod 9, with rolled threads, did not exhibit intergranular cracking, indicating an EHE threshold of 0.85 Fu. Rod 10 and Rod 11, with cut threads, broke at the first thread engagement with the nut and displayed evidence of intergranular cracking during SEM examination. This indicates that EHE initiated at 0.85 Fu, with an EHE threshold of 0.80 Fu for Rod 10 and Rod 11.

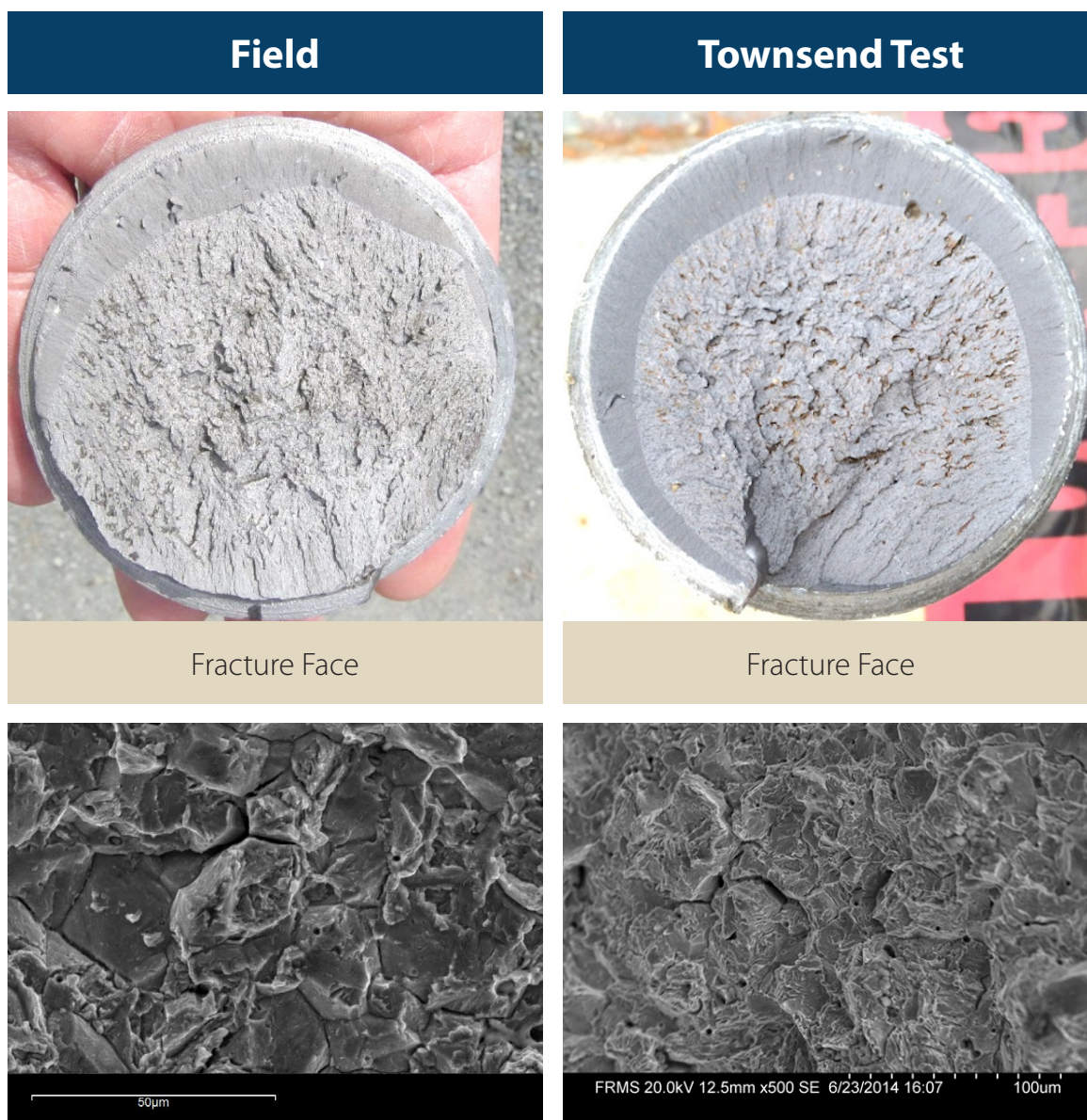
A comparison between the results for Rods 8 and 9 (rolled threads) and those for Rods 10 and 11 (cut threads) indicates that the EHE resistance of rolled threads is superior to that of cut threads. This is consistent with the work of others [6] who have found that thread rolling after heat treatment significantly increases resistance to stress-

corrosion cracking, owing to cold work and residual compressive stresses created at thread roots as a result of the thread rolling process.

Phase 3 — 2008 Pier E2 — Rods 12-13

Both 2008 rods failed at loads of 0.70 Fu, which indicates a threshold of 0.65 Fu. The macroscopic appearance of the fracture surfaces, and the intergranular nature of the fracture surface observed in the SEM, indicate that these rods failed by a hydrogen embrittlement mechanism. Given that the results of Phase 5 (as discussed below) show that the IHE threshold for this group of rods is significantly higher than 0.65 Fu, it can be unequivocally concluded that the rods in Phase 3 failed solely as a result of EHE. The similarities both in failure loads (0.70 Fu) and fracture appearances of the 2008 rods in Test IV and that of the failures of the 2008 rods that occurred on Pier E2 (see Figure 3.1-9) demonstrate that Test IV is duplicating hydrogen damage as observed with the 2008 fractures. It also demonstrates that soaking in corrosive water for long times is not necessary to produce EHE.

Figure 3.1-9: Test IV — Townsend Test Results Comparison



Hardness values near the outer surfaces of the 2010 Rods 1-4 and 2008 Rods 12 and 13 are virtually identical at HRC 37. Two possible explanations for the lower threshold of the 2008 rods as compared to the 2010 Pier E2 rods have been considered:

- Differences in the electrode potential between the 2008 rods (-1.01 V_{sc}e) and the 2010 rods (-0.92 V_{sc}e).
- Differences in the Charpy impact energy between the 2008 rods (14 to 15 ft-lbs) and the 2010 rods (37 to 38 ft-lbs).

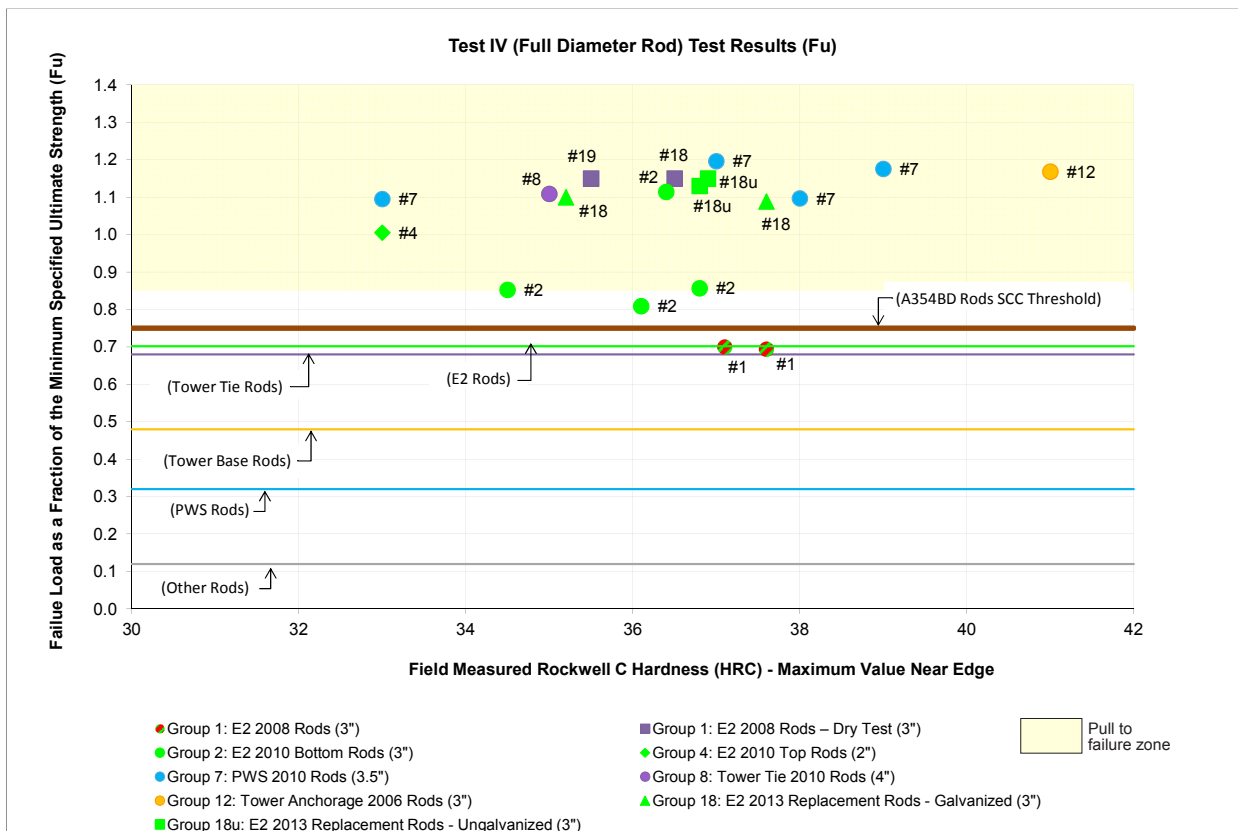
Phase 4 – 2013 Pier E2 (Galvanized and Ungalvanized) – Rods 14–17

All rods, both galvanized (Rods 14 and 15) and ungalvanized (Rods 16 and 17), which were fabricated from a different alloy (4340), endured for the entire 24 days of testing, and were then pulled to failure at peak loads above 100% Fu. Moreover, evaluation of the fracture surfaces revealed only ductile fracture features. This indicates that the 2013 rods are resistant to EHE up to 0.85 Fu, with or without a galvanized coating.

Assuming that the surface hardness is similar to that of the other rods in Test IV, the results of Phase 4 could indicate that the higher fracture toughness of the 2013 rods resulted in greater resistance to EHE. However, it is noted that hardness profiles measured at the rod ends before testing exhibited an M-Shape, which increases the possibility that the higher EHE threshold of the 2013 rods results from lower surface hardness. This points to the need to determine the actual microhardness profiles of the Phase 4 rods and is included in the PFA.

Figure 3.1-10 shows the pull to failure force and displacement. Rod 14 failed at the first thread at the nut engagement, while Rods 15, 16, and 17 failed in a ductile manner with necking away from the nut. Intergranular cracking (SCC initiation) was not observed in any of these rods, which all exhibited ductile tensile or ductile shear fracture morphology.

Figure 3.1-10: Test IV Failure Loads for A354BD Rods



The fact that all Phase 4 rods had to be pulled to failure after the six-day hold at 0.85 Fu may also indicate that there is no effect of the galvanized coating on the EHE threshold of this very high-toughness material up to a level of 0.85 Fu. Hardness profiles, which are currently underway, are also needed to determine if the behavior of these rods is a result of higher fracture toughness or lower surface hardness.

Phase 5 – 2008 Pier E2 Rods Tested in the Dry – Rods 18–19

Phase 5 was conducted in the same manner as Phases 1 to 4, but without the presence of salt water, thus ruling out any possibility of EHE. As such, Phase 5 is a test for IHE of the rods as they were at the time of the test, whether or not hydrogen from fabrication had diffused out of the steel since the samples were cut and extracted from Pier E2.

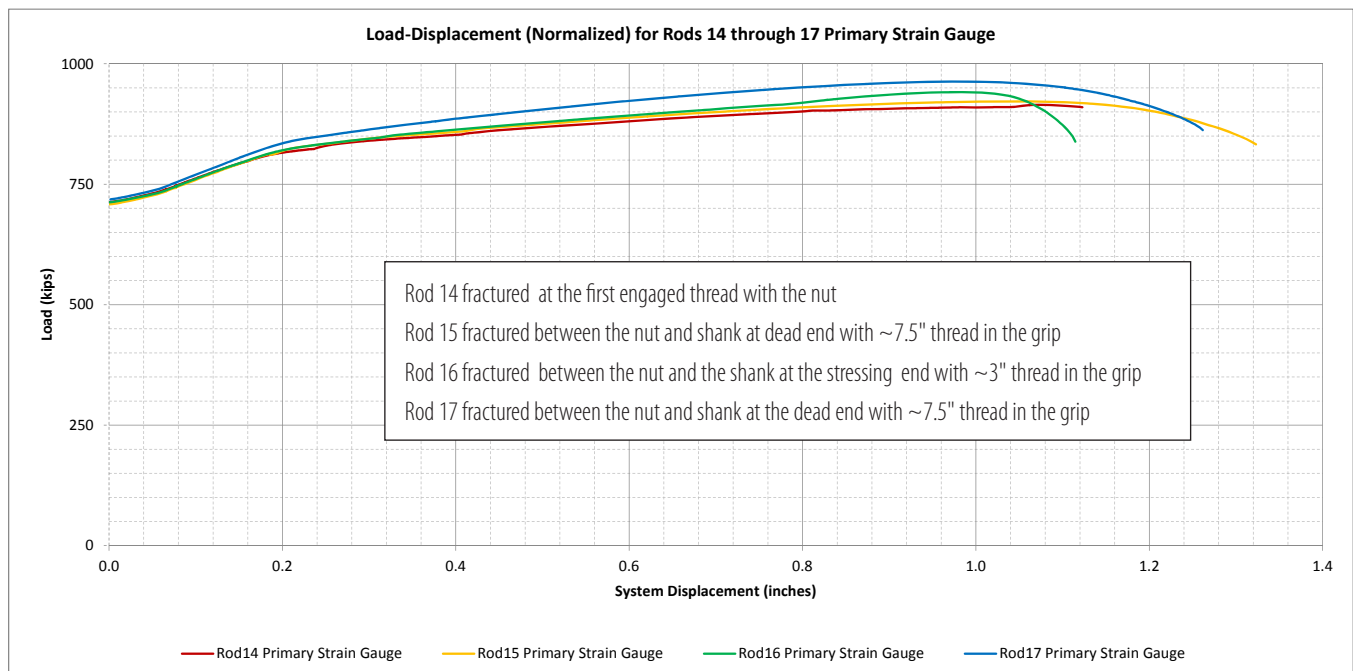
Without water, the 2008 rods in Phase 5 endured the 24 days of testing without breaking and were then pulled to failure with a peak load of 1.15 Fu, which is the same as the Test III-M tensile tests. SEM examination found no evidence of intergranular cracking (SCC initiation). The IHE threshold is 0.85 Fu. The finding that the IHE threshold is significantly higher than the EHE threshold of 0.65 Fu for this material is in agreement with the findings of the 1975 publication [3].

The fact that the 2008 rods in Phase 5 were unaffected by IHE up to at least 0.85 Fu means that the 2008 Phase 3 Rods which broke at 0.70 Fu could have failed as a result of EHE. Because the characteristics of 2008 rods that failed on the SAS are identical to those tested in Phase 3, it can be concluded that the mechanism of failure is fully consistent with EHE, and that there is no reason to believe that IHE was involved.

3.1.5 Summary of Results

A plot of the failure loads for all the rods tested is provided in Figure 3.1-11.

Figure 3.1-11: Load Displacement Graphs for Rods 14–17



Test IV duplicated the failures of 2008 rods on Pier E2 in terms of breaking loads and mechanism of failure. This provides confidence in the results obtained with these and the other rods, as follows.

1. The EHE threshold of the 2010 Pier E2 rods is 0.75 Fu.

2. The EHE threshold of the 2008 Pier E2 rods is 0.65 Fu.
3. The difference between the 2008 and 2010 Pier E2 thresholds can be attributed to differences in toughness and a higher iron content of the galvanized coating on the 2010 rods (the higher iron content reduces the electrochemical driving force for hydrogen deposition on the steel).
4. EHE threshold of the various 2010 and 2006 rods varies from 0.80 Fu to 0.85 Fu.
5. The EHE threshold of 3.5-inch PWS rods with threads rolled after heat treatment is 0.85 Fu, and is superior to that of similar rods with cut threads, with a threshold of 0.80 Fu.
6. The EHE threshold of black 2013 Pier E2 rods is 0.85 Fu.
7. The EHE threshold of galvanized 2013 Pier E2 rods is 0.85 Fu.
8. The IHE threshold of 2008 rods is 0.85 Fu.

3.2 TEST V — INCREMENTAL STEP LOAD TESTING: "RAYMOND TEST"

The objectives of Test V are to determine the SCC stress intensity thresholds for the material of the various groups of rods and independently determine the threshold load for SAS Bridge rods. Since many specimens can be obtained throughout a cross section of a 3-inch-long threaded segment of the rod, the effects of varying manufacturing and environmental variables such as potential on the hydrogen embrittlement threshold of the threaded rods can be evaluated. Fractographic analysis, using a Scanning Electron Microscope (SEM), was conducted on the tested specimens whose fracture surfaces were produced under known testing conditions, for comparison to the results of the post fracture analysis (PFA) of the threaded rods.

In addition, the rods were thoroughly characterized metallurgically relative to hardness (HRC), Open Circuit Corrosion Potential (OCP) of the coating, Fracture Toughness (K_{Ic}/K_{Ictod}), Internal Hydrogen Embrittlement (IHE), and Environmental Hydrogen Embrittlement (EHE) at the center (Center), mid radius (MR), and outside diameter (OD) of the rods when exposed to a 3.5% salt water environment with an applied potential simulating the galvanic effect of zinc coating.

3.2.1 Test Protocol and Test Rigs

Testing was conducted per ASTM Standards: ASTM F2078 (HE Terminology), ASTM F1624 (IHE, EHE threshold), ASTM E1681 (SLT-EAC threshold), ASTM E18 (HRC), ASTM E23 (Charpy), and ASTM E399/E812/E1290 (Fracture Toughness) for each rod sample provided.

Test Method Description

The test procedure provides an accelerated method to measure the threshold stress or threshold stress intensity for the onset of hydrogen stress cracking in steel. The procedure conforms to ASTM F1624 and is based on determining the onset of subcritical crack growth with a progressively decreasing, step-modified, strain-rate test under displacement control. The threshold load, (P_{th}), is obtained on completion of a minimum of two tests. The threshold is the lowest value of two consecutive tests when the difference between them is within 5% of the fast fracture strength (FFS). For example, if the FFS is 100 lbs., and the first EHE test had a load of 35 lbs., and the second EHE test had a load of 32 lbs., the threshold load would be 32 lbs., because the two EHE tests were within 5 lbs. (5% of FFS) of each other. Once an invariant value is obtained, no further tests are required. Otherwise, additional tests are performed following the protocol of Section 8.1.6 in ASTM F1624 until an invariant value within 5% of FFS is obtained from two consecutive tests.

A fatigue pre-cracked specimen is used to determine the material property ($K_{Ic}/K_{Ictod}/K_{Isc}$) in accordance with ASTM F1624 and the other referenced specifications. Tests to determine the effective threshold stress intensity in a salt water environment for the threaded and galvanized conditions ($K_{I\theta}$) use a specimen with the threads removed intact. The $K_{I\theta}$ tests conform to all other F1624 requirements and can be used to directly predict the performance of the threaded rod in service and in the Townsend Test.

Terminology/Symbols

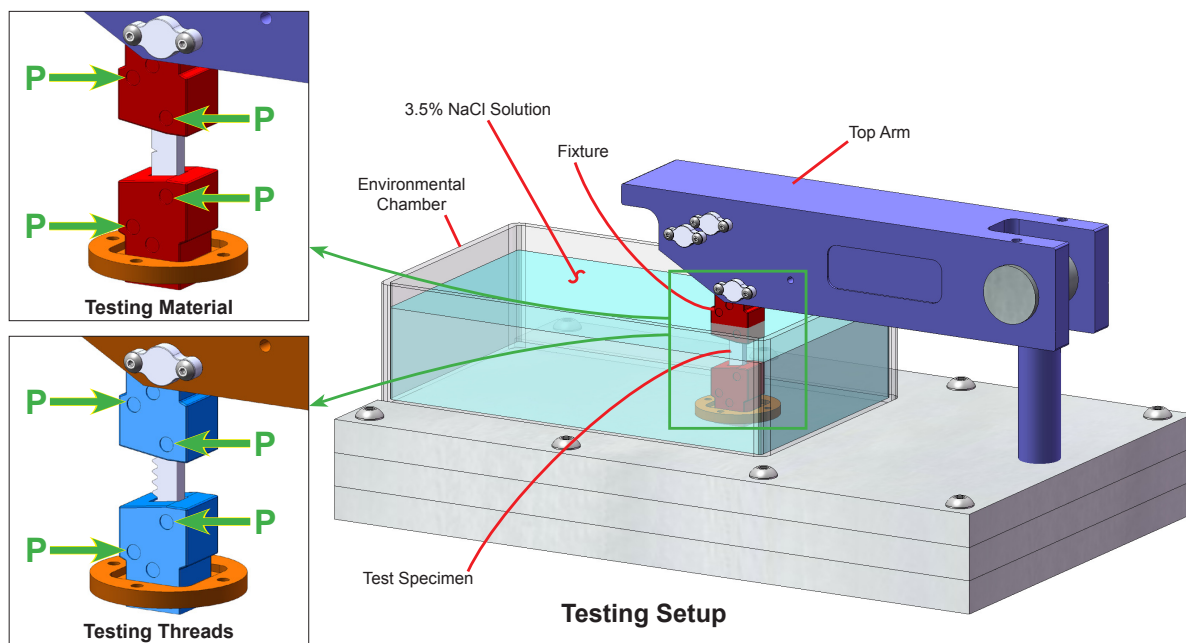
See Glossary

The test sample designation is as follows: Group ID-V-Number. For example 3-V-1 is Sample Number 1 cut from a Group 3 rod (E2 shear key upper rod, see Table 3.1-2).

Testing Equipment

Test Machine: Testing was conducted using a computerized, four-point bend, digital displacement controlled loading frame that is capable of stepping in 0.5% load steps and is programmed to increase incrementally in steps of load and time to vary the effective strain rate at the root of the notch between 10^{-4} and 10^{-9} s^{-1} . Bend test machines manufactured by Fracture Diagnostics International (FDI) were used for this test program (see Figure 3.2-1).

Figure 3.2-1: Bend Test Machine for Incremental Step Loading, Manufactured by FDI



Fixtures: Various types of adapters were used in four-point bending to transmit the measured load applied by the testing equipment to the test specimen.

Test Environment: Testing was conducted in two environments. Fast-fracture tests and IHE tests were conducted in air. For EHE tests, specimens were immersed into a 3.5% NaCl solution under potentiostatic control by imposing a galvanic cathodic potential in NaCl solution contained in an appropriate inert container.

Potentiostatic Control: The corrosion potential of the specimen was controlled with reference to a Saturated Calomel Electrode (SCE). The imposed potential was active and ranged from -0.85 V to -1.2 V versus SCE (V_{SCE}) in a 3.5% NaCl solution. Based on a Boeing Aircraft audited and approved of the potentiostat/environmental chamber, the measuring error is less than 10 mV out of 1106 mV.

*Test Protocol Details**Specimen Machining*

Rod samples were received at LRA and visually examined for general condition and major defects. Samples varied in length from 6 inches to 24 inches. A 2.5-inch long Charpy-sized segment was cut from the sample and specimens were machined from this segment by electrical discharge machining (EDM). Two types of specimens were prepared. One type of specimen was cut from the outer edge of the segment and included the thread and the hot dipped galvanized zinc (HDG-Zn) coating. The nominal dimensions of the threaded specimens (OD_{th}) are 0.4-inch wide by 0.45-inch thick by 2.5-inches long. A section was removed from the backside of the specimen to reduce the specimen thickness at the thread root to 0.4-inch. A second type of specimen was cut from the interior of the segment. ASTM E1290-99, single edged notched bend, SEN(B) specimens were cut from the interior of the rod to Charpy-size dimensions of 0.4-inch wide by 0.4-inch thick by 2.25-inches long. A slot, 0.1-inch deep, was cut by EDM in the center of each specimen as a starter slot for fatigue pre-cracking. The location from which an interior specimen was removed was noted and specimens were tested as outer diameter, mid-radius, or center specimens. The two types of specimens are shown in Figure 3.2-2 and Figure 3.2-3, and the distribution of specimens in a rod is illustrated in Figure 3.2-4 and Figure 3.2-5.

Figure 3.2-2: A Charpy-sized, Single Edge Notched Bend, ASTM E1290 SEN(B), Specimen

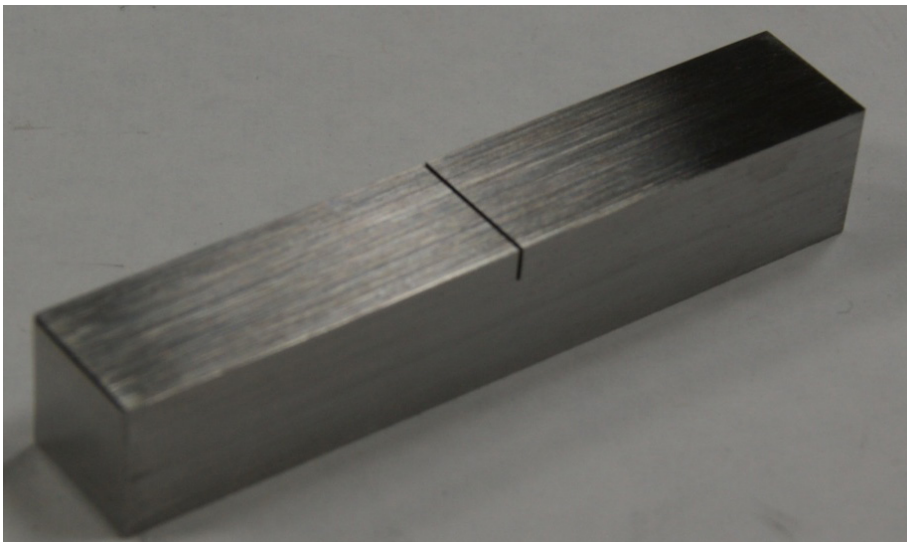


Figure 3.2-3: A Charpy-sized, Threaded Specimen for Determining KI_p



Figure 3.2-4: Machining Plan for a 3-inch Diameter Rod

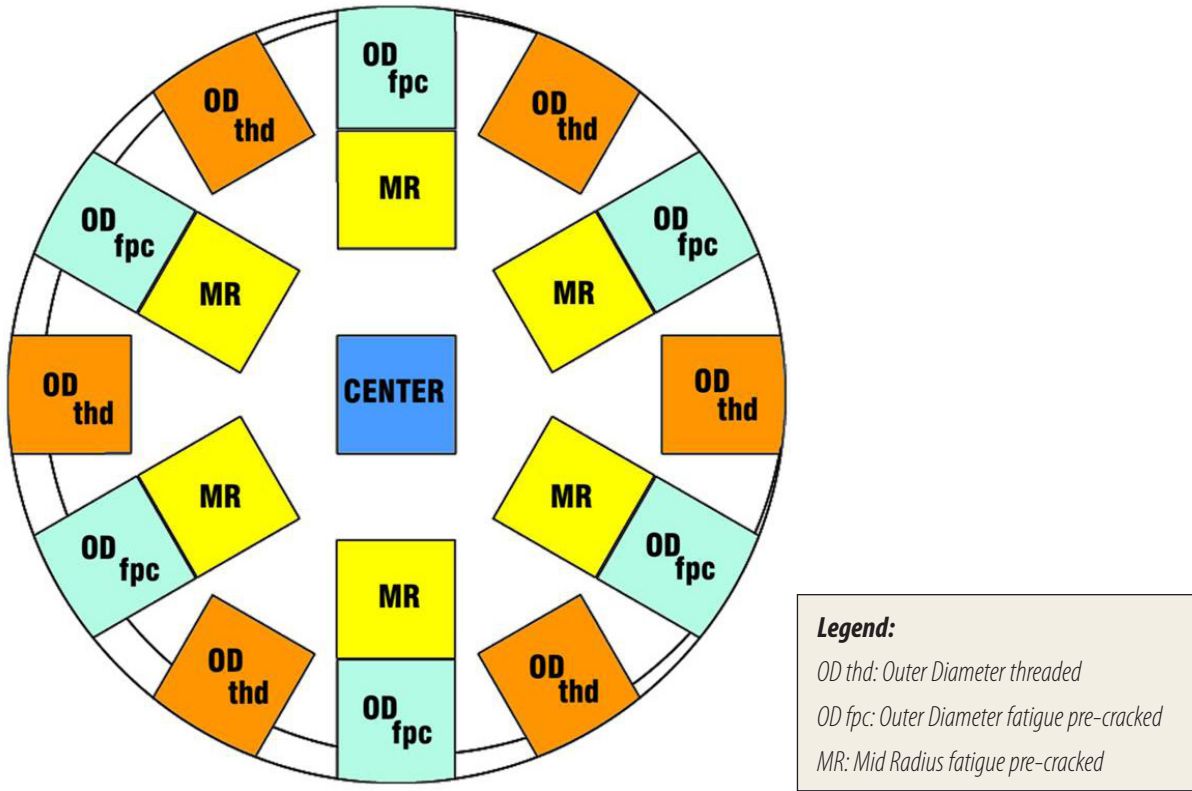
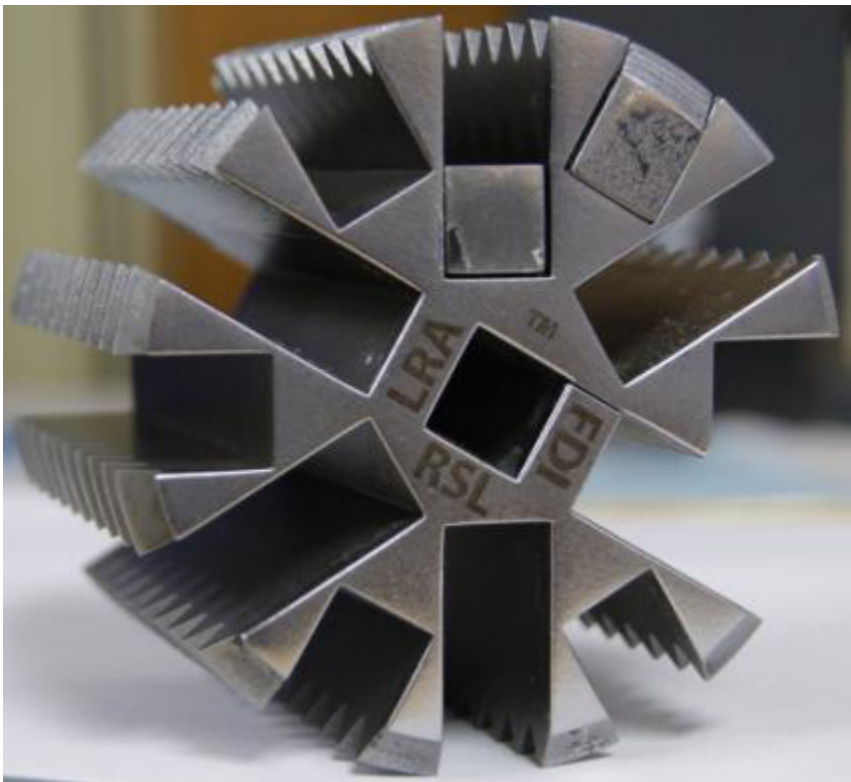


Figure 3.2-5: Rod Sample with Specimens Removed



Specimen Preparation

After the specimens are removed from the rod by EDM, they are lightly sanded and cleaned. SEN(B) specimens are wet sanded with 240, 320, and/or 600 grit sandpaper to remove EDM recast (a thin coating of molten material redeposited on the specimen during the EDM process). Specimens are then cleaned in an Alconox cleaning solution, rinsed in acetone, and dried.

Hardness Test

The hardness of each specimen is measured using a Rockwell Hardness Tester (Wilson Instrument Division, American Chain and Cable Co.). Rockwell hardness C (HRC) scale is used in accordance with ASTM E18. The hardness is measured at six points on the side of the specimen spanning its length. The hardness can be used to estimate the ultimate tensile strength of the specimen using ASTM E140.

Fatigue Pre-cracking

Prior to testing, single edge notched bend Charpy-sized specimens are fatigue pre-cracked. The EDM slot was extended by fatigue approximately 0.08 to 0.10-inch. The precise depth of the pre-crack is measured following testing. The final stress intensity used during fatigue pre-cracking (typically 15 ksi $\sqrt{\text{in}}$) was less than 60% of the measured stress intensity for crack initiation (which is typically 25 ksi $\sqrt{\text{in}}$ to 35 ksi $\sqrt{\text{in}}$). A Physmet FCM-300B pre-cracking machine was used to pre-crack the specimens as required. This unique piece of equipment uses constant displacement rings to produce cracks ranging from 0.005-inch to 0.250-inch in fewer than 10 minutes. Threaded specimens were not fatigue pre-cracked.

Fast-Fracture Test

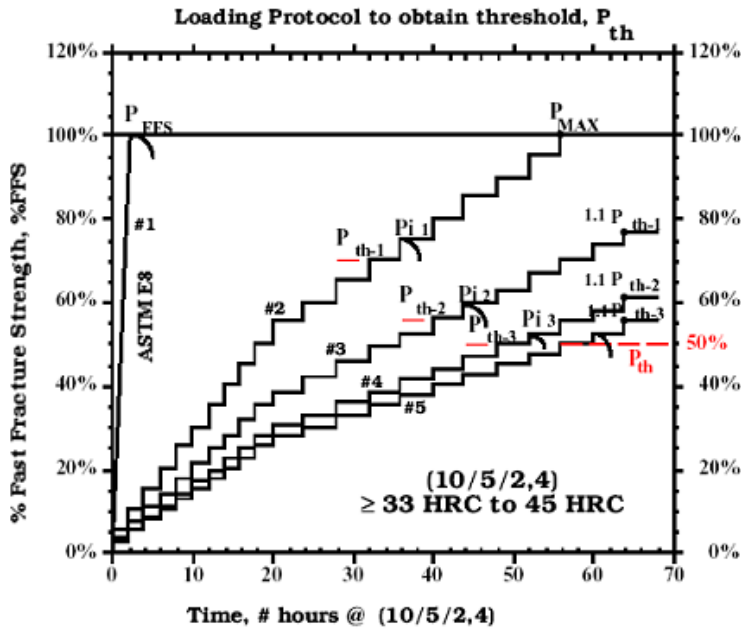
To provide baseline reference data for each rod and specimen type, a specimen of each rod and type is tested to rupture using a rate consistent with ASTM E8. This establishes a fast-fracture strength (FFS) or load (P_{FFS}) for a given specimen geometry.

RSL™ Testing

The test procedure provides an accelerated method to measure the threshold stress or threshold stress intensity for the onset of hydrogen stress cracking in steel. The procedure conforms to ASTM F1624 and is based on determining the onset of subcritical crack growth with a step modified, incrementally increasing, slow strain rate test under displacement control. The threshold load (P_{th}), is obtained on completion of a minimum of two tests. The threshold is the lowest value of two consecutive tests when the difference between them is within 5% of the fast-fracture strength, FFS. Once an invariant value is obtained, no further tests are required. Otherwise, additional tests must be performed following the protocol of Section 8.1.6 in ASTM F1624 until an invariant value within 5% of FFS is obtained from two consecutive tests. Of the two tests, the lowest value is used.

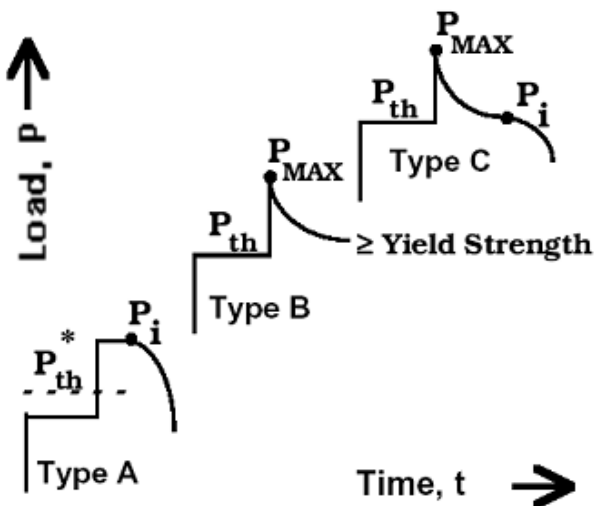
Figure 3.2-6 shows a typical progression of tests from Section 8.1.6 in ASTM F1624. The curve at the left labeled “ASTM E8” shows the load/time curve for the fast-fracture test that determines P_{FFS} . The first RSL test is performed at 5% steps of P_{FFS} , initially 10 each, two-hour steps followed by four-hour steps until the specimens fracture (labeled P_{i-1}) and the step before the fracture step is the threshold load (labeled $P_{\text{th}-1}$). The next test is performed with steps of 5% of P_{target} of 1.1 times $P_{\text{th}-1}$ to find $P_{\text{th}-2}$, and so on as shown in Figure 3.2-6.

Figure 3.2-6: Schematic of a (10/5/2,4) Step Loading Profile to Determine Threshold for the Hardness of Steel ≥ 33 HRC to 45 HRC



ASTM F1624 was originally developed for testing aerospace steels with a hardness of 50 HRC. Because of the low-strength steel being tested, the net-section stress in bending at which the sub-sized specimen cracks is likely to be above the yield stress of the steel. At these stress levels, significant plastic deformation at room temperature is possible and will produce a load drop that can be confused with crack extension. Figure 3.2-7 shows the load drop curvature that can be used to separate the crack initiation load from yielding.

Figure 3.2-7: Definition of Crack Initiation Load, P_i Load and Threshold Load, P_{th}



Hydrogen embrittlement or Stress Corrosion Cracking will produce an accelerating curve that appears as a concave downward Type A load time curve as shown in Figure 3.2-7. On the other hand, yielding will produce a Type B load time curve that is concave upwards.

Often, cracking will initiate after some delay in a step. When this occurs, the curve will take on a sigmoidal shape as shown in Figure 3.2-7 as a Type C curve. If the test does not attain a load drop of 5%, the test will increase to the next load step, generating a serrated load-time curve above the threshold. To definitively detect this threshold load, a change in stiffness is measured.

Multiple specimens are tested per ASTM F1624. By decreasing the load step, the effective strain rate is decreased from specimen to specimen. The minimum or invariant value of the stress intensity (KI_{SCC} , KI_{IHE} , or KI_{EHE}) or stress for a given geometry with regard to the loading rate before the onset of crack growth is defined as the threshold for the onset of crack growth due to hydrogen embrittlement.

Impact after Test

After RSL testing has been completed, the specimen is ultrasonically cleaned in Alconox followed by acetone and dried in air. The specimen is then baked at 400°F for one hour to heat tint the cracked surface and then broken by impact to expose the fracture face using the CIM-24 Physmet Charpy Impact Machine, which is capable of testing materials with energy capacities up to 24 ft-lbs. Heat tinting aids any subsequent SEM examination by marking the extent of SCC cracking.

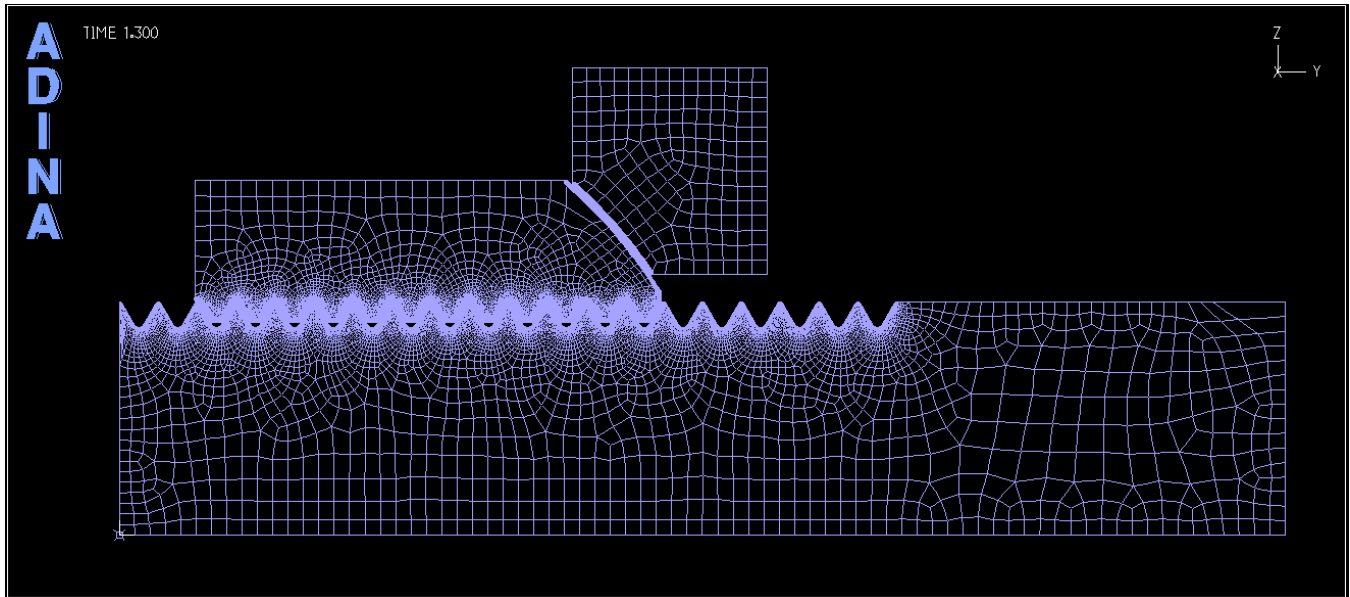
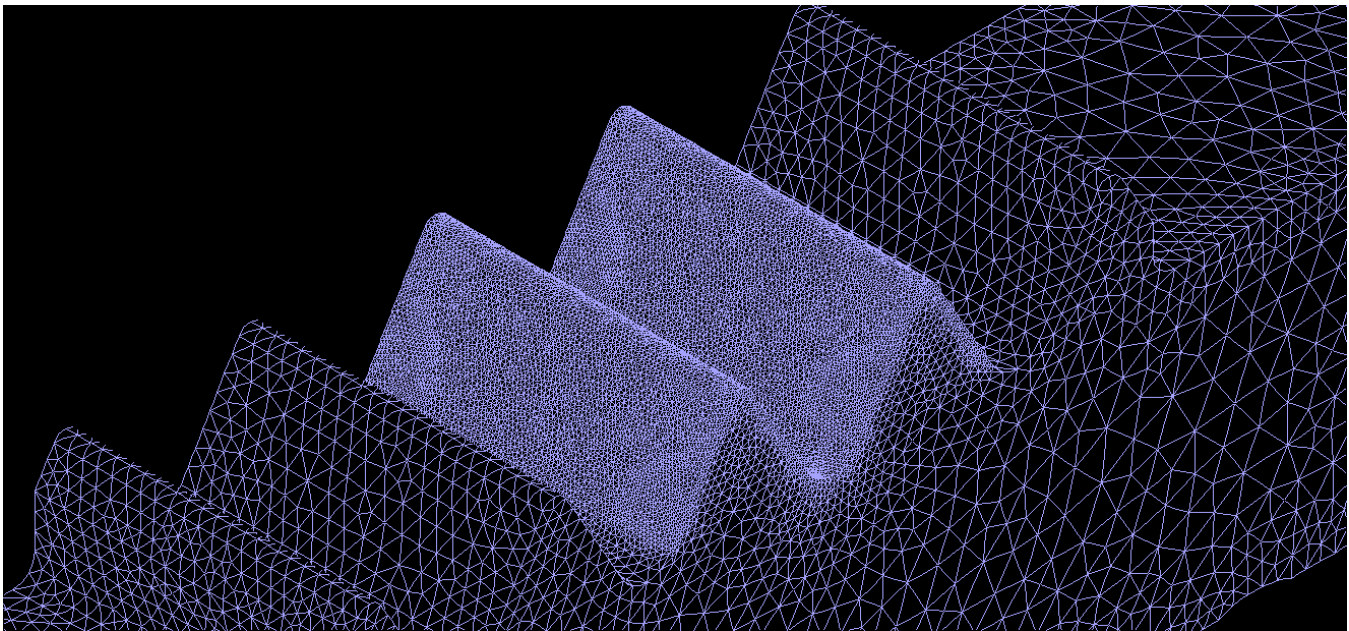
For fatigue pre-cracked specimens, the actual length of the pre-crack cannot be measured until after the test is complete and the specimen is broken open. In addition, for the fatigue pre-cracked FFS test, heat tinting allows the extent of crack tearing to be measured to ensure that a valid crack tip opening displacement (CTOD) test was performed.

3.2.2 FEM Validation

Correlation with Full-Size Test (FEM)

Fracture mechanics analyses were used to relate test loads from small-sized threaded specimens tested in bending to equivalent loads for full-sized rods tested in tension. This approach is well established in the literature [7] for relating different specimen geometries for high-strength aerospace materials, and has also been used for testing A490 bolt geometries [8]. Because the stress intensity equation is used on a threaded or notched specimen with a radius ρ and not with a sharp crack, $KI\rho$, is used as the "effective" stress intensity factor.

To establish the correlation between the small specimen geometries and the full-sized threaded rods, finite element analyses were conducted on models of Test IV of full-sized rods shown in Figure 3.2-8 and on Test V idealized threaded specimens shown in Figure 3.2-9. Strain, strain energy density, and plastic axial stress results from the two analyses were equated to obtain correlations between rod and specimen loads. Essentially, the same correlation was obtained for the three metrics. The correlations may be used to find a rod load corresponding to a specimen load obtained in a test.

Figure 3.2-8: Test IV Model Mesh**Figure 3.2-9: Test V Model Mesh**

Relating the FEM analysis to Test Data

The fracture mechanics approach is to model the notch as a sharp crack and use existing models to calculate the stress intensity for the geometry of the notch. In the case of the full sized threaded rod, the geometry modeled is a circumferentially notched round bar tested in tension, NRB(T), with an outer diameter of the thread major diameter and with the notch diameter of the thread minor diameter. Once this geometry is modeled, the relationship between applied axial load and stress intensity can be readily calculated from equations in the literature [9, 10]. For the small-sized specimen, the geometry modeled is a single-edge notched specimen tested in bending, SEN(B).

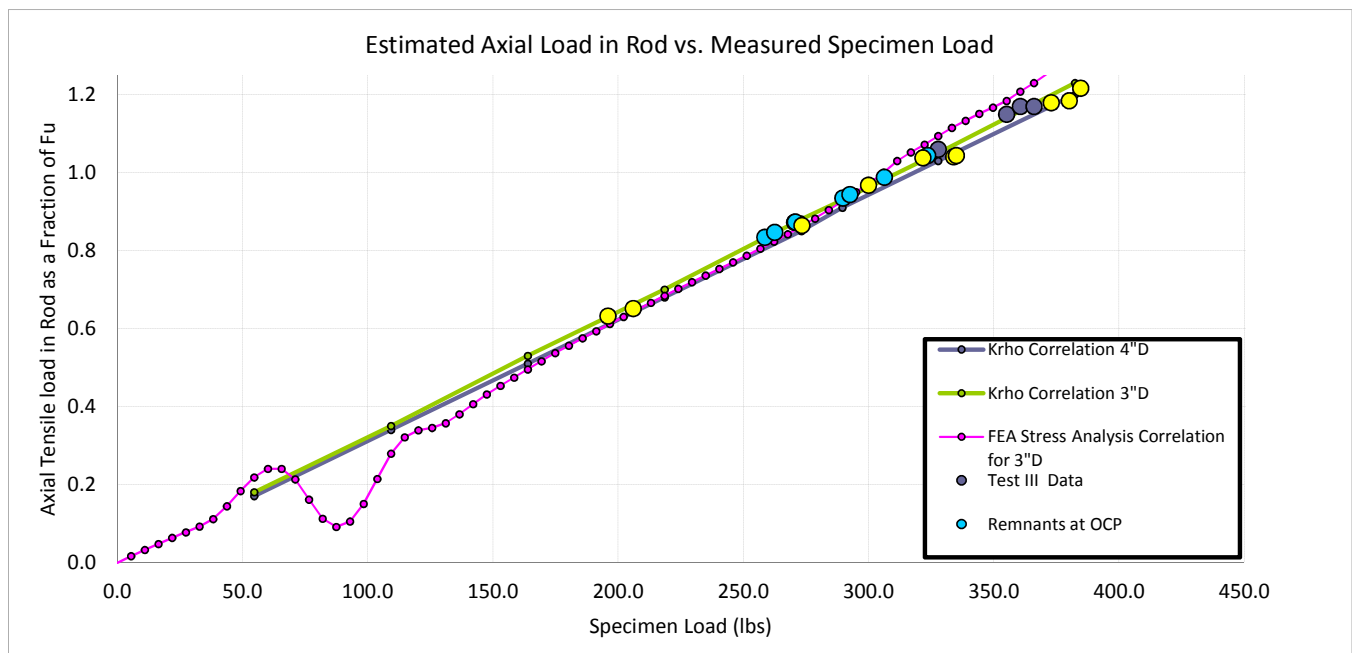
The concept is that the material response is measured as the stress intensity at which cracking initiates and will be the same stress intensity for both the NRB(T) and SEN(B). Measuring the crack initiation stress intensity factor using a small-sized specimen will allow the prediction of the crack initiation stress intensity factor for the full-sized

threaded rod and subsequently predicting the fracture load as a ratio to the rod specified ultimate tensile strength. The measured value of threshold KI_p for each rod can be used to calculate the threshold load for the idealized specimen used in the FEM analysis since KI_p accounts for any small changes in the geometry of the test specimen from variation in the rod thread geometry and machining tolerances in fabrication of the specimen.

Test V tests were performed with a conservative applied potential of $-1.106 V_{sce}$, which is more severe than what galvanized rods are likely to experience due to the galvanic potential or even the open circuit potential (OCP) from the galvanizing. Typically, the potential applied to the rods from the galvanizing is more positive and on the order of $-0.9 V_{sce}$. A special test program was performed to determine the effect of applied potential on the measured value for KI_p for threaded specimens and the results are published in another section of this report. Also measured, as part of Test V, was the galvanic potential or OCP of the galvanizing for each rod. Using the correlation developed, a value for KI_p at the galvanizing OCP can be estimated from the KI_p measured at $-1.106 V_{sce}$. Once $KI_{p_{OCP}}$ is known, the failure load for the threaded rod (F_u) can be predicted.

To verify the fracture mechanics correlation, Figure 3.2-10, the relationship between both the specimen fracture load and specimen threshold load, calculated from their corresponding measured stress intensity, KI_p , are compared to the same load parameters calculated with FEM analysis. Also compared are the threshold data from Test V, adjusted for the measured OCP of the rod.

Figure 3.2-10: Estimated Rod F_u vs. Specimen Threshold Load



As can be seen in Figure 3.2-10, the stress-intensity correlation agrees well with the FEM correlation. Test IV Phase I testing found that, out of four rods tested, one had a threshold of $0.75 F_u$, two had a threshold of $0.80 F_u$, and one had a threshold greater than $0.85 F_u$. The data from remnants from Test IV, Phase I Rods and their sister rods identified as 3-V-xx rods (blue data points) match well to the Test IV and Test III results.

3.2.3 Summary of Results

Effect of Hardness, HRC, on Measured Threshold- fpc

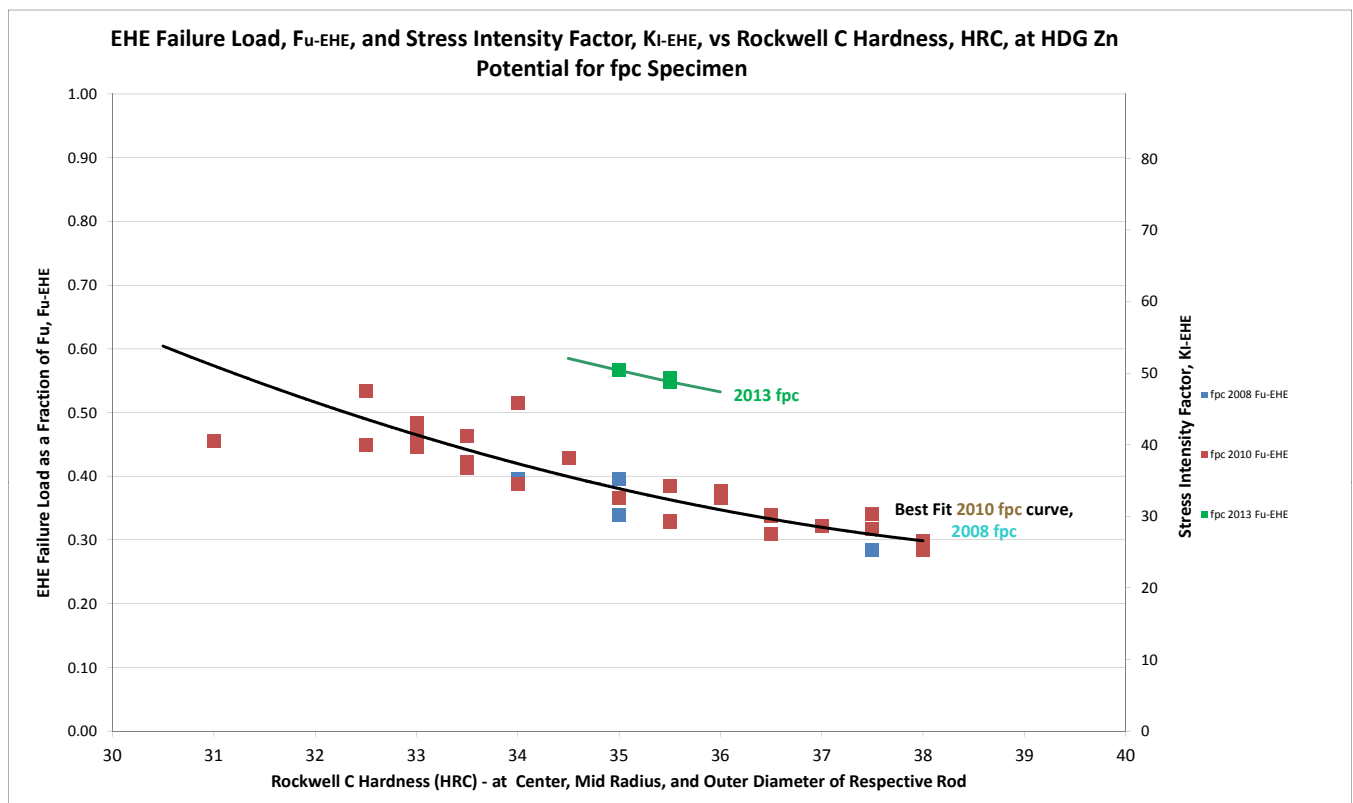
The test results for the 16 rod samples as well as samples from the remnants of the dead (non stressed) end of the four rods tested in Test IV Phase I are shown in the following figures. Fu Ratio is the maximum load of FFS converted via fracture mechanics equations to FFS of a rod.

Observations that can be drawn from this data are:

1. The results of Test V agree with the SCC conclusions established in Test IV
2. The results of Test V indicate the SCC threshold is greater than the applied load for the SAS Rods
3. The 2008-fpc specimens are at the minimum values of the 2010-fpc specimens

The EHE threshold stress-intensity values for fatigue pre-cracked specimens tested at -1.106 Vsce and adjusted for Zn potential (-1.06 Vsce) are plotted in Figure 3.2-11. A second order polynomial was best fit to the fpc data in Figure 3.2-11. The equation and results are discussed in Appendix M. Not shown in the figure is the “Townsend Curve” i.e. the curve relating KI_{sc} to hardness that Dr. Townsend found in his 1975 paper [3]; however the Townsend Curve approximately matches the Test V fatigue pre-cracked data. The adjustment for potential is as presented in Figure 3.2-12. The fpc KI_{sc} data for the SAE 4140 steel rods when corrected for the zinc potential are consistent with the Townsend Curve for Vsce-Zn, appear to be independent of microstructure, and only depend on hardness of the specimen. The fpc specimens indicate the 2013 material is the most environmental corrosion-resistant of the rods obtained for Test V.

Figure 3.2-11: EHE Threshold Force Ultimate and Stress Intensity



Neither the 2008 nor the 2010 specimens tested exhibited IHE (threaded and fpc specimens). However, there was concern expressed that process hydrogen could have diffused out of the uncoated surfaces of samples since the rod

samples were removed from the bridge and in storage at room temperature for up to six months before testing. Extra precautions were taken with the freshly galvanized 2013 rods to minimize any escape of hydrogen by storing specimens in a freezer and the results of these specimens further supported the original conclusions.

Effectiveness of Applying a Holiday to the Test V Test Specimens

Objective: Analyze the effectiveness of scribing a holiday (or break) in the galvanized coating on threaded samples RSL™ tested in 3.5% NaCl at -1.106 V_{sce}.

Background

In service, parts can easily be damaged or dinged resulting in damaged coatings and exposing the bare steel of the part. If the correct environment is present, a galvanic couple will occur between the coating and the bare steel, charging hydrogen into the exposed steel. The threaded samples are given a holiday to simulate this situation. Since the specimen is potentiostatically charged with hydrogen on all surfaces of the specimen, the presence of galvanizing should have no electrochemical effect on the test. There was concern that for Test IV, placing the holiday too deep may score the underlying steel, effectively adding defects at the holiday. This was tested in Test V by placing a holiday in one of the three threads tested for each specimen. Theoretically, the sample should fail approximately 30%, or one-third, of the time in the thread with the holiday.

Experimental Procedure

A holiday or scribe mark was placed on one of the middle threads of the threaded SEN(B) samples, which were tested in four-point bending in 3.5% NaCl environment at -1.106 V_{sce}. The holiday was created on the sample using a 0.008-inch diameter diamond wire. The holiday was inspected by optical inspection via microscope to verify that most but not all of the galvanizing was removed.

Results

Currently 40 EHE threaded samples have been tested. Of these 40 samples with holidays, only 18 samples actually fractured in the thread root with the holiday on it and 22 fractured in a thread root that did not contain a holiday. Samples did not always fracture in the holiday or even in one of the middle threads.

Discussion

There are typically three thread roots in the stressed area of the test sample, rarely four. So if the fracture location were entirely random, it would be expected that fractures would occur in the thread root with the holiday about 33% of the time. In fact, it occurred in the thread with the holiday 45% of the time, indicating that the presence of the holiday may have affected the fracture initiation location to some extent. However, the average stress intensity measured when the sample initiated a crack in the thread with a holiday was 62.8 ksi/in, while the stress intensity measured when the sample initiated a crack in a thread without a holiday was 63.6 ksi/in, a statistically insignificant amount, indicating that the presence of the holiday did not affect the test results.

Conclusion

Applying a holiday in the thread root of the threaded SEN(B) samples does not significantly influence their fracture behavior on the threaded Charpy-sized specimen; but due to the limited area of the specimen being coated, a large influx of hydrogen resulted throughout the specimen, results that are not unexpected. Only if the specimens had been completely galvanized would the presence of a holiday be influential in the initiation of a hydrogen-induced stress-corrosion crack.

Effect of Applied Potential on Measured Threshold

The freely corroding or Open Circuit Potential of the galvanizing on the rods varied from rod to rod from a low of -1.1 Vsce to a high of -0.85 Vsce. Testing performed on other, non-SAS, higher-strength steels (on the order of 50 HRC) for ASTM F1940 found a significant variation of measured threshold due to applied potential within these limits. In order to determine the effect of applied potential on the measured threshold Fu for galvanized rods with a value of hardness on the order of 36 HRC, a special project was performed.

Summary of Protocol

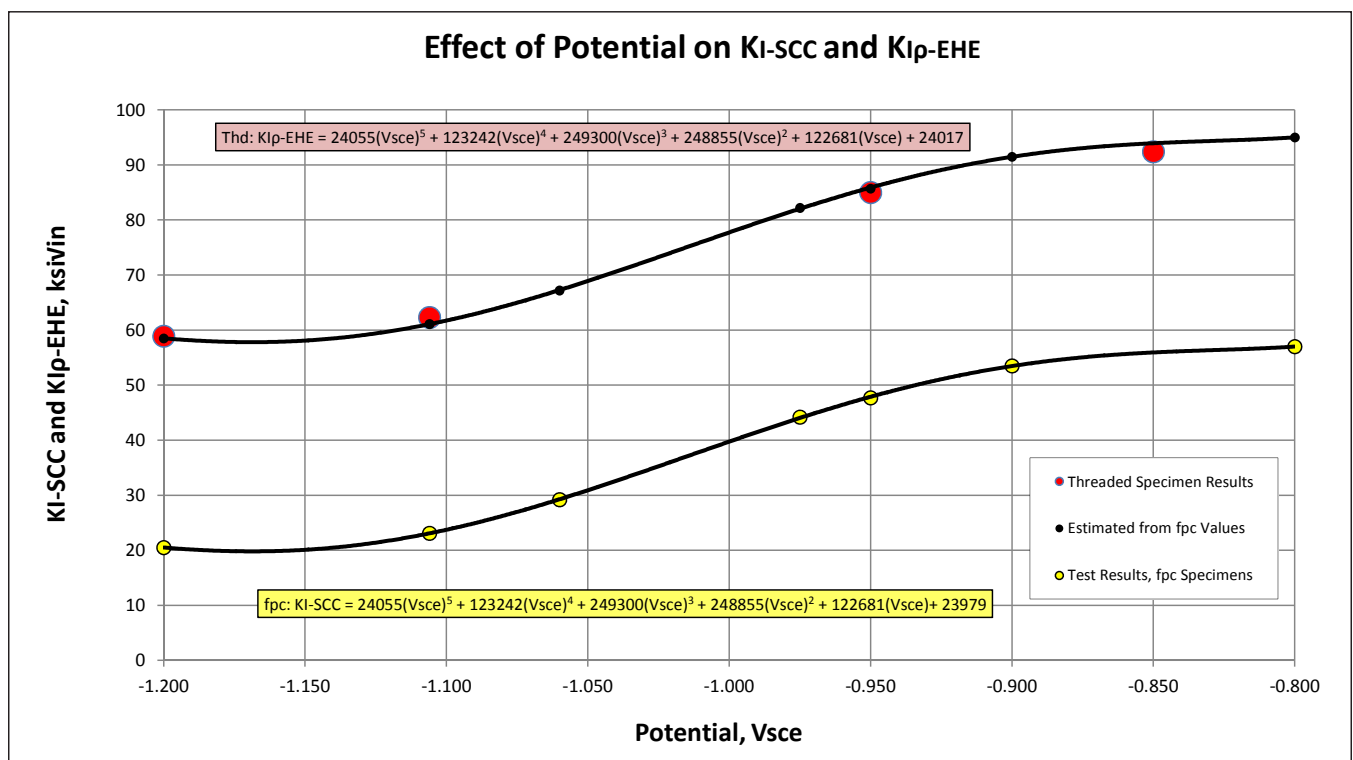
Using the protocol developed for measuring KI_{sc} of fatigue pre-cracked specimens for the threaded rods, the threshold stress intensity was measured for fatigue pre-cracked specimens under varying applied potentials. Fatigue pre-cracked specimens from the same heat of steel and essentially the same hardness were used. After testing the fatigue pre-cracked specimens, threaded specimens were tested at various potentials to verify the effect of potential on threaded specimens. The current to the specimens was adjusted as necessary to maintain the potential between the specimen and the bath to the desired potential.

Specimens used were from the OD of rods 3-V-9, 3-V-11, and 3-V-12. For the fatigue pre-cracked specimens, the applied potentials were -1.20 Vsce, -1.106 Vsce, -1.06 Vsce, -0.975 Vsce, -0.90 Vsce, and -0.800 Vsce. For the threaded specimens, the applied potentials were -1.2 Vsce, -1.106 Vsce, -0.95 Vsce, and -0.85 Vsce.

Results

Figure 3.2-12 shows that while KI_{sc} is effectively level below -1.10 Vsce, and above -0.90 Vsce, there is significant change in KI_{sc} between -1.1 Vsce and -0.9 Vsce, with KI_{sc} changing from 23 ksi√in at -1.1 Vsce to 53 ksi√in at -0.9 Vsce. The upper curve in Figure 3.2-12 shows the polynomial trend line through the fpc data shifted upward by 38 ksi√in. Also shown in Figure 3.2-12 are the results of testing threaded specimens at various potentials, showing that shifting the trend line up matches the threaded results.

Figure 3.2-12: Effect of Applied Polarization Potential on the Measured KI_{sc} and KI_{IP}-EHE



A fifth order polynomial was fit to the fpc data in Figure 3.2-12. The upper curve, which is 38 ksi√in greater than the fpc curve, can be used to estimate the effect of OCP on the measured KI_p and %Fu for full-sized threaded rods by subtracting the value of the curve at the test potential (62 ksi√in at -1.106 Vsce) from the measured value for KI_p for the rod and adding the value of the curve at the rod potential.

Summary of Threaded Test V Data Adjusted to Test IVs Respective Rod ID #

The results for Test V are included in Appendix M. The results for Test V are adjusted for potential and hardness as shown in the previous sections so that they could be compared to the Test IV results.

Figure 3.2-13 shows a plot of minimum F_u -EHE against HRC with 2008 Test V data adjusted to the corresponding Test IV rod potential and hardness as described above. In other words, the Test IV data was preserved and the Test V data was adjusted for potential and hardness. The figure shows the range of values for each test series. Tables of results can be seen in Appendix M.

Figure 3.2-13: Test V 2008 SCC Specimen Fracture Load in Salt Water Adjusted to Test IV Hardness of 37 HRC and Rod Potential (F_u -SCC)

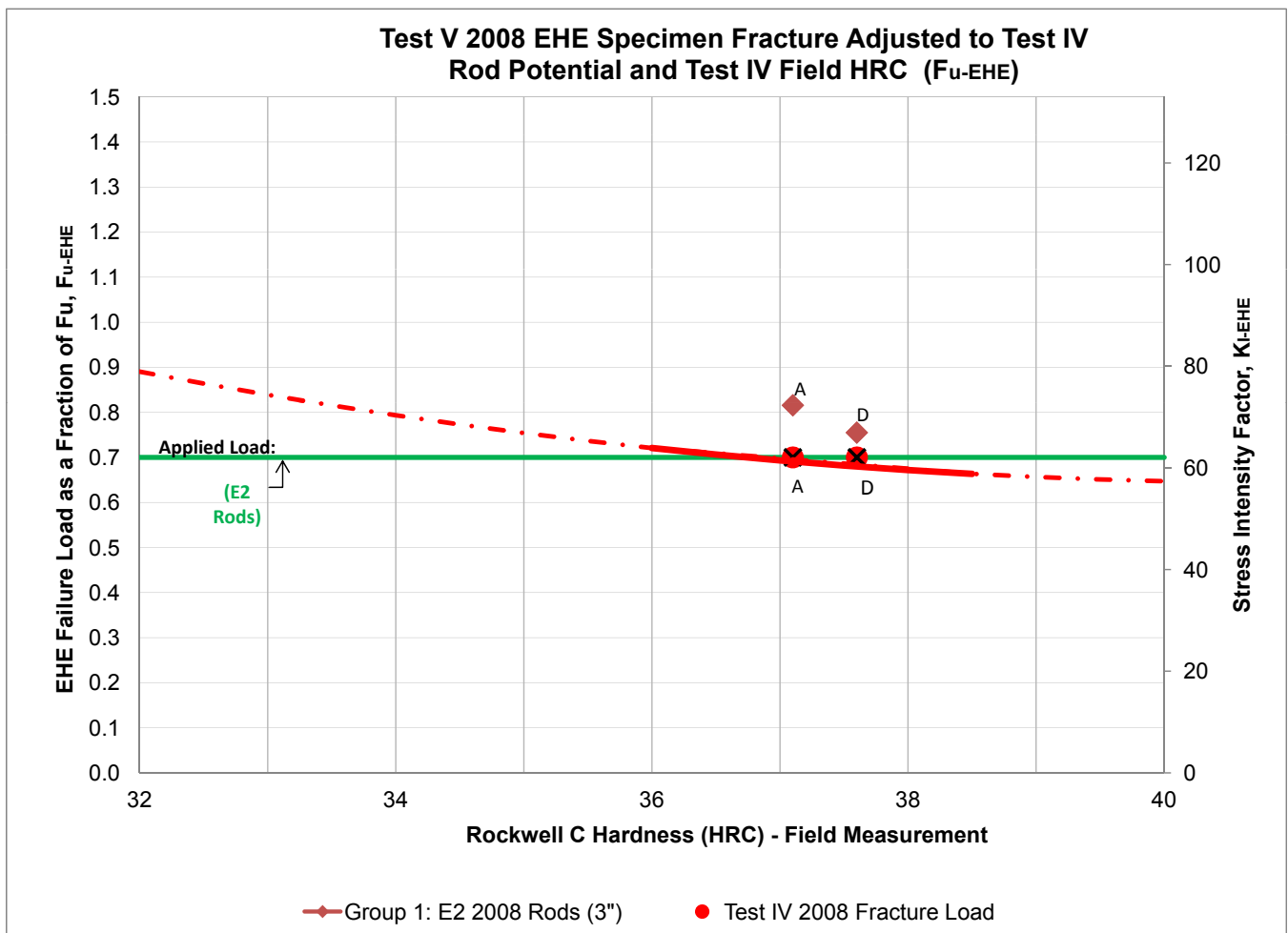
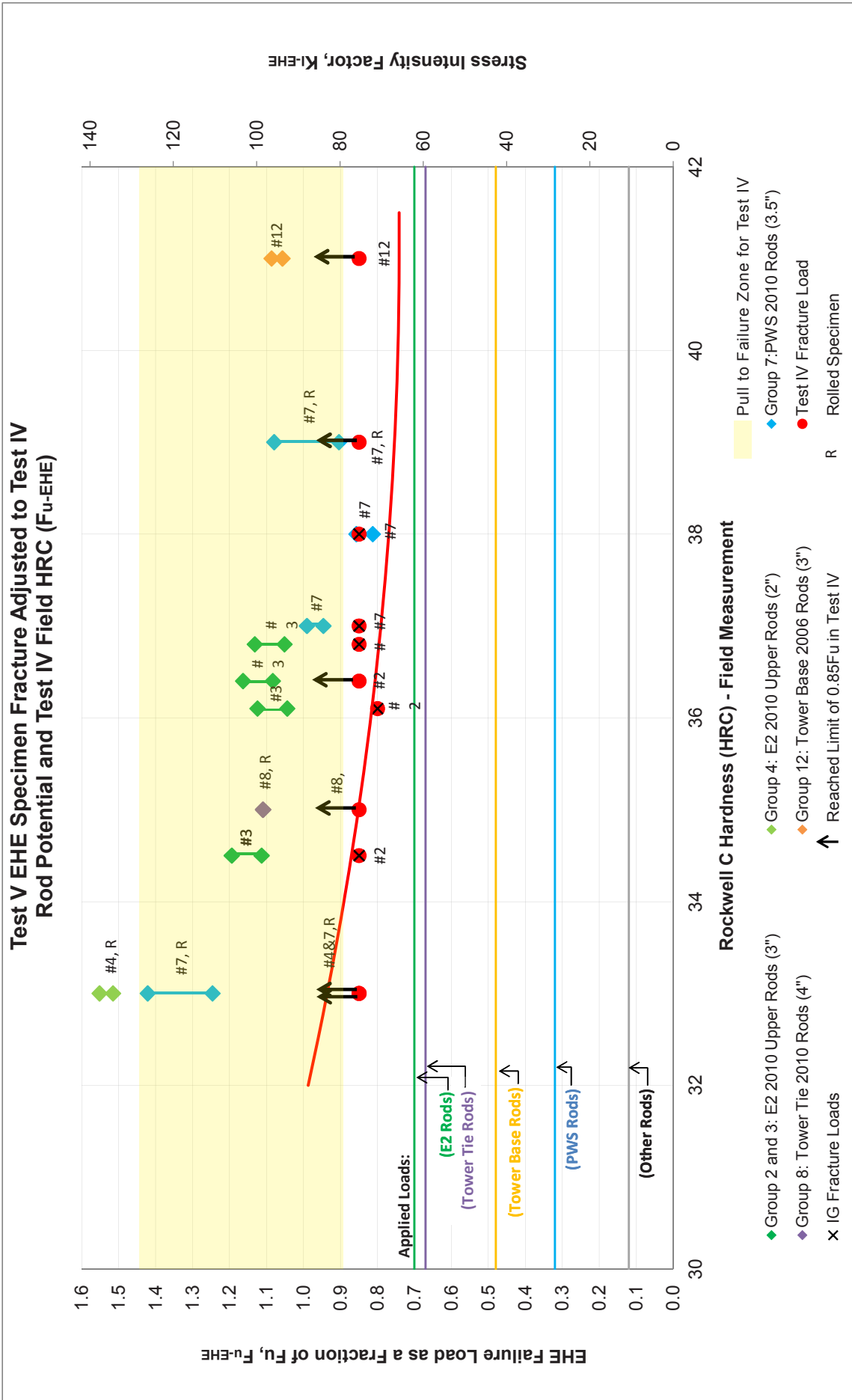


Figure 3.2-14 shows a plot of minimum F_u -EHE against HRC with 2010 Test V data adjusted to the corresponding Test IV rod potential and hardness as described above. Again, the Test IV data was preserved and the Test V data was adjusted for potential and hardness. The figure shows the range of values for each test series. These results also show all rods are significantly above the applied load demand in the SAS. Tables of results can be seen in Appendix M.

Figure 3.2-14: Test V 2010 and 2006 EHE Specimen Fracture Load in 3.5% Salt Water Adjusted to Test IV Rod Potential (Fu EHE) and Hardness (HRC)



Threshold Stress Intensity

- The $K_{I,p}$ and $K_{I,sc}$ were determined for each rod sample provided (see Appendix M).
- The $K_{I,sc}$ data for the SAE 4140 steel rods are consistent with the Townsend Curve for V_{scc-Zn} , are independent of microstructure, and only dependent on hardness of the specimen.
- The $K_{I,p}$ data for the 2010 rods are higher than $K_{I,p}$ data for the 2008 rods.
- The $K_{I,p}$ data for rod samples with rolled threads are 10–20% higher than the $K_{I,p}$ data for the cut thread rod samples.

The observations that can be drawn from these data are:

1. The results of Test V agree with the conclusions established in Test IV.
2. The results of Test V indicate the SCC threshold is greater than the applied loads for the SAS.
3. The results of Test V for the 2008 rods show the threshold for these rods is lower than the originally applied load but is greater than the reduced load (0.40 F_u).
4. The results of Test V for the 2013 rods show the threshold for these rods is higher than the threshold for the 2010 rods.
5. Neither the 2008 nor the 2010 specimens exhibited IHE.

3.2.4 Conclusions

1. The FEM analysis and testing correlation to Test IV justifies the use of the “effective” fracture mechanics parameter $K_{I,p}$ to correlate small-specimen test results to full-sized threaded rod performance, both structurally and relative to degradation due to environmental exposure.
2. The results of Test V agree with the SCC conclusions established in Test IV.
3. The results of Test V indicate the SCC threshold is greater than the applied load for the SAS.
4. The results of Test V for the 2008 rods show the threshold for these rods is lower than the originally applied load but is greater than the reduced load (0.40 F_u), and predict the March 2013 fractures.
5. The results of Test V for the 2013 rods show the threshold for these rods is higher than the threshold for the 2010 rods.

3.3 TEST VI — ADDITIONAL VERIFICATION TESTING: “GORMAN TEST”

The objective of Test VI is to further verify, using slower rates than specified in ASTM F1624, the values of K_{I-EHE} or $K_{I,p}$ determined by the Test V tests performed at the LRA/RSL™ Labs in Newport Beach, California, similar to tests performed on 10-32 machine screws.

Test VI was proposed to address the concern that there may be crack initiation mechanisms that require longer time than Test V provides to reveal themselves. For example, it was speculated that oxide wedging may apply stress to an otherwise arrested crack after some delay, causing it to extend at a lower load than would be measured by the accelerated loading profile from ASTM F1624 used for Test V.

Test VI was divided into two parts. In Part 1, the Test V thresholds were validated via loading rates slower than specified in ASTM F1624. In Part 2, the Test V thresholds will be validated using sustained loading tests above, at, and below the threshold.

3.3.1 Part 1: Extended RSL Testing

Test Protocol and Test Rigs

Test VI, Part 1 is an extension of Test V. Therefore, the test procedure and equipment for Test VI, Part 1 were the same as those used for Test V with the following exception: the loading rate was significantly slower. In Test V, the loading rate had dwell times of four hours as the fracture load was approached. In Test VI, the first specimens were tested with dwell times of eight hours. This dwell time was increased with subsequent specimens to decrease the loading rate (strain rate) until an invariant threshold value was attained. The loading rates in Test VI were significantly slower than Test V and also were significantly slower than called for in ASTM F1624 (see Figure 3.3-1).

Three fpc specimens and three threaded specimens were tested to verify the KI-EHE or KI- thresholds determined during Test V. Testing was conducted with an applied potential that was the same as used for the corresponding tests in Test V (-1.106 V_{sce}) and adjusted to Zn Potential (-1.06 V_{sce}). A table of results can be seen in Appendix N.

Results

Test V thresholds at -1.106 V_{sce} were verified using slower loading rates and can be seen in Figure 3.3-2. The test data from Test VI and Test V are plotted at -1.06 V_{sce} as a function of loading rate. See Appendix N for the test results.

Figure 3.3-1: Test V, 4-hr and Test VI, 8-hr, 16-hr Threaded EHE-RSL for Shear Key (Top)

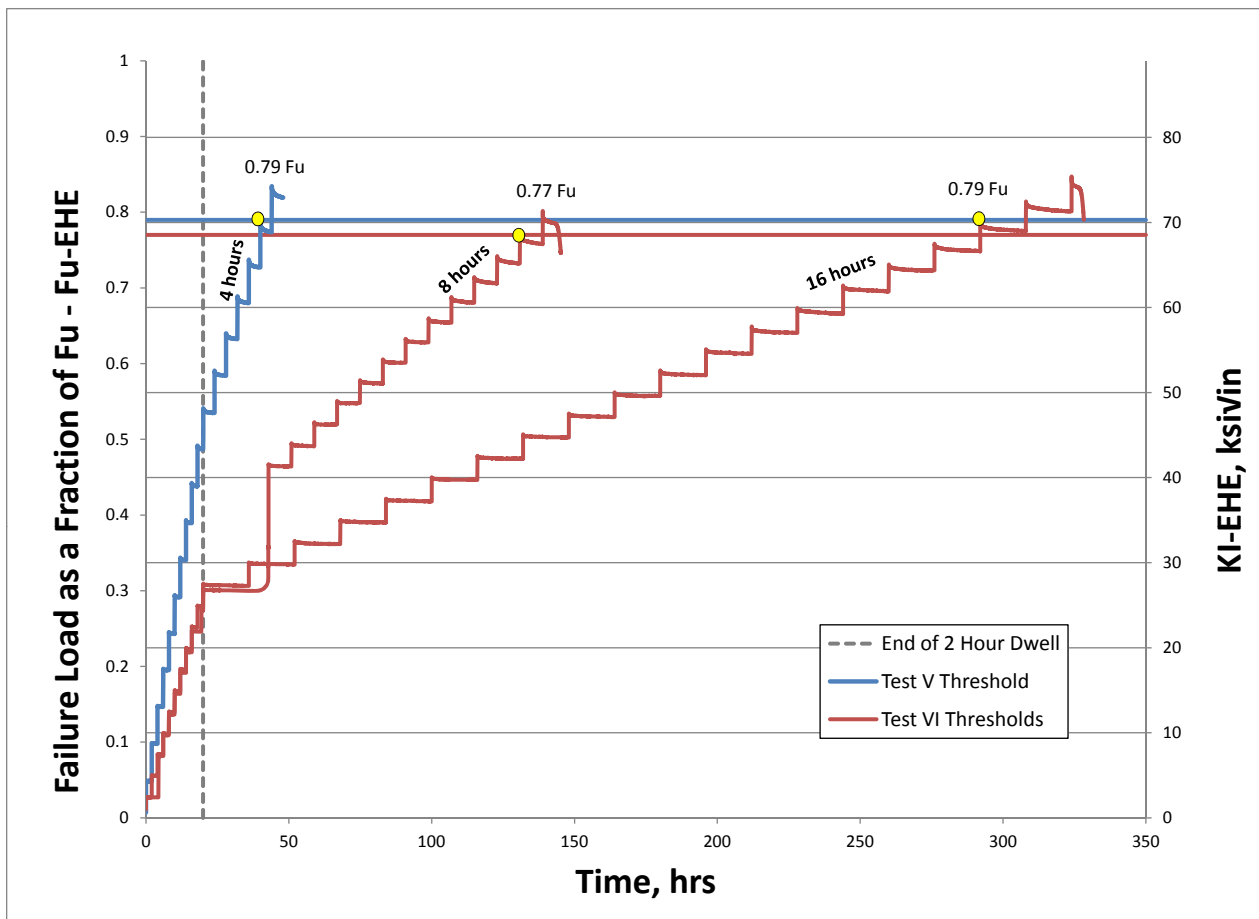
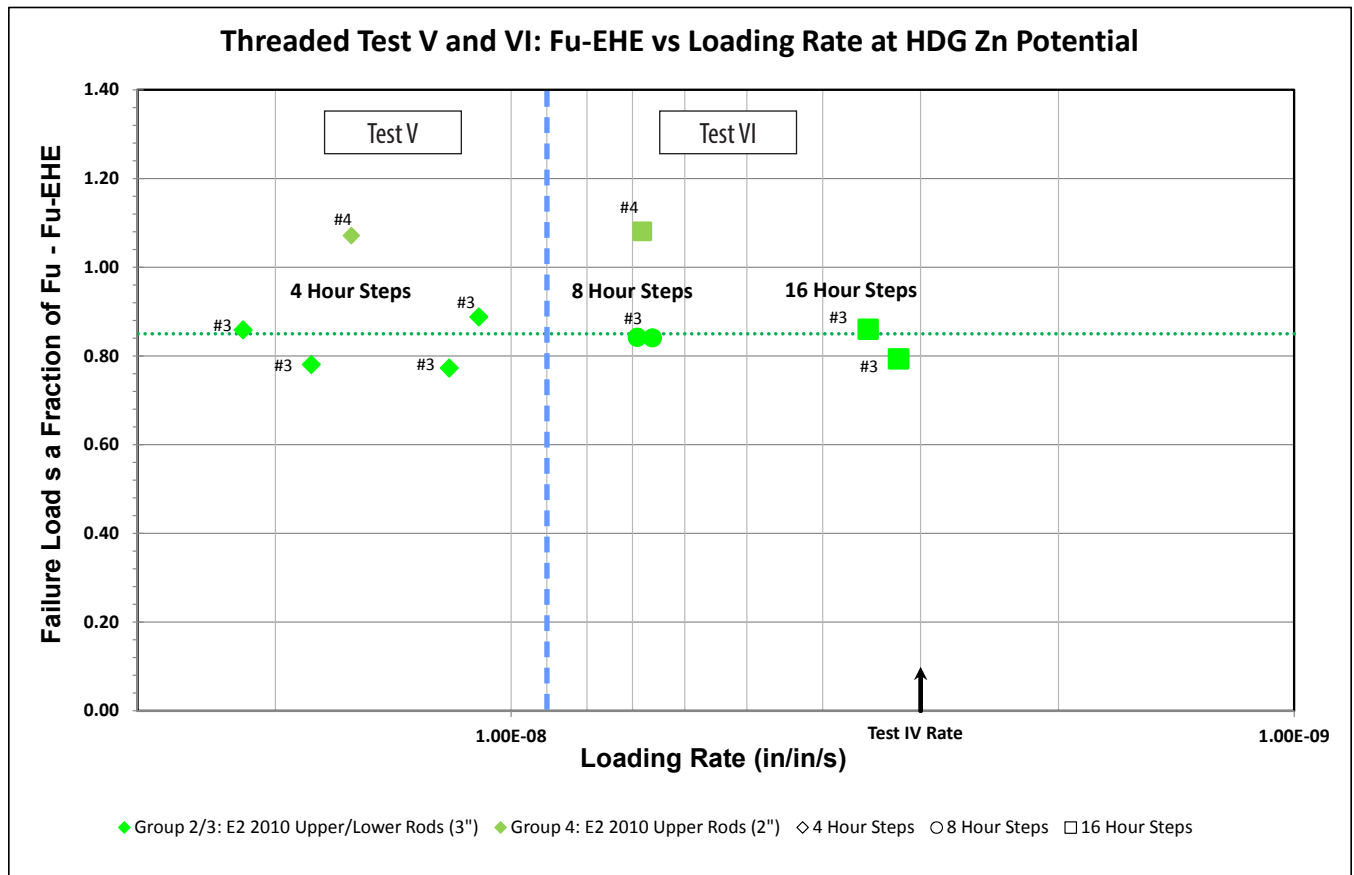


Figure 3.3-2: Threaded Test V and VI: Fu-EHE vs Loading Rate at -1.06V_{sce}



3.3.2 Part 2: Sustained Load Testing

Sustained Load Test Rigs

Three test rigs were designed, fabricated, and assembled for sustained load testing of small specimens. A schematic representation of the test rigs is shown in Figure 3.3-3 and a photograph of the three rigs is shown in Figure 3.3-4.

Figure 3.3-3: Components of the Sustained Load Test Rigs

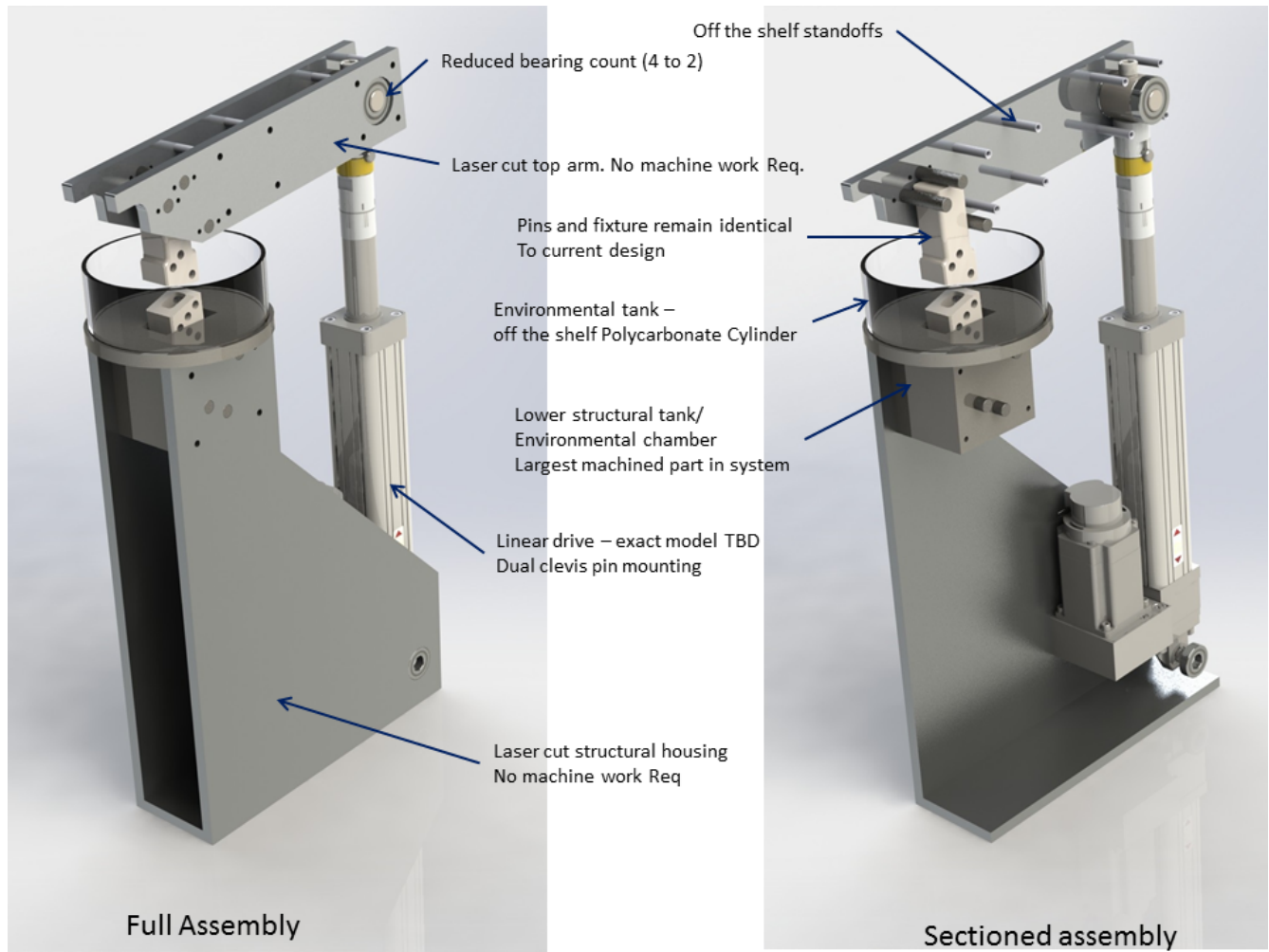


Figure 3.3-4: Three Sustained Load Test Rigs Undergoing Final Check-out Prior to Calibration



Specimen Fabrication

Specimens for sustained load testing were threaded Charpy-sized specimens as described in Test V, Section 3.2.

Test Protocol

Three threaded Charpy-sized specimens will be tested with constant loads using the sustained load test rigs. The test method should be generally consistent with ASTM E1681. The constant loads will range from about 0.10 F_u above to 0.10 F_u below, corresponding to the load that developed the $K_{I\dot{p}}$ value in Test V. The tests will be continued until specimen failure or 5000 hours. The specimens will be suspended in sodium chloride solution and be instrumented such that the time of failure is recorded. Testing is conducted with an applied potential that is the same as used for the corresponding tests in Test V.

The loading shall be as follows:

- a. 1-test loaded @ threshold
- b. 1-test loaded @ threshold +0.10 F_u
- c. 1-test loaded @ threshold -0.10 F_u

The water bath is recirculated, oxygenated, and monitored for the test duration.

After completion of 5000 hours, the specimen will be heat tinted and broken. The fracture surfaces will be examined in the SEM to identify the morphology of any pre-existing fracture.

Results

Testing will be completed in March 2015, and included in Appendix N.

3.3.3 Summary of Results and Conclusions, Test VI

1. Test VI Part 1 validated that the Test IV and Test V strain rates were sufficient to reach a threshold.
2. No additional crack initiation mechanisms were identified by decreasing the loading rate in Test VI, equivalent to extending the RSL-dwell time to eight hours or 16 hours, which approaches the Test IV loading rate.
3. Part 2 of the Gorman Test is expected to further substantiate conclusion No. 2 by applying a sustained-load test for 5000 hours, and will be concluded in March 2015.

4. TESTING PROGRAM SUMMARY AND RECOMMENDATIONS

4.1 BACKGROUND AND OBJECTIVES

The primary objective of the testing program is to evaluate the suitability of the various types of ASTM A354 Grade BD (A354BD) rods used in the SAS to perform their function during their design life. The A354BD rods must perform at their permanent tension levels, with essentially no risk of failure, whether due to mechanical overload or time-dependent mechanisms. The testing was designed to:

- Verify the mechanical properties and chemical composition of all types of A354BD rods used on the bridge, to determine the mechanical properties of these structural components and to evaluate the uniformity of these properties across the various lots.
- Determine the rods' resistance to Stress Corrosion Cracking (SCC), both for Internal Hydrogen Embrittlement (IHE) and for Environmental Hydrogen Embrittlement (EHE).
- Test the failed rods with similar protocols to ascertain the similarities and differences between these groups of rods.

To address the above objectives, the testing program included the following:

- Test I, Test II, and Test III: Mechanical Properties and Chemistry Analysis
- Test IV, Test V, and Test VI: Time-dependent SCC testing

In addition to these tests, other investigations were conducted such as visual inspection of all accessible rods in the field, review of all construction and fabrication records, and in-situ borescope examination of the accessible 2008 rod cavities in Pier E2 capbeam. The borescope examination revealed the presence of water inside four of the five rod cavities and voids in the grout at the bottom rod connection, inside the bottom chamber (top hat).

Table 4.1-1 provides a summary of the fabrication and construction records.

Table 4.1-1: Comparison of 2006, 2008, 2010, and 2013 Rods

		Tower Foundation	Pier E2		
		2006 Rods	2008 Rods	2010 Rods	2013 Rods
Fabrication	Steel	SAE 4140	SAE 4140	SAE 4140	SAE 4340
	Vacuum Degassing	<i>under review</i>	No	Yes	Yes
	Heat Treatment	Induction	Furnace (Double Heat Treatment)	Induction	Induction
	Magnetic Particle Testing (MT)	No	No	Yes	Yes
	Elongation (14% min required)	15% to 21%	12.5% to 15%	14% to 17%	16% to 21%
	Electrode Potential	-0.87 Vsce	-1.01 Vsce	-0.92 Vsce	-0.95 Vsce
Construction	Schedule	Fabricated 2006, Installed 2007, Grouted 2010, 1st Tension 2010/2011, Final Tension 2013	Fabricated 2008, Installed 2008, Grouted 2013, Tensioned March 2013	Fabricated 2010, Installed 2012, Grouted 2013, Tensioned April 2013	Fabricated 2013/2014, Installed Feb 2014, Grouted Feb/Mar 2014, Tensioned Mar 2014
	Environment	<i>under review</i>	Water removed from base of rod several times during construction	Through Rods No standing water issue	Through Rods No standing water issue
	Grouting	<i>under review</i>	After rod failure, pockets of water/air discovered in grouted Top Hat in 4 of 5 boroscope explorations of rod cavities	Through Rods. No indications of grouting issues.	Through Rods. No indications of grouting issues.
	Thread Deformation	No	Yes	No	No

4.2 SUMMARY OF RESULTS OF TESTS I, II, AND III

The following provides a summary of the main results of field and laboratory testing:

- An extensive field hardness survey confirmed that all rods on the SAS Bridge have hardness within the expected range. No abnormal readings were found. The results indicate that the bolts within a production batch have similar tensile strength and were subjected to similar heat treatment.
- The field hardness readings were verified by a side-by-side comparison with the hardness readings taken with standard laboratory testing equipment.
- Full-diameter and laboratory tests of the rods confirmed that the A354BD rods remaining in the SAS Bridge meet the strength requirements.
- The chemistry of the A354BD rods remaining on the SAS Bridge was found to be very uniform and suggests that SAE 4140 was the base alloy for all rods except the 2013 rods, which conformed to SAE 4340.
- The 2008 A354BD rods exhibited lower Charpy V-notch toughness than the samples from other A354BD rods in the bridge with the exception of one other heat (used in Group 8 and 9 material).

Table 4.2-1 provides a summary of these results.

Table 4.2-1: Test I, II, III, and III-M Results Summary

		Summary of Tests I, II, III, and III-M (all rods)			
		2006 Rods	2008 Rods	2010 Rods	2013 Rods
Mechanical Testing	Hardness — Lab (R/2) (HRC)	35	36	34	35
	Hardness — Lab (Edge) (HRC)	34	38	35	36
	Toughness — CVN (ft-lb)	35	14	37	48
	Full Size Tensile (ksi)	159	161	153	162

4.3 SUMMARY OF RESULTS OF TEST IV

A plot of the failure loads for all tested rods is provided in Figure 4.3-1. The service demand load levels are shown as horizontal lines in the figure for each category of rod. The yellow zone shows the results for specimens that did not break at 0.85 Fu or below and that were subsequently pulled to failure. The “SCC Threshold” line is drawn 5% below the lowest value measured in the test for rods that remained in the SAS. Test IV duplicated the failures of 2008 rods on Pier E2 in terms of breaking loads and mechanism of failure.

The test results can be summarized as follows:

- The EHE threshold of the 2010 Pier E2 rods is 0.75 Fu.
- The EHE threshold of the 2008 Pier E2 rods is 0.65 Fu.
- The difference between the 2008 and 2010 Pier E2 thresholds can be attributed to differences in toughness and a higher iron content of the galvanized coating on the 2010 rods (the higher iron content reduces the electro-chemical driving force for hydrogen deposition on the steel).
- EHE threshold of the various 2010 and 2006 rods varies from 0.80 Fu to 0.85 Fu.
- The EHE threshold of 3.5-inch PWS rods with threads rolled after heat treatment is 0.85 Fu, and is superior to that of similar rods with cut threads, with a threshold of 0.80 Fu.
- The EHE threshold of black 2013 Pier E2 rods is 0.85 Fu.
- The EHE threshold of galvanized 2013 Pier E2 rods is 0.85 Fu.
- The IHE threshold of 2008 rods is 0.85 Fu.

As shown in Figure 4.3-1 and Figure 4.3-2, the pretension load of the 2008 rods (0.70 Fu) is higher than the corresponding EHE threshold (0.65 Fu), which is consistent with the failures that occurred at Pier E2. More importantly, these figures show that the design loads of all rods presently in service on the SAS are less than the corresponding SCC threshold levels determined in Test IV, and that with a supplemental corrosion barrier, the long term capacity of the A354BD rods is 1.0 Fu or greater.

Figure 4.3-1: Test IV Failure Loads for A354BD Rods

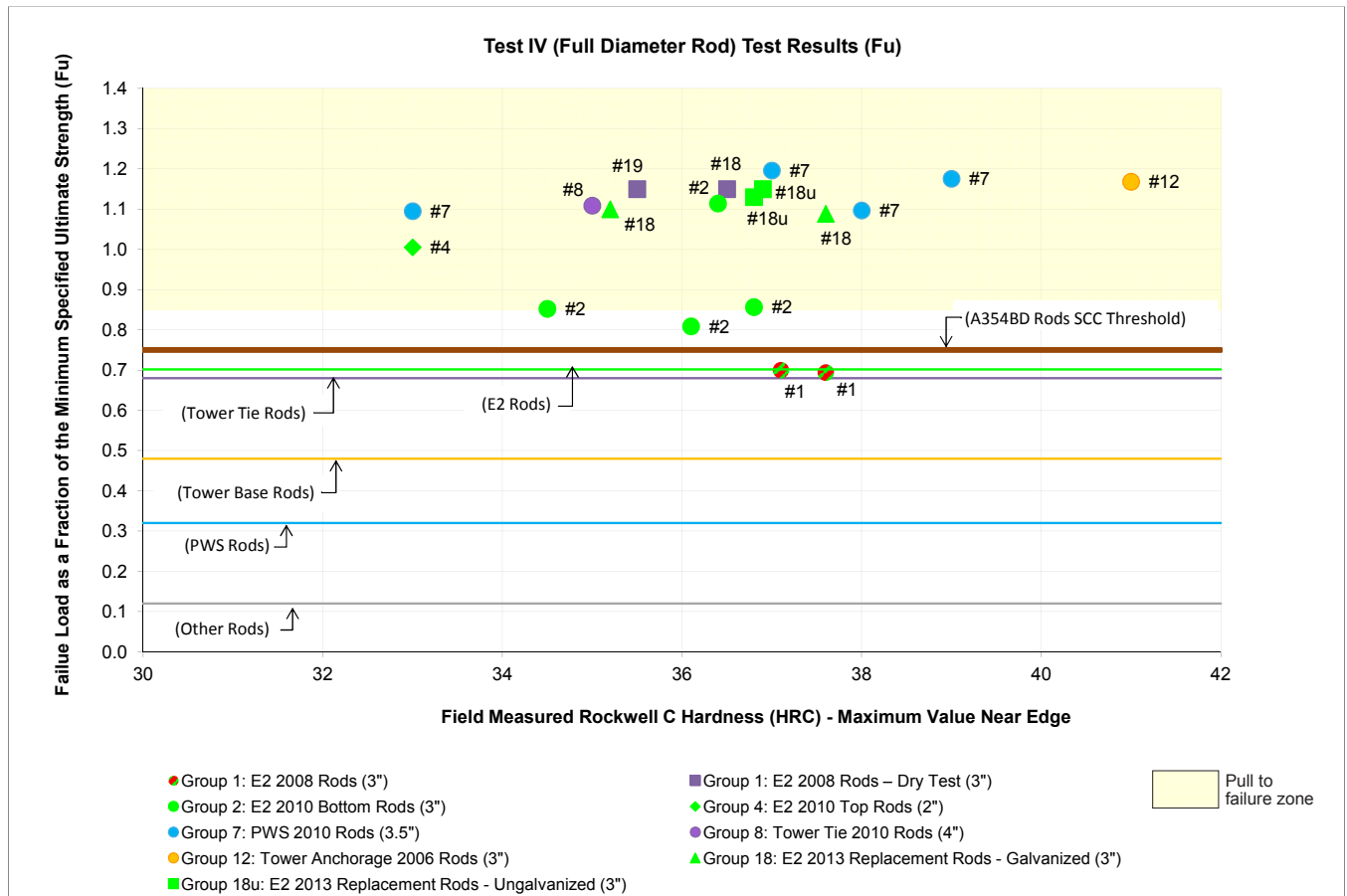


Figure 4.3-2: Test IV EHE Threshold and Applied Load Summary

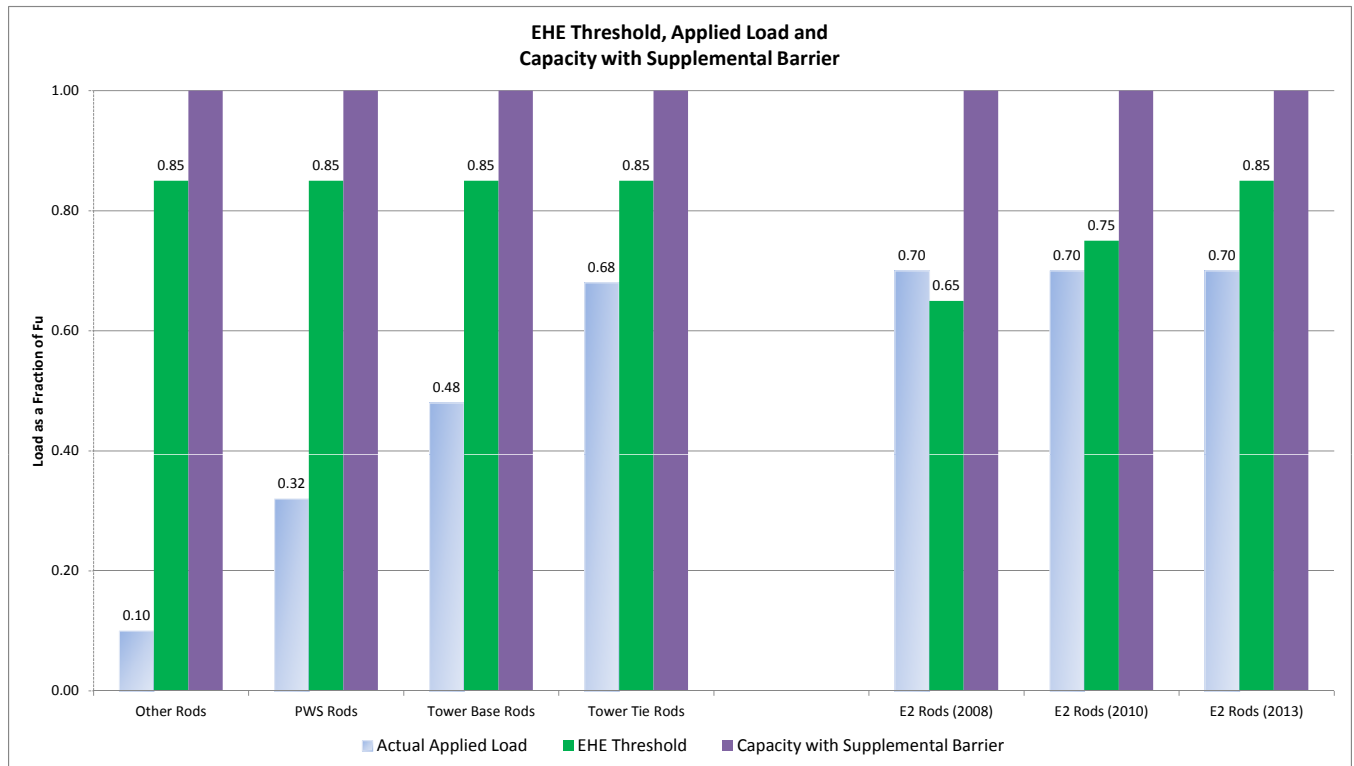


Figure 4.3-3: Load Displacement Graphs for Rods 14 -17 (2013 Galvanized and Ungalvanized)

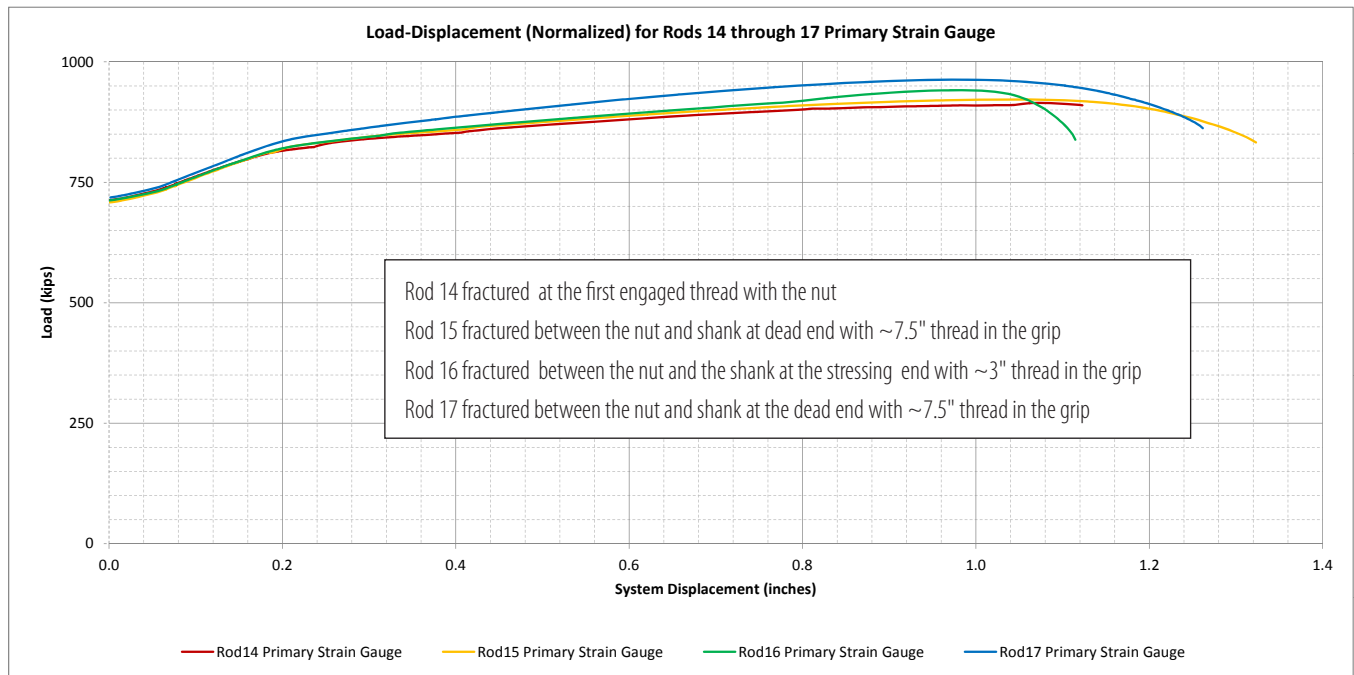


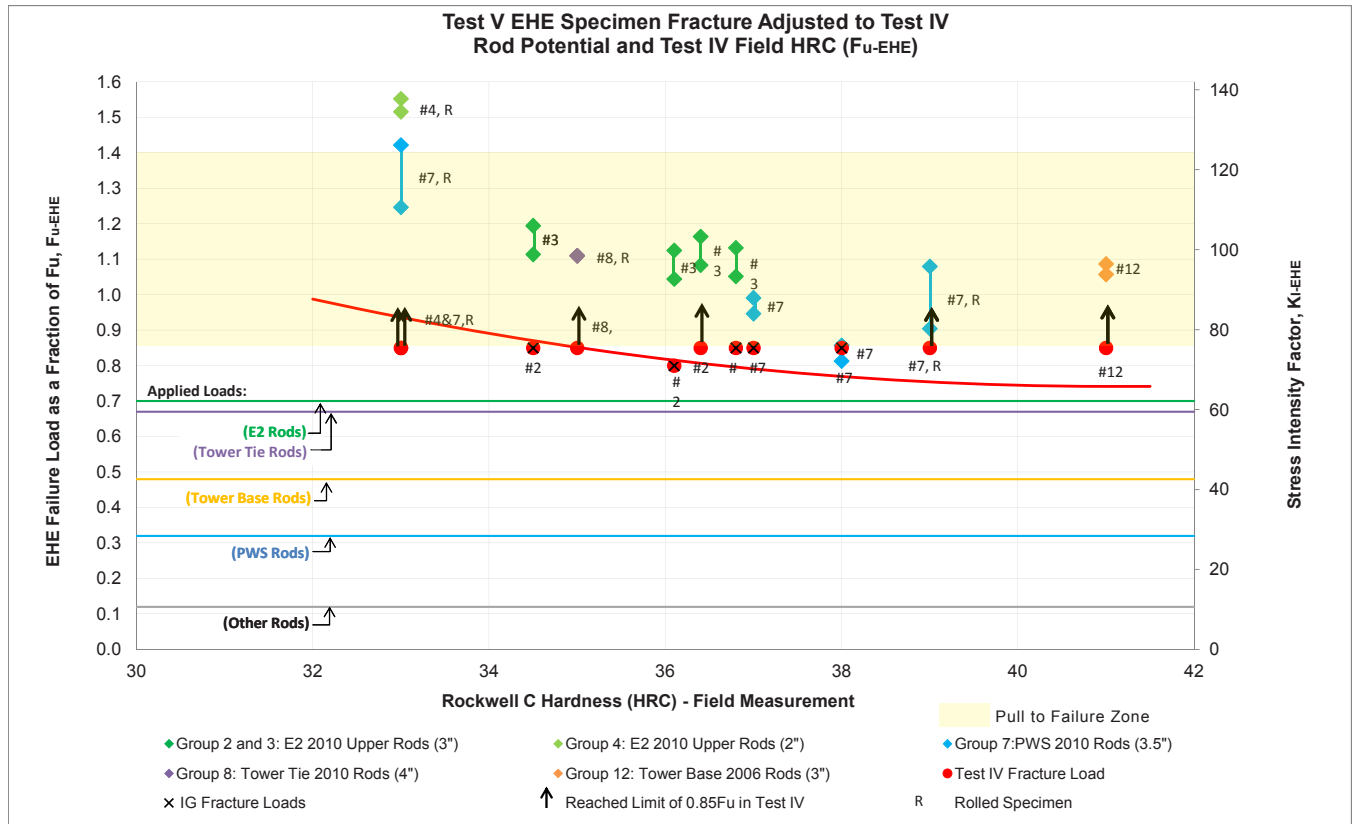
Figure 4.3-3 shows the load-displacement of the galvanized and ungalvanized 2013 rods after being subjected to step load of Test IV and reaching 0.85 Fu without failure. There are no notable differences in their load-displacement characteristics.

4.4 SUMMARY OF RESULTS OF TEST V

Threshold Stress Intensity – K_{I_p} and $K_{I_{sc}}$ values were determined for each rod sample provided. The $K_{I_{sc}}$ data are consistent with the Townsend Curve for $V_{sc}e-Zn$, independent of microstructure, and, for the SAE 4140 steel rods, only dependent on hardness of the specimen. The K_{I_p} data for the 2010 rods are higher than K_{I_p} data for the 2008 rods. In particular, the K_{I_p} data for rod samples with rolled threads are 10-20% higher than the K_{I_p} data for the cut-thread rod samples. Based on this limited data, neither the 2008 nor the 2010 specimens tested exhibit IHE.

The results of Test V corroborate the SCC threshold established in Test IV with full-diameter rods as shown in Figure 4.4-1.

Figure 4.4-1: Test V Specimen SCC Failure Load in Salt Water at Rods Potential (F_u)

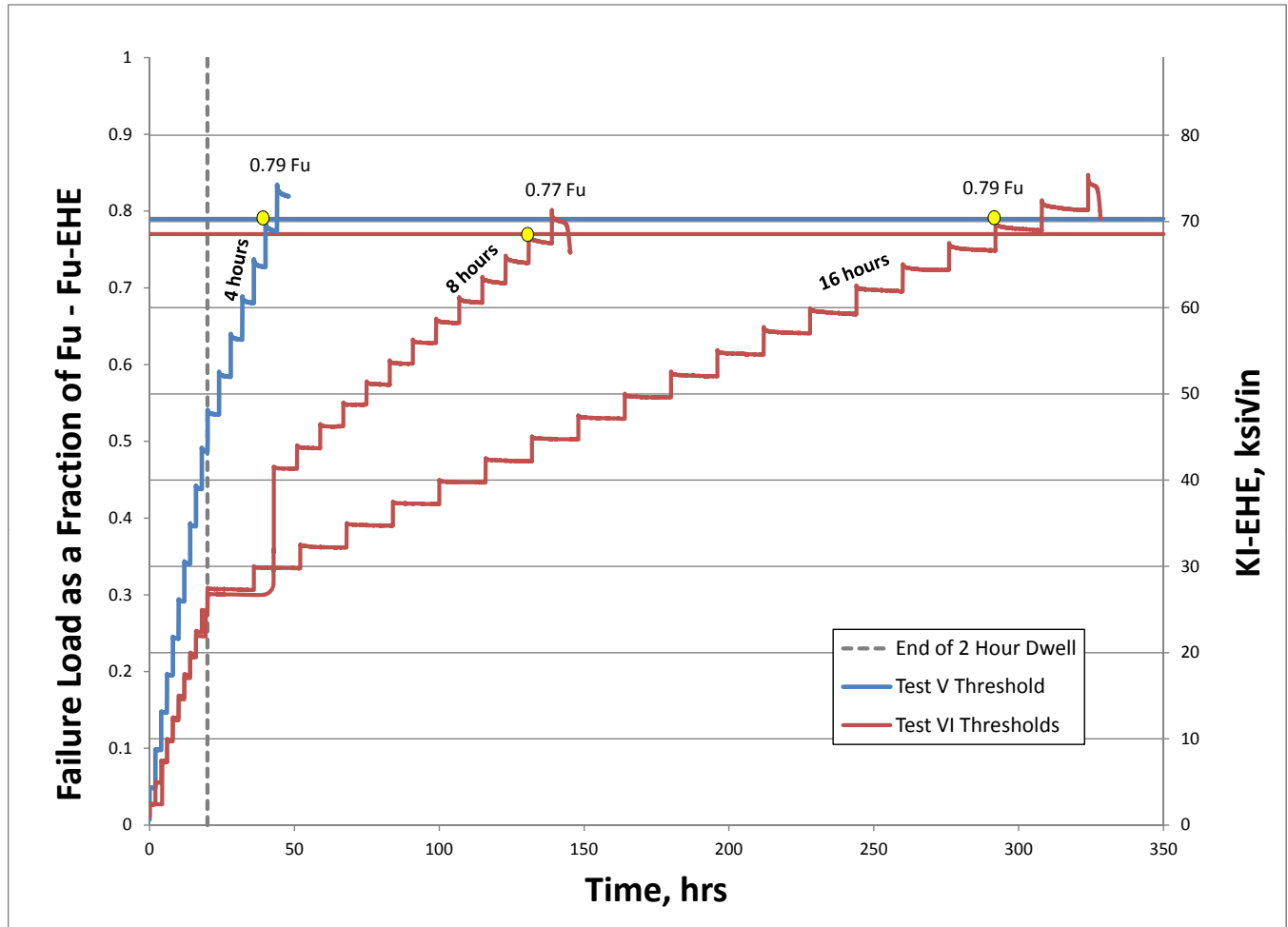


4.5 SUMMARY OF RESULTS OF TEST VI

Part 1

The test data from Test V and Test VI are plotted as a function of loading rate in Figure 4.5-1.

Figure 4.5-1: Test V and Test VI Load Rating



- Test VI validated that the Test IV and Test V strain rates were sufficient to reach a threshold.
- No additional crack initiation mechanisms were identified by decreasing the loading rate in Test VI, equivalent to extending the RSL-dwell time to eight hours or 16 hours.

Part 2

The sustained load test, to be completed in March 2015, consists of applying a sustained-load above, at, and below the threshold for 5000 hours. When completed, a report will be issued and included in Appendix N.

4.6 SUMMARY AND RECOMMENDATIONS

4.6.1 Summary

- 2008 A354BD Rods – These rods are no longer in use on the SAS
 - Test IV replicated the field results with the rods failing at 0.70 Fu when exposed to salt water thereby validating Test IV protocol.
 - IHE threshold is 0.85 Fu, which indicates that the 2008 rods in the field failed due to EHE.
 - Top and bottom segments of the same rod failed at same load level of 0.70 Fu.
- 2006/2010/2013 A354BD Rods
 - In Test IV, all rods failed at 0.80 Fu or greater, indicating that the SCC threshold of these rods can be conservatively set at 0.75 Fu.
 - Test V and Test VI are consistent with the threshold established in Test IV.
 - Rods with threads rolled after heat treatment exhibit superior resistance to SCC than cut threads.
 - Rods with higher toughness (higher CVN) exhibit higher SCC threshold.
 - The threshold of both galvanized and ungalvanized 2013 rods in Test IV is 0.85 Fu.

4.6.2 Conclusions and Recommendations

- The 2008 rods failed in the field due to EHE.
- The testing program established a conservative threshold in an aggressive salt water environment equal to 0.75 Fu for all A354BD rods on the SFOBB-SAS. This threshold is larger than the applied pre-tension loads.
- It is concluded that the A354BD rods in service on the SAS are safe, as they are not susceptible to SCC at the design loads and conditions, and no reduction in pre-tension is required.
- Galvanized A354BD rods on the SFOBB-SAS shall be protected from exposure to water by having at least one supplemental barrier against moisture such as: dehumidification, paint system, grout, or grease caps. This is expected to ensure that the long-term capacity of A354BD rods is greater than 1.0 Fu.
- The A354BD rods on the SAS shall be inspected and maintained per the SAS maintenance manual. The operating and maintenance instructions for the SAS will include requirements that the supplemental corrosion protection features of the A354BD rods be periodically checked and that they be maintained in a condition that ensures protection of the rods from exposure to aggressive conditions.

The following additional actions are also recommended based on recent field inspections of A354BD rods by Caltrans Construction (refer to Appendix O):

- It is reported that Pier E2 Bearings and Shear Key Top Housing Rods (Group 3 and 4) are painted for the exposed portions outside the structure, but are not painted for the portions inside the structure. A supplemental barrier for all portions of these rods shall be provided.
- The grease caps at the top of Pier E2 Rods (Group 2) were reported to be leaking. These grease caps shall be repaired and sealed to eliminate leakage.
- Water was recently observed at a number of Tower Anchorage Anchor Rod locations (Groups 12 and 13). The source of water shall be fully investigated and addressed.

5. GLOSSARY, ABBREVIATIONS, AND ACRONYMS

A354BD Anchor Rod: An anchor rod conforming to the ASTM A354 specification, which covers the chemical and mechanical requirements of quenched and tempered alloy steel bolts, studs and other externally threaded rods 4-inches and under in diameter. BD designates a grade specified in ASTM A354. The minimum tensile strengths of Grade BD rods are 150 ksi for ¼-inch to 2½-inch diameter rods and 140 ksi for over 2½-inch diameter rods.

American Society for Testing and Materials (ASTM): The organization was originally established as American Society for Testing Materials. The name was changed in the 1960's to American Society for Testing and Materials. It is now designated ASTM International. It currently has 143 technical committees that write standards, and there are more than 12,500 standards being maintained. The objectives of the Society include improving product quality, enhancing safety, facilitating market access, promoting trade, and building consumer confidence.

Anchor rod: A rod used to attach objects or structures to concrete. It generally includes two threaded ends, to which nuts and washers are attached to maintain loads in the rod.

Bake: Heat to a temperature, below the tempering or aging temperature of the metal or alloy, in order to remove hydrogen before embrittlement occurs by the formation of microcracks.

Bearing: A component located to transfer loads between the bridge structure and a supporting pier or abutment.

Brittleness: The tendency of a material to break at a very low strain, elongation, or deflection, and to exhibit a clean fracture surface with no indications of plastic deformation.

Charpy V-Notch test: An impact test (ASTM E23) in which a rectangular specimen with a “V”-shaped notch cut into the midpoint of the length is struck by a pendulum-mounted striker. The energy that is absorbed in fracture is calculated by comparing the height to which the striker would have risen had there been no specimen to the height to which it actually rises after fracture of the specimen.

Corrosion: The deterioration of a material, usually a metal, that results from a chemical or electrochemical reaction with its environment.

Crack: Line of fracture without complete separation.

Deck: The roadway portion of a bridge, including shoulders. In SAS, the deck is made up of steel orthotropic box girder.

Ductility: The ability of a material to deform plastically before fracturing.

Electrode Potential: The potential of an electrode, or galvanic couple, measured against a suitable reference electrode.

Elongation: A measure of the ductility of a material (the percentage stretch in the length of a test specimen). It is the amount of strain a material can experience before failure in a tensile test. A ductile material will record a high elongation, while brittle materials, such as ceramics, tend to show very low elongation.

Embrittlement: The loss of ductility or toughness or both, of a material, usually a metal or alloy.

Environmental hydrogen embrittlement (EHE): Hydrogen embrittlement caused by hydrogen introduced into a steel/metallic alloy from an environmental source coupled with stress either residual or externally applied.

Fatigue: A cyclic cracking mechanism that is progressive and localized, caused by repetitive loading over time at stress ranges below the yield strength, and is commonly transgranular.

fpc: fatigue precrack. A sharp crack that is deliberately placed at the root of a notched test specimen by applying a cyclic load at sufficient load and number of cycles to initiate a crack in order to prepare it for a fracture mechanics test for toughness or stress corrosion cracking.

Fracture strength: The normal stress at the beginning of fracture.

Galvanizing: A means of applying a protective zinc coating that will corrode in preference to the steel substrate.

Hardness Rockwell C Scale (HRC): The Rockwell scale is a hardness scale based on the indentation resistance of a material. There are several alternative scales, with the most commonly used being the “B” and “C” scales. HRC is a gauge of the hardness of a material based on a test that measures the depth of penetration by an indenter under a large load compared to the penetration made by a preload as specified in ASTM E18.

Hardness: Resistance of a material to small-area surface deformation, which is indicative of properties such as strength and abrasion resistance.

Heat treatment: Heating and cooling processes that produce metallurgical changes in the metallic alloy, which alter the mechanical properties and microstructure of the metal.

Hot-dip galvanizing (HDG): Applying a coating of zinc by immersion in a bath of molten zinc.

Hydrogen embrittlement (HE): Embrittlement caused by the presence of hydrogen within a metal or alloy.

Internal hydrogen embrittlement (IHE): Hydrogen embrittlement caused by absorbed atomic hydrogen into the steel/metallic alloy from an industrial hydrogen emitting process coupled with stress, either residual or externally applied.

KIctod: Elastic-plastic estimate of K_{Ic} using the crack tip opening displacement (ASTM E1290).

K_{Ic} : Fracture toughness, a material property that defines the critical conditions for fracture under linear elastic plane strain tensile loading conditions. It is determined with a fpc specimen (ASTM E399/E1820).

KI-EHE: Invariant value of the EHE threshold stress intensity — test conducted in aqueous solution under cathodic hydrogen charging conditions. Not geometry-dependent. It is determined with a fpc specimen.

KI-IHE: Invariant value of the IHE threshold stress intensity — test conducted in air. It is determined with a fpc specimen.

KI_{sc}: Threshold stress intensity for the onset of crack growth in an environment — the invariant value of the threshold stress intensity for stress corrosion cracking — test conducted under open circuit corrosion potential or freely corroding conditions. It is determined with a fpc specimen.

KI_ρ: The effective fracture toughness of a notched instead of an fpc specimen, where ρ is the radius of the notch, which in the case of a threaded rod is the root radius of the thread. It is a geometry-dependent value that depends on root radius of the thread and the rod properties.

KI_ρ-EHE: Invariant value of the EHE threshold effective stress intensity. The test is conducted in aqueous solution under cathodic hydrogen charging conditions, possibly due to galvanic coupling with coating, and the value is – dependent on root radius. It is determined with a notched specimen.

KI_ρ-IHE: Invariant value of the IHE threshold effective stress intensity factor. The test is conducted in air, and the value is dependent on root radius. It is determined with a notched specimen.

KI_ρ-max: The maximum value of the effective stress intensity in a KI fracture toughness test. It is determined with a notched specimen.

K_{max}: The maximum stress intensity factor in a KI_{ctod} or KI_c test. It is determined with either a fpc or notched specimen.

Magnetic particle testing (MT): A non-destructive method for detecting cracks and other discontinuities at or near the surface in ferromagnetic materials, such as iron, nickel, cobalt, and some of their alloys. Magnetic particle testing may be applied to raw material, semi-finished material, finished material, and welds, regardless of heat treatment or lack thereof.

Martensite: A metallurgical phase of some iron-carbon alloys that forms if the material is rapidly cooled from a high temperature. Generally this material is hard and brittle until tempered.

Morphology: The characteristics of a fractured surface (e.g., intergranular, transgranular, cleavage).

Orthotropic box girder (OBG): A structural steel box that is stiffened either longitudinally or transversely, or in both directions, to allow the roadway to directly bear vehicular loads and to contribute to the bridge structure's overall load-bearing behavior.

Pickling: (1) Treating a metal or alloy in a chemical bath to remove scale and oxides (e.g., rust) from the surface. (2) Complete removal of rust and mill scale by acid pickling, duplex pickling, or electrolytic pickling. The action of the acid on the metal results in the generation of hydrogen, some of which can be absorbed by the steel.

Pier E2: The first pier east of the main tower of the self-anchored suspension span, and where the twin steel orthotropic box girder roadways bear.

Pier: A vertical structure that supports the ends of a multi-span superstructure at a location between abutments.

Rising Step Load (RSL): A step modified slow strain rate test method to quantitatively measure the threshold stress intensity for the onset of subcritical crack growth (ASTM F1624).

Self-anchored suspension (SAS): The SAS portion of the new East Span of the San Francisco–Oakland Bay Bridge connects the Yerba Buena Island Transition Structures with the Skyway. A single continuous cable is anchored within the eastern end of the roadway, carried over the tower, wrapped around the two side-by-side decks at the western end carried back over the tower, and re-anchored at the eastern end of the roadway. The 2,047-foot-long SAS has a single 525-foot-tall steel tower, and is designed to withstand a massive earthquake.

Shear key: A shaped joint between two prefabricated elements that can resist shear through the geometric configuration of the joint. In the SAS, the shear keys are elements adjacent to the bearings that resist lateral seismic loads on the roadways.

Skyway: The Skyway portion of the new East Span of the San Francisco–Oakland Bay Bridge is a 1.2-mile-long, elevated viaduct connects to SAS, with two parallel roadways that accommodate five lanes of traffic plus two 10-foot- wide shoulders in each direction.

Strain rate: The rate of relative length deformation with time due to an applied stress.

Strain: Deformation of a material caused by the application of an external force.

Stress corrosion cracking (SCC): Cracking of a material produced by the combined action of corrosion and sustained tensile stress (residual or applied). In this report, the term is used to cover any non-ductile fracture of high strength steel at stresses below its ultimate tensile strength in a corrosive environment.

Stress: The intensity of force acting in or on a material, expressed as force per unit area.

Stress–intensity factor (K): The magnitude of the mathematically ideal crack–tip stress field (stress field singularity) in a homogeneous linear–elastic body.

Susceptibility to hydrogen embrittlement: A material property that is measured by the threshold stress intensity factor for hydrogen-induced stress cracking, K_{Isc} , K_{I-IHE} , or K_{I-EHE} , which can be a function of hardness and microstructure.

Tensile load: A force that attempts to pull apart or stretch an object in the direction of the applied load
Tension test: A test in which a tensile force applied in the axial direction of a specimen as per ASTM E8.
Tension: A force that stretches or pulls on a material in the direction of the applied load.

Threshold (th): A point, separating conditions that will produce a given effect, from conditions that will not produce the effect.

Threshold stress (σ_{th}): A stress, below which no hydrogen stress cracking will occur and above which time-delayed fracture will occur.

Threshold stress intensity (K_{th}): The stress intensity, below which no hydrogen stress cracking will occur and above which, time-delayed fracture will occur.

Townsend test: An accelerated test to determine the susceptibility of a material to stress corrosion cracking. The material is tested in a 3.5% sodium chloride solution while tensioned progressively in step loads over time until failure.

Ultimate tensile strength (UTS): The maximum stress that a material can withstand while being stretched or pulled before failing or breaking.

Vacuum degassing: A process where molten metal (commonly steel) is placed in a vacuum to remove excess hydrogen and/ or carbon.

Yerba Buena Island Transition Structures: Connects the SAS to the Yerba Buena Island tunnel and provide the transition from the East Span's side-by-side traffic to the upper and lower decks of the tunnel and the West Span.

6. REFERENCES

1. SFOBB Contract Change Order No. 312.
2. Boyd, Walter K. and Hyler, W.S. "Factors Affecting Environmental Performance of High-Strength Bolts." Journal of Structural Division 99(7) (1973). Print.
3. Townsend Jr., H.E., "Effects of Zinc Coatings on the Stress Corrosion Cracking and Hydrogen Embrittlement of Low-Alloy Steel." Metallurgical Transactions A 6A (1975). Print.
4. P. S. Tyler, M. Levy, and L. Raymond, Investigation of the Conditions for Crack Propagation and Arrest under Cathodic Polarization by Rising Step Load Bend Testing, Corrosion, Vol. 47, No. 2, pp. 82-87 (1991).
5. Olsen, C., "Fatigue Crack Growth Analyses of Aerospace Threaded Fasteners: Part I: State of Practice Bolt Crack Growth Analyses Methods, in Structural Integrity of Fasteners." STP 1487 (2007).
6. Kephart, A.R. "Benefits of Thread Rolling Process to the Stress Corrosion Cracking and Fatigue Resistance of High Strength Fasteners." Symposium on Environmental Degradation of Materials in Nuclear Power System – Water Reactors. 1993.
7. NMAB 328 "Rapid, Inexpensive Tests for Determining Fracture Toughness", National Academy of Sciences, Washington, D.C. 1976
8. Raymond, L., "The Susceptibility of Fasteners to Hydrogen Embrittlement and Stress Corrosion Cracking", Chapter 39, "Handbook of Bolts and Bolted Joints" by John H. Bickford & Sayad Nassar, Published by Marcel Dekker, 1998
9. Tada, Hiroshi, "The Stress Analysis of Cracks Handbook," Paris Productions, Inc., St. Louis, Missouri, 1985.
10. Raymond, L., "Fracture Mechanics Applied to Tensile Fasteners" American Fastener Journal, Part 1, "Failure Mode" Oct/Nov, 1989, Part 2, "Material Selection" Jan/Feb, 1990, Part 3, "Environmental Effects" Mar/Apr, 1990, Part 4, "Test Methods" May/June, 1990, Part 5, "Hydrogen Embrittlement" Sep/Oct, 1990.
11. Dull, D.L., and Raymond, L., "Electrochemical Techniques", Hydrogen Embrittlement Testing, ASTM STP 543, June 1972, page 20.

ASTM REFERENCES

ASTM Standard A143, 2007, "Standard Practice for Safeguarding Against Embrittlement of Hot-Dip Galvanized Structural Steel Products and Procedure for Detecting Embrittlement," ASTM International, West Conshohocken, PA, 2003, DOI: 10.1520/A0143_A0143M-07R14, www.astm.org.

ASTM Standard A354, 2011, "Standard Specification for Quenched and Tempered Alloy Steel Bolts, Studs, and Other Externally Threaded Fasteners," ASTM International, West Conshohocken, PA, 2003, DOI: 10.1520/A0354-11, www.astm.org.

ASTM Standard A1038, 2013, "Standard Test Method for Portable Hardness Testing by the Ultrasonic Contact Impedance Method," ASTM International, West Conshohocken, PA, 2003, DOI: 10.1520/A1038, www.astm.org.

ASTM Standard E18, 2014, "Standard Test Methods for Rockwell Hardness of Metallic Materials," ASTM International, West Conshohocken, PA, 2003, DOI: 10.1520/E0018, www.astm.org.

ASTM Standard E23, 2012, "Standard Test Methods for Notched Bar Impact Testing of Metallic Materials," ASTM International, West Conshohocken, PA, 2003, DOI: 10.1520/E0023-12C, www.astm.org.

ASTM Standard E140, 2012, "Standard Hardness Conversion Tables for Metals Relationship Among Brinell Hardness, Vickers Hardness, Rockwell Hardness, Superficial Hardness, Knoop Hardness, Scleroscope Hardness, and Leeb Hardness," ASTM International, West Conshohocken, PA, 2003, DOI: 10.1520/E0140, www.astm.org.

ASTM Standard E384, 2011, "Standard Test Method for Knoop and Vickers Hardness of Materials," ASTM International, West Conshohocken, PA, 2003, DOI: 10.1520/E0384-11E01, www.astm.org.

ASTM Standard E399, 2012, "Standard Test Method for Linear-Elastic Plane-Strain Fracture Toughness K_{Ic} of Metallic Materials," ASTM International, West Conshohocken, PA, 2003, DOI: 10.1520/E0399, www.astm.org.

ASTM Standard E812, 1997, "Standard Test Method for Crack Strength of Slow-Bend Precracked Charpy Specimens of High-Strength Metallic Materials (Withdrawn 2005)," ASTM International, West Conshohocken, PA, 2003, DOI: 10.1520/E0812-91R97, www.astm.org.

ASTM Standard E1290, 2008, "Standard Test Method for Crack-Tip Opening Displacement (CTOD) Fracture Toughness Measurement (Withdrawn 2013)," ASTM International, West Conshohocken, PA, 2003, DOI: 10.1520/E1290-08E01, www.astm.org.

ASTM Standard E1681, 2013, "Standard Test Method for Determining Threshold Stress Intensity Factor for Environment-Assisted Cracking of Metallic Materials," ASTM International, West Conshohocken, PA, 2003, DOI: 10.1520/E1681, www.astm.org.

ASTM Standard F606, 2014, "Standard Test Methods for Determining the Mechanical Properties of Externally and Internally Threaded Fasteners, Washers, Direct Tension Indicators, and Rivets," ASTM International, West Conshohocken, PA, 2003, DOI: 10.1520/F0606-14, www.astm.org.

ASTM Standard F1624, 2012, "Standard Test Method for Measurement of Hydrogen Embrittlement Threshold in Steel by the Incremental Step Loading Technique," ASTM International, West Conshohocken, PA, 2003, DOI: 10.1520/F1624-12, www.astm.org.

ASTM Standard F1940, 2007, "Standard Test Method for Process Control Verification to Prevent Hydrogen Embrittlement in Plated or Coated Fasteners," ASTM International, West Conshohocken, PA, 2003, DOI: 10.1520/F1940-07A, www.astm.org.

ASTM Standard F2078, 2008, "Standard Terminology Relating to Hydrogen Embrittlement Testing," ASTM International, West Conshohocken, PA, 2003, DOI: 10.1520/F2078-08A, www.astm.org.

ASTM Standard F2660, 2013, "Standard Test Method for Qualifying Coatings for Use on A490 Structural Bolts Relative to Environmental Hydrogen Embrittlement," ASTM International, West Conshohocken, PA, 2003, DOI: 10.1520/F2660, www.astm.org.

7. APPENDICES

Only cover pages of appendices provided for reference. Full appendices provided under separate cover.

- A. Presentations to TBPOC
- B. E2 Shear Keys S1/S2 Design Alternatives
- C. S1/S2 Alternative Load Path (Shimming) Report
- D. A354BD Rods Project Specifications
- E. Hood Canal Floating Bridge Report (3/20/2014 Revision)
- F. Borescope Investigation of Pier E2 Rods Holes, SMR Reports (2011 and 2013)
- G. BAMC's Borescope Report (04/17/2014 Revision 3)
- H. E2 Shear Key Rod Failure Fracture Analysis Report
- I. Theory of Hydrogen Embrittlement and Stress Corrosion Cracking
- J. Test I, II, III, M-Shape, II-M, III-M Reports
- K. Test IV Plans and Field Reports
- L. Test IV Post-Fracture Analysis Reports
- M. Test V Details and Data Report
- N. Test VI Details and Data Report
- O. Field Inspection Report on the Tower Anchorage Anchor Rods

*Appendix A –
Presentations to TBPOC*



July 24, 2014
Toll Bridge Program Oversight Committee

A354BD Rods Testing Program Current Results

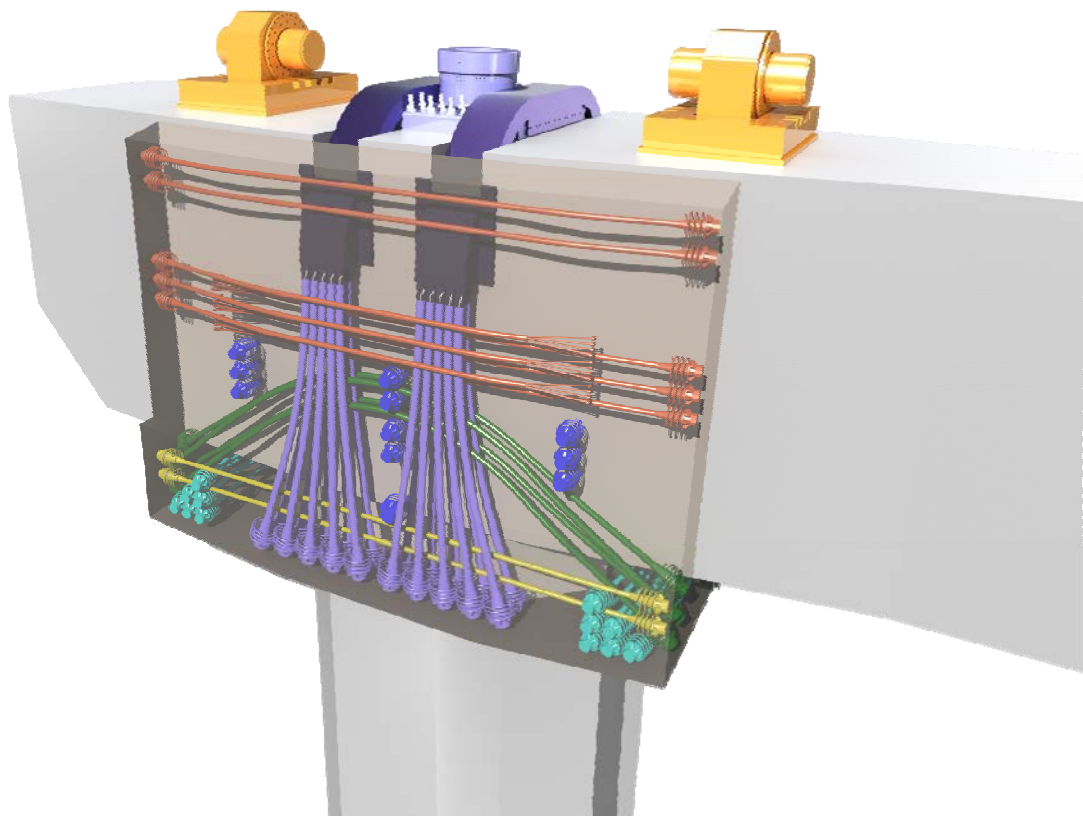


August 28, 2014
Toll Bridge Program Oversight Committee

A354BD Rods Testing Program Current Results

*Appendix B –
E2 Shear Keys S1/ S2 Design Alternatives*

San Francisco-Oakland Bay Bridge Self-Anchored Suspension Span (SFOBB-SAS)



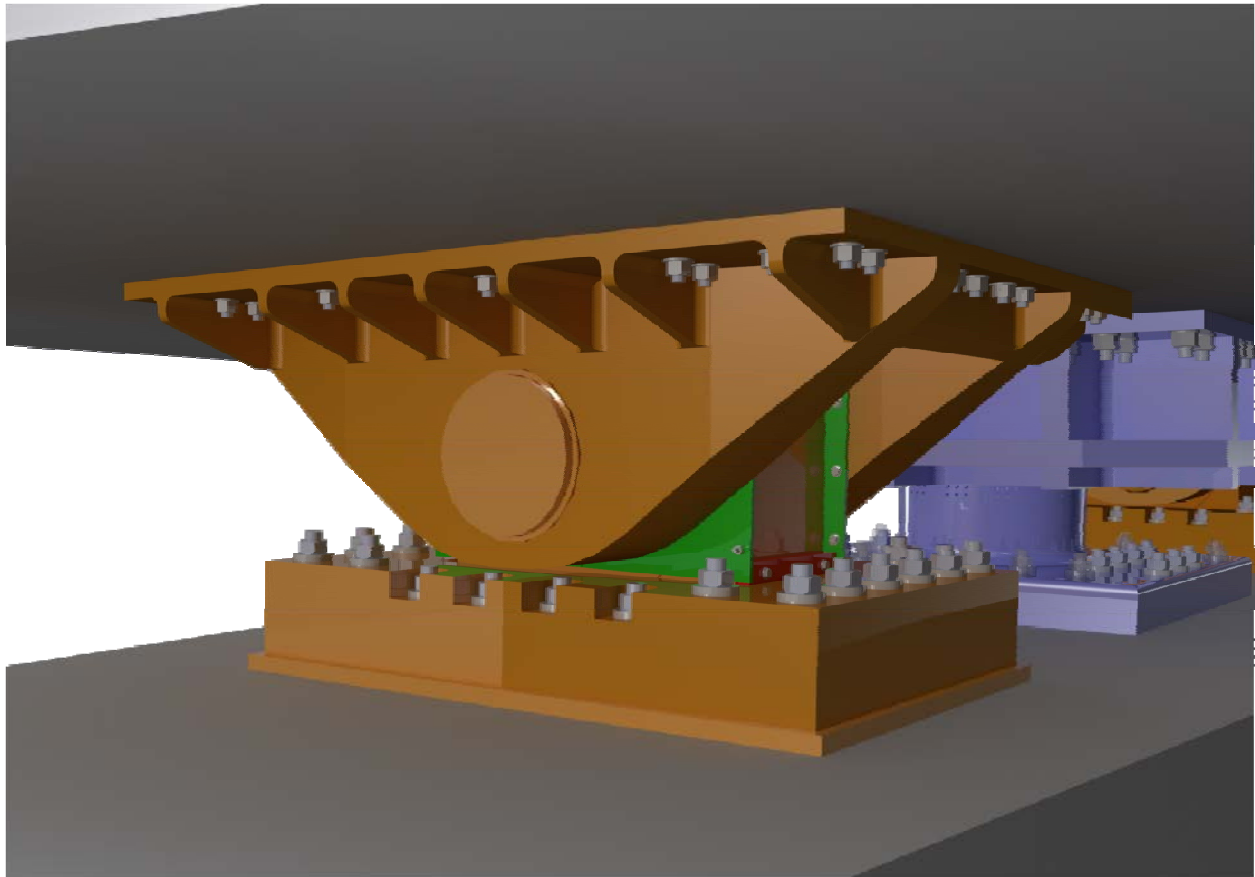
NEW DESIGN OF SHEAR KEYS S1 & S2

August 2, 2013



*Appendix C –
S1/ S2 Alternative Load Path (Shimming)
Report*

San Francisco-Oakland Bay Bridge Self-Anchored Suspension Span (SFOBB-SAS)



SEISMIC EVALUATION OF SAS AT E2 PIER PRIOR TO COMPLETION OF SHEAR KEYS S1 & S2

July 15, 2013



*Appendix D –
A354BD Rods Project Specifications*



STATE OF CALIFORNIA
DEPARTMENT OF TRANSPORTATION

**NOTICE TO CONTRACTORS
AND
SPECIAL PROVISIONS
FOR CONSTRUCTION ON STATE HIGHWAY IN
THE CITY AND COUNTY OF SAN FRANCISCO
AT YERBA BUENA ISLAND**

DISTRICT 04, ROUTE 80

For Use in Connection with Standard Specifications Dated JULY 1999, Standard Plans Dated JULY 1999, and Labor Surcharge and Equipment Rental Rates.

(INFORMAL BIDS CONTRACT)

CONTRACT NO. 04-0120E4

04-SF-80-13.4,13.8

ACBRIM-080-(094)N

***** CONFORMED COPY FOR INTERNAL USE ONLY; NOT FOR PUBLIC DISTRIBUTION.*****

**Bids Open: January 21, 2003
Dated: October 17, 2003**

OSD

<i>Addendum 1</i>	<i>November 20, 2003</i>	<i>Addendum 5</i>	<i>January 7, 2004</i>
<i>Addendum 2</i>	<i>November 24, 2003</i>	<i>Addendum 6</i>	<i>January 12, 2004</i>
<i>Addendum 3</i>	<i>December 12, 2003</i>	<i>Addendum 7</i>	<i>January 14, 2004</i>
<i>Addendum 4</i>	<i>December 19, 2003</i>	<i>Addendum 8</i>	<i>January 16, 2004</i>



STATE OF CALIFORNIA
DEPARTMENT OF TRANSPORTATION

**NOTICE TO CONTRACTORS
AND
SPECIAL PROVISIONS**

**FOR CONSTRUCTION ON STATE HIGHWAY IN
SAN FRANCISCO COUNTY IN SAN FRANCISCO
FROM 0.6 KM TO 1.3 KM EAST OF THE YERBA BUENA TUNNEL EAST PORTAL**

DISTRICT 04, ROUTE 80

**For Use in Connection with Standard Specifications Dated JULY 1999, Standard Plans Dated JULY 1999, and Labor
Surcharge and Equipment Rental Rates.**

CONTRACT NO. 04-0120F4

04-SF-80-13.2/13.9

***** CONFORMED THROUGH ADDENDUM NO. 7 ***
May 25, 2006 edition**

**Bids Open: March 22, 2006
Dated: August 1, 2005**

OSD

List of ASTM's

- ASTM A 354
- ASTM A 490
- ASTM A 123/ A 123M
- ASTM A 143/ A 143M
- ASTM F 606
- ASTM F 2329

ASTM specifications are not reproduced in this appendix due to ASTM copyright restrictions.

Interested readers are referred to www.astm.org for material purchasing details.

DEPARTMENT OF TRANSPORTATION - District 4 Toll Bridge Program

333 Burma Rd.
Oakland, CA 94607
(510) 622-5660, (510) 286-0550 fax



*Flex your power
Be energy efficient!*

October 31, 2008

Contract No. 04-0120F4
04-SF-80-13.2 / 13.9
Self-Anchored Suspension Bridge
Letter No. 05.03.01-002906

Michael Flowers
Project Executive
American Bridge/Fluor, A JV
375 Burma Road
Oakland, CA 94607

Dear Michael Flowers,

Authority to Proceed – CCO 91 - Additional Magnetic Particle Testing of Anchor Rods/Bolts

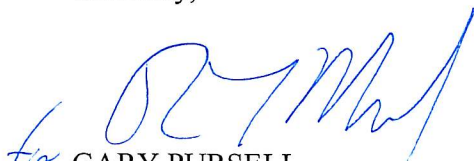
In accordance with Section 4-1.03, "Extra Work," of the Standard Specifications, ABF is directed to perform additional Magnetic Particle Testing (MT) in accordance with ASTM specification A490, on cable bracket anchor rods, main cable anchor rods and other ASTM 354, Grade BD anchor rods and bolts to be tensioned in excess of 0.5Fu. This additional work will be covered under Contract Change Order (CCO) No. 91.

The items requiring additional MT include the following:

1. East Saddle tie rod
2. Pier E2 Shear Key - anchor rods connecting stub to the E2 concrete cross beam
3. Pier E2 Shear Key - anchor bolts connecting OBG with shear key housing
4. Spherical Bushing Bearings (Pier E2) - anchor rods connecting hold down to E2 concrete cross beam
5. Spherical Bushing Bearings (Pier E2) - anchor bolts to OBG
6. Spherical Bushing Bearings (Pier E2) -Spherical bushing assembly bolts
7. Cable bracket anchor rods
8. Main Cable anchor rods

Please contact Brian Boal at 510-622-5191 if you have any questions.

Sincerely,


for GARY PURSELL
Resident Engineer

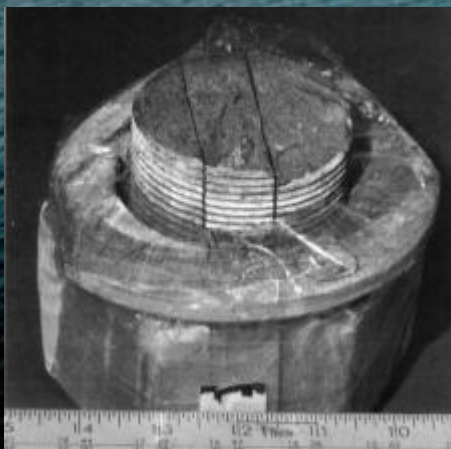
cc: Rick Morrow, Brian Boal, Gary Lai, Scott Fabel, Jinesh Mehta
file: 05.03.01, 49.091

*Appendix E –
Hood Canal Floating Bridge Report
(3/20/2014 Revision)*

HOOD CANAL FLOATING BRIDGE

High Strength Anchor Bolts
Example of Application of Greased and
Sheathed Double Corrosion Protection Systems

DRAFT



For:
San Francisco-Oakland Bay Bridge
SAS pier E2 Anchor Bolts Study
By the Bay Area Management
Consultants (BAMC) For the Bay Area
Toll Authority (BATA)

March 20, 2014

*Appendix F –
Borescope Investigation of Pier E2 Rods
Holes, SMR Reports (2011 and 2013)*

PROJECT INFORMATION

04-0120F4

Self-Anchored Suspension Bridge

SUBJECT

Borescope Investigation of Pier E2 Rod Holes – 2011

BACKGROUND

A total of 288 ASTM A354 Gr. BD bearing and shear key anchor rods have been installed in Pier E2, per the contract requirements; 96 of these 3-inch hot-dip galvanized rods are shear key anchor rods that were embedded in concrete at Pier E2. The shear key anchor rods were fabricated in 2008 and assembled inside pipe sleeves in Shear Keys S1 and S2 after release to the jobsite. The locations of the shear keys (S1 and S2) are highlighted in Figure 1. The area around the pipe sleeves was grouted five years later, in 2013.

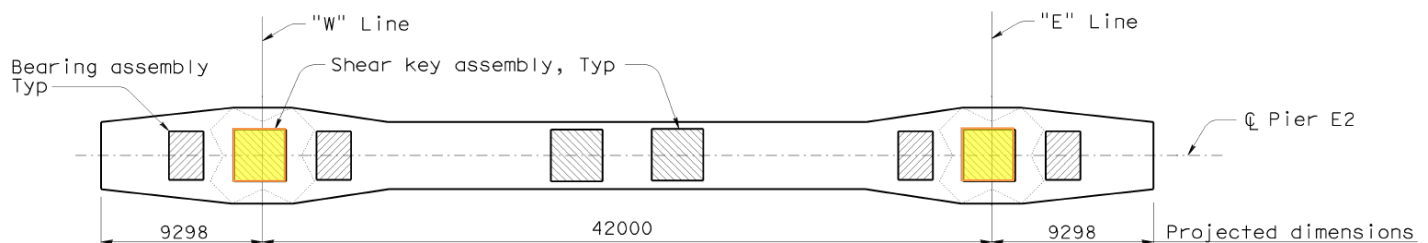


Figure 1: Locations of Shear Keys S1 (left) and S2 (right) on Pier E2

As shown in **Figure 2**, the details of the rods in S1 and S2 are different from the details for the bearing anchor rods. The embedment of the shear key E2 rods in concrete prevents access from below. Prior to installation of the shear keys, the rods had to be flush with the Pier E2 top surface; therefore, pipe sleeves were installed below the bearing plate to allow for the rods to be temporarily lowered (**Figures 3 and 4**). The area inside the temporary pipe sleeve was to be grouted after the rods were raised to their final position during installation of the shear key.

PROJECT INFORMATION

04-0120F4

Self-Anchored Suspension Bridge

SUBJECT

Borescope Investigation of Pier E2 Rod Holes – 2013

BACKGROUND

A total of 288 ASTM A354 Gr. BD bearing and shear key anchor rods have been installed in Pier E2. 96 of these 3-inch hot-dip galvanized rods are shear key anchor rods that were embedded in concrete. The rods were fabricated in 2008 and assembled inside pipe sleeves in Shear Keys S1 and S2. The area around the pipe sleeves was grouted five years later, in 2013.

Once the grouting was complete, in Mar. 2013, thirty-two (32) of the shear key anchor rods fractured shortly after tensioning. The specific rods are highlighted in **Figure 1**. The top portions of the rods were extracted in segments for fracture analysis. It was not possible to retrieve the bottom fracture surfaces. The Department requested that METS investigate the interior of the rod holes with a borescope to evaluate the in-situ conditions and provide images of the fracture region.

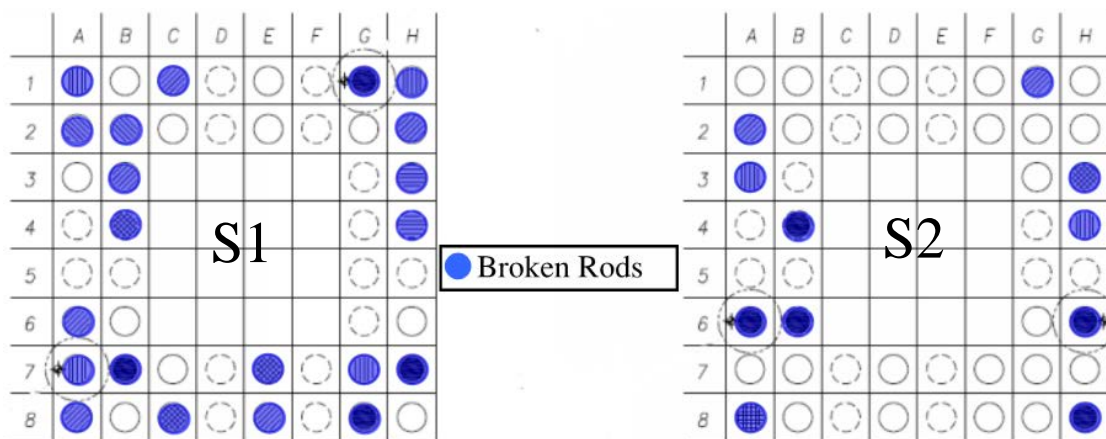


Figure 1: Locations of Failed Rods in Shear Keys S1 & S2

*Appendix G –
BAMC's Borescope Report
(04/17/2014 Revision 3)*

DRAFT REPORT

Review of the Failed E2 Embedded Anchor Rod Boroscope Investigation



Rev. 3: April 17, 2014

For:

San Francisco-Oakland Bay Bridge (SFOBB)
SAS Pier E2 Anchor Bolts Study

By:

Bay Area Management Consultants (BAMC) for the Bay Area Toll
Authority (BATA)

*Appendix H –
E2 Shear Key Rod Failure Fracture
Analysis Report*

PROJECT INFORMATION

Project# 04-0120F4

SUBJECT

Metallurgical Analysis of Bay Bridge Broken Anchor Rods S1-G1 & S2-A6

METALLURGICAL TEAM

The testing and analysis of the failed anchor rods from shear keys S-1 and S-2 was performed jointly by Salim Brahimi, Rosme Aguilar and Conrad Christensen.

Mr. Brahimi is a consultant to ABF (American Bridge Fluor – joint venture). He is the president of IBECA Technologies. He is a licenced member of the Quebec Order of Professional Engineers and has over 24 years of experience in the fastener industry. Mr. Brahimi holds a masters of materials engineering from McGill University in Montreal. He is the current chairman of the ASTM Committee F16 on Fasteners. He also serves on the ISO TC2 (Technical Committee on Fasteners), ASTM committees B08 (Coatings), E28 (Mechanical Testing), A01 (Steel), F07 Aerospace and Aircraft, Industrial Fasteners Institute (IFI) Standards and Technical Practices Committee, and the Research Council on Structural Connections (RCSC). Mr. Brahimi is recognized and highly respected throughout the fastener industry as a leading expert in fastener manufacturing, fastener metallurgy, application engineering, corrosion prevention, failure analysis and hydrogen embrittlement.

Mr. Aguilar is the Branch Chief of the California Department of Transportation (Caltrans) Structural Materials Testing Branch, responsible for quality assurance testing of structural materials product used in construction projects throughout the state. He has over thirty (30) years of work experience as an Engineer. Twenty three (23) of these years as a Transportation Engineer in Caltrans, two (2) years as a Quality Assurance Auditor for INTEVEP, S.A. (The Technological Research Institute of the Venezuelan Petroleum Industry), and five (5) years as a Researcher in the area of New Products Development at SIDOR (a Venezuelan Steel Mill). Mr. Aguilar holds a Master of Science in Metallurgy (1982) and a B.S. in Metallurgical Engineering (1980) from the University of Utah, Salt Lake City, Utah. He is a Registered Professional Civil Engineer in the State of California. His areas of expertise and responsibility are Quality Assurance and materials testing but in addition he has performed or assisted in the performance of numerous materials characterization and failure analysis for Caltrans and other state agencies.

Mr. Christensen is a consultant to the California Department of Transportation (Caltrans). He is the principal and founder of Christensen Materials Engineering, which provides laboratory testing and materials engineering services. He has over 32 years of experience as a metallurgist specializing in materials testing and failure analysis. His areas of expertise include: microscopic

Appendix I –
Theory of Hydrogen Embrittlement and
Stress Corrosion Cracking
by
H.E. Townsend

Hydrogen Embrittlement and Stress Corrosion Phenomena

1. Mechanisms of Hydrogen Embrittlement

This purpose of this Appendix is to review the hydrogen embrittlement and stress corrosion cracking of steels, particularly as it relates to galvanized ASTM A354 BD rods.

In general, hydrogen can affect the mechanical behavior of steels in several ways. For mild steels, dissolved hydrogen can produce loss of ductility at low concentrations, and blistering due to internal pressure of molecular hydrogen at high concentrations. At high temperatures, hydrogen can react with the carbon in steels to form methane, with significant loss of mechanical properties. In the case of high strength steels, small amounts (0.01-0.1 ppm) of dissolved hydrogen can cause slow crack growth under sustained tensile loads leading to brittle fracture.

When high-strength steels are subjected to sustained tensile loads under normal ambient conditions, dissolved hydrogen is attracted to regions of high tensile stress. As it diffuses to high-stress regions, it is adsorbed on planes of weakness, such as grain boundaries and cleavage planes, where it reduces the attractive forces between iron atoms. When the force required for decohesion of these planes is reduced to less than that required to cause plastic flow, slow crack growth occurs.

As described by Petch and Stables [1], and Petch [2], decohesion occurs because of a reduction in surface energy due to the adsorption of hydrogen.

It is now widely accepted that stress corrosion cracking of high-strength, quenched-and-tempered steel exposed to aqueous environments proceeds by a hydrogen embrittlement mechanism. Others have reviewed theory, testing, and phenomenology of stress corrosion cracking and hydrogen embrittlement in high-strength metals in detail [3-6].

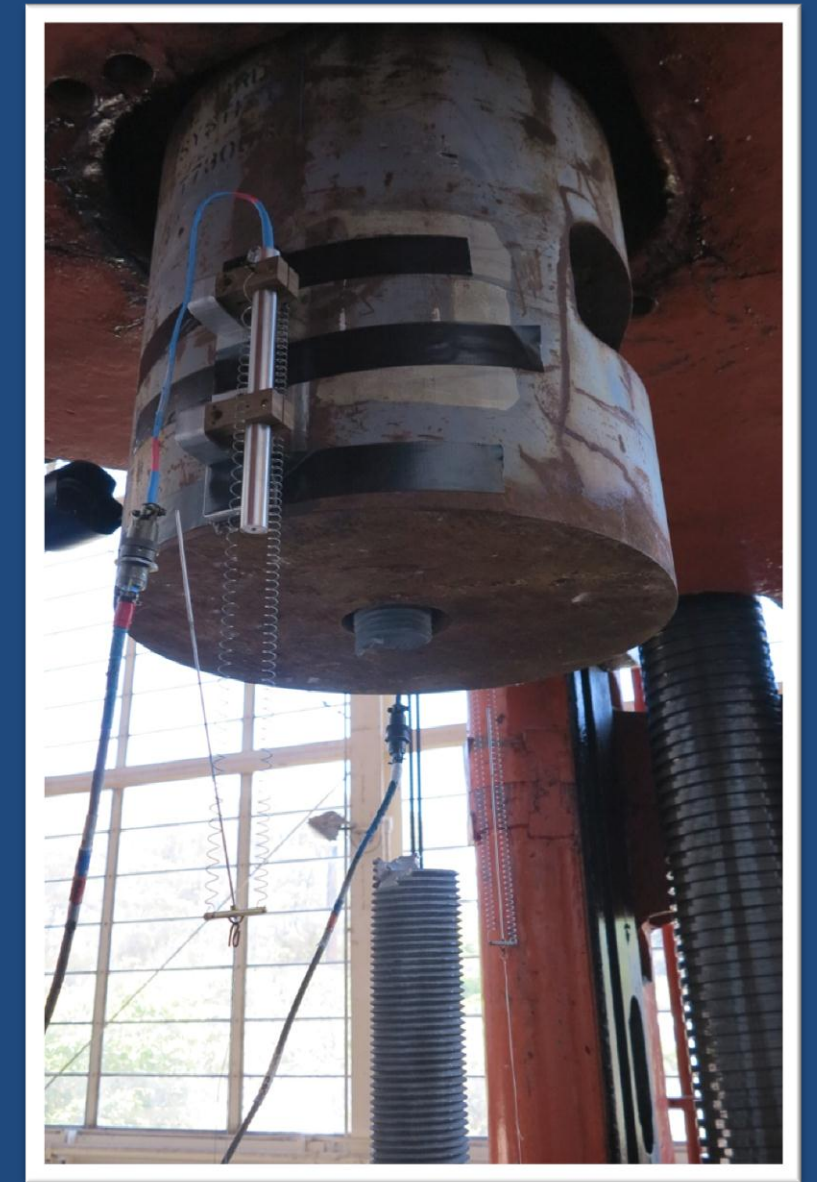
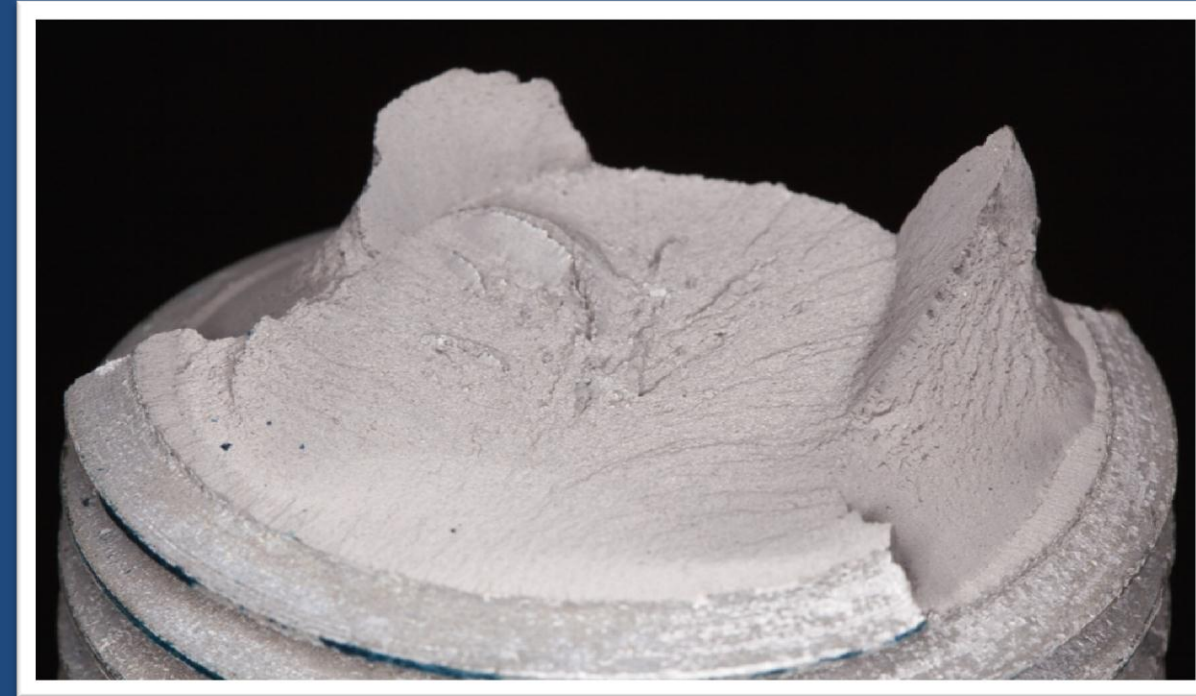
Three essential factors are simultaneously required to produce hydrogen embrittlement as shown in Figure 1.

*Appendix J –
Test I, II, III, M-Shape, II-M, III-M Reports*

Appendix J –

Test I, II, III, M-Shape, II-M, III-M Reports

Test I, II & III



SAS A354BD TESTING PROGRAM RESULTS

Test I, II & III

Appendix J –

Test I, II, III, M-Shape, II-M, III-M Reports

M-Shape, II-M, III-M (Forthcoming)

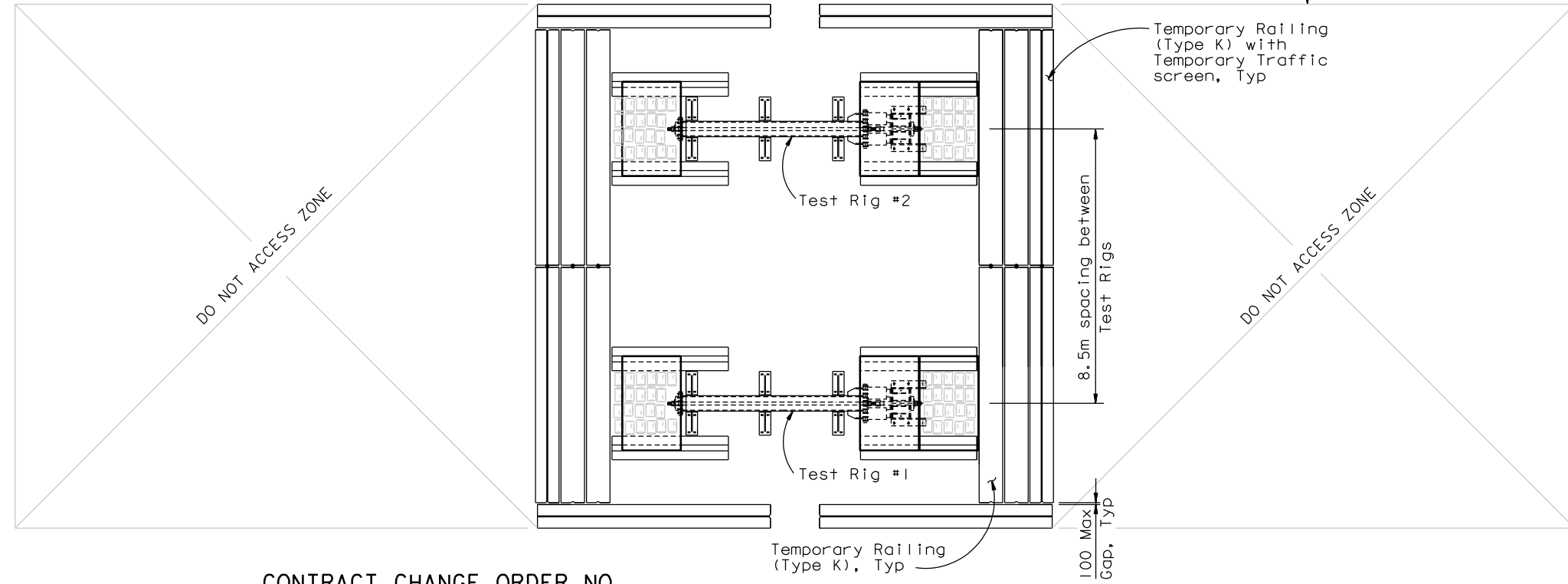
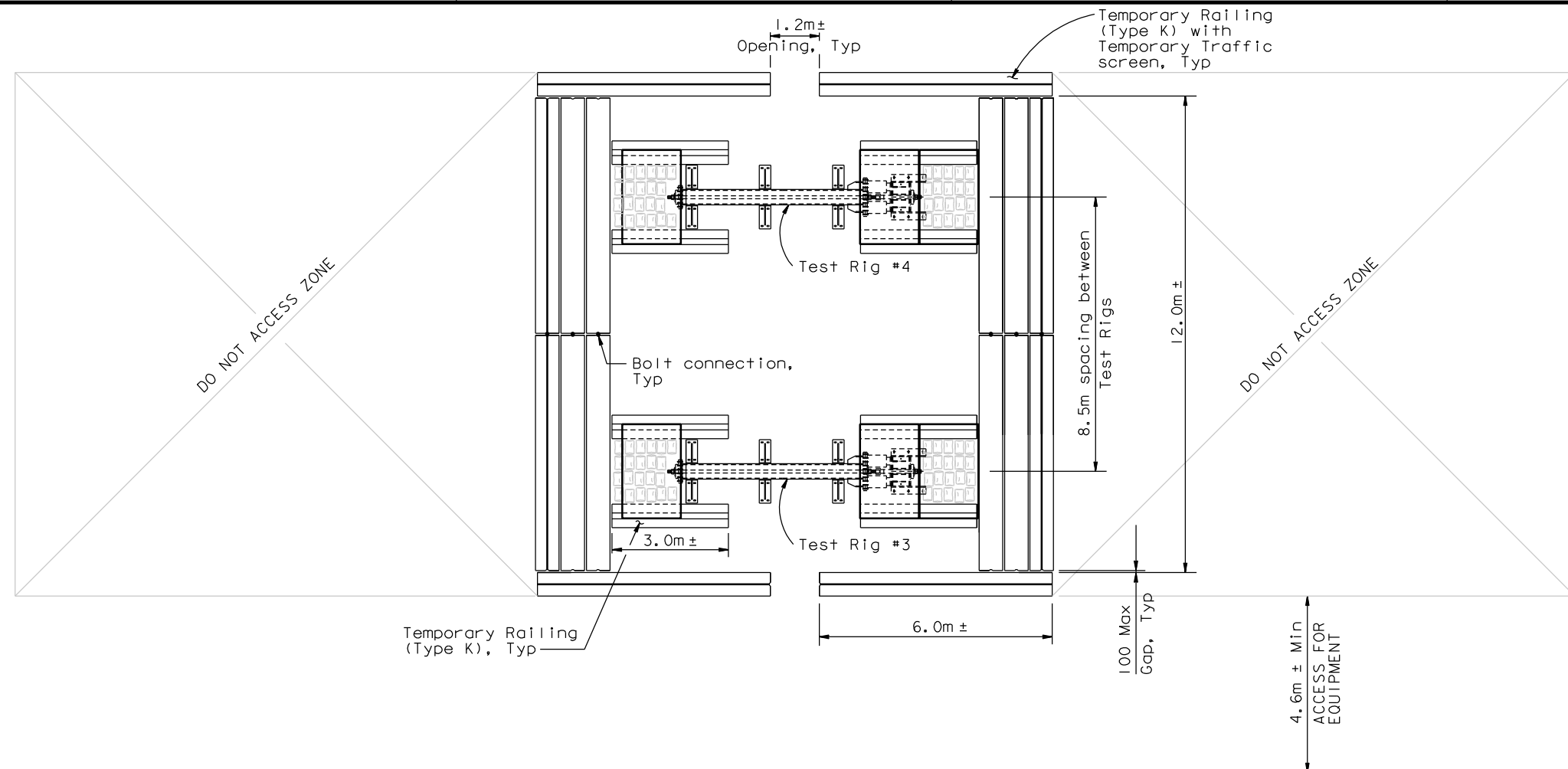
*Appendix K –
Test IV Plans and Field Reports*

*Appendix K –
Test IV Plans and Field Reports
Test IV Plans*



DIST.	COUNTY	ROUTE	KILOMETER POST TOTAL PROJECT	SHEET NO.	TOTAL SHEETS
04	SF	80	13.2/13.9	888SI	1204

REGISTERED ENGINEER - CIVIL 05-22-13 PLANS APPROVAL DATE <small>The State of California or its officers or agents shall not be responsible for the accuracy or completeness of electronic copies of this plan sheet.</small> T.Y. LIN / MOFFATT & NICHOL 825 BATTERY STREET SAN FRANCISCO, CA 94111 <small>Caltrans now has a web site! To get to the web site, go to: http://www.dot.ca.gov</small>	



GENERAL NOTES:

PRE-FABRICATION INSPECTION:

Prior to fabrication of the test rig, existing built-up box sections and existing jacking chairs shall be inspected for:

- Surface damage/ defects on structural steel.
- All fillet and PJP welds shall be 100% VT and 100% MT.
- All CJP welds shall be 100% VT, 100% MT, and 100% UT.
- Geometric tolerance shall conform to the requirements of the AISC Code of Standard Practice, Section 6.4; as well as the requirements in AWS D1.1, Section 5.23, as applicable. Twist of existing built-up box sections shall not exceed 0.002 radians per meter of length or 0.005 radians in overall length, whichever is less.

Weld acceptance criteria shall be that specified in AWS D1.1 for statically loaded, non-tubular connections.

Existing built-up box sections and existing jacking chairs with damage/ defects or do not meet the requirements above are not permitted to be used in the fabrication of the test rig. It is acceptable to repair the existing built-up box sections and existing jacking chairs to meet the requirements.

STRUCTURAL STEEL:

Unless noted otherwise:

- New structural steel shall conform to ASTM A572 Grade 50 (Fy=345 MPa).
- Structural steel with welded connections shall meet minimum CVN of 27 J @ 21C.
- Bolts for structural steel shall conform to ASTM A325M. All bolts and bolt holes may be substituted with imperial sizes of larger diameter. Bolted connections shall conform to the requirements in the Research Council on Structural Connections, "Specification for Structural Joints Using ASTM A325 or A490 Bolts," 2004 (RSCS Specification)
- Bolts shall have threads excluded from shear plane. Faying surfaces shall be Class A or above.
- Welding shall be in accordance with AWS D1.1/ D1.1M: 2002.
- Deposited weld filler material shall meet minimum CVN of 27 J @ -20C.
- Filler material shall have 483 MPa tensile strength minimum.
- All fillet and PJP welds shall be 100% VT and 100% MT.
- Weld acceptance criteria shall be that specified in AWS D1.1 for statically loaded, non-tubular connections.
- Geometric tolerance shall conform to the requirements of the AISC Code of Standard Practice, Section 6.4; as well as the requirements in AWS D1.1, Section 5.23, as applicable.

CONTRACT CHANGE ORDER NO. _____ SHEET ____ OF ____ PLAN - GENERAL ARRANGEMENT

REQUESTS FOR INFORMATION NOT ADDRESSED IN THIS CCO REMAIN IN FORCE

ALL DIMENSIONS ARE IN MILLIMETERS UNLESS OTHERWISE SHOWN

SAN FRANCISCO OAKLAND BAY BRIDGE EAST SPAN SEISMIC SAFETY PROJECT	
SELF-ANCHORED SUSPENSION BRIDGE (SUPERSTRUCTURE & TOWER)	
TEST RIG DETAILS NO. 1	
BRIDGE NO. 34-0006L/R	PROJECT ENGINEER M. Nader
KILOMETER POST 13.2/13.9	DESIGNER A. Akinsanya / W. Long
REVISION DATES (PRELIMINARY STAGE ONLY)	SHEET OF 47 IS 1

DESIGN OVERSIGHT	DATE	DESCRIPTION	BY	CH'D	CCO#
	05/22/13	REMOVE, REPLACE, AND TEST SAMPLE RODS	CC	MN	314

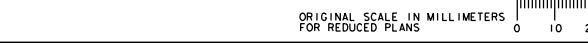
DESIGN	BY	C. Choi	CHECKED	N. Vo
DETAILS	BY	G. Mok	CHECKED	J. Denis
QUANTITIES	BY	G. MOK	CHECKED	J. Denis

PREPARED FOR THE STATE OF CALIFORNIA DEPARTMENT OF TRANSPORTATION	
BRIDGE NO.	34-0006L/R
KILOMETER POST	13.2/13.9

PROJECT ENGINEER	M. Nader
DESIGNER	A. Akinsanya / W. Long
DATE	05/22/13

Rev. Date: 5-18-98

ORIGINAL SCALE IN MILLIMETERS FOR REDUCED PLANS



CU 04 EA 0120F1

DISREGARD PRINTS BEARING EARLIER REVISION DATES

100% PS&E
 DATE PLOTTED => 23 MAY 2013
 TIME PLOTTED => 09:14:45
 USERNAME => PHUG

*Appendix K –
Test IV Plans and Field Reports*

Field Reports -

Load vs. Time Plots

Jacking Summaries (Load & Displacement)

Break Summary

VGO Report Test IV Phase 1

*VGO Report Test IV Phase 2**

*VGO Report Test IV Phase 3**

*VGO Report Test IV Phase 4**

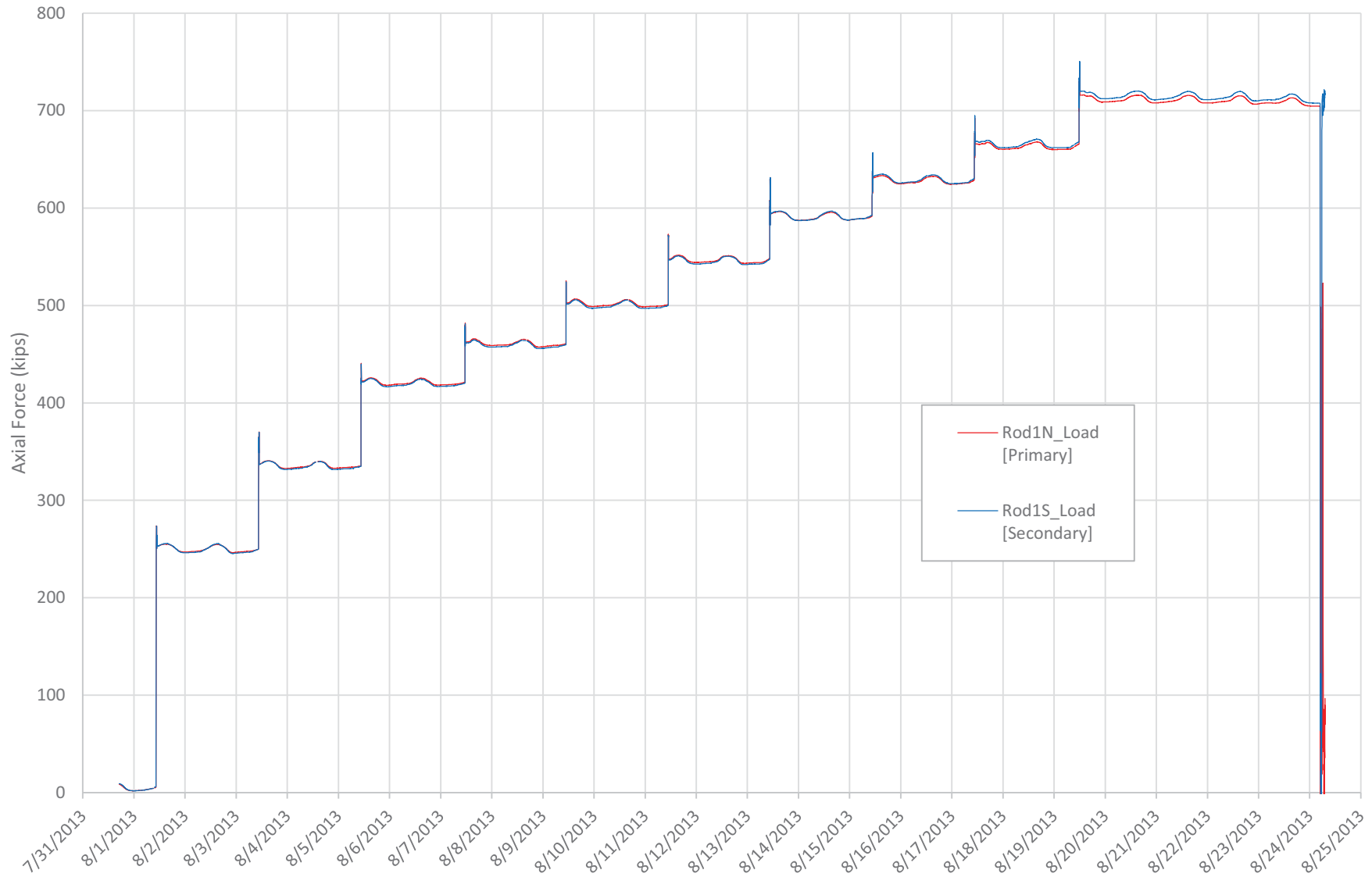
*VGO Report Test IV Phase 5**

** Reports Forthcoming-Jacking Summaries Included*

A354BD Rod Summary

Rod Group #2

Rod 1 (B1-F4) Axial Force



Jacking Operation Summary Data

Rod Group #2

Rod 1 (B1-F4)						
% Fu	Date & Time	Rod1N_Load (kips) [Primary]	Rod1S_Load (kips) [Secondary]	Rod1_DispAvg (inch)	Peak Jacking Load (kips)	Peak Jacking Displacement (in)
0.30	8/1/13 10:55 AM	253	253	0.358	273	0.398
0.40	8/3/13 10:55 AM	337	337	0.480	370	0.542
0.50	8/5/13 11:01 AM	422	421	0.605	441	0.648
0.55	8/7/13 11:37 AM	463	462	0.664	482	0.710
0.60	8/9/13 11:03 AM	502	501	0.725	527	0.776
0.65	8/11/13 11:02 AM	547	546	0.793	574	0.849
0.70	8/13/13 11:47 AM	594	594	0.863	631	0.937
0.75	8/15/13 10:57 AM	631	632	0.918	655	0.977
0.80	8/17/13 10:59 AM	666	668	0.972	692	1.034
0.85	8/19/13 12:06 PM	716	720	1.051	747	1.119

Rod Group #2

Rod 2 (B2-F5)						
% Fu	Date & Time	Rod2N_Load (kips) [Primary]	Rod2S_Load (kips) [Secondary]	Rod2_DispAvg (inch)	Peak Jacking Load (kips)	Peak Jacking Displacement (in)
0.30	8/9/13 10:43 AM	259	257	0.382	278	0.415
0.40	8/11/13 11:20 AM	344	342	0.509	371	0.561
0.50	8/13/13 11:07 AM	428	425	0.634	482	0.728
0.55	8/15/13 11:13 AM	460	457	0.683	484	0.737
0.60	8/17/13 11:18 AM	508	505	0.753	534	0.813
0.65	8/19/13 1:07 PM	547	544	0.814	576	0.881
0.70	8/21/13 10:53 AM	591	587	0.883	617	0.947
0.75	8/23/13 11:53 AM	638	635	0.957	671	1.029
0.80	8/25/13 11:06 AM	676	672	1.012	708	1.085
0.85		N/A			N/A	N/A

Rod Group #2

Rod 3 (S3-D2)						
% Fu	Date & Time	Rod3N_Load (kips) [Primary]	Rod3S_Load (kips) [Secondary]	Rod3_DispAvg (inch)	Peak Jacking Load (kips)	Peak Jacking Displacement (in)
0.30	8/19/13 1:33 PM	255	252	0.363	289	0.190
0.40	8/21/13 11:40 AM	342	340	0.488	359	0.525
0.50	8/23/13 1:17 PM	417	414	0.593	439	0.639
0.55	8/25/13 11:25 AM	464	461	0.658	487	0.709
0.60	8/27/13 10:38 AM	508	505	0.725	530	0.775
0.65	8/29/13 10:53 AM	550	546	0.785	574	0.839
0.70	8/31/13 9:31 AM	591	588	0.845	615	0.901
0.75	9/2/13 9:35 AM	627	624	0.898	656	0.962
0.80	9/4/13 11:15 AM	667	664	0.954	697	1.020
0.85	9/6/13 10:43 AM	710	707	1.019	762	1.116

Rod Group #2

Rod 4 (S4-E2)						
% Fu	Date & Time	Rod4N_Load (kips) [Primary]	Rod4S_Load (kips) [Secondary]	Rod4_DispAvg (inch)	Peak Jacking Load (kips)	Peak Jacking Displacement (in)
0.30	8/5/13 9:16 AM	260	259	0.269	276	0.301
0.40	8/7/13 10:45 AM	337	335	0.380	359	0.425
0.50	8/9/13 11:23 AM	425	423	0.505	453	0.563
0.55	8/11/13 10:40 AM	462	460	0.561	489	0.618
0.60	8/13/13 10:22 AM	508	505	0.623	534	0.678
0.65	8/15/13 11:31 AM	547	543	0.679	571	0.734
0.70	8/17/13 11:37 AM	590	586	0.745	617	0.805
0.75	8/19/13 11:32 AM	628	623	0.802	659	0.867
0.80	8/21/13 11:22 AM	669	663	0.868	699	0.935
0.85	8/23/13 1:00 PM	712	704	0.934	747	1.009

Notes: Data taken at indicated time, shortly after lockoff on nut. Peak Jacking Load is from the Primary strain gages and over the entire Jacking Process.
 Peak Jacking Displacement is from the calculated average of the displacement transducers taken at the same point in time as the Peak Jacking Load.

PHASE 1

(Test Rigs #1-4)
(Rods 1-4)

Rod Group #2	
Test Rig #1 - Rod 1	
2010 Rod, Rod ID B1-F4	
8/19/2013 12:06	Jack to 0.85 Fu
8/24/2013 4:55	Rod Breaks
4.7	days at 0.85 Fu
113	hours at 0.85 Fu

Rod Group #2	
Test Rig #2 - Rod 2	
2010 Rod, Rod ID B2-F5	
8/25/2013 11:06	Jack to 0.80 Fu
8/26/2013 16:48	Rod Breaks
1.2	days at 0.80 Fu
30	hours at 0.80 Fu

Rod Group #2	
Test Rig #3 - Rod 3	
2010 Rod, Rod ID S3-D2	
9/6/2013 10:43	Jack to 0.85 Fu
9/12/2013 9:30	Tensioned to Failure
5.9	days at 0.85 Fu
143	hours at 0.85 Fu

Rod Group #2	
Test Rig #4 - Rod 4	
2010 Rod, Rod ID S4-E2	
8/23/2013 13:00	Jack to 0.85 Fu
9/11/2013 11:20	Rod Breaks
8.9	days at 0.85 Fu
214	hours at 0.85 Fu

Tension to Failure Step delayed beyond 140 hours because of jobsite scheduling issues

PHASE 2

(Test Rigs #5-11)
(Rods 5-11)

Rod Group #4	
Test Rig #5 - Rod 5	
2" dia., E2 Bearing Upper Rod, spare rod	
1/30/2014 10:33	Jack to 0.85 Fu
2/5/2014 8:04	Tensioned to Failure
5.9	days at 0.85 Fu
142	hours at 0.85 Fu

Rod Group #12	
Test Rig #6 - Rod 6	
3" dia., Tower Anchor Rod, Vulcan, rod ID b2W-6	
2/1/2014 10:30	Jack to 0.85 Fu
2/7/2014 8:11	Tensioned to Thread Strip
5.9	days at 0.85 Fu
142	hours at 0.85 Fu

Rod Group #8	
Test Rig #7 - Rod 7	
4" dia., Tower Saddle Tie Rod, rod ID 5	
1/28/2014 10:34	Jack to 0.85 Fu
2/10/2014 11:55	Tensioning Ends w/o Break
13.1	days at 0.85 Fu
313	hours at 0.85 Fu

Tension to Failure Step delayed beyond 140 hours because of jacking equipment issues

Rod Group #7	
Test Rig #8 - Rod 8	
3.5" dia., PWS Anchor Rod, Rolled Threads, rod ID E-118, Heat OYI	
1/28/2014 10:45	Jack to 0.85 Fu
2/3/2014 8:00	Tensioned to Failure
5.9	days at 0.85 Fu
141	hours at 0.85 Fu

Rod Group #7	
Test Rig #9 - Rod 9	
3.5" dia., PWS Anchor Rod, Rolled Threads, rod ID W-074, Heat OTD	
1/26/2014 10:38	Jack to 0.85 Fu
2/1/2014 8:30	Tensioned to Failure
5.9	days at 0.85 Fu
142	hours at 0.85 Fu

Rod Group #7	
Test Rig #10 - Rod 10	
3.5" dia., PWS Anchor Rod, Cut Threads, rod ID E-036, Heat OTD	
1/24/2014 11:42	Jack to 0.85 Fu
1/30/2014 7:54	Tensioned to Failure
5.8	days at 0.85 Fu
140	hours at 0.85 Fu

Rod Group #7	
Test Rig #11 - Rod 11	
3.5" dia., PWS Anchor Rod, Cut Threads, rod ID E-110, Heat OOF	
1/22/2014 13:26	Jack to 0.85 Fu
1/28/2014 8:11	Tensioned to Failure
5.8	days at 0.85 Fu
139	hours at 0.85 Fu

PHASE 3

(Test Rigs #12 & 13)
(Rods 12 & 13)

Rod Group #1	
Test Rig #12 - Rod 12	
2008 Rod, ID S2-A8, Heat MJF-32, Top	
4/15/2014 10:35	Jack to 0.70 Fu
4/17/2014 6:37	Rod Breaks
1.8	days at 0.70 Fu
44	hours at 0.70 Fu

Rod Group #1	
Test Rig #13 - Rod 13	
2008 Rod, ID S2-A8, Heat MJF-32, Bottom	
4/15/2014 10:43	Jack to 0.70 Fu
4/18/2014 3:39	Rod Breaks
2.7	days at 0.70 Fu
65	hours at 0.70 Fu

0.70 Fu Step extended beyond 48 hours because of safety issues with high AE activity at scheduled time of tensioning step

PHASE 4

(Test Rigs #14-17)
(Rods 14-17)

Rod Group #18	
Test Rig #14 - Rod 14	
2013 Rod, ID EB-2-03, Galvanized	
7/1/2014 9:34	Jack to 0.85 Fu
7/7/2014 8:34	Tensioned to Failure
6.0	days at 0.85 Fu
143	hours at 0.85 Fu

Rod Group #18	
Test Rig #15 - Rod 15	
2013 Rod, ID EB-2-08, Galvanized	
7/1/2014 9:46	Jack to 0.85 Fu
7/7/2014 11:52	Tensioned to Failure
6.1	days at 0.85 Fu
146	hours at 0.85 Fu

Rod Group #18	
Test Rig #16 - Rod 16	
2013 Rod, ID SK-3-06, Ungalvanized	
7/3/2014 9:35	Jack to 0.85 Fu
7/9/2014 8:25	Tensioned to Failure
6.0	days at 0.85 Fu
143	hours at 0.85 Fu

Rod Group #18	
Test Rig #17 - Rod 17	
2013 Rod, ID SK-3-13, Ungalvanized	
7/3/2014 9:50	Jack to 0.85 Fu
7/9/2014 11:51	Tensioned to Failure
6.1	days at 0.85 Fu
146	hours at 0.85 Fu

PHASE 5

(Test Rigs #18 & 19)
(Rods 18 & 19)

Rod Group #1	
Test Rig #18 - Rod 18	
Dry 2008 Rod, ID S1-A7, Bottom	
9/5/2014 9:22	Jack to 0.85 Fu
9/11/2014 8:06	Tensioned to Failure
5.9	days at 0.85 Fu
143	hours at 0.85 Fu

Rod Group #1	
Test Rig #19 - Rod 19	
Dry 2008 Rod, ID S2-H6, Bottom	
9/5/2014 9:33	Jack to 0.85 Fu
9/11/2014 9:34	Tensioned to Failure
6.0	days at 0.85 Fu
144	hours at 0.85 Fu

Townsend Test – Phase I

September 25th, 2014

VGO Project #13106

Prepared For:

**Brian A. Petersen
Project Director
American Bridge/Fluor JV
375 Burma Road
Oakland, CA 94607**



1330 SE 6th
Portland, OR 97214
Tel (503)239-6000
Fax (503)239-6100

Jacking Operation Summary Data

Rod 5 (2" dia., E2 Bearing Upper Rod, spare rod)						
% Fu	Date & Time	Rod5N_Load (kips) [Primary]	Rod5S_Load (kips) [Secondary]	Rod5_DispAvg (inch)	Peak Jacking Load (kips)	Peak Jacking Displacement (in)
0.30	1-12-2014 11:57am	117	117	0.140	131	0.158
0.40	1-14-2014 11:54am	152	152	0.178	168	0.200
0.50	1-16-2014 12:41pm	188	188	0.219	206	0.243
0.55	1-18-2014 11:34am	208	208	0.240	225	0.264
0.60	1-20-2014 1:53pm	229	229	0.263	247	0.289
0.65	1-22-2014 1:34pm	246	246	0.285	266	0.313
0.70	1-24-2014 11:53am	266	265	0.309	283	0.336
0.75	1-26-2014 10:48am	283	282	0.337	301	0.366
0.80	1-28-2014 10:54am	301	301	0.382	324	0.415
0.85	1-30-2014 10:33am	321	320	0.487	344	0.507

Rod 6 (3" dia., Tower Anchor Rod, Vulcan, rod ID b2W-6)						
% Fu	Date & Time	Rod6N_Load (kips) [Primary]	Rod6S_Load (kips) [Secondary]	Rod6_DispAvg (inch)	Peak Jacking Load (kips)	Peak Jacking Displacement (in)
0.30	1-14-2014 12:55pm	260	260	0.156	299	0.184
0.40	1-16-2014 12:57pm	342	342	0.205	380	0.234
0.50	1-18-2014 11:45am	421	421	0.251	452	0.278
0.55	1-20-2014 2:06pm	469	470	0.279	506	0.310
0.60	1-22-2014 1:43pm	503	504	0.299	540	0.331
0.65	1-24-2014 12:41pm	552	552	0.329	594	0.364
0.70	1-26-2014 10:56am	589	589	0.352	633	0.390
0.75	1-28-2014 11:03am	627	628	0.375	675	0.416
0.80	1-30-2014 10:44am	671	671	0.404	725	0.447
0.85	2-1-2014 10:30am	713	714	0.433	762	0.476

Rod 7 (4" dia., Tower Saddle Tie Rod, rod ID 5)						
% Fu	Date & Time	Rod7N_Load (kips) [Primary]	Rod7S_Load (kips) [Secondary]	Rod7_DispAvg (inch)	Peak Jacking Load (kips)	Peak Jacking Displacement (in)
0.30	1-10-2014 10:57am	470	470	0.239	554	0.280
0.40	1-12-2014 10:37am	620	620	0.303	670	0.333
0.50	1-14-2014 10:37am	776	773	0.369	830	0.403
0.55	1-16-2014 10:45am	855	850	0.402	910	0.440
0.60	1-18-2014 10:33am	940	933	0.438	1,001	0.479
0.65	1-20-2014 11:47am	1,017	1,008	0.468	1,090	0.516
0.70	1-22-2014 11:50am	1,092	1,079	0.494	1,157	0.539
0.75	1-24-2014 10:59am	1,166	1,151	0.527	1,236	0.575
0.80	1-26-2014 10:16am	1,248	1,232	0.567	1,324	0.618
0.85	1-28-2014 10:34am	1,327	1,310	0.612	1,423	0.671

Rod 8 (3.5" dia., PWS Anchor Rod, Rolled Threads, rod ID E-118, Heat OVI)						
% Fu	Date & Time	Rod8N_Load (kips) [Primary]	Rod8S_Load (kips) [Secondary]	Rod8_DispAvg (inch)	Peak Jacking Load (kips)	Peak Jacking Displacement (in)
0.30	1-10-2014 11:12am	358	358	0.178	400	0.206
0.40	1-12-2014 10:42am	468	469	0.226	513	0.258
0.50	1-14-2014 10:43am	590	591	0.281	638	0.317
0.55	1-16-2014 10:50am	641	642	0.305	690	0.343
0.60	1-18-2014 10:46am	701	703	0.332	752	0.373
0.65	1-20-2014 12:02pm	759	760	0.358	817	0.404
0.70	1-22-2014 11:57am	819	820	0.386	881	0.434
0.75	1-24-2014 11:07am	875	876	0.413	942	0.465
0.80	1-26-2014 10:26am	940	940	0.447	1,009	0.502
0.85	1-28-2014 10:45am	998	996	0.49	1,080	0.548

Rod 9 (3.5" dia., PWS Anchor Rod, Rolled Threads, rod ID W-074, Heat OTD)						
% Fu	Date & Time	Rod9N_Load (kips) [Primary]	Rod9S_Load (kips) [Secondary]	Rod9_DispAvg (inch)	Peak Jacking Load (kips)	Peak Jacking Displacement (in)
0.30	1-8-2014 10:45am	354	355	0.180	395	0.211
0.40	1-10-2014 11:45am	472	474	0.237	533	0.284
0.50	1-12-2014 10:55am	583	587	0.286	636	0.332
0.55	1-14-2014 11:03am	644	648	0.315	695	0.367
0.60	1-16-2014 11:11am	703	708	0.343	756	0.396
0.65	1-18-2014 11:03am	760	766	0.369	819	0.427
0.70	1-20-2014 12:57pm	819	826	0.397	885	0.461
0.75	1-22-2014 12:53pm	878	885	0.426	942	0.491
0.80	1-24-2014 11:21am	937	946	0.456	1,006	0.525
0.85	1-26-2014 10:38am	993	1,004	0.486	1,068	0.560

Rod 10 (3.5" dia., PWS Anchor Rod, Cut Threads, rod ID E-036, Heat OTD)						
% Fu	Date & Time	Rod10N_Load (kips) [Primary]	Rod10S_Load (kips) [Secondary]	Rod10_DispAvg (inch)	Peak Jacking Load (kips)	Peak Jacking Displacement (in)
0.30	1-6-2014 10:54am	358	358	0.118	401	0.143
0.40	1-8-2014 11:04am	468	467	0.169	511	0.196
0.50	1-10-2014 12:39pm	584	582	0.223	633	0.256
0.55	1-12-2014 11:08am	646	644	0.250	697	0.285
0.60	1-14-2014 11:18am	704	702	0.278	761	0.320
0.65	1-16-2014 11:35am	761	757	0.307	820	0.350
0.70	1-18-2014 11:15am	821	817	0.335	886	0.382
0.75	1-20-2014 12:52pm	878	874	0.365	963	0.421
0.80	1-22-2014 11:12pm	944	938	0.395	1,016	0.450
0.85	1-24-2014 11:42am	992	985	0.422	1,076	0.483

Rod 11 (3.5" dia., PWS Anchor Rod, Cut Threads, rod ID E-110, Heat OOF)						
% Fu	Date & Time	Rod11N_Load (kips) [Primary]	Rod11S_Load (kips) [Secondary]	Rod11_DispAvg (inch)	Peak Jacking Load (kips)	Peak Jacking Displacement (in)
0.30	1-4-2014 12:43pm	353	352	0.174	393	0.204
0.40	1-6-2014 11:09am	468	468	0.230	519	0.266
0.50	1-8-2014 11:26am	583	582	0.283	636	0.325
0.55	1-10-2014 12:52pm	642	641	0.313	696	0.357
0.60	1-12-2014 11:26am	700	697	0.340	755	0.387
0.65	1-14-2014 11:42am	761	758	0.370	820	0.421
0.70	1-16-2014 11:55am	822	818	0.400	890	0.456
0.75	1-18-2014 11:26am	876	871	0.428	945	0.486
0.80	1-20-2014 1:38pm	935	929	0.459	1,011	0.521
0.85	1-22-2014 1:26pm	993	986	0.490	1,066	0.553

Note: Data taken at indicated time, shortly after lockoff on nut. Peak Jacking Load is from the Primary strain gages and over the entire Jacking Process. Peak Jacking Displacement is from the calculated average of the displacement transducers taken at the same point in time as the Peak Jacking Load.

Jacking Operation Summary Data

Rod 12 (2008 Rod, ID S2-A8, Heat MJF-32, Top)						
% Fu	Date & Time	Rod12N_Load (kips) [Primary]	Rod12S_Load (kips) [Secondary]	Rod12_DispAvg (inch)	Peak Jacking Load (kips)	Peak Jacking Displacement (in)
0.30	4/3/14 10:33 AM	253	253	0.134	279	0.154
0.40	4/5/14 10:26 AM	341	341	0.177	372	0.201
0.50	4/7/14 10:30 AM	419	419	0.214	455	0.243
0.55	4/9/14 10:36 AM	466	465	0.239	503	0.272
0.60	4/11/14 10:35 AM	508	507	0.261	554	0.299
0.65	4/13/14 10:14 AM	553	552	0.285	596	0.323
0.70	4/15/14 10:35 AM	594	593	0.307	645	0.350
0.75						
0.80						
0.85						

Rod 13 (2008 Rod, ID S2-A8, Heat MJF-32, Bottom)						
% Fu	Date & Time	Rod13N_Load (kips) [Primary]	Rod13S_Load (kips) [Secondary]	Rod13_DispAvg (inch)	Peak Jacking Load (kips)	Peak Jacking Displacement (in)
0.30	4/3/14 10:42 AM	260	257	0.143	285	0.165
0.40	4/5/14 10:35 AM	341	339	0.181	371	0.209
0.50	4/7/14 10:41 AM	422	419	0.219	459	0.253
0.55	4/9/14 10:45 AM	465	462	0.242	506	0.280
0.60	4/11/14 10:41 AM	506	504	0.262	550	0.302
0.65	4/13/14 10:20 AM	548	546	0.283	594	0.325
0.70	4/15/14 10:43 AM	595	593	0.307	649	0.354
0.75						
0.80						
0.85						

Note: Data taken at indicated time, shortly after lockoff on nut. Peak Jacking Load is from the Primary strain gages and over the entire Jacking Process. Peak Jacking Displacement is from the calculated average of the displacement transducers taken at the same point in time as the Peak Jacking Load.

Jacking Operation Summary Data

Rod 14 (2013 Rod, ID EB-2-03, Galvanized)						
% Fu	Date & Time	Rod14N_Load (kips) [Primary]	Rod14S_Load (kips) [Secondary]	Rod14_DisplacementAvg (inch)	Peak Jacking Load (kips)	Peak Jacking Displacement (in)
0.30	6/13/14 9:40 AM	262	265	0.371	282	0.410
0.40	6/15/14 9:11 AM	339	343	0.488	358	0.527
0.50	6/17/14 9:42 AM	425	429	0.608	444	0.652
0.55	6/19/14 9:39 AM	460	465	0.659	482	0.712
0.60	6/21/14 9:23 AM	507	512	0.730	529	0.783
0.65	6/23/14 9:30 AM	546	552	0.787	567	0.842
0.70	6/25/14 9:30 AM	592	598	0.857	617	0.917
0.75	6/27/14 9:33 AM	631	637	0.913	657	0.977
0.80	6/29/14 9:27 AM	670	677	0.972	698	1.040
0.85	7/1/14 9:34 AM	720	728	1.052	754	1.128

Rod 15 (2013 Rod, ID EB-2-08, Galvanized)						
% Fu	Date & Time	Rod15N_Load (kips) [Primary]	Rod15S_Load (kips) [Secondary]	Rod15_DisplacementAvg (inch)	Peak Jacking Load (kips)	Peak Jacking Displacement (in)
0.30	6/13/14 9:58 AM	255	255	0.332	275	0.376
0.40	6/15/14 9:24 AM	339	340	0.457	356	0.497
0.50	6/17/14 9:50 AM	421	422	0.571	438	0.616
0.55	6/19/14 9:50 AM	463	463	0.635	482	0.683
0.60	6/21/14 9:34 AM	510	511	0.708	531	0.758
0.65	6/23/14 9:40 AM	550	551	0.767	572	0.817
0.70	6/25/14 9:40 AM	589	590	0.824	611	0.879
0.75	6/27/14 9:43 AM	635	636	0.889	660	0.949
0.80	6/29/14 9:39 AM	673	674	0.946	699	1.008
0.85	7/1/14 9:46 AM	713	713	1.007	740	1.072

Rod 16 (2013 Rod, ID SK-3-06, Ungalvanized)						
% Fu	Date & Time	Rod16N_Load (kips) [Primary]	Rod16S_Load (kips) [Secondary]	Rod16_DisplacementAvg (inch)	Peak Jacking Load (kips)	Peak Jacking Displacement (in)
0.30	6/15/14 8:24 AM	254	254	0.361	270	0.395
0.40	6/17/14 9:58 AM	337	337	0.474	354	0.514
0.50	6/19/14 10:02 AM	419	419	0.594	438	0.638
0.55	6/21/14 9:43 AM	461	461	0.657	481	0.705
0.60	6/23/14 9:49 AM	508	507	0.722	529	0.772
0.65	6/25/14 9:49 AM	546	545	0.781	568	0.833
0.70	6/27/14 9:52 AM	587	586	0.836	609	0.893
0.75	6/29/14 9:46 AM	627	626	0.896	651	0.956
0.80	7/1/14 9:57 AM	678	677	0.972	709	1.043
0.85	7/3/14 9:35 AM	717	716	1.033	747	1.104

Rod 17 (2013 Rod, ID SK-3-13, Ungalvanized)						
% Fu	Date & Time	Rod17N_Load (kips) [Primary]	Rod17S_Load (kips) [Secondary]	Rod17_DisplacementAvg (inch)	Peak Jacking Load (kips)	Peak Jacking Displacement (in)
0.30	6/15/14 8:36 AM	252	252	0.313	268	0.347
0.40	6/17/14 10:09 AM	340	339	0.445	359	0.487
0.50	6/19/14 10:11 AM	420	418	0.559	439	0.605
0.55	6/21/14 9:52 AM	462	459	0.624	485	0.677
0.60	6/23/14 9:58 AM	508	505	0.688	533	0.743
0.65	6/25/14 10:00 AM	549	546	0.751	572	0.805
0.70	6/27/14 10:01 AM	586	582	0.798	610	0.857
0.75	6/29/14 9:55 AM	630	626	0.859	656	0.923
0.80	7/1/14 10:07 AM	677	672	0.929	704	0.997
0.85	7/3/14 9:50 AM	718	712	0.992	758	1.075

Note: Data taken at indicated time, shortly after lockoff on nut. Peak Jacking Load is from the Primary strain gages and over the entire Jacking Process.
 Peak Jacking Displacement is from the calculated average of the displacement transducers taken at the same point in time as the Peak Jacking Load.

Jacking Operation Summary Data

Rod 18 (Dry 2008 Rod, ID S1-A7, Bottom)						
% Fu	Date & Time	Rod18N_Load (kips) [Primary]	Rod18S_Load (kips) [Secondary]	Rod18_DispAvg (inch)	Peak Jacking Load (kips)	Peak Jacking Displacement (in)
0.30	8-18-2014 9:32am	260	258	0.136	283	0.156
0.40	8-20-2014 9:41am	339	337	0.175	368	0.200
0.50	8-22-2014 9:32am	421	418	0.213	455	0.243
0.55	8-24-2014 9:29am	465	462	0.234	504	0.268
0.60	8-26-2014 9:29am	503	500	0.252	542	0.289
0.65	8-28-2014 9:27am	548	544	0.275	592	0.316
0.70	8-30-2014 9:29am	586	582	0.295	633	0.338
0.75	9-1-2014 9:29am	633	628	0.321	682	0.365
0.80	9-3-2014 9:19am	673	668	0.341	724	0.388
0.85	9-5-2014 9:22am	712	707	0.364	768	0.414

Rod 19 (Dry 2008 Rod, ID S2-H6, Bottom)						
% Fu	Date & Time	Rod19N_Load (kips) [Primary]	Rod19S_Load (kips) [Secondary]	Rod19_DispAvg (inch)	Peak Jacking Load (kips)	Peak Jacking Displacement (in)
0.30	8-18-2014 9:39am	256	257	0.133	280	0.154
0.40	8-20-2014 9:47am	335	337	0.170	370	0.198
0.50	8-22-2014 9:41am	422	423	0.213	460	0.245
0.55	8-24-2014 9:35am	468	470	0.236	508	0.271
0.60	8-26-2014 9:35am	504	505	0.253	544	0.291
0.65	8-28-2014 9:41am	551	553	0.279	595	0.320
0.70	8-30-2014 9:38am	590	591	0.298	633	0.341
0.75	9-1-2014 9:35am	636	638	0.324	686	0.368
0.80	9-3-2014 9:30am	677	678	0.346	727	0.393
0.85	9-5-2014 9:33am	716	717	0.368	773	0.422

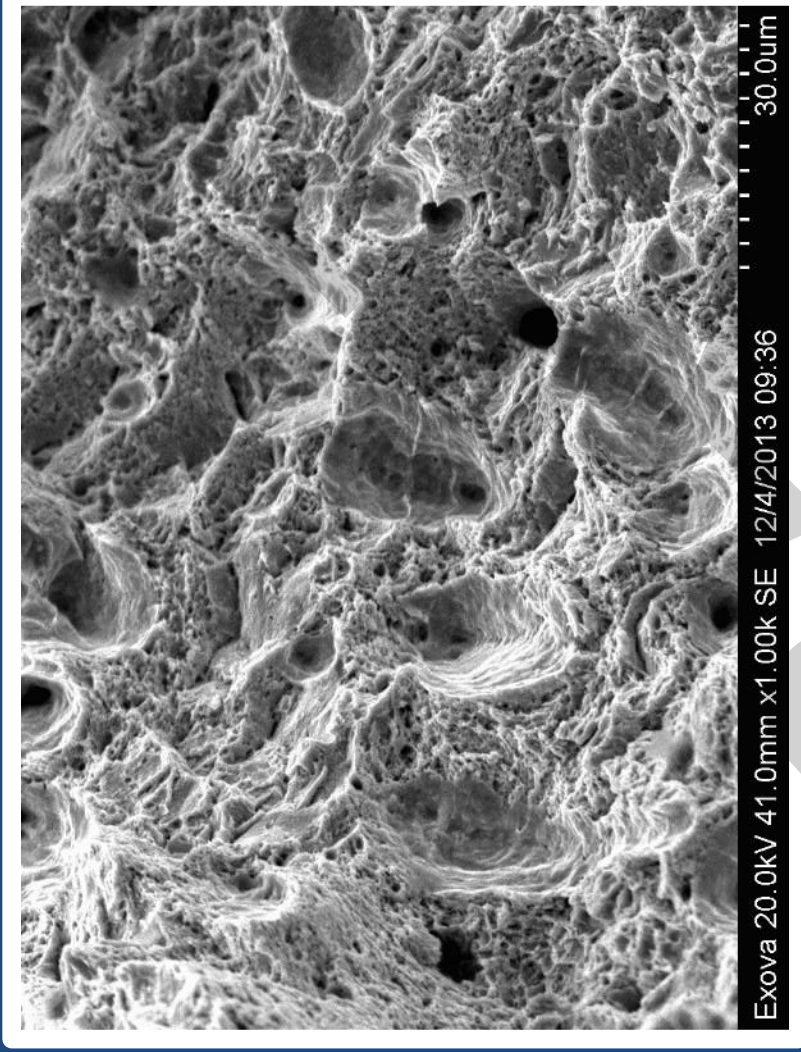
Note: Data taken at indicated time, shortly after lockoff on nut. Peak Jacking Load is from the Primary strain gages and over the entire Jacking Process.
Peak Jacking Displacement is from the calculated average of the displacement transducers taken at the same point in time as the Peak Jacking Load.

Location and Item	Component Description	Rod (no head) or Bolt (with head)	Threads Cut or Rolled	Supplier	Diameter (in)	Overall Length (ft)	Overall Length (mm)	Quantity Installed (not including spares)	De-Humidified Zone?	Tighten Method	Final Tension (fraction of Fu or UTS)	Date Tension or Loading Complete	Date Re-Inspected (by 4/8/13)	Date Re-Inspected (by 4/23/13)	Date Re-Inspected (by 5/5/13)	Date Re-Inspected (by 5/28/13)	Date Re-Inspected (by 7/8/13)	Date Re-Inspected (by 9/1/13)	Notes							
E2 Bearings and Shear Keys	1	E2 Shear Key - Connect to Concrete - Above Column, Under OBG [S1, S2]	rod	Cut	Dyson	3	17.2 10.0	5235 3035	60 36	96	No	Tension	0.7	3/5/2013	daily check	daily check	daily check	saddle construction in progress	saddle construction in progress	saddle construction in progress	Tensioned to 0.75 Fu, with lockoff at ~ 0.7 Fu 32 of 96 rods broke after tensioning, then tension level lowered Saddle alternative takes the place of these rods; rods detensioned					
	2	E2 Shear Key - Connect to Concrete - Above Bent Cap, Under Crossbeam [S3, S4]	rod	Cut	Dyson	3	21.9	6676	96												192	No	Tension	0.7	4/1/2013	daily check
	3	E2 Bearing - Connect to Concrete - Under OBG [B1, B2, B3, B4]	rod	Cut	Dyson	3	22.6 22.2	6902 6777	64 32	320	No	Tension	0.7	4/9/2013	daily check	daily check	daily check	daily check	daily check	daily check						
		E2 Shear Key - Connect to OBG [S1, S2]	rod	Cut	Dyson	3	4.4 1.8	1337 537	96 64												320	No	Tension	0.7	9/12/2012	4/6/2013 4/8/2013
	4	E2 Shear Key - Connect to Crossbeam [S3, S4]	rod	Cut	Dyson	3	4.3 1.7	1312 512	96 64	224	No	Tension	0.7	9/12/2012	4/6/2013	4/17/13 to 4/23/13	5/3/2013	5/28/2013	7/6/2013	8/29/2013						
	5	E2 Bearing - Connect to OBG [B1, B2, B3, B4]	rod	Rolled	Dyson	2	3.6	1105	224												96	No	Tension	0.61	July 2009	not accessible
	6	E2 Bearing Assembly Bolts (Spherical Bushing Halves)	rod	Cut	Dyson for Lubrite for Hochang	1	2.4	733	96	336	No	snug + 1/4 turn	~0.4	January 2010	4/6/2013 (for 32 accessible bolts)	4/23/2013 (for 32 accessible bolts)	5/3/2013 (for 32 accessible bolts)	not accessible	7/6/2013 (for 32 accessible bolts)	not accessible						
Cable Anchorage	7	PWS Anchor Rods - PWS Socket to Anchorage	rod	55 Cut (20%) 219 Rolled (80%)	Dyson	3-1/2	27.9 to 31.8	8500 to 9700	274												Yes	Load Transfer	0.26	9/26/2012	4/6/2013	4/20&22/2013
										0.29	N/A	N/A	N/A	N/A	N/A	N/A	N/A	N/A	N/A	N/A			With DL + Added DL			
										0.32	N/A	N/A	N/A	N/A	N/A	N/A	N/A	N/A	N/A	N/A			N/A	N/A	N/A	Service Load (Group 1)
										0.35	N/A	N/A	N/A	N/A	N/A	N/A	N/A	N/A	N/A	N/A			N/A	N/A	N/A	SEE (Seismic)
Top of Tower	8	Tower Saddle Tie Rods	rod	Rolled	Dyson	4	6.0 to 17.5	1840 to 5325	25	Yes	Tension	0.41	7/14/2012	N/A	N/A	N/A	N/A	N/A	N/A	Load During Construction - Tensioned to 0.5 Fy						
	9	Turned Rods at Tower Saddle Segment Splices	rod	Cut	Dyson	3 @ Threads [-3-1/16 @ Shank]	1.5	463	100	Yes	Tension	0.45	4/6/2011	4/6/2013	4/19/2013	5/3/2013	5/24/2013	7/2/2013	8/29/2013	Additional tension in tie rods from cable with service load						
							1.4	415	8		snug	~0.1	7/14/2012								Located at the 2 field splices connecting the 3 tower saddle segments; 100 rods tensioned prior to saddle erection; 8 rods only snug tight after tie rod tensioning due to conflict with tie rods.					
	10	Tower Saddle to Grillage Anchor Bolts	Hex Bolt	Cut	Dyson	3	1.2	360	90	Head Yes, Nut No	snug	~0.1	3/25/2013	4/6/2013	4/19/2013	5/3/2013	5/24/2013	7/2/2013	8/29/2013	Snug tightened before and after load transfer: Initial Tension complete on 5/20/2011; final tension complete on 3/25/2013.						
11	Tower Outrigger Boom (for Maintenance) at Top of Tower	Hex Bolt	Cut	Dyson	3	2.1	630	4	No	snug	~0.1	July 2012	4/6/2013	4/19/2013	5/4/2013	5/24/2013	7/2/2013	8/29/2013	Act as pins for swinging out and then securing the maintenance outrigger boom at the top of 2 of 4 tower head chimneys. At each boom, one bolt is loaded and other bolt is unloaded in the current boom position. The currently unloaded bolt will be installed snug tight when the boom is swung out for use (future position).							
Bottom of Tower	12	Tower Anchor Rods - Tower at Footing (3" Dia)	rod	Cut	Vulcan Threaded Products for KOS for KFM (04-0120E4)	3	25.6	7789	388	Upper Rod Yes, Lower Rod in Concrete/Grout	Tension	0.48	4/17/2013	N/A	4/20/2013 4/22/2013	5/5/2013	5/23/2013	7/6/2013	8/30/2013	Tensioned to 1800 kN = 404.7 kips; Tension before and after load transfer: Initial Tension Late 2010 through Early 2011; Final Tension 2013						
	13	Tower Anchor Rods - Tower at Footing (4" Dia)	rod	Cut		4	25.7	7839	36		Tension	0.37	4/17/2013	N/A	4/20/2013 4/22/2013	5/5/2013	5/23/2013	7/6/2013	8/30/2013	Tensioned to 2530 kN = 568.8 kips; Tension before and after load transfer: Initial Tension Late 2010 through Early 2011; Final Tension 2013						
East Saddles	14	East Saddle Anchor Rods	rod	Cut	Dyson for JSW	2	2.6	800	32	Yes	snug	~0.1	May 2010	4/7/2013	4/21/2013	5/3/2013	5/23/2013 5/24/2013	7/2/2013	8/29/2013	specified gap under nut/washer at one end of rod and 2 nuts snug against each other at other end of rod -> snug tight for portion of rod						
	15	East Saddle Tie Rods	Hex Bolt	Cut	Dyson	3	4.7	1420	18	Yes	snug	~0.1	4/13/2012	N/A	N/A	N/A	N/A	N/A	N/A	Snug tightened before load transfer						
East Cable	16	B14 Cable Bands - Cable Brackets - at East End of Bridge - Strongback Anchor Rods	rod	Rolled	Dyson	3	10.3 to 11.1	3129 to 3372	24	No	Tension	0.16	2/8/2013	4/7/2013	4/21/2013	5/4/2013	5/24/2013	5/28/2013	7/3/2013	8/29/2013	pre-compress neoprene between strongback and cable band					
																	5/23 & 24/2013	7/2/2013	8/29/2013	Additional tension in tie rods from cable with service load						
W2 Bent Cap	17	W2 Bikepath Anchor Rods	Hex Bolt	Cut	Dyson	~1-3/16 [Metric M30]	1.4 to 1.5	420 to 460	43	No	snug	~0.1	N/A	N/A	N/A	N/A	N/A	N/A	N/A	Details for bikepath connections are being redesigned and are not final. The 18 anchor rods at the bottom connections will be abandoned. The 25 anchor rods at the top connections may be used and supplemented with additional anchor rods. These rods will be tensioned on the separate YBITS-2 Contract.						

Total = 2306

New or updated information after 5/6/2013 Update is highlighted Red

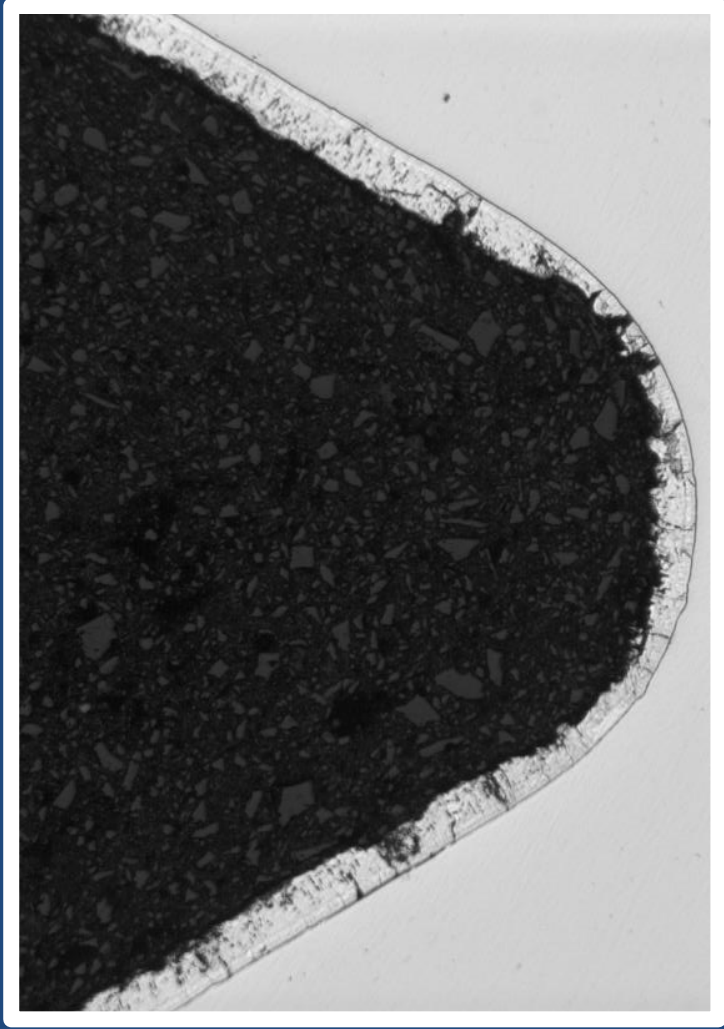
*Appendix L –
Test IV Post-Fracture Analysis Reports*



TOWNSEND TEST POST FRACTURE ANALYSIS

August 19, 2014

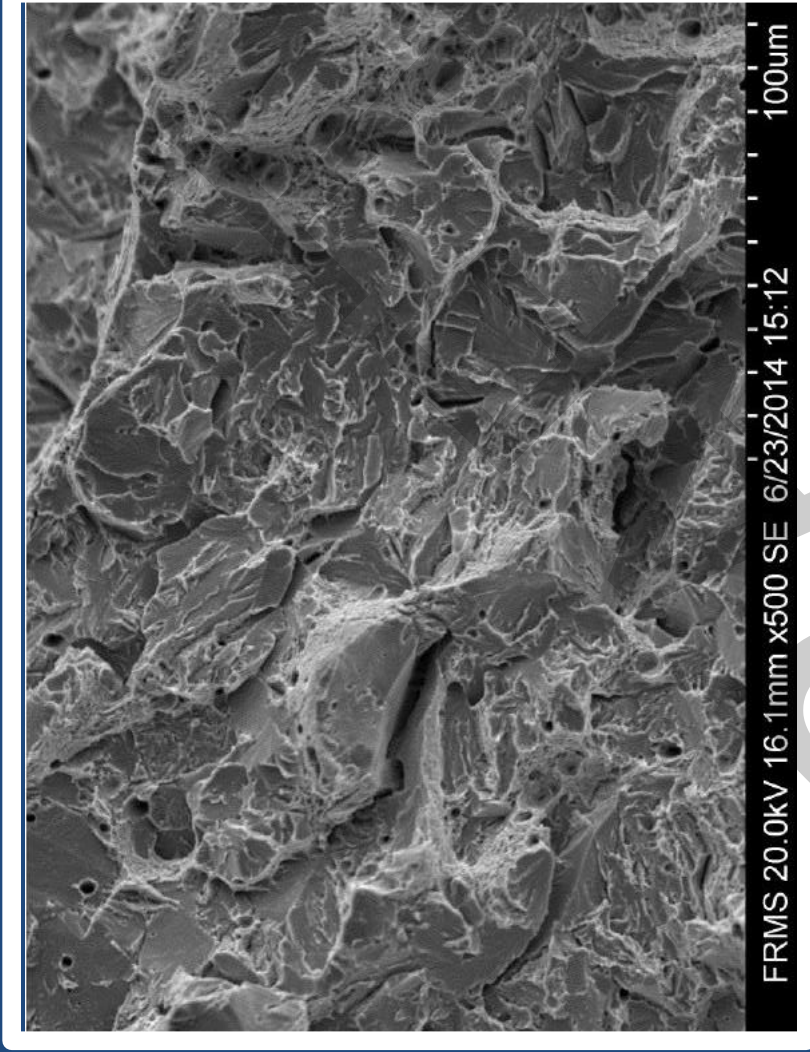
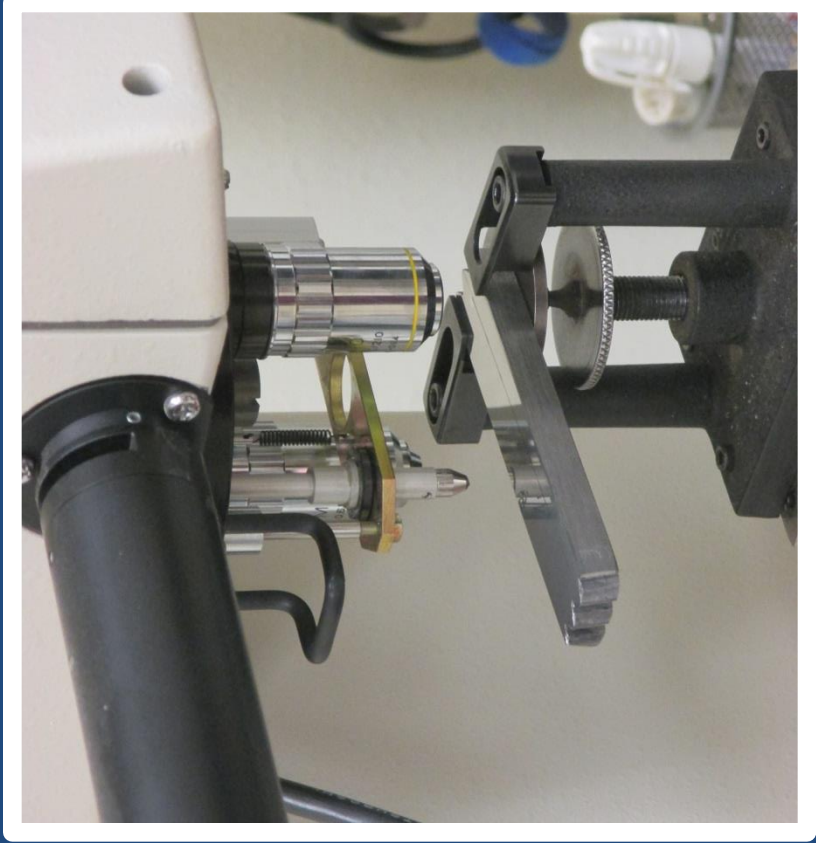
Rods #1-4



TOWNSEND TEST POST FRACTURE ANALYSIS

August 15, 2014

Rods #5-11 (Draft)



TOWNSEND TEST POST FRACTURE ANALYSIS

August 15, 2014

Rods #12-13 (Draft)

*Appendix M –
Test V Details and Data Report*

LRA – Fast Fracture Strength, K_{max}

K_{max} is calculated from the maximum load achieved during the FFS test for a specimen. F_u -max is the maximum load of FFS converted via fracture mechanics equations to FFS of rod. The fast fracture strength values for the samples are plotted in Figure M-1 as a function of hardness and listed in Table M-1.

Some initial conclusions that can be drawn from this data are:

- (1) K_{max} increases with hardness, increasing in groups from Center, Mid-Radius (MR), Outer Diameter (OD), to Threaded,
- (2) K_{max} for the threaded specimens is higher than the K_{max} for fpc specimens,
- (3) All rolled thread specimens reached test limit without cracking, and
- (4) The 2008-fpc specimens are at the minimum values of the 2010-fpc specimens and the 2008 threaded-cut specimens are within range of 2010 threaded-cut specimens.

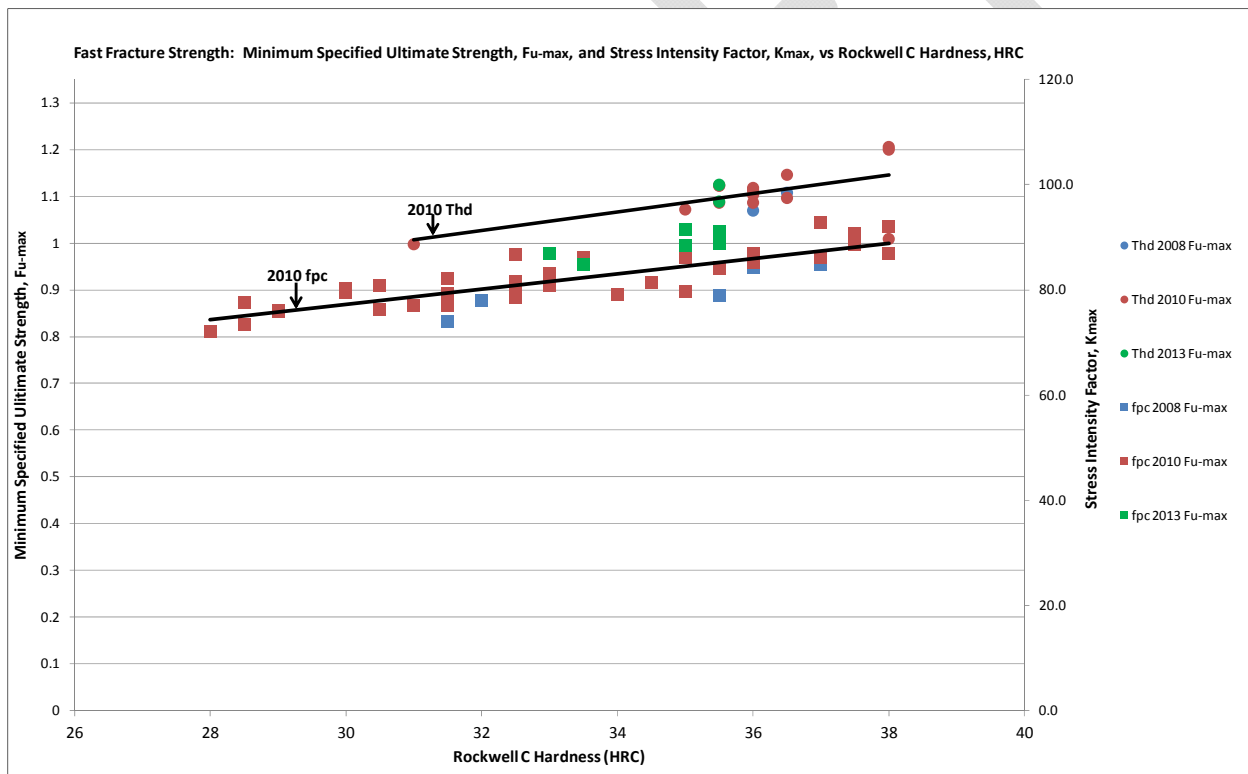


Figure M-1. Fast Fracture Strength: F_u -max and K_{max} vs HRC

*Appendix N –
Test VI Details and Data Report*

LRA – Environmental Hydrogen Embrittlement, KI-EHE

Table N-1 lists the EHE threshold stress intensity values for both fatigue pre-cracked and threaded specimens that were tested at -1.106 Vsce and adjusted to the potential for zinc (-1.06 Vsce). The fatigue pre-cracked data were generated from specimens from material from Rod ID 3, Shear Key Anchor Bolts-Top and can be compared to the results for fpc specimens from the same rods. Included in the threaded tests were specimens from Rod ID 4, Pier E2 Bearing Bolts-Top Housing which had rolled threads.

These results are directly comparable with Test V EHE Thresholds at HDG Zn Potential listed in Table M-3 in Appendix M.

Table N-1. Environmental Hydrogen Embrittlement Results at -1.106 Vsce Adjusted to V-HDG-Zn, KIp and Fu-EHE

LRA - EHE Testing in 3.5% NaCl charged at -1.106 Vsce and Adjusted for HDG Zn Potential									
Test	ID	Rod	Dia.	Structural Component	Comments	Threaded			
						HRC	Kp	Fu	RSL method
Thd, Test VI	3	3-VI-9	3"	Shear Key Anchor Bolts-Top	Same Heat as ID 2 (Rods #1 through #4 Test IV)	36.5	70.2	0.79	(10/5/2,16)
	3	3-VI-11	3"	Shear Key Anchor Bolts-Top	Same Heat as ID 2 (Rods #1 through #4 Test IV)	36.0	74.5	0.84	(10/5/2,8)
	4	4-VI-1	2"	Structural Components: Pier E2 Bearing Bolts-Top Housing	Rolled Threads (Rod #5 Test IV)	36.0	92.3	1.08	(10/5/2,16)
fpc (OD), Test VI	3	3-VI-9	3"	Shear Key Anchor Bolts-Top	Same Heat as ID 2 (Rods #1 through #4 Test IV)	36.0	31.5	0.36	(10/5/2,16)
	3	3-VI-11	3"	Shear Key Anchor Bolts-Top	Same Heat as ID 2 (Rods #1 through #4 Test IV)	36.0	32.8	0.37	(10/5/2,8)
	3	3-VI-12	3"	Shear Key Anchor Bolts-Top	Same Heat as ID 2 (Rods #1 through #4 Test IV)	36.0	33.6	0.38	(10/5/2,8)

*Appendix O –
Field Inspection Report on the Tower
Anchorage Anchor Rods
(Forthcoming)*

